Environmental Drivers of Northeast Atlantic food webs

Amy. L. Shurety

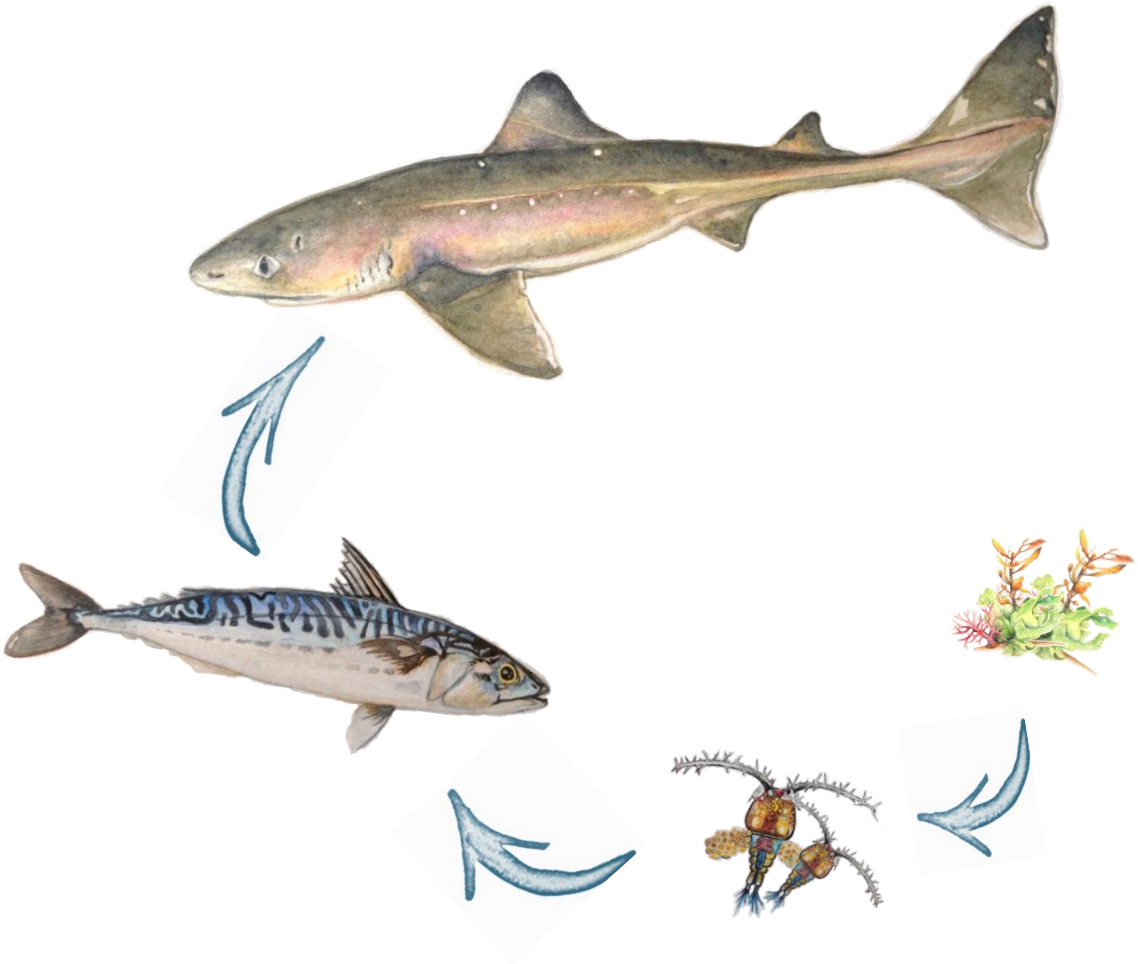

A thesis submitted for the degree of Doctor of Philosophy in Environmental Sciences

School of Life Sciences

University of Essex

March 2026

To my son, Oliver

may the world always hold its wonders for you to explore

And to my husband, Chris

my world is full of wonder because of you

Abstract

Marine ecosystems are increasingly reshaped by interacting environmental stressors driven by global change, affecting the provision of ecosystem goods and services. This thesis adopts a multi-scale food web approach to quantify how increasing temperatures and commercial fishing alter trophic structure and function and ultimately ecosystem resilience across the Northeast Atlantic, progressing from pairwise interactions to food webs across large spatio-temporal gradients. Analysis of stomach contents records spanning 35 years demonstrates that an allometric constraint underpinning food webs, the predator–prey mass ratio, increases with temperature, which is amplified in areas under high commercial fishing, indicating that trophic size structure is dynamic across environmental conditions. These changes are driven primarily by physiologically driven declines in prey body mass. Scaling up beyond pairwise interactions, 4,728 spatially resolved empirical food webs were constructed across the North Sea from 1997 to 2015 using stomach content and survey data, providing an unprecedented representation of trophic interactions and energy flow. Ecological network analysis revealed that temperature and commercial fishing jointly reshape food web structure and function, with consequences for ecosystem resilience. Colder, less exploited systems retain greater trophic complexity, energy availability, and pathway redundancy, whereas warmer and heavily exploited systems exhibit simplified, more tightly organised trophic networks with reduced energy availability and pathway redundancy. Temporal analysis showed that North Sea food webs have become less complex, more structurally organised and energetically constrained over recent decades. These results reflect a shift in ecosystem resilience from ecosystems characterised by adaptive flexibility toward ecosystems structured for energetic efficiency and persistence. Localised analyses reveal substantial spatial heterogeneity, highlighting that regional trends can obscure localised variation in ecosystem resilience. By providing a spatially resolved empirical baseline, this work advances understanding of how environmental change reshapes marine ecosystem resilience, supporting spatially targeted ecosystem-based management informed by climate change and sustainable fisheries.

Contribution statement

I hereby declare that the chapters and associated papers that make up this thesis are the result of my own work. My supervisory team (Dr Eoin O'Gorman, Prof Tom Cameron, Dr Murray Thompson and Dr Elena Couce) provided conceptual and methodological guidance and revision feedback. Various external collaborators (Dr John Pinnegar, Dr Brian Fath and Dr Elena Rovenskaya) also provided invaluable input, including contributing data, methodological help and editorial feedback.

Acknowledgements

Academia can impose heavy expectations and rigid relationships that can hinder growth rather than encourage it. I chose this PhD partly because it was funded (let's all be honest with each other), but also partly because I had a great feeling about who would become my supervisors. That mattered to me, and I am glad I trusted it.

Eoin, thank you for creating such a warm and supportive environment in which I could grow, combining open, easy conversations with thoughtful and structured guidance, and for your generosity with time and understanding. Elena, thank you for your warm and approachable support, for sharing your wealth of knowledge so generously, including the baby sleeping advice! Murray, thank you for sharing your expertise and for being so friendly and encouraging throughout this journey, it felt like you always had an open door despite it being online. Tom thank you so much for your encouragement, and steady guidance throughout this PhD.

You all made it easy for me to pursue this PhD while concurrently fulfilling my dream of becoming a mum, something I do not take for granted, as I am sure not every PhD mum-to-be would feel that way. Thank you. I hope to stay in contact with all of you way into the future.

To my lifelong friends along the way (too many to name), you made this journey so much richer through entertaining office chats, interesting lab group meetings, warm friendships, and endless encouragement. Thank you.

Thank you to Sam for the beautiful water colour drawings.

My IIASA YSSP cohort, YSSP was one of the most rewarding experiences of my PhD. I arrived focused on advancing my career but returned with an overflowing heart and mind.

To my Dad, Mum and Sister. Thank you for being my foundation and my springboard into a career in environmental research, and for always supporting me from day one.

To my little family. Oliver, you are truly the light of my life, and I hope this allows me to build a better future for you. Chris, thank you for being so selfless so I could achieve my dream. This PhD is a reflection of your support, and in truth, your name should be written next to mine, as it is in life.

Contents

Abbreviations

ADBM	Allometric Diet Breadth Model
AIC	Akaike Information Criterion
AMI	Average Mutual Information
APL	Average Path Length
CPOM	Coarse Particulate Organic Matter
DAPSTOM	Integrated Database and Portal for Fish Stomach Records
DATRAS	ICES Database of Trawl Surveys
ENA	Ecological Network Analysis
FCI	Finn Cycling Index
FPOM	Fine Particulate Organic Matter
GES	Good Environmental Status
ICES	The International Council for the Exploration of the Sea
PPMR	Predator to Prey Body Mass Ratio
OSPAR	Oslo and Paris Convention for the protection of European Seas
SST	Sea Surface Temperature
TST	Total System Throughflow

1 General Introduction

1.1 Background on main themes

1.1.2 Ecosystem resilience

An ecosystem is a biological community of interacting organisms and their physical and chemical environment (DeAngelis, 1980; Odum, 1980), forming a complex network of interactions. To sustain this complexity, ecosystem components and interactions continually change in response to environmental conditions, restructuring in ways that support long-term functioning. Consequently, there is no single “optimal” ecosystem structure; instead, systems self-organise and adapt. This capacity for self-organisation and restructuring is underpinned by ecosystem resilience (Holling, 1973), which is closely linked to the structure of ecosystem interactions (O’Gorman et al., 2019; Scharler et al., 2018). Gunderson, (2000) described self-organisation as interactions between structure and function that produce emergent patterns regardless of initial conditions. Resilience therefore determines how ecosystems respond to environmental gradients and disturbances.

Ecosystem resilience has been defined in many ways, leading to conceptual ambiguity. O’Leary et al., (2017), for example, identified nine different definitions. Early interpretations largely equated resilience with stability and the maintenance of equilibrium (Folke, 2006; Gunderson, 2000; Scharler et al., 2018). Holling, (1973), however, reframed resilience as an ecosystem’s capacity to absorb disturbances, both natural and anthropogenic, while maintaining function and integrity, even if the system shifts away from its previous equilibrium. This perspective emphasises adaptive capacity, allowing ecosystems to reorganise or transform while continuing to function.

Adaptive responses may involve regime shifts, defined as low-frequency, high-magnitude changes in ecosystem structure or functioning that move a system into an alternative stable state with distinctly different dynamics (Gunderson, 2000; Scheffer and Carpenter, 2003). The basin-of-attraction analogy (Figure 1.1) illustrates how resilience determines whether a system remains within its current state or transitions to another.

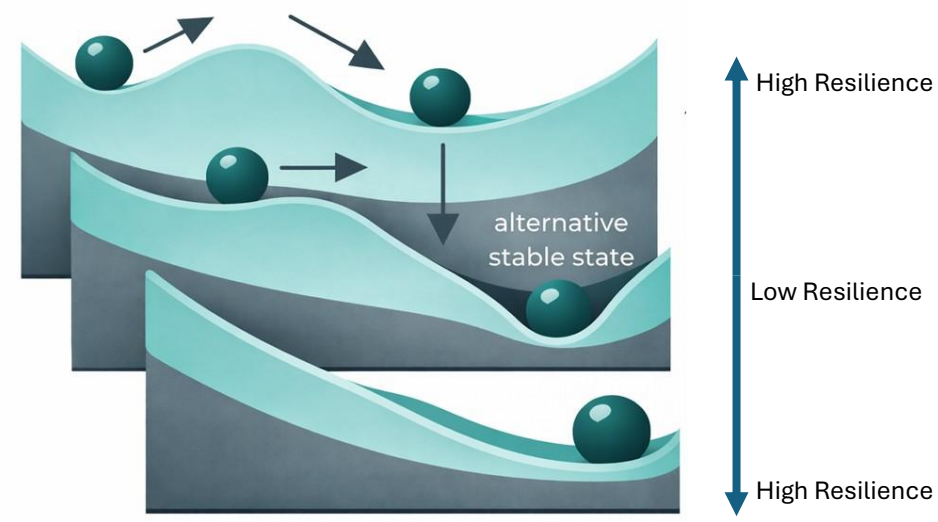

Figure 1.1: The basin of attraction analogy whereby a system (ball) is able to stay within its basin depending on its resilience. If an ecosystem moves into another basin a regime shift has taken place whereby a system has undergone substantial re-structuring (adapted from Gunderson, 2000). I acknowledge the use of AI in helping me construct this figure (OpenAI, 2025)

From a network perspective, resilience has been linked to a balance between redundancy and organisation (Figure 1.2) (Kharrazi et al., 2020; Ulanowicz, 2009). For example, in ecological networks, redundancy, such as multiple species performing similar ecological functions or parallel energy pathways, provides buffering capacity when disturbances disrupt individual components. At the same time, the organisation of interactions within networks supports efficient transfer of matter such as energy and stable functioning of the system such as biological activity (Hirata and Ulanowicz, 1986; Kharrazi et al., 2020, 2016). Together, these properties allow systems to absorb disturbances while maintaining overall system functioning.

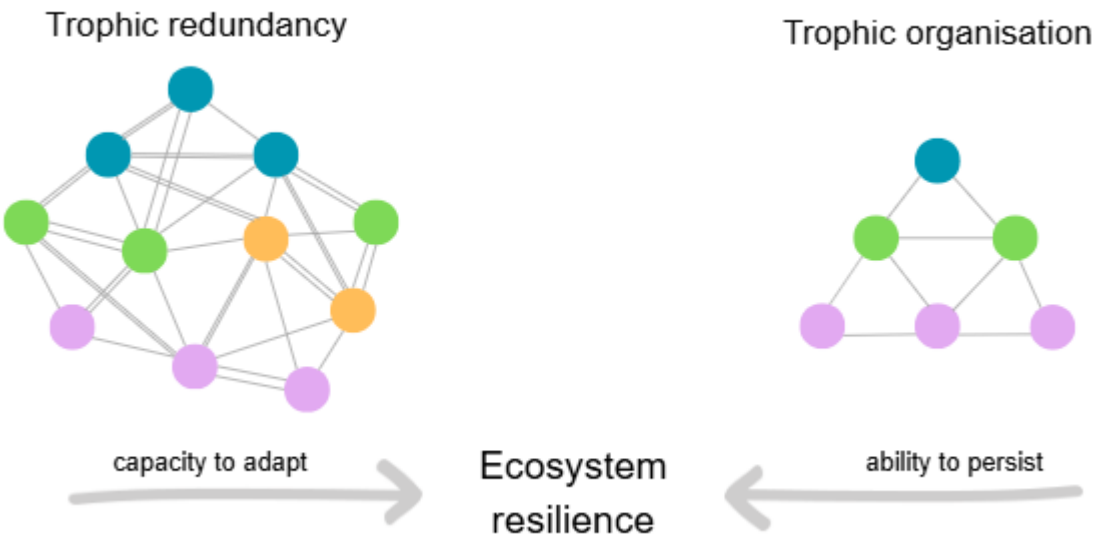

Figure 1.2: A conceptual, diagram illustrating the balance between trophic redundancy, allowing capacity to adapt through functional similar trophic pathways (redundancy), and trophic organisation enabling persistence through efficient energy transfer (Holling, 1973).

In ecological terms, resilience enables recovery from both natural and human-induced disturbances (Folke, 2006; Holling, 1973; Scharler et al., 2018) and is therefore fundamental to sustainability. The continued provision of ecosystem goods and services depends on the capacity to maintain functioning despite increasing pressures. As contemporary ecosystems face more frequent and intense disturbances, resilience has become increasingly critical.

1.1.3 Food webs

A food web is a network representation widely used in ecological research to understand ecosystem structure, functioning, and resilience (Belgrano, 2004; Frelat et al., 2022; Link, 2002; McCormack et al., 2021; Pimm, 1982). It describes the trophic interactions through which energy and biomass are transferred among organisms within an ecosystem (Belgrano, 2004; Petchey et al., 2008; Pimm, 1982). Within this framework, nodes typically represent species, functional groups, or trophic compartments, while links represent feeding interactions that govern the direction and magnitude of energy flow (Figure 1.3).

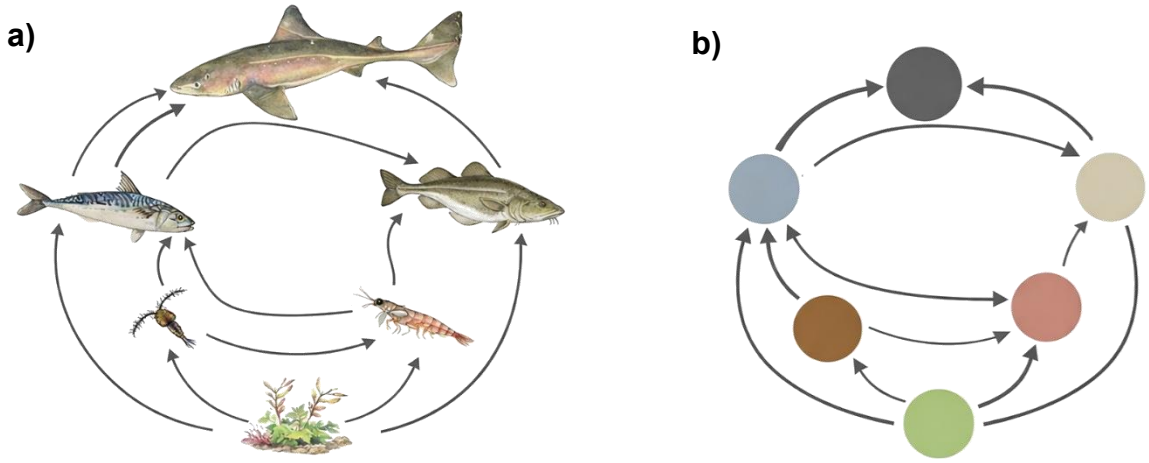

Figure 1.3: Illustration of how **a)** ecological food webs can be represented as **b)** networks. **a)** Organisms including phytoplankton, zooplankton, krill, mackerel, cod, and dogfish are depicted. **b)** These organisms are represented as nodes within a network. Trophic interactions between consumers and their resources (i.e., the flow of energy) are represented as links between nodes, with link weights reflecting the magnitude of energy transferred through each trophic interaction. Watercolour illustrations used to construct this illustration were created by Samantha Venter.

The structure that regulates energy flow encapsulates the multitude of interactions and feedbacks that shape overall ecosystem functioning, such as productivity and nutrient recycling (Petchey et al., 2008; Pimm, 1982, 1980; Tang et al., 2024). A central challenge in ecological research is reconciling the need to understand the complexity in dynamic ecosystem interactions with the demand for simple, robust management guidance. Network approaches offer a powerful framework to address

this challenge by providing a quantitative representation of structure, function relationships within complex systems. Networks are used across disciplines, from social and infrastructure systems to biological and ecological systems (Cumming, 2016). They also overlap across disciplinary boundaries, for example in fisheries where ecological food webs intersect with social networks of resource users (Bodin et al., 2006). As integrative tools, networks facilitate interdisciplinary research and are particularly attractive to policy makers due to their capacity to distil complex ecosystem dynamics into interpretable, quantitative insights (Cumming, 2016; Fath et al., 2019).

Within food webs energy generally flows from abundant, small-bodied primary producers and consumers at lower trophic levels to larger-bodied, less abundant predators at higher levels, with allometric body-size scaling providing a fundamental organising principle (Brose et al., 2006; O'Gorman et al., 2019). Historically, food webs have been conceptualised as hierarchical trophic pyramids, reflecting thermodynamic constraints and the progressive loss of energy between successive trophic levels (Lindeman, 1942a; Woodson et al., 2018). However, real food webs are rarely strictly linear or pyramidal. Instead, they often exhibit complex topology, including modular structure, omnivory, feedback loops, and highly connected nodes associated with functional hubs or keystone species that disproportionately influence network stability (Newman and Girvan, 2004). Food webs are inherently dynamic, with trophic interactions, energy pathways, and species roles continually reorganising in response to environmental variability across space and time (Bartley et al., 2019; Kortsch et al., 2019; Perkins et al., 2010; Tylianakis and Morris, 2017).

Food web structure fundamentally constrains ecosystem functioning because the arrangement of trophic interactions determines how energy and biomass are transferred, regulated, and stabilised within ecosystems (Frelat et al., 2022; Petchey et al., 2008; Pimm, 1982; Ulanowicz, 1996). Interaction strengths, the distribution of trophic links, and the balance between top-down and bottom-up control collectively shape productivity, nutrient cycling, and population dynamics (McCann et al., 1998; Pace et al., 1999). Early theoretical work suggested that increasing complexity in trophic interactions could destabilise communities (Hastings, 1988; May, 1973; Pimm, 1980), yet subsequent research suggests that complexity in trophic interactions such as compartmentalisation or redundancy in energy flows could

dampen oscillatory dynamics by localising disturbance (McCann et al., 1998; Rooney et al., n.d.; Thébault and Fontaine, 2010). Energy flux through trophic pathways further mediates ecosystem resilience, as alterations to trophic level structure or interaction strengths can reduce the efficiency of energy transfer and increase vulnerability to perturbation (Scharler et al., 2018; Ulanowicz et al., 2009). Thus, food web architecture is not merely descriptive but mechanistic, governing how ecosystems respond to environmental variability, absorb disturbance, and maintain functional integrity under environmental change.

Despite their conceptual power, historically quantitative food-web analyses have been constrained by extensive data requirements, and limited standardisation across studies (Thompson et al., 2020). Food webs are typically constructed by combining information on species composition with evidence of trophic interactions, using a range of complementary methodological approaches. Direct dietary methods, such as stomach-content analysis, provide taxon-specific evidence of realised predator–prey links, although they can be biased toward larger or hard-bodied prey that persist longer in digestive tracts (Hyslop, 1980). DNA metabarcoding can improve the detection of rare, soft-bodied, or highly digested prey that may be missed by visual identification, while stable isotope analysis integrates assimilated resource use over longer time periods and can be used to infer trophic position and energy pathways within the system (Blackman et al., 2022; Casey et al., 2019; Post, 2002). However, accurate characterisation of trophic interactions still requires intensive sampling across taxa and life stages, and rare species or weak interactions are frequently under-represented. Nevertheless, dietary data have enabled the development of size-structured and empirically grounded food webs that capture key aspects of ecosystem organisation and energy transfer (Woodson et al., 2018). In parallel, modelling approaches have been developed to overcome empirical limitations and explore dynamic ecosystem processes. Where direct interaction data are limited, food webs are often supplemented with literature-derived interactions, trait-based inference, or mass-balance approaches. Mass-balance and dynamic simulation models such as Ecopath with Ecosim (Christensen and Walters, 2004) use biomass, production, consumption, and diet data to quantify energy budgets and trophic flows under different exploitation scenarios. Mechanistic frameworks including the Allometric Diet Breadth Model (ADBM) (Petchey et al., 2010) predict interaction

structure based on body-size constraints, while tools such as Fluxweb (Gauzens et al., 2019) estimate energy fluxes from network topology and species traits. As such, food-web construction is rarely based on a single method, but instead depends on combining empirical dietary evidence, biochemical tracers, published trophic information, and modelling approaches.

1.1.4 Global change

Ecosystems across the globe are subject to a wide array of environmental gradients. Patterns observed in ecosystem structure and function are known to be associated with environmental gradients (Coghlan et al., 2022; Kortsch et al., 2019; Thompson et al., 2020; Tylianakis and Morris, 2017). These gradients can be a result of both large and small-scale natural and anthropogenic stressors that are both increasing in intensity and frequency (Halpern et al., 2008). Such stressors include climate change and over-fishing which are both extremely relevant in all marine ecosystems (Howarth et al., 2018).

1.1.4.1 Climate change

Temperature represents a major environmental gradient structuring marine ecosystems, driving species distributions and community composition (Boyce et al., 2008, 2015; Kortsch et al., 2019) as well as regulating key physiological processes, including growth, metabolism and energetic demand (Brown et al., 2004; Capuzzo et al., 2018; Cheung et al., 2013). Environmental temperature varies naturally through seasonal and interannual cycles, however anthropogenic activities have amplified natural variation in temperatures, known as climate change. Climate change is a pervasive driver of ecological change across marine systems (Doney et al., 2012; Hoegh-Guldberg and Bruno, 2010), altering both abiotic conditions and the biological processes they regulate.

In marine ecosystems, climate change manifests most prominently through rising sea surface temperature (SST) and ocean acidification (Brierley and Kingsford, 2009; Harley et al., 2006). Globally, SST has increased by approximately 0.65 °C since the 1950s (Gulev et al., 2023), with further warming projected. Elevated SST drives species range shifts, often poleward or into deeper waters, as mobile species move to suitable thermal habitats (Bryndum-Buchholz et al., 2020; Poloczanska et al., 2016). Marine species inhabiting warmer environments frequently exhibit

narrower thermal tolerances, increasing sensitivity to additional warming (Sunday et al., 2010). In the North Sea, for example, warming in the late 1990s was associated with the expansion of horse mackerel and marked shifts in zooplankton communities (Heath, 2005), illustrating how temperature-driven range shifts can reorganise trophic interactions.

Range shifts of species is one reason why increasing temperature alters food webs through both direct and indirect pathways. Changes in species abundance and richness can rewire the network of specialist and generalist consumers (Schwarz et al., 2017), introducing new or specialising trophic interactions (Bartley et al., 2019; Pecuchet et al., 2020). Temperature-dependent metabolic scaling further increases consumer energetic demand, often favouring smaller-bodied species and altering predator–prey body size structure (Brown et al., 2004; Schwarz et al., 2017). Such shifts propagate through networks, modifying trophic energy flux and potentially impacting ecosystem resilience (Coghlan et al., 2022; du Pontavice et al., 2020).

Collectively, previous research demonstrates that rising SST fundamentally restructures marine food webs by reshaping species distributions, interaction strengths, body size structure and energy pathways. As warming intensifies, understanding how SST reorganises food web structure and function is essential for anticipating changes in ecosystem resilience and sustaining the goods and services provided by marine systems.

1.1.4.2 Commercial fishing

Historically commercial fishing has resulted in the unsustainable removal of commercial fish species from marine ecosystems, leading to altered trophic interactions through the disproportionate extraction of targeted species (Pauly et al., 1998). Globally, approximately 60% of assessed fish populations are fully exploited or overexploited (FAO, 2016), and globally total fisheries catch increased markedly throughout the twentieth century in response to escalating global protein demand (Link and Watson, 2019). Although fishing pressure is commonly quantified using landings data and catch-per-unit-effort metrics, these indicators provide limited insight into ecosystem-wide direct and indirect consequences (Reum et al., 2019a). For example, the collapse of cod stocks in the Northwest Atlantic facilitated increases in forage fish and invertebrates, resulting in persistent alternative species

composition (Frank et al., 2005). Such ecosystem-level reconfigurations highlight the importance of moving beyond single-species management toward ecosystem-based fisheries management frameworks that explicitly account for trophic structure and energy flow (Fath et al., 2019; Schückel et al., 2022).

Commercial fisheries have historically targeted large-bodied, high-trophic-level species (Baum and Worm, 2009; Jennings et al., 2002; Pauly and Palomares, 2005), resulting in the selective removal of older, more fecund individuals and a truncation of population age and size structure. This selective extraction steepens community size-spectrum slopes and reduces the relative abundance of apex predators (Howarth et al., 2018). Size-based ecosystem theory predicts that such truncation disrupts trophic interactions and the flow of energy across food webs (Andersen and Beyer, 2015; Blanchard et al., 2017). In addition, fisheries-induced evolution may favour earlier maturation at smaller body sizes, further reinforcing long-term shifts in community structure (Heino et al., 2015). As a result extensive evidence indicates that commercial exploitation reduces the mean trophic level of marine catches, a phenomenon termed “fishing down the food web” (Pauly et al., 1998; Pauly and Palomares, 2005). The loss of top predators generates strong top-down effects that propagate through food webs, often increasing the abundance of meso-predators and lower trophic-level species (Bascompte et al., 2005; Pauly and Palomares, 2005). This process can intensify predation pressure on forage fish and benthic invertebrates, thereby restructuring community composition (Prugh et al., 2009). Empirical studies from multiple marine systems demonstrate that predator depletion can trigger trophic cascades, alter competitive interactions, and shift dominance toward opportunistic or fast-growing species (Baum and Worm, 2009; Lynam et al., 2017). Such cascades occur when declines at one trophic level propagate to adjacent levels through direct and indirect trophic interactions (Reum et al., 2019a), potentially resulting in regime shifts (Scheffer and Carpenter, 2003). Declines in biodiversity associated with overfishing can destabilize ecosystem functioning by reducing functional redundancy and weakening compensatory dynamics among species (Daskalov et al., 2007; Naeem, 2009).

Therefore, commercial fishing not only reduces target stock biomass but fundamentally restructures marine food webs by altering size distributions, species compositions and weakening natural top-down control by lowering mean trophic

level. Understanding such impacts of commercial fishing is essential for predicting long-term ecosystem responses and designing management strategies that preserve both biodiversity and ecosystem function.

1.1.4.3 Cumulative Impacts

Environmental gradients such as SST and commercial fishing do not act in isolation but rather act in unison resulting in synergistic or cumulative impacts within ecosystems (Korpinen and Andersen, 2016; Molinos and Donohue, 2010). For example, researchers believe that variability brought on by climate change has made North Sea fish stocks such as cod more vulnerable to overfishing impacts by reducing recruitment success, prey availability and age-structure of commercial populations (Bryndum-Buchholz et al., 2020; Heath, 2005; Kirby et al., 2009; Lynam et al., 2017). Climate-driven range shifts of top predators toward cooler regions, combined with their selective removal by overfishing, can amplify trophic cascades within marine food webs (du Pontavice et al., 2020). Despite these cross-scale impacts, fisheries and climate management have historically focused on single-species assessments and/or independent drivers of change. Increasingly, emphasis is needed on ecosystem-based management approaches that account for impacts across all levels of biological organisation, from species to whole systems as well as cumulative impacts of environmental global change (Bartley et al., 2019; Link and Watson, 2019).

1.1.5 Spatial temporal scales

Environmental gradients take shape over both space and time, leading to calls for adaptive management and assessments that fully incorporate differences between spatiotemporal scales. This is particularly important in marine ecosystems, which are highly connected and characterised by diffuse boundaries compared to terrestrial systems (Link, 2002). Such connectivity allows physical, biological and anthropogenic drivers to propagate across large areas, reinforcing the need to consider cross-scale interactions when evaluating ecosystem structure and functioning in the context of environmental global change.

Food webs are inherently diverse, complex and variable across space (e.g., local, regional and global) and time (e.g., seasonal, interannual and decadal) (Albouy et

al., 2014; Frelat et al., 2022; McCormack et al., 2021; Petchey et al., 1999). This variability arises from spatial and temporal heterogeneity in abiotic conditions, such as temperature and nutrient availability, as well as biotic processes including species interactions, productivity and phenology (Boyce et al., 2015; Frelat et al., 2022; Kortsch et al., 2015; McCormack et al., 2021; Molinos and Donohue, 2010). Recognising and explicitly incorporating this variability into food web construction and analysis is therefore vital, as static or single-scale representations risk overlooking key dynamics that structure trophic interactions.

Body size and mobility further complicate food web structure across scales. Larger or more mobile predators typically occupy broader habitat ranges, often traversing ecosystem boundaries and participating in multiple, spatially distinct food webs (McCormack et al., 2021). Climate change is a major driver of species range shifts, altering the spatial overlap among predators and prey and reshaping trophic interactions (du Pontavice et al., 2020; Flanagan et al., 2019). Such range shifts can only be fully understood when examined across species' geographical ranges and relevant spatial scales. Furthermore, many marine species exhibit long life spans accompanied by substantial ontogenetic size changes (Link, 2002), necessitating explicit consideration of life-stage and size-structured dynamics in food web analyses. For example, Thompson et al., 2020 demonstrated that in the North Sea, species biomass is distributed across broad feeding and environmental niches, both of which shift markedly over time.

Environmental and anthropogenic stressors also vary across ecosystem types and spatio-temporal scales (du Pontavice et al., 2020; Molinos and Donohue, 2010). Shelf and coastal seas, for instance, are often more vulnerable to human activities due to their proximity to population centres and exposure to multiple stressors, including fishing, nutrient loading and habitat modification (Capuzzo et al., 2018). Importantly, ecosystem responses to perturbations may exhibit significant lag times (Thompson et al., 2020). Impacts do not always manifest immediately, as changes must propagate through networks of direct and indirect interactions before system-level effects become apparent (Allesina et al., 2006). Accounting for these delayed and scale-dependent responses is essential for understanding ecosystem resilience, anticipating regime shifts, and designing adaptive management strategies that are robust to ongoing environmental change.

1.2 Background on relevant ecological theory

1.2.1 Body mass scaled trophic interactions

Trophic interactions such as predator–prey relationships are non-random and governed by fundamental ecological principles, including behavioural and physiological traits (Bascompte et al., 2005; Howarth et al., 2018; Petchey et al., 2008). Body size is a strong predictor of species interactions in marine systems and is closely linked to trophic level, resource access, and vulnerability to predation and disturbance (Brose et al., 2006; Gauzens et al., 2019; Nordström et al., 2015; Petchey et al., 2010; Schneider et al., 2012; Thompson et al., 2020; Woodson et al., 2018). Therefore, diets are largely size-structured, with predators typically consuming smaller prey, leading to consumer groups that are broadly organised by body size (Howarth et al., 2018; Petchey et al., 2008; Reum et al., 2019a). Diet breadth also increases with body size, as allometric foraging allows larger species to exploit a wider range of prey sizes (Petchey et al., 2008).

Consequently, body size has been increasingly adopted as a universal ecological trait by major research initiatives, including the European Science Foundation Research Network (Petchey and Belgrano, 2010; Thompson et al., 2020). However, further progress is needed to integrate body size into universally comparable indicator frameworks and understand any nuances in trophic scaling under changing environmental conditions.

Predator prey body mass ratio (PPMR) is a metric used to quantify the body mass scaling between consumer and resource (Reum et al., 2019b). Established ecosystem modelling techniques make use of PPMR to predict trophic interactions (Brose et al., 2006; Petchey et al., 2010; Plank et al., 2017), however it is considered as a static value which does not account for the known variability in dynamics that influence the body mass of both predators and prey. PPMR is known to be dependent on species composition as well as individual predator attributes (Reum et al., 2019b; Reum and Hunsicker, 2012; Wilson and Kimmel, 2021). Changing PPMR has repercussions for ecosystem stability (Plank and Law, 2012) due to changing strength of energy transfer between species (Barnes et al., 2010; Emmerson and Raffaelli, 2004). Therefore, studies to assess the variability of PPMR across spatial gradients of species composition and other environmental conditions would enhance

its use in predicting trophic interactions within marine ecosystems (Barnes et al., 2010; Coghlan et al., 2022; Reum et al., 2019b).

1.3 Background on key methodological approaches

1.3.1 Flux web

The Fluxweb package (Gauzens et al., 2019) was developed in using R v4.2.2 (R Core Team, 2024) to predict the weight of interactions within food webs using the equation below (equation 1.1). Data needed to construct a *fluxweb* model includes a matrix of trophic interactions, vector of total population biomass, vector of the average body masses and a vector of the organism types (i.e., plant, animal or detritus) (Gauzens et al., 2019). Prey preference can also be included as an optional parameter. The *fluxweb* package outputs a matrix of energy fluxes between nodes, which can be used to construct weighted food webs (Bazin et al., 2025; Gauzens et al., 2019; Kortsch et al., 2021). The model also assumes a steady state system where losses by predation or physiological processes equal gains from consumption (Gauzens et al., 2019).

$$\sum_j W_{ji} F_i e_{ij} = X_i + \sum_j W_{ij} F_j.$$

(equation 1.1)

where F_i is the sum of all ingoing energy flux from species j, W_{ij} defines the proportion of F_i obtained from species j, e defines species feeding efficiency, and X_i represents the energetic loss from species i. The equation was solved by calculating the sum of ingoing fluxes for each species within the food web.

Quantifying energy fluxes will give insight into ecosystem characteristics such as productivity and herbivory (Gauzens et al., 2019). Furthermore, the package allows the computation of a stability metric which describes to extent to which the system is able to return to equilibrium (Gauzens et al., 2019). The *fluxweb* package has been used to predict external impacts such as changing temperatures on food web structure (Bazin et al., 2025; O'Gorman et al., 2019). Data availability on the weight

of trophic interactions is often limited due to the degree of sampling effort required, making *fluxweb* a valuable tool for food web research.

1.3.2 Ecological Network Analysis

Ecological metrics are powerful tools for distilling the complexity of ecosystems into simple, quantitative information that can communicate changes in structure and function (Table 1.1). They are widely used to evaluate ecosystem responses to environmental change, including shifts in food web organisation under external pressures. Beyond change detection, metrics also serve to define ecosystems, a critical step for comparing ecosystem status across space and time (Cumming and Peterson, 2017)

Ecological Network Analysis (ENA) provides a rigorous framework for calculating key metrics that quantify ecosystem structure and function (Table 1.1). ENA has been applied across a diversity of systems, including estuaries (Mukherjee et al., 2015), soils (Creamer et al., 2016), urban-industrial ecosystems (Morris et al., 2021), marine environments (Tomczak et al., 2013) and freshwater ecosystems (Li et al., 2009), and is supported by an R package, *enaR* (Borrett and Lau, 2014). These metrics help bridge scientific understanding and management relevance by providing standardised, reproducible metrics.

Metrics must be clearly defined, simple, measurable and interpretable across disciplines to be effective in policy and management (Hák et al., 2016; Levett, 1998). An example in practice is the increasing use of mean trophic level in fisheries management as an indicator of top-down pressure from harvesting, which typically declines with rising fishing intensity (Link and Watson, 2019; Pauly et al., 1998; Pauly and Palomares, 2005). Similarly, connectance, a measure of interaction density within a food web, provides insight into complexity and potential biodiversity loss (Dunne et al., 2002; Frelat et al., 2022; O'Gorman et al., 2019), with declines potentially indicating reduced ecosystem resilience (Pecuchet et al., 2020). Total system throughput (TST) is another key metric of overall system size and growth, integrating biomass and productivity to reflect functional capacity and ecosystem resilience (Finn, 1980, 1976). TST has been shown to scale with total biomass and growth (de la Vega et al., 2018; Mukherjee et al., 2015).

International assessment frameworks are increasingly using ecological metrics in policy evaluations. For example, the Oslo and Paris Convention for the protection of European Seas (OSPAR) Quality Status Report 2023 (Schückel et al., 2022) uses a suite of ENA-derived metrics to assess the state of marine food webs across the North-East Atlantic. These metrics are explicitly linked to Marine Strategy Framework Directive criteria and help inform regional evaluations of food web status and progress toward Good Environmental Status (GES) (OSPAR, 2023; Schückel et al., 2022).Despite their utility in both science and policy assessments, there remains a need to integrate a broader suite of metrics, underpinned by robust spatial and temporal empirical evidence, into routine ecological assessments and policy frameworks to better capture cumulative pressures and ecosystem responses (Fath et al., 2019; Schückel et al., 2022; Thompson et al., 2025).

627 Table S1: Key information on each network-level metric used to analyse variation in
628 food web structure and function within this thesis.

Metric	Definition	Equation	Unit	Reference
Connectance	Connectance is the proportion of observed flows in a network relative to the maximum number of possible flows	$Connectance = n(n - 1)L$ Where *L* is the number of realized trophic/flow links and n is the number of nodes		Pimm, 1982
Mean trophic level	We used the prey average trophic level which is defined as a consumer's average position above its prey in the network, expressed as 1 + the mean trophic level of those prey species.	$TL_i = 1 + \frac{1}{n_i} \sum_{j \in prey(i)} TL_j$ Where *TLi* is the trophic level of species *i*, *prey(i)* is the set of prey species consumed by *i* and *ni* is the number of prey species *i*		(Hudson et al., 2013; Levine, 1980)
Modularity	Modularity measures how strongly a food web is divided into communities, by comparing the actual density of trophic links within groups to the density expected if trophic links were placed at random.	$Q = \frac{1}{2m} \sum_{i.j} (A_{ij} - \frac{k_i k_j}{2m}) \delta(c_i, C_j)$ Where A_{ij} is the adjacency matrix, k_i is the degree of node *I, m* is the total number of edges and (C_i, C_j) equals 1 if nodes *i* and *j* are in the same community, else 0		Newman and Girvan, 2004

Table S1 continued

Metric	Definition	Equation	Unit	Reference
Average path length (APL)	The mean of the shortest path lengths between all pairs of nodes.	$APL = \frac{1}{N(N-1)}\sum_{i \neq j} d_{ij}$ Where d_{ij} is the shortest path length between nodes *i* and *j*, and *N* is the total number of nodes in the network		Dunne et al., 2002; Watts and Strogatz, 1998
Total system throughflow (TST)	The total amount of energy (e.g. carbon) of all flows in the system.	$TST = \sum_{i=1}^{n} T_i$ Where *Ti* is the instantaneous rate at which matter or energy moves through a node	mgC·m^{-2}·time^{-1}	Finn, 1976
Finn cycling index (FCI)	Equates to the recycling activity of the system, specifically the proportion of the total flow (TST) within the system that is recycled	$FCI = \frac{T_c}{TST}$ Where T_c is the amount of cycles flow and *TST* is the total system throughflow	Percentage (%)	Finn, 1976
Omnivory	Measures the degree to which nodes have trophic links across multiple trophic levels	$Omnivory = \frac{N_{omn}}{N}$ Where N_{om} is the number of omnivorous nodes (i.e. species who feed on prey from more than two trophic levels) and *N* is the total number of nodes		Pimm and Lawton, 1978; Williams and Martinez, 2004

Table S1 continued

Metric	Definition	Equation	Unit	Reference
Redundancy	A measure of the number and distribution of parallel pathways found in a system	$Redundancy = -\sum_{ij}\left(\frac{T_{ij}}{T_{..}}\right) log_2(\frac{T_{ij}^2}{T_{i.}T_{.j}}$ Where Σ_{ij} is the sum of all flows from node *i* to *j*, T_{ij} is the flow from node *i* to *j* and $T_{..}$ is the total system throughput (TST)	bits	Ulanowicz, 2004
Average mutual information (AMI)	A measure of the overall organisation within a system, namely how efficient and direct communication is between any two nodes	$AMI = \sum_{ij}\left(\frac{T_{ij}}{T_{..}}\right) log_2(\frac{T_{ij}T_{..}}{T_{i.}T_{.j}}$ Where Σ_{ij} is the sum of all flows from node *i* to *j*, T_{ij} is the flow from node *i* to *j* and $T_{..}$ is the total system throughput (TST).	bits	Ulanowicz, 2004
Robustness	Indicates the trade-off between efficiency and redundancy	$R = -\alpha Log(\alpha)$ Where α = *AMI / Redundancy*		Ulanowicz et al., 2009

1.4 Study Site: Northeast Atlantic

The Northeast Atlantic extends from the Arctic to the Iberian Peninsula and the European continental shelf to the Mid-Atlantic Ridge, including the Norwegian Sea, Greenland Sea, Barents Sea, North Sea, Celtic Sea, English Channel and the Bay of Biscay (Figure 1.4). The Northeast Atlantic has a predominantly temperate climate, with spatiotemporal variability strongly influenced by the North Atlantic Oscillation (Hurrell, 1995; von Schuckmann et al., 2024). In the Northeast Atlantic climate change and overfishing are prominent anthropogenic pressures causing variation in environmental gradients (Bryndum-Buchholz et al., 2020; Heath, 2005; Lynam et al.,

2017; Thompson et al., 2020). SST within the North Sea has increased by 0.2 – 0.4 ° C per decade (Dye et al., 2013) and is expected to increase three times faster than the global average (Bryndum-Buchholz et al., 2020).

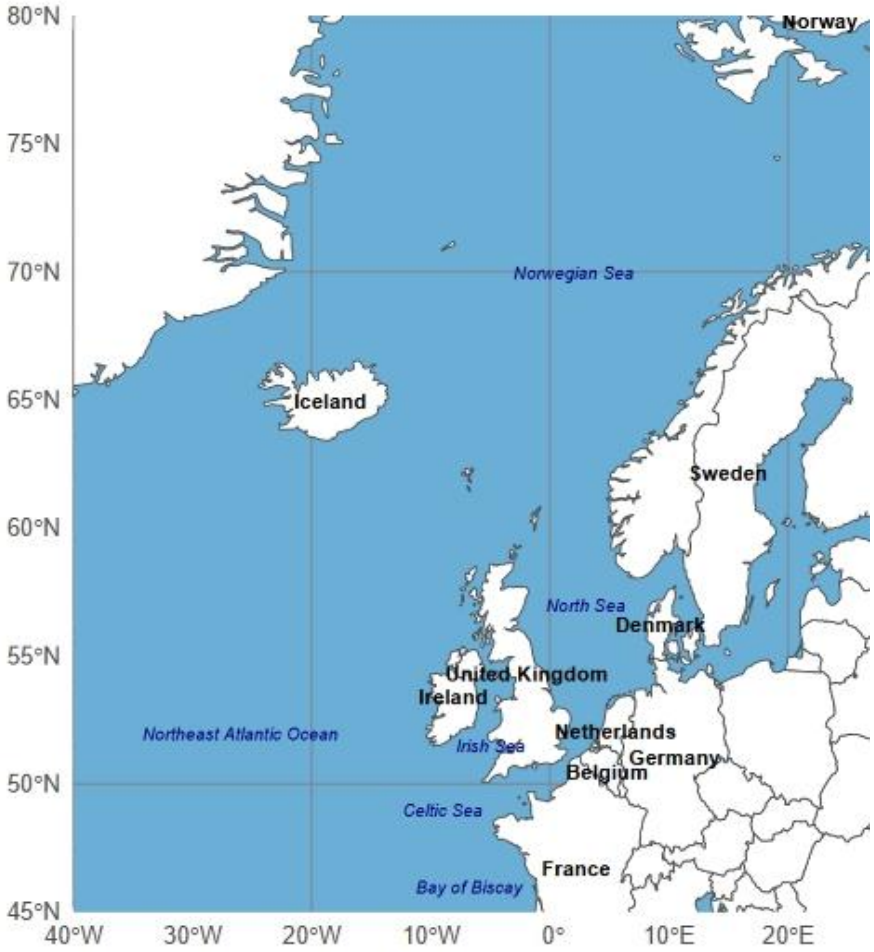

Figure 1.4: The Northeast Atlantic region where this thesis focuses its research.

The Northeast Atlantic is considered to be instrumental in global fisheries production (Bryndum-Buchholz et al., 2020) as it provides approximately 5% of the global fish harvest (Kirby et al., 2009). As a result, however the Northeast Atlantic and in particular the North Sea is one of the most heavily fished ecosystems in the world (Heath, 2005) with fish stocks declining drastically between the 1950s and 1980s (Capuzzo et al., 2018). Recently, commercial fishing pressure within the region has declined (Couce et al., 2020) due to concern for Northeast Atlantic fish stocks causing authorities to rethink management implementation in the 1990s and 2000s. Some stock recovery was seen (Capuzzo et al., 2018; Engelhard et al., 2014), however, the ecosystem-wide consequences of this reduction, as well as the legacy

effects of historically intense exploitation, remain poorly understood. A few examples of North Sea commercial fish species include cod, whiting, haddock, sprat, sand eel and herring (Figure 1.4) (Clark et al., 2003; Kirby et al., 2009; Lynam and Riberio, 2022; Lynam et al., 2017; Stäbler et al., 2018). Large sampling records are available for the Northeast Atlantic, this together with its importance for protein production and the clear impacts of both fisheries and climate change make it a fruitful case study for food web modelling studies.

A typical North Sea food web incorporates basal resources such as phytoplankton, lower trophic levels including zooplankton, followed by small pelagic fish such as herring and sprat, with larger demersal fish, marine mammals and seabirds occupying the upper trophic levels (Figure 1.5) (Fauchald et al., 2011; Heath, 2005; Lynam et al., 2017; Mackinson and Daskalov, 2007; Silberberger et al., 2018). However, North Sea food webs vary markedly across spatial scales. Heath, 2005 described the pelagic food web (1973–2000) as predominantly governed by bottom-up control, whereas benthic components were more strongly influenced by top-down processes. This spatial heterogeneity in trophic regulation has led to suggestions that the North Sea be managed as distinct zones to better account for regional variability in ecosystem structure and functioning (Frelat et al., 2022).

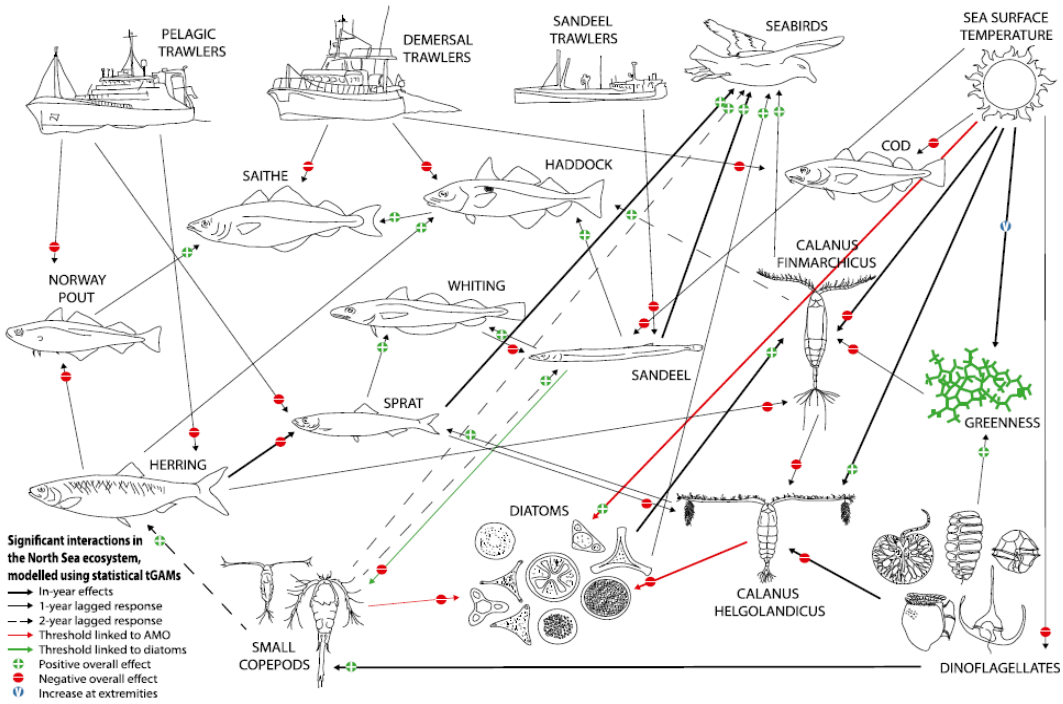

Figure 1.5: An example of a North Sea food web and key commercial fisheries (Lynam et al., 2017).

1.5 Thesis outline

The overarching objective of this thesis is to understand past and spatial variation in trophic interactions and food webs across the Northeast Atlantic, with a particular focus on two key environmental drivers: SST and commercial fishing. Central themes that underpin the thesis and overlap between chapters are 1. ecosystem resilience; 2. marine trophic interactions and food webs, and 3. large scale spatial and temporal gradients of SST and commercial fishing (Figure 1.5).

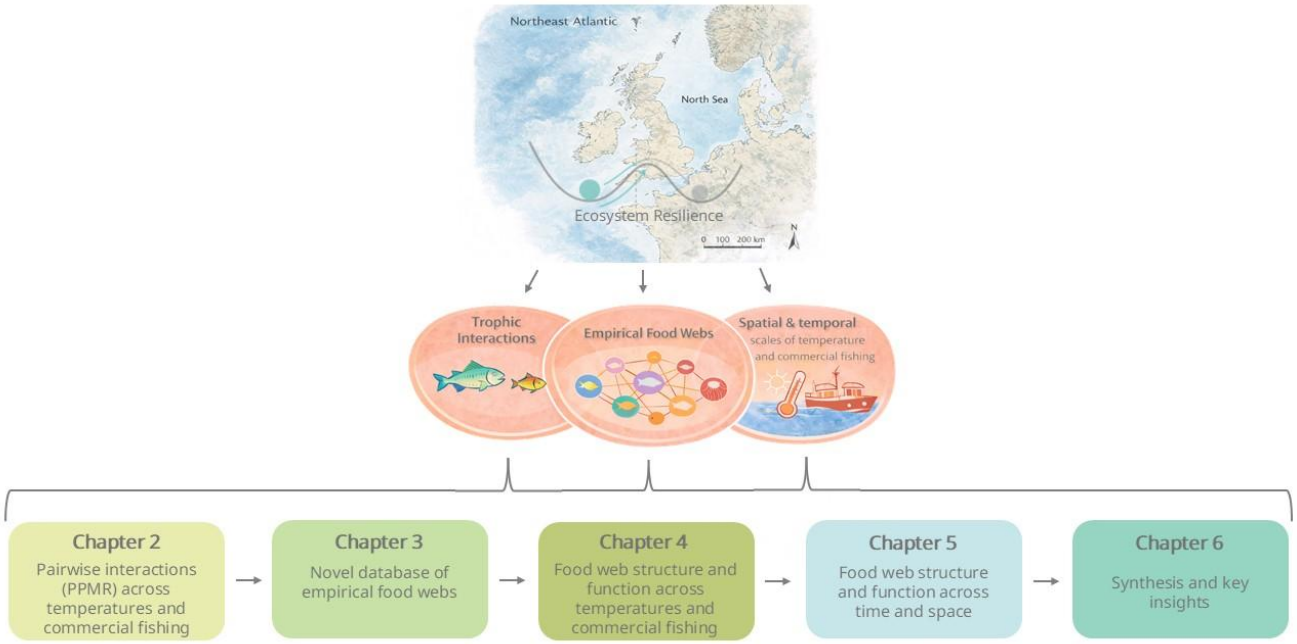

Figure 1.5: A conceptual diagram illustrating the thesis outline. Across the thesis chapters trophic interactions and empirical food webs were used to assess ecosystem resilience within the Northeast Atlantic on the backdrop of large-scale gradients in SST and commercial fishing. I acknowledge the use of AI in helping me construct this figure (OpenAI, 2025).

Each chapter builds progressively by addressing scale from different biological and environmental perspectives. Chapter two focuses on pairwise trophic interactions to examine how large-scale regional environmental drivers influence food web dynamics. Chapter three expands the level of biological organisation by constructing multi-species meta-webs, allowing assessment of emergent structural and functional properties beyond pairwise interactions in chapters four and five.

Spatial and temporal scales are explicitly addressed across chapters. Chapters two and four apply a space-for-time substitution approach to infer long-term change in trophic structure from spatial gradients, while chapter five adopts a more integrative perspective, examining environmental drivers of food web variation through time at localised spatial resolutions.

Collectively, the thesis progresses from simple binary interaction metrics to complex meta-food web analyses across local and regional contexts. By integrating variation

across space and time, this work provides novel insights into the structure and functioning of northern temperate marine food webs under environmental change.

The thesis expands on existing theoretical and applied methodologies within food web research such as resilience theory and ENA (Fath et al., 2007; Holling, 1973; Kay et al., 1989). We also make use of modelling techniques to analyse variation in food web structure and function as well as estimating energy flux through the food webs (Gauzens et al., 2019).

Chapter two focusses on pairwise trophic interactions, specifically PPMR, across SST and commercial fishing gradients of the Northeast Atlantic. By making use of an unprecedented stomach contents database this chapter provides insight into how the body mass scaling of predators and prey changes with increasing SST and if this is moderated by the interacting impacts of commercial fishing. The chapter highlights the dynamic nature of marine trophic interactions and the fundamental ecological principles, such as allometric scaling, that underpin them.

Chapter three outlines the design of a methodological framework that constructs weighted empirical food webs. Using this dynamic methodology, together with large environmental datasets, this chapter addresses the lack of large-scale, long-term food web data by constructing 4,728 empirical food webs across the North Sea at 50 km resolution annually from 1997–2015. This novel database of empirical food webs provides the foundation for assessing environmental change and benchmarking food web structure and function within marine ecosystems.

Chapter four draws on the empirical food web database together with ENA to examine how variation in food web structure and function is jointly shaped by spatial and temporal gradients in North Sea SST and commercial fishing pressure. By quantifying key food web properties this chapter provides broad insight into the structural and energetic constraints governing marine ecosystem resilience across the North Sea region.

Chapter five builds on the benchmarking of North Sea food web structure and function by shifting focus to temporal dynamics of key network-level metrics. By examining change through time, the chapter provides insight into long-term variation in ecosystem resilience. In addition, analyses of localised temporal trends generate insights for spatially explicit ecosystem-based management.

Chapter six summarises the key observations and insights across all data chapters. Providing a synthesised overview of the *environmental drivers of Northeast Atlantic food webs* and contextualising it into the wider context of research on marine ecology, food webs, and ecological resilience.

2 Commercial fishing amplifies impacts of increasing temperature on predator-prey interactions in marine ecosystems

Published in Nature Communications

2.1 Abstract

Predator-prey interactions determine food web structure, energy flux, and ecosystem stability. Increasing temperatures and commercial fishing both alter body size distributions that underpin predator-prey interactions, but empirical evidence of their individual and combined effects is limited. We studied how the predator to prey body mass ratio (PPMR) changed as a function of temperature and fishing effort in over 50,000 predator stomachs collected across the Northeast Atlantic over 35 years. PPMR increased with temperature, an effect that is exacerbated by greater fishing effort, driven by intraspecific decreases in prey body mass in heavily fished areas. To compensate for smaller prey (both within and across species) in warmer waters and areas of high fishing, predators targeted the largest prey available to them, but this is insufficient to alter the community-wide increase in PPMR. Higher PPMR is associated with weaker trophic interactions that dampen strong oscillatory dynamics but could also reduce energy transfer efficiency within ecosystems, both of which can affect ecosystem stability. These results could help underpin ecosystem-based management and sustainable fisheries by providing estimates of how future climate warming might interact with fishing to affect energy flux through marine food webs.

2.2 Introduction

Marine food webs are highly size structured, consisting of many small organisms and few large organisms (Reum et al., 2019a; Tucker and Rogers, 2014). Trophic interactions tend to involve larger consumers eating smaller resources due to gape limitation and the lower risk of injury or wasted energy (Heneghan et al., 2019; Petchey et al., 2008). The size-structuring of marine food webs has given rise to their historical conceptualisation as trophic pyramids where the vast majority of biomass and productivity is concentrated at lower trophic levels made up of smaller organisms (e.g., plankton, small fish) with decreasing biomass and productivity at higher trophic levels that consist of larger intermediate and top predators (e.g., large fish, marine mammals) (Lindeman, 1942a). Thus, body mass is considered a master trait due to the constraints it imposes on trophic relations and is a useful tool for gaining insight into and modelling trophic interactions (Ducrotoy et al., 2000; Reum et al., 2019a). For instance, the relative sizes of predators and their prey measured via predator-prey mass ratios (PPMR) are a key constraint on how energy flows through ecosystems (Schneider et al., 2012; Wang and Brose, 2018).

Predator-prey interactions act as highways of energy flow, creating avenues whereby the direct and indirect effects of species can propagate throughout entire ecosystems (Levin, 1998; O'Gorman et al., 2019). Trophic interactions are vulnerable to global environmental change (Kortsch et al., 2019; Pörtner et al., 2022), but the intricacies of the response are less well known (Frelat et al., 2022; Link and Watson, 2019; Nakazawa et al., 2011). Marine ecosystems exhibit large natural variability in temperature due to latitude, seasonality, and depth, but climate change is causing relatively rapid increases in sea surface temperatures (SST) beyond this natural variability (Flanagan et al., 2019; Pecuchet et al., 2020). For example, SST in the Northeast Atlantic has increased by as much as 0.5 °C in the last century (Gulev et al., 2023), which has been linked to changes in biodiversity and food web structure (Baum and Worm, 2009; Boyce et al., 2015; Kortsch et al., 2019; Lynam et al., 2017). Warmer waters are known to favour smaller species due to temperature dependencies of distribution, physiology, and productivity (Cheung et al., 2013; Daufresne et al., 2009). Decreasing body mass is recognised as a ubiquitous response to increasing temperature, which can be due to physiological drivers such as increased metabolic demands keeping species smaller and the age at maturity lower (Brown et al., 2004;

Sheridan and Bickford, 2011), or through changes in community composition that favour smaller species (Cheung et al., 2013; Coghlan et al., 2024).

Commercial fishing is a global anthropogenic pressure ubiquitous in marine ecosystems, particularly in the Northeast Atlantic where the biomass of many fish species has declined dramatically over the past century (Capuzzo et al., 2018; Howarth et al., 2018; Link and Watson, 2019). Similar to the observed impacts of increasing temperatures, fishing also results in an increase in the relative abundance of smaller species, as commercial fishing practices are well known to target larger fish due to their commercial value (Baum and Worm, 2009; Pauly and Palomares, 2005). By selecting for larger fish, commercial fisheries also impact the age-structure of fish communities (Berkeley et al., 2004; Hsieh et al., 2010). Commercial fishing has a heterogenous distribution in space and time and could therefore lead to complex effects on trophic interactions when combined with changes in temperature. For example, the combination of commercial fishing and increasing temperature has been shown to alter the recruitment, abundance, distribution, body condition, prey availability, and spawning success of marine organisms (Báez et al., 2021; Kirby et al., 2009; Lynam et al., 2017). Despite the growing body of evidence highlighting the impacts of both commercial fishing and temperature on the size structuring of marine food webs, few studies have investigated the potential for complex interacting effects of these drivers on PPMR. It is important to address this because current models that forecast fish stocks under climate change use a fixed PPMR (Perkins et al., 2022), not accounting for the physiological and compositional plasticity of species when exposed to environmental stressors.

To improve our predictive capacity, it is important to first understand the historical variation in PPMR across largescale gradients of temperature and commercial fishing pressure. PPMR is an excellent predictor of the identity and strength of predator-prey interactions and thus for quantifying ecosystem energy flux (Gauzens et al., 2019; Petchey et al., 2008). Physiological and compositional changes, such as decreasing body mass and fluctuating species richness and prey availability, driven by increasing temperature and targeted fishing practices could alter PPMR, which in turn has the potential to rewire whole food webs (Brose et al., 2006; Thompson et al., 2023) and disrupt ecosystem functioning and stability (Lynam et al., 2017; Schneider et al., 2012; Tucker and Rogers, 2014). Altered PPMR at the community-level is thus likely to be

underpinned by disproportionate changes in the relative size of predators and their prey driven either by physiological mechanisms, such as altered metabolism or growth leading to a systematic reduction in body size of many species in the community (i.e. intraspecific processes), or compositional mechanisms, such as systematic changes in the number of small or large species within the community (i.e. interspecific processes). Disentangling the relative importance of these mechanisms is key to understanding and forecasting the effects of temperature and commercial fishing on the size-structure of trophic interactions.

Here, we employ a space-for-time substitution to quantify PPMR across spatial gradients of temperature and fishing effort, which could help predict how energy fluxes in the Northeast Atlantic may respond to future global change. Given that PPMR has a negative relationship with body mass (Riede et al., 2011; Thompson et al., 2025; Tucker and Rogers, 2014), a reduction in the mean body size of the community at higher temperatures and/or commercial fishing pressure should lead to an increase in PPMR since smaller predators consume relatively smaller prey. We test the following hypotheses: (1) PPMR is positively related to temperature and fishing; (2) PPMR values are highest where temperature and fishing are both high; (3) increases in PPMR are related to both physiological processes (e.g. altered metabolic rate, which may underpin changes in body mass) and compositional processes (changes in taxonomic composition). The central goal of our study was to empirically quantify change in PPMR along a temperature gradient, and test how this was affected by commercial fishing effort. Given how critical PPMR is in determining energy flux through marine food webs and their stability (Otto et al., 2007; Schneider et al., 2012; Tucker and Rogers, 2014; Wang and Brose, 2018), this understanding could be beneficial for improving projections of fish stocks and optimising multi-species fisheries management under future scenarios of climate change and commercial fishing.

2.3 Methods

The study relies on historical stomach-content records publicly available from the Cefas Data Hub (Pinnegar et al., 2023), Copernicus (Donlon et al., 2012; Good et al., 2020; Stark et al., 2007a) and the JRC Data catalogue (Zanzi and Holmes, 2017). No new animal sampling was undertaken, and therefore ethical approval and informed consent were not required. Data were used in accordance with institutional and national regulations.

2.3.1 Study region

The fish stomach survey data for this study were collected from 1981-2016 in an area of the Northeast Atlantic spanning 35° of latitude and 70° of longitude, incorporating the Bay of Biscay, Celtic Sea, North Sea, Norwegian Sea, and Greenland Sea (Figure 1a). The geographic area has a temperate climate in the south and a polar climate to the north (Ducrotoy et al., 2000). The region provides ecosystem goods and services to large populations across many countries in western Europe, including valuable commercial fish stocks, with mature oil and gas fields, rapidly developing offshore wind infrastructure and important carbon sinks (Ducrotoy et al., 2000; Engelhard et al., 2014; Forsyth and Kay, 1980). The Northeast Atlantic thus experiences some of the strongest anthropogenic impacts globally (Halpern et al., 2008; Lynam et al., 2017; Rutterford et al., 2023). Extensive and often coordinated international research has also been conducted, providing extensive datasets and sampling records (ICES, 2026).

2.3.2 Stomach content dataset

Observations of PPMR were taken from the Dapstom stomach content database (Pinnegar et al., 2015). We utilised a total of 313,953 individual observations from 53,444 individual stomachs of 88 unique predator species. These observations were made on 1,862 different research hauls across the Northeast Atlantic (44° N to 79.5 ° N and 28.5 E° to 41.9° W) from 1981 to 2016. Predators were always identified to species level, with prey identified to the highest possible taxonomic level, i.e. species where possible, but often to family level. All prey species were considered (i.e. both fish and invertebrates). Fullness of stomach or level of digestibility were not considered and so the estimates of body mass may be subject to some associated uncertainty. Additional variables taken from the database included the total number of prey species per predator stomach i.e. prey abundance, the geographical coordinates, and the year and month each sample was collected. These variables were included in the study as any change in PPMR can be driven by multiple and not mutually exclusive processes, e.g. changes in predator body size, prey body size, predator behaviour to select different sized prey, or the behaviour of prey to avoid predation based on their body size.

Biomass-weighted PPMR was calculated for each individual predator using the equation 2.1 (Reum et al., 2019b):

$$PPMR = \frac{M_i}{\frac{1}{n}\sum_{j=1}^{n} Mj}$$

(equation 2.1)

where M_i is the body mass of predator species *i*, M_j is the body mass of prey taxon *j*, and *n* is the total abundance of prey in the stomach. Wet weight (g) was defined as body mass.

2.3.3 Sea-surface temperature dataset

Daily sea surface temperature (SST) data (°C) from both satellite and in situ observations were extracted from the Copernicus open access data repository (Donlon et al., 2012; Good et al., 2020; Stark et al., 2007a). Throughout the rest of the study, SST is simply referred to as temperature. The spatial resolution of the temperature data was 0.05° longitude x 0.05° latitude and covered every month from 1981 to 2016. The average temperature (°C) was calculated per month and matched to PPMR data sampled in the following month to account for any lag effects (i.e. if a predator's stomach contents were sampled in May 1992, then the corresponding temperature would be the monthly average of April 1992). Other environmental variables used for modelling purposes included salinity, chlorophyll (ug/l), and the average water column depth (m), which were taken from the ICES open-source data portal (ICES Data Portal, Dataset on Ocean HydroChemistry, Extracted June 12, 2023. ICES, Copenhagen). These ecologically relevant variables were included as they could cause background variation in PPMR. The mean of each environmental variable was calculated for each month of every year (1981–2016) and matched to the following month of PPMR data. The longitude and latitude coordinates were to four decimal points. Due to spatiotemporal limitations in the environmental data layers available, 43% of PPMR observations did not have corresponding salinity or chlorophyll data.

2.3.4 Commercial fishing effort dataset

We make use of The Scientific, Technical and Economic Committee for Fisheries (STECF) trawling effort dataset, available from the JRC Data catalogue, because of

its extensive coverage in space and time which corresponded with our PPMR observations (STECF, 2017). The STECF data provides annual fishing hours per ICES rectangle (0.5° latitude by 1° longitude) across areas of the Northeast Atlantic. We downloaded the data for the region 49.25° N to 63.25° N and 7.5° W to 12.5° E, covering the period 2002 to 2022. The data is a compilation of member state submissions in response to the Data Collection Framework (DCF) Fishing Effort Regimes Data Call in 2017 (Zanzi and Holmes, 2017). The STECF dataset used in this study included data from Belgium, Denmark, Netherlands, United Kingdom, France, Germany, and Sweden. Fishing effort was matched to the PPMR observations based on the year and ICES rectangle in which the sampling took place. This resulted in 131,767 PPMR observations in the Northeast Atlantic from 2002-2016 with a corresponding measure of fishing effort in hours per year (Figure 2.1c). For visualisation purposes, the fishing effort data was divided into three bins each containing an equal number of observations, and the median of each bin was calculated for fitting regression lines to plots. An overview of the data construction can be found in Figure S2.2.

2.3.5 Statistical analysis

All statistical analyses were conducted using R v4.2.2 (R Core Team, 2024). A mixed effects model was used to test the relationship between temperature and either PPMR, predator body mass (g), prey body mass (g), prey abundance per predator stomach (prey count), or prey species richness per predator stomach. The response variables were $\log_{10}$ transformed to meet the assumptions of normality and homogeneity (Figure S2.3). The model included the fixed effect of mean temperature (°C, continuous variable) and random effects for chlorophyll (ug/l, continuous), salinity (‰, continuous), depth (m, continuous), number of years since the start of the study period (continuous), ICES rectangle (categorical), season (categorical), predator species identity (categorical), and predator stomach identity (categorical).

The same five response variables (PPMR, predator body mass, prey body mass, prey count, and prey species richness) were then separately included in models containing main and interactive effects of mean temperature (°C, continuous variable) and mean commercial fishing effort (hours per year, continuous variable) for the subset of data that included information on fishing effort. The response variables were again $\log_{10}$ transformed to meet the assumptions of normality and homogeneity (Figure S2.4). The

random effect structure remained the same as above. For all models, linear and polynomial versions were compared using Akaike information criterion (AIC; Akaike, 1974)., with the linear models found to be the best fit in seven out of ten comparisons (Table S2.3).

Lastly, nMDS ordination plots were constructed for both the full temperature dataset and the fishing effort data subset. Prey were aggregated into families for consistency and to help with model convergence, and plotted against mean temperature, prey body mass, and fishing effort vectors.

2.4 Results

2.4.1 Effects of increasing temperature and fishing effort on PPMR

Across the Northeast Atlantic, there was a significant increase in PPMR with increasing temperature (t_{64764} = 23.29; p < 0.001, R^2 = 0.45; Figure 2.1a, b). This suggests that predators and their prey diverged in size at higher temperature (Figure 2.1b). PPMR was predicted to increase by 30% across the temperature gradient, or 1.8 % per 1 °C. Latitude was a major contributor to the effect of temperature on PPMR, with less contribution of season and water column depth (Figure S2.1). The increase in PPMR was amplified in areas with more commerical fishing, with a significant interactive effect of temperature and fishing effort on PPMR (t_{62436} = 2.99, p = 0.003, R^2 = 0.48, Figure 2.1c, d). PPMR increased at both high and low fishing effort, but the increase in PPMR with increasing temperature was more pronounced in areas that were more heavily fished (Figure 2.1d). In areas of low commercial fishing, PPMR was predicted to increase by 22 % across the temperature gradient, or 1.3 % per 1 °C, whereas in areas of high commercial fishing, PPMR was predicted to increase by 82 % across the temperature gradient, or 4.8 % per 1 °C.

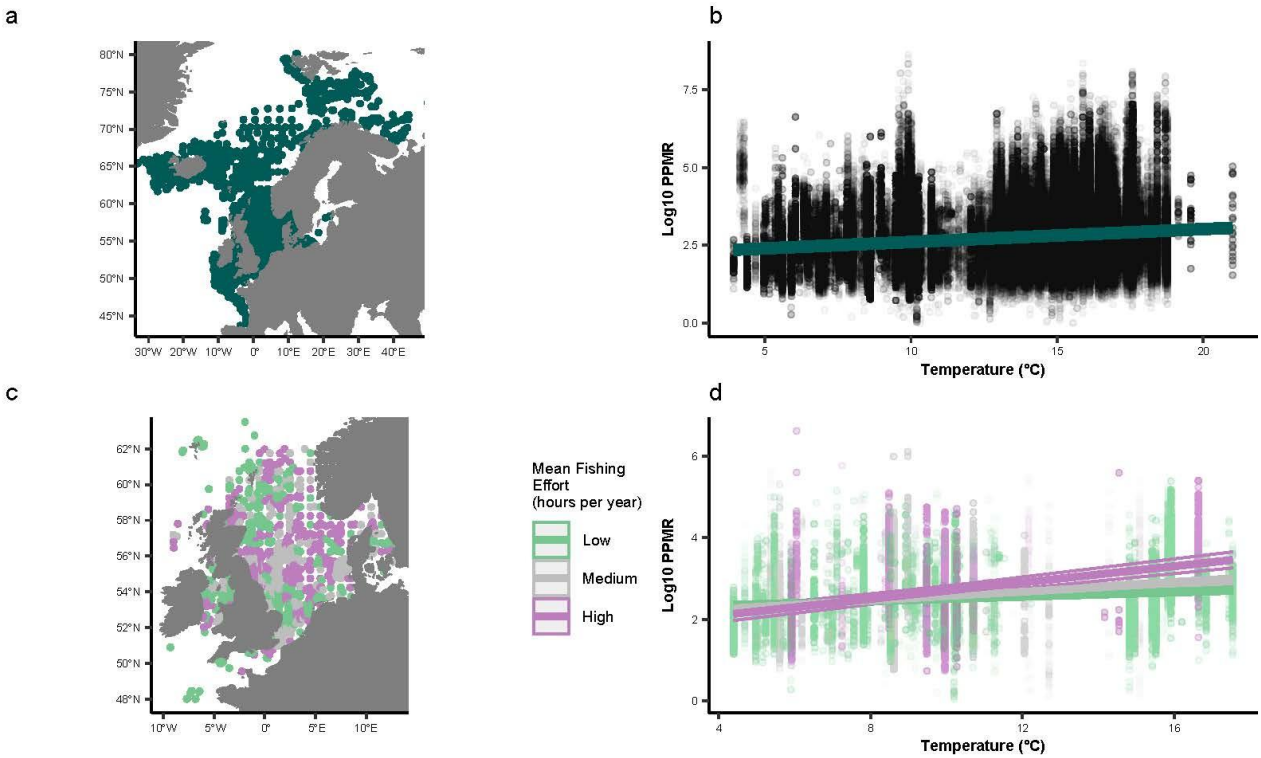

974

975 Figure 2.1: They key findings of temperature and commercial fishing driven changes
976 in PPMR across the Northeast Atlantic. **a,** A map of the Northeast Atlantic study region
977 illustrating all sites (points) that were sampled over the period 1981 to 2016. **b,** the
978 relationship between temperature (°C) and $\log_{10}$ predator prey body mass ratio
979 (PPMR) with the fitted linear mixed effects model ($y = 2.2 + 0.041x$). Temperature
980 refers to mean SST (°C). **c,** A map illustrating the sampled sites (points) that had
981 corresponding commercial fishing data available. **d,** The interactive effect of
982 commercial fishing on the relationship between temperature and PPMR. Commercial
983 fishing effort was analysed as a continuous variable, but for the purposes of
984 visualisation, low (45–566 hours per year), medium (576–878 hours per year), and
985 high (903-3,479 hours per year) levels of fishing effort are indicated in the figure. **d:**
986 low fishing effort: $y = 2.2 + 0.03x$; medium fishing effort: $y = 2 + 0.053x$ and high
987 fishing effort: $y = 1.7 + 0.1x$. The maps were created using the maps R package
988 (Becker et al., 2023).

2.4.2 Effects of only temperature on body mass, prey count, and prey richness

There was no significant effect of temperature on the mean body mass of the predators sampled (t_{6660} = 1.93, p = 0.053, Figure 2.2a), i.e. using the larger dataset without fishing effort data included. Mean predator body mass was also relatively consistent at the species level across the entire temperature gradient with no significant effect of temperature on 82% of predator species, accounting for 99% of predator biomass (Table 2.1, Table S2.1). In contrast, there was a significant decrease in the mean body mass of prey individuals with increasing temperature (t_{64764} = -7.58, p < 0.001, R^2 = 0.83, Figure 2.2b), indicating that reductions in prey body mass were a primary driver of the increase in PPMR with increasing temperature. Note that we refer to “prey” here as any organism found in the diet of the fish predators, even if those species could be predators themselves. At the species level, there was a decrease in mean individual prey body mass with increasing temperature for 58% of prey species, accounting for 77 % of prey biomass (Table 2.1, Table S2.2), indicating that intraspecific responses to increasing temperature played a major role in determining the observed changes in PPMR.

Table 2.1: The percentage of each predator and prey species, their respective biomasses, and average individual body size response to increasing temperature using the larger dataset without fishing effort data included.

	Predator species	Predator biomass	Prey species	Prey biomass
No change	81.6	99.4	32.3	23.0
Increase	5.3	0.1	14.0	0.2
Decrease	13.2	0.5	58.2	76.8

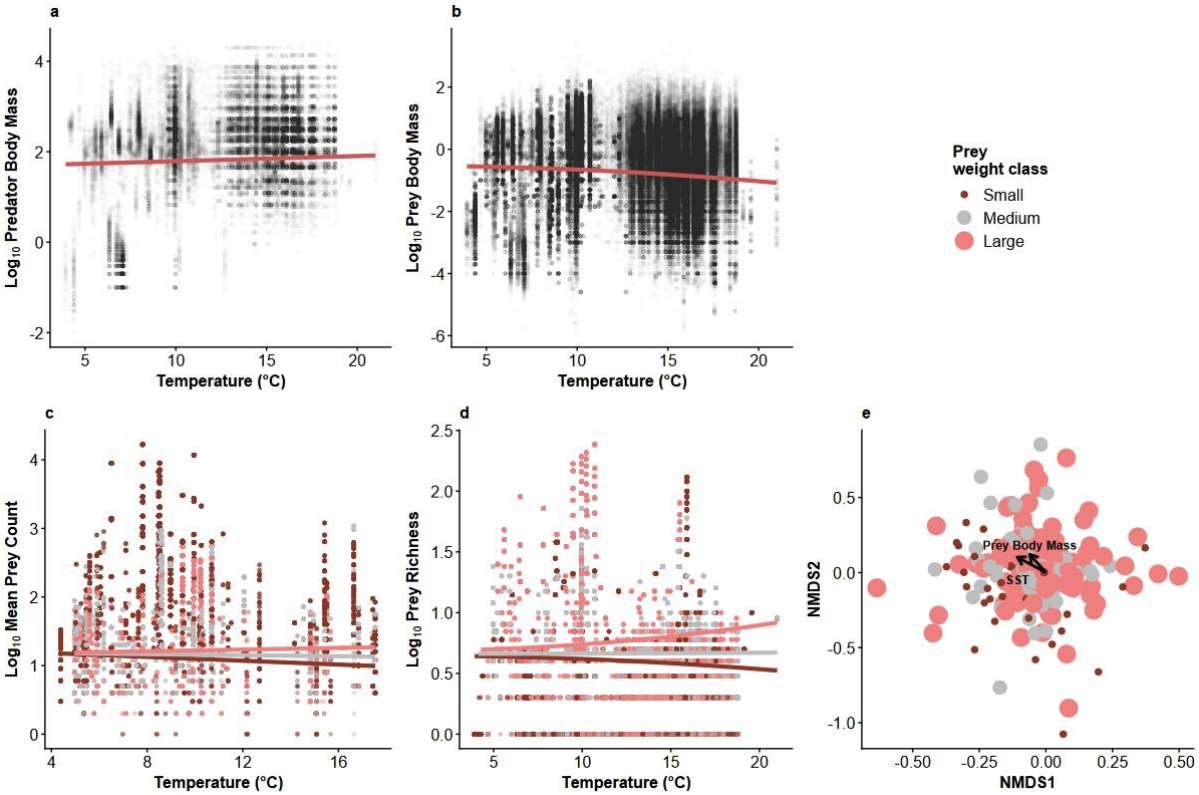

Figure 2.2: The effect of temperature (°C) on underlying predator and prey variables including **a,** $\log_{10}$ predator body mass (g) ($y = 2.3 + 0.0029x$), **b,** $\log_{10}$ prey body mass (g) ($y = -0.53 - 4.2 \times 10^{-16} - 0.0012x$), **c,** $\log_{10}$ prey count (number of individuals per stomach) and **d**, $\log_{10}$ species richness (number of species per stomach) in the Northeast Atlantic between 1981 and 2016. The results of **c,** $\log_{10}$ prey count and **d,** $\log_{10}$ species richness were further categorised into prey weight classes by small (0-0.072 g); medium (0.072 – 1.25 g) and large (1.25 – 2,137 g) prey body mass (**c:** small species: $y = 1.2 - 0.009x$; large species: $y = 1.1 + 0.021x$; **d:** small species: $y = 0.65 + 2.6 \times 10^{-17}x - 0.00028x^2$; large species: $y = 0.69 + 4 \times 10^{-17} + 0.00053x^2$). **e,** nMDS illustrating the weak effect of temperature on the size of prey taxa in the community, with short temperature and body mass vectors that are orthogonal to one another. The colour and size of the points represent the size classes of the prey taxa.

The prey count (t_{6660}= -4.91, p < 0.001, R^2 = 0.64, Figure 2.2c) and prey species richness (t_{6660} = -6.42, p < 0.001, R^2 = 0.82, Figure 2.2d) within predator stomachs significantly increased with increasing temperature. There was a significant interaction between prey size class and temperature for both prey count (t_{6660} = 13.07, p = < 0.001, R^2 = 0.64, Figure 2.2c) and prey species richness (t_{6660} = 27.43, p < 0.001, R^2 = 0.82, Figure 2.2d). Here, predators increasingly targeted larger prey from a bigger

pool of species as temperature increased. However, the nMDS analysis did not indicate any strong relationship between the size of the prey taxa consumed and mean temperature (Figure 2.2e), indicating no clear evidence for compositional changes contributing to the decrease in mean prey body mass with increasing temperature.

2.4.3 Interactive effects of temperature and fishing effort on body mass, prey count, and prey richness

The consistency of sampled predator body mass across the temperature gradient was maintained despite additional impacts of commercial fishing, with no significant interactive effect of temperature and fishing effort (t_{6085} = -0.71, p = 0.478, Figure 2.3a). There was a significant interactive effect of temperature and commercial fishing on individual prey body mass (t_{62436} = -9.92, p < 0.001, R^2 = 0.83; Figure 2.3b), however, with an increase in prey body mass at low fishing effort and a decline in prey body mass at high fishing effort (Figure 2.3b). Fishing effort also significantly altered the positive relationship between prey count and temperature (t_{6085} = 15.0, p < 0.001, R^2 = 0.79, Figure 2.3c), with a reduction in the number of prey of all sizes consumed with increasing temperature at low fishing effort, but an increase in the number of prey of all sizes consumed with increasing temperature at high fishing effort. There was a significant interactive effect of temperature and commercial fishing on prey species richness (t_{6085}= 5.19, p < 0.001, R^2 = 0.84, Figure 2.3d). Here, there was a greater increase in prey species richness with temperature as prey size class increased and as fishing effort increased. The nMDS plot showed a tendency for larger prey taxa to be found in areas of increased commercial fishing although mean fishing effort only accounted for 4 % of the variation in body size (R^2 = 0.04, Figure 2.3e). Mean prey body mass was also not strongly associated with mean temperature or fishing effort.

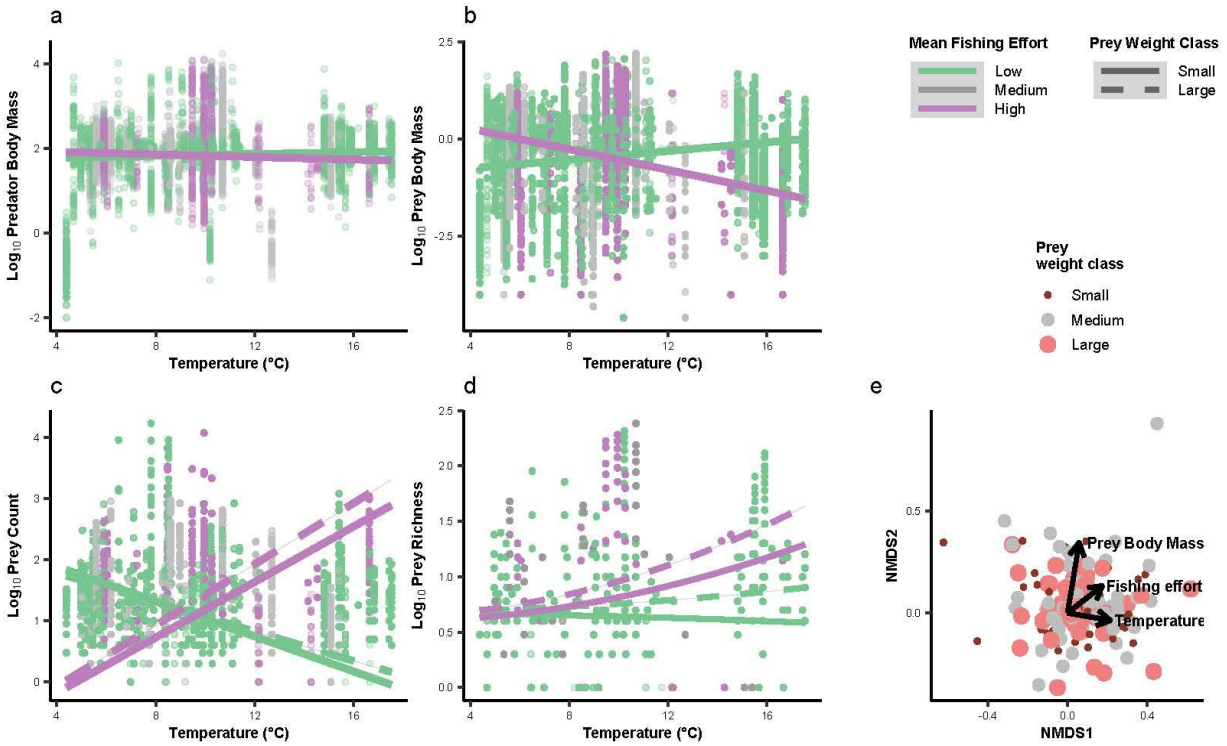

Figure 2.3: The interactive effect of temperature (°C) and commercial fishing on underlying predator and prey variables including **a,** $\log_{10}$ predator body mass (g), **b,** $\log_{10}$ prey body mass (g), **c,** $\log_{10}$ prey count (number of individuals per stomach) and **d**, $\log_{10}$ species richness (number of species per stomach) in the Northeast Atlantic between 1981 and 2016. Commercial fishing effort was analysed as a continuous variable, but for the purposes of visualisation, low (45 – 566 hours per year), medium (576 – 878 hours per year), and high (903 – 3,479 hours per year) levels of fishing effort are indicated in the figure. Trend lines based on the predicted values of the mixed effects model were plotted for low (**a**: $y = 1.6 + 0.026x$; **b:** $y = -1.1 + 0.0039x$) and high commercial fishing (**a**: $y = 1.8 + 0.0081x$; b: $y = 1.9 + 0.003x$). The results of **c,** $\log_{10}$ prey count and **d,** $\log_{10}$ species richness were further categorised into prey weight classes by small (0-0.072 g); medium (0.072 – 1.25 g) and large (1.25 – 2,137 g) prey body mass. (**c:** low fishing effort and small species: $y = 2.5 - 0.14x$; high fishing effort and small species: $y = -1.1 + 0.23x$; low fishing effort and large species: $y = 2.3 - 0.12x$; high fishing effort and large species: $y = -1.1 + 0.25x$; **d:** low fishing effort and small species: $y = 0.67 - 4.3 \times 10^{-17}x - 0.00027x^2$; high fishing effort and small species: $y = 0.59 - 3.5 \times 10^{-17}x + 0.0023x^2$; low fishing effort and large species: $y = 0.69 - 2.3 \times 10^{-17}x + 7 \times 10^{-4}x^2$;

high fishing effort and large species: $y = 0.63 - 5.8 \times 10^{-17}x + 0.0033x^2$). **e,** nMDS illustrating the weak effects of temperature and fishing effort on the size of prey taxa, with temperature and body mass vectors orthogonal to one another and a weak correlation between body mass and commercial fishing effort (R^2 = 0.04). The colour and size of the points represent the size classes of the prey taxa.

2.5 Discussion

We provide empirical evidence that commercial fishing amplifies the increase in PPMR with increasing temperature in the Northeast Atlantic, as sampled predators in warmer waters with higher fishing effort typically consumed the smallest prey relative to their body size. This suggests that increased water temperature within heavily fished ecosystems of the Northeast Atlantic could cause predator and prey body mass to diverge from one another. A larger community-level PPMR typically results in a less efficient flow of energy through food webs (Barnes et al., 2010), which could reduce the persistence of apex predators and overall system stability (Jennings and Warr, 2003). Quantifying the effects of multiple stressors on predator-prey interactions across large spatiotemporal gradients is thus crucial to gain insight into how ecosystems could respond to global change and improve ecosystem-based management. Our space-for-time substitution provides insights into past variation and potential adaptation of trophic interactions to environmental drivers such as higher temperatures, given the long timescales over which ecosystems have been exposed to these conditions, i.e. organisms may be thermally adapted after many generations at higher temperatures, which is not possible to study in short-term experiments involving acute temperature exposures.

The observed reduction in the mean body mass of the prey community at higher temperatures was underpinned by overall intraspecific reductions in body size. This indicates a physiological response to increasing temperature, which can occur through changes in metabolism, ontogeny, and thermoregulation, all of which can contribute to the evolution and persistence of smaller sized species in warmer waters. Metabolic rates are known to rise with temperature and as a result increase the energetic requirements of organisms (Brown et al., 2004). This is exacerbated by reduced oxygen in warmer waters further constraining energetic demands which can be more easily maintained by smaller individuals (Baudron et al., 2014; Cheung et al., 2013; Forster and Hirst, 2012; Pauly, 2019). The increase in metabolism causes

species to have faster growth rates and shorter generation times, which can also contribute to decreased body mass if species mature and reproduce quicker in warmer areas (Kuparinen et al., 2011; Neuheimer and Grønkjær, 2012) (though note there are exceptions to this general rule (Wootton et al., 2022)). Furthermore, when close to the upper limits of their thermal ranges, smaller individuals thermoregulate more efficiently than larger individuals as they are better able to lose excess heat due to their large surface area-to-volume ratio (Goldenberg et al., 2022). Our results show that individual body mass within the majority of sampled prey species decreased with increasing temperature. Other studies have also found temperature-driven decreases in the size of individual Northeast Atlantic species such as plaice, *Pleuronectes platessa* (Baudron et al., 2014) and Atlantic cod, *Gadus morhua* (Tirsgaard et al., 2015), due to the temperature-dependent physiology of marine species.

Changes in PPMR could also be a consequence of altered community composition (Cheung et al., 2013; Fernandes et al., 2013; Harley et al., 2006; Perry et al., 2005; Reum et al., 2019b; Thompson et al., 2025), however, no clear evidence of size-based compositional changes behind the increase in PPMR were observed in our study. In other words, while the taxonomic composition of prey species may have changed from colder to warmer waters, the number of small and large taxa was still similar. Despite the similar size composition of prey species across the temperature gradient, there was a community-wide intraspecific decrease in prey body mass at higher temperatures and fishing effort, i.e. driven by reductions in size within rather than across species. The sampled predators responded to the intraspecific decrease in prey body mass by selecting the largest individuals available to them and a greater diversity of large prey, which could be a result of optimal foraging in order to maintain energetic requirements (Ortiz et al., 2023). Nevertheless, the overall reduction in average size of the prey community meant that PPMR increased with both temperature and fishing effort. Changes in the abundance and selectivity of predators could also reflect changes in the environmental abundance and distribution of prey. To test this would require information on the quantity of prey in the environment as well as in the stomachs of predators, but these data are not yet routinely collected at the scale needed for this study.

Commercial fishing is known to be a strong driver behind the size-structure within marine ecosystems, sometimes even more so than increasing temperature (Agnetta et al., 2024; Blanchard et al., 2005). Here we found that commercial fishing amplified the increase in PPMR across the temperature gradient of the Northeast Atlantic. In particular, commercial fishing magnified the reduction in the body mass of prey species with increasing temperature, which underpinned the increase in PPMR in warmer waters with more fishing. The long-term targeting of larger individuals by fisheries reduces the body mass of commercially valuable species (Baum and Worm, 2009; Genner et al., 2010; Pauly and Palomares, 2005; Preciado et al., 2019; Wood et al., 2024). For example, Atlantic mackerel (*Scomber scombrus*), haddock (*Melanogrammus aeglefinus*) and European plaice (*Pleuronectes platessa*) are all commercially important species within the prey community that exhibited a decline in body mass. This is supported by previous research within the Northeast Atlantic showing that the average body mass of mature mackerel declined by as much as 175 g per year from 1983 to 2013 (Olafsdottir et al., 2016), a mature haddock by as much as 9 % from 1970 to 2008 (Shackell et al., 2010), and the maximum body mass of plaice by 28 % throughout the 20th century (Mollet et al., 2016), with direct links to the intensification of commercial fishing. Smaller species have become increasingly abundant in fisheries landings due to the collapse of many larger commercial species (Jennings et al., 2002; Liang and Pauly, 2017a), suggesting that the impacts of fisheries are not just found at higher trophic levels. Large-scale ecosystem degradation is occurring simultaneously through destructive fishing methods, such as trawling, that reduce habitat diversity and food availability, which could impact trophic interactions throughout the size-spectrum of a food web (Halpern et al., 2008; Liang and Pauly, 2017b).

The sampled Northeast Atlantic predators in this study were seemingly more resilient to increasing temperature, with no change in body mass across the temperature gradient or in response to fishing. The consistency in predator body mass could be due to sampling bias of the survey trawls targeting larger, commercially important fish species, i.e. smaller species not captured by the trawls may also be predators in the wider food web, and so the lack of temperature effect on predator body size is largely constrained to organisms in the 1 to 10,000 g size range. The trawls had no

control over the prey composition included, i.e. since the prey in the stomach contents were selectively sampled through feeding by the predators.

Our original hypothesis that PPMR would increase with temperature in the Northeast Atlantic was underpinned by the expectation of widespread reductions in body mass in warmer waters (i.e. for both predators and prey). Given the observed negative relationship between PPMR and body size (Riede et al., 2011; Thompson et al., 2025; Tucker and Rogers, 2014), a community with a smaller average body mass should thus have a larger PPMR. This hypothesis was only substantiated by a decrease in prey body mass, not also predator body mass as anticipated. Thus, the overall increase in PPMR with temperature was driven by a different mechanism to our expectation, i.e. contrasting effects of temperature on large and small organisms leading to a divergence in their size ratio. Differential effects of temperature on the body size of trophic groups have recently been described in coastal reef ecosystems, with a similar reduction in the size of smaller fish with increasing temperature and no change in larger piscivores (Coghlan et al., 2024). This highlights the importance of further research to explore the underlying mechanisms to improve our understanding of how warming may affect different food web compartments and thus overall functioning and stability.

Increasing PPMR, as seen here across the temperature and fishing effort gradients of the Northeast Atlantic, is associated with a greater prevalence of weak interactions (Brose et al., 2006), which can help to buffer against the destabilising, oscillatory dynamics of strong trophic interactions (McCann et al., 1998). Weak interactions are often associated with more generalist predator diets that hold more trophic redundancy, i.e. more pathways for energy to flow through the food web (Bondavalli and Bodini, 2014; McCann et al., 1998). Flexible foraging or generalised predation can also prevent the over-dominance or over-predation of particular prey species under different environmental conditions, helping to increase ecosystem stability (Van Baalen et al., 2001). Case studies have shown that the impacts of species loss are more unpredictable in food webs that have lower redundancy (Albouy et al., 2014). On the other hand, weak per capita interactions can also result in species needing to consume more or larger prey to meet their energetic requirements (Ortiz et al., 2023), leading to stronger population-level interaction strengths. This was observed in the Northeast Atlantic as sampled predators were found to be targeting

more individuals and species of larger prey in warmer waters. This highlights how temperature can interact with factors like PPMR and the associated indirect changes to trophic interaction strengths to alter entire community size spectra (Coghlan et al., 2024). Thus, the consequences of increasing PPMR for the persistence of species and overall energy flux through food webs is still uncertain, and is an area requiring urgent attention in future studies.

PPMR is a valuable metric to monitor ecosystem changes as it is a good predictor of trophic interactions, governs how energy flows through ecosystems (Hunsicker et al., 2011; Reum et al., 2019a; Tucker and Rogers, 2014), can estimate community size-spectrum (Coghlan et al., 2022) and as a result, is a fundamental input into size-based models of ecosystem dynamics such as the Allometric Diet Breadth Model (Petchey et al., 2008; Reum et al., 2019a). In such models, PPMR is normally treated as a constant parameter (Perkins et al., 2022) without accounting for systematic variability under different environmental conditions. Here we show that PPMR should instead be considered as a dynamic parameter to account for the heterogeneity of body mass across environmental gradients. Future research could analyse how changes in PPMR propagate through entire food webs, e.g., via dynamical models, to further understand how energy stocks and fluxes are affected by such change.

Our study suggests that impacts of climate change, such as increasing temperature, will be more pronounced in areas favoured by commercial fisheries, providing evidence to promote ecosystem-based management especially in regions experiencing notable increases in temperature and high commercial fishing to better maintain predator-prey interactions. This illustrates the complex nature of changing environmental gradients on marine food webs and highlights the importance of ecosystem-based management that considers the individual and synergistic impacts of multiple environmental change drivers. Thus, climate change policies and fisheries management should be integrated in order to make meaningful impacts when managing the trophic structure of marine ecosystems.

2.6 Data Availability

The data used within this study can be accessed through the University of Essex research open access data repository (A.L. Shurety, M.S.A. Thompson, E. Couce, T.

Cameron and E.J. O'Gorman, Commercial fishing amplifies impacts of increasing temperature on predator-prey interactions in marine ecosystems. University of Essex Research Data Repository. 10.5526/ERDR-00000220. 2025). This study also made use of the DAPSTOM database (Pinnegar, 2014) which can be found on the Cefas data hub : https://www.cefas.co.uk/data-and-publications/fish-stomach-records/. As well as sea surface temperature records (Donlon et al., 2012; Good et al., 2020; Stark et al., 2007a) and fishing effort data (Zanzi and Holmes, 2017).

2.7 Code Availability

The code used within this study is available via GitHub:
https://github.com/amyshurety/PPMR_Atlantic_Publication/tree/main

2.8 Supplementary Information

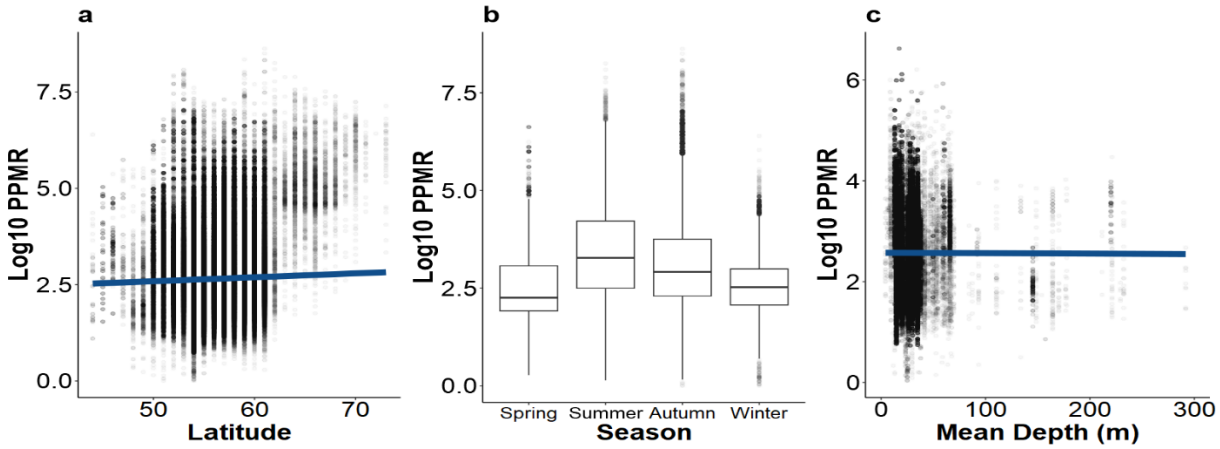

Figure S2.1: Effects of latitude, season, and mean depth on the predator-prey body mass ratio (PPMR). (a) There was a significant increase in $\log_{10}$ PPMR with increasing latitude ($t_{64886} = 27.83$, $p < 0.001$, $R^2 = 0.73$). (b) There was no significant effect of season on $\log_{10}$ PPMR ($F_3 = 1.88$, $p = 0.171$). (c) There was no significant effect of depth on log10 PPMR ($t_{64886} = 0.92$, $p = 0.361$).

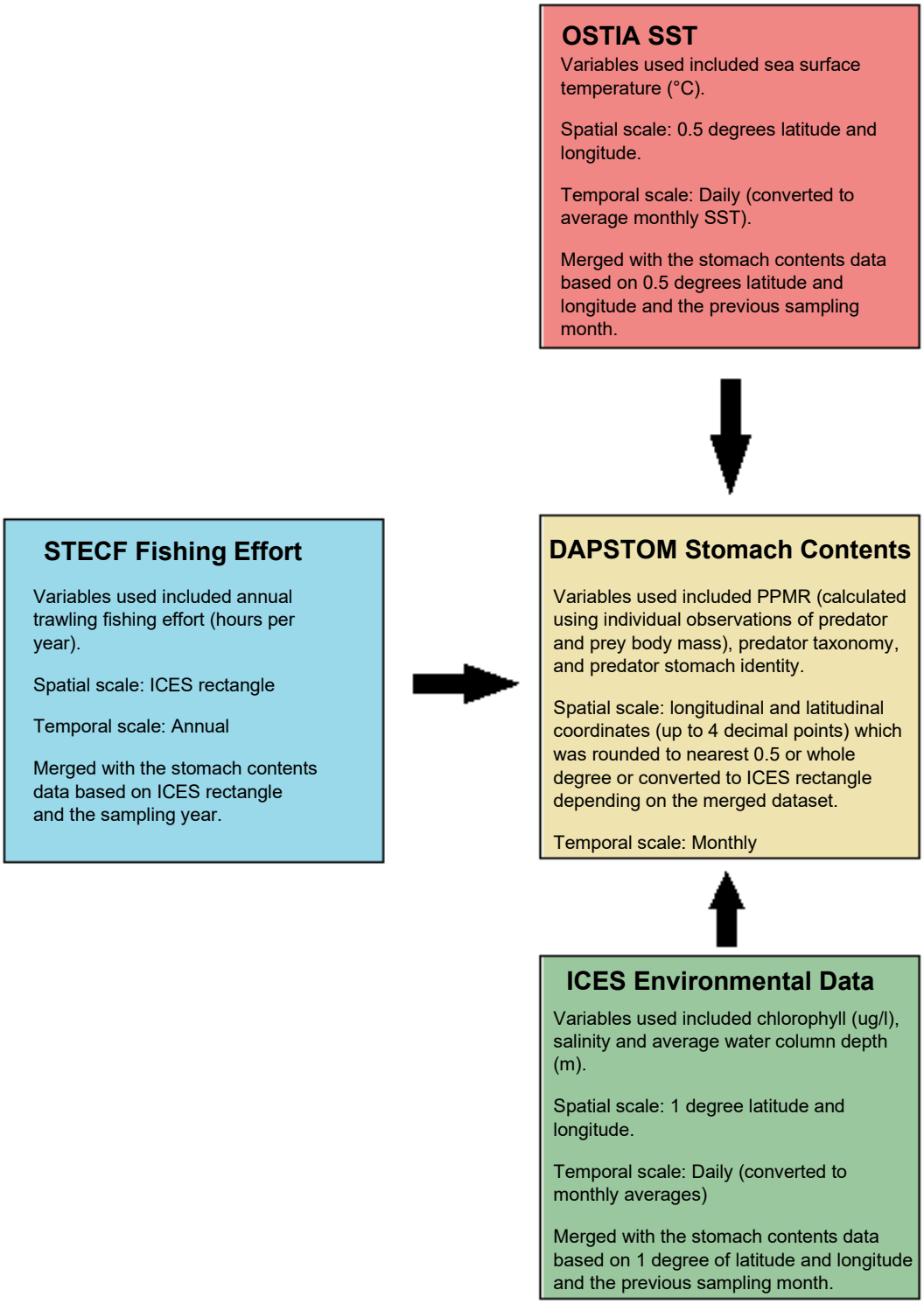

Figure S2.2: A flow diagram illustrating the steps taken to join the four different datasets used within this study.

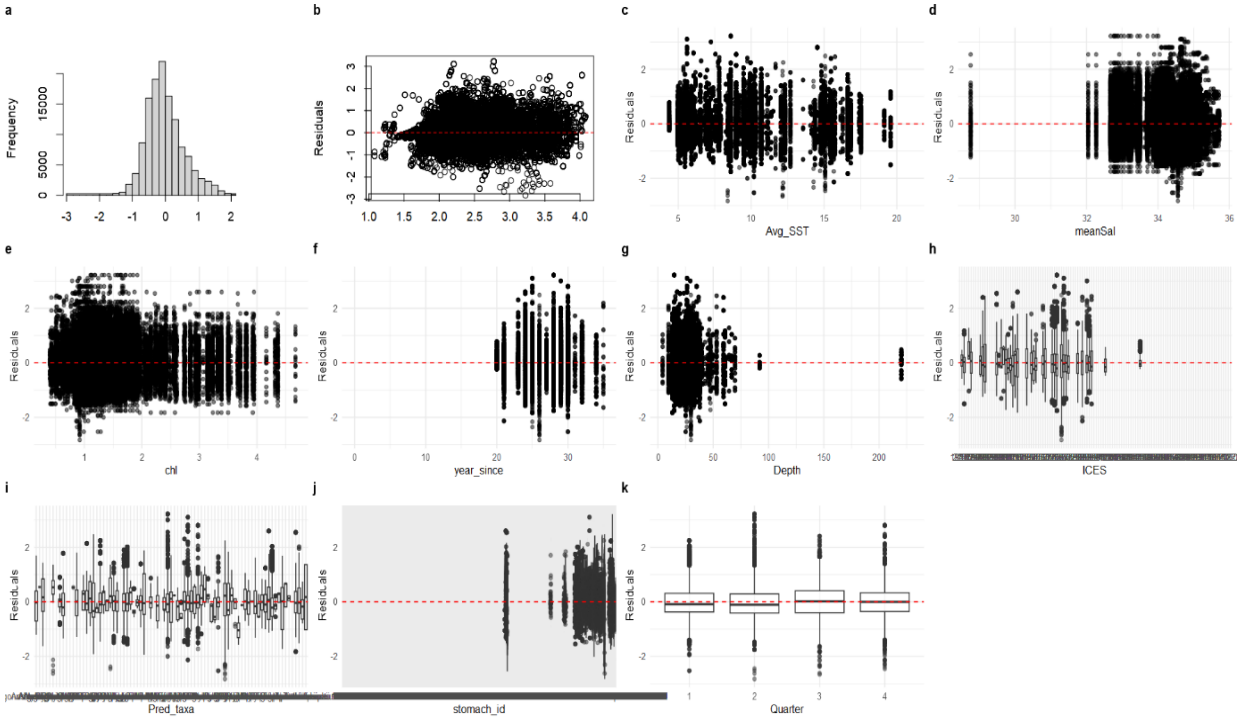

Figure S2.3: Diagnostic plots of the model for PPMR vs temperature (Figure 1B, n = 64765). (a) Histogram of the residuals, (b) scatterplot of fitted vs residual values, and (c-k) scatterplots of residuals vs each covariate in the model.

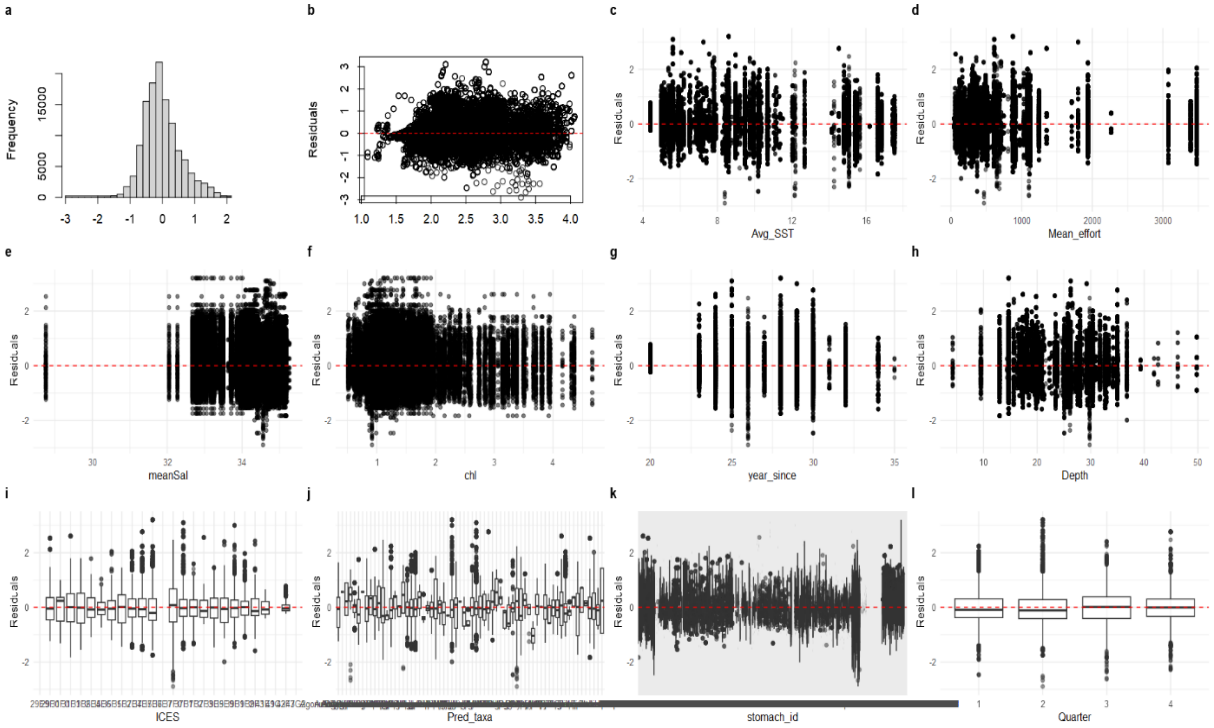

Figure S2.4: Diagnostic plots of the model for PPMR vs the interaction of temperature and fishing effort (Figure 1C, n = 62437). (a) Histogram of the residuals, (b) Scatterplot of fitted vs residual values, and (c-l) scatterplots of residuals vs each covariate in the model.

Table S2.1: The results of a linear regression of body mass (g) vs temperature (°C) for each individual predator species included in the study with their corresponding percentage of total biomass across all species (%).

Species	Df	slope	t-value	p-value	% biomass
Agonus cataphractus	954	-0.0122	0.0136	-0.8986	0.0352
Alloteuthis subulata	386	0.0752	0.05	1.5031	0.0131
Amblyraja radiata	3633	0.0028	0.0072	0.3859	0.7332
Ammodytes	14	0.1029	0.2295	0.4486	0.0006
Anarhichas lupus	70	-0.0243	0.0472	-0.5147	0.0327
Anguilla anguilla	30	0.0466	0.0523	0.8925	0.0033
Argentina sphyraena	306	0.0237	0.0705	0.3359	0.0204
Argentinidae	1045	-0.1683	0.0605	-2.7792	0.0708
Arnoglossus laterna	401	0.0217	0.0104	2.079	0.0193
Brosme brosme	10	0.0779	0.1488	0.5235	0.0029
Callionymus lyra	2156	-0.0192	0.0034	-5.7288	0.1416
Capros aper	304	0.0725	0.0758	0.9573	0.0187
Cepola macrophthalma	288	-0.4492	0.1282	-3.5034	0.0215
Chelidonichthys cuculus	3340	0.0253	0.0044	5.7514	0.4646
Chelidonichthys lucerna	968	0.0149	0.0299	0.4994	0.1976
Chelon labrosus	66	-0.0711	0.0785	-0.9061	0.0042
Ciliata mustela	114	-0.0168	0.024	-0.6997	0.0083
Clupea harengus	35106	-0.1035	0.0026	-39.7035	2.7795
Conger conger	334	-0.0734	0.0392	-1.8707	0.1748
Dicentrarchus labrax	127	0.0254	0.03	0.8449	0.0097
Echiichthys vipera	12169	-0.0017	0.0015	-1.0936	0.7304
Enchelyopus cimbrius	248	-0.0206	0.0342	-0.6014	0.0226
Engraulis encrasicolus	26	0.1504	0.1619	0.929	0.0019
Eutrigla gurnardus	39687	0.0114	0.0008	14.1139	4.4904
Gadiculus argenteus	13	-1.0581	3.0759	-0.344	0.0004
Gadus morhua	125677	0.2384	0.0005	488.0396	37.3059
Gaidropsarus vulgaris	260	0.1239	0.0698	1.7758	0.0406

Table S2.1 continued

Species	Df	slope	t-value	p-value	% biomass
Galeus melastomus	230	-0.1356	0.1159	-1.1692	0.029
Glyptocephalus cynoglossus	254	0.0701	0.062	1.1315	0.0414
Gobiidae	470	-0.0492	0.01	-4.8929	0.0101
Gobiusculus flavescens	129	-0.0233	0.0533	-0.4363	0.0011
Helicolenus dactylopterus	51	-0.4203	0.1921	-2.1884	0.005
Hippoglossoides platessoides	1269	0.0215	0.0085	2.5301	0.1137
Hippoglossus hippoglossus	6	0.1102	0.1573	0.7008	0.0025
Hyperoplus lanceolatus	1148	0.0033	0.005	0.6652	0.0849
Lepidorhombus whiffiagonis	2925	-0.0268	0.0216	-1.2372	0.4381
Leucoraja naevus	543	-0.0525	0.0187	-2.8107	0.1298
Limanda limanda	56388	<0.0001	0.0012	0.0084	5.8963
Lipophrys pholis	224	0.0384	0.0323	1.1902	0.0026
Lophius piscatorius	838	-0.0332	0.0143	-2.3185	0.4105
Maurolicus muelleri	220	0.4669	3.516	0.1328	0.0041
Melanogrammus aeglefinus	59139	-0.0291	0.0009	-31.099	10.1355
Merlangius merlangus	150622	0.1745	0.0004	462.084	14.4708
Merluccius merluccius	2975	0.0851	0.0091	9.3361	0.7765
Microchirus variegatus	264	0.0121	0.0134	0.8987	0.017
Micromesistius poutassou	7800	-0.0204	0.0021	-9.6621	0.594
Microstomus kitt	1507	0.0129	0.0046	2.8082	0.2064
Molva molva	460	-0.0562	0.0374	-1.5021	0.1926
Mullus surmuletus	289	0.0117	0.011	1.066	0.0351
Mustelus asterias	123	-0.4985	0.2059	-2.4216	0.0248
Myoxocephalus scorpius	249	0.0069	0.0144	0.4772	0.0307

Table S2.1 continued

Species	Df	slope	t-value	p-value	% biomass
Osmerus eperlanus	2	-0.7479	1.2859	-0.5816	<0.0001
Pholis gunnellus	217	-0.1561	0.0189	-8.243	0.0064
Phycis blennoides	2	10.418	11.3788	0.9156	0.0005
Platichthys flesus	847	-0.077	0.0085	-9.0797	0.1326
Pleuronectes platessa	40952	0.0133	0.0013	10.6027	5.3984
Pollachius pollachius	851	-0.0447	0.023	-1.9397	0.41
Pollachius virens	7627	0.0923	0.0031	29.5236	2.7729
Pomatoschistus minutus	13	-0.0082	0.0515	-0.1585	0.0003
Raja clavata	1499	-0.0616	0.0064	-9.5572	0.5425
Raja montagui	646	-0.0422	0.0119	-3.541	0.1523
Sardina pilchardus	56	-0.0077	0.1802	-0.0427	0.0066
Scomber scombrus	27988	-0.0088	0.001	-8.7132	5.3332
Scophthalmus maximus	707	-0.0789	0.0098	-8.0846	0.1912
Scophthalmus rhombus	1781	-0.0799	0.0066	-12.1826	0.5388
Scyliorhinus canicula	3302	-0.0036	0.0073	-0.4983	0.7549
Solea solea	876	0.0442	0.0054	8.207	0.1192
Sprattus sprattus	28697	-0.0155	0.0043	-3.6067	0.9655
Squalus acanthias	965	0.1286	0.01	12.8128	0.3281
Taurulus bubalis	202	-0.2194	0.0168	-13.0942	0.0078
Trachurus trachurus	2875	0.0166	0.0041	4.0323	0.4342
Trigloporus lastoviza	244	-0.004	0.1256	-0.0315	0.0357
Trisopterus esmarkii	577	0.263	0.0104	25.2188	0.0192
Trisopterus luscus	2494	0.0279	0.0037	7.4572	0.3641
Trisopterus minutus	3185	-0.0024	0.0048	-0.5069	0.2222
Zeus faber	1294	0.0369	0.0102	3.6286	0.2667

1267

Table S2.2: The results of a linear regression of body mass (g) vs temperature (°C) for each individual prey species included in the study with their corresponding percentage of total biomass across all species (%).

Species	Df	slope	t-value	p-value	% biomass
Abra alba	4372	-0.0094	0.0052	-1.8208	0.3591
Abra prismatica	26	0.0023	0.0464	0.0489	0.0027
Acartia clausi	67	0.1574	0.0297	5.3038	0.0069
Alloteuthis subulata	70	-0.2914	0.1723	-1.6905	0.0318
Ammodytes	9190	-0.0458	0.0011	-40.3889	4.2664
Ampelisca	710	-0.0403	0.0061	-6.6473	NA
Amphipoda	1248	0.0537	0.0035	15.4342	NA
Amphiura filiformis	6301	-0.1358	0.0019	-72.0354	NA
Anapagurus laevis	29	<0.0001	0.0562	<0.0001	0.0075
Annelida	5532	-0.1012	0.0022	-45.1269	NA
Antalis entalis	44	0.0045	0.0929	0.0487	0.0104
Aphrodita aculeata	675	0.1042	0.0104	10.0331	0.4652
Argentina sphyraena	28	-0.107	0.0268	-3.9961	0.0164
Arnoglossus laterna	28	0.018	0.0242	0.7467	0.0134
Arthropoda	22668	0.2233	0.0015	152.9064	NA
Atelecyclus rotundatus	28	-0.0895	0.0317	-2.827	0.0121
Balanus crenatus	9	-0.04	0.0465	-0.8603	0.0005
Bathyporeia pelagica	28	0.0609	0.1383	0.4404	0.0007
Bodotria scorpioides	12	<0.0001	5.0946	<0.0001	NA
Brachynotus sexdentatus	16	<0.0001	0.1219	<0.0001	0.0052
Buccinum undatum	148	0.2894	0.0559	5.1776	0.0542
Buglossidium luteum	170	-0.0263	0.0101	-2.602	0.1322
Calanoida	2977	-0.0424	0.0053	-7.9871	NA
Calanus	5582	-0.0713	0.0049	-14.6381	NA
Callianassa subterranea	307	<0.0001	0.0357	<0.0001	0.3209
Callionymus lyra	1103	-0.0137	0.0036	-3.7796	0.7601
Calocaris macandreae	1560	-0.0404	0.0069	-5.8901	0.5017
Cancer pagurus	44	-0.1695	0.0274	-6.1905	0.0239

Table S2.2 continued

Species	Df	slope	t-value	p-value	% biomass
Cancridae	3890	-0.0855	0.0027	-31.6956	1.1772
Candacia armata	55	<0.0001	0.2866	<0.0001	0.0075
Capitella capitata	23	0.1759	0.0514	3.4229	NA
Caprella monocera	27	0.0843	0.0845	0.9979	0.0008
Carcinus maenas	32	0.0381	0.0314	1.2117	0.0373
Cerastoderma edule	13	0.0025	0.0356	0.0707	0.0081
Chlamys opercularis	64	-0.0043	0.0287	-0.151	0.0282
Chordata	13544	0.0107	0.0021	5.0849	NA
Clupea harengus	619	-0.0966	0.0162	-5.9716	0.7648
Clupeidae	226	-0.0178	0.0128	-1.3939	0.1399
Cnidaria	98	-0.1115	0.0157	-7.0942	0.0733
Corophium volutator	20	<0.0001	0.041	<0.0001	0.0005
Corystes cassivelaunus	761	-0.1228	0.0044	-28.0762	0.272
Coscinodiscus	111	0.1815	0.0496	3.6622	0.0119
Crangon allmanni	9	-4.7387	4.0903	-1.1585	0.0024
Crangon crangon	18	-0.1146	0.0412	-2.7835	0.0049
Crangonidae	2624	-0.0276	0.0028	-9.7756	0.724
Crepidula fornicata	16	-0.049	0.049	-0.9992	0.0005
Ctenophora	54	-0.0108	0.0195	-0.5545	0.0129
Cultellus pellucidus	167	-0.1394	0.0134	-10.4412	0.0369
Cumacea	91	0.0171	0.0131	1.3042	NA
Cylichna cylindracea	91	<0.0001	0.1212	<0.0001	0.0157
Decapoda	2873	0.0044	0.0024	1.8256	NA
Dendronotus frondosus	16	4.3066	3.8564	1.1167	0.0018
Diptera	11	-0.0098	0.0486	-0.2022	0.0009
Ebalia cranchii	55	0.1224	0.0288	4.2443	0.0132
Echiichthys vipera	74	-0.0656	0.0127	-5.172	0.0718
Echinocardium cordatum	71	-0.0583	0.0197	-2.9528	0.0357
Echinocyamus pusillus	160	0.0208	0.0102	2.0348	0.011
Echinodermata	132	-0.0129	0.0115	-1.1246	0.0245

Table S2.2 continued

Species	Df	slope	t-value	p-value	% biomass
Echiurus echiurus	116	-0.0728	0.0181	-4.0284	0.0459
Enchelyopus cimbrius	96	0.6455	0.1125	5.7379	0.1225
Ensis	181	0.0119	0.01	1.1979	0.0553
Eteone longa	65	<0.0001	0.051	<0.0001	0.0021
Euphausiidae	7336	-0.0428	0.0032	-13.5687	1.2991
Euspira	64	<0.0001	0.0322	<0.0001	0.0127
Funiculina quadrangularis	12	<0.0001	0.1698	<0.0001	0.0084
Gadidae	3738	0.6711	0.0088	75.8459	1.6039
Gadus morhua	416	-1.0092	0.2342	-4.3084	0.0389
Gaidropsarus	148	-0.4251	0.0807	-5.2677	0.1372
Galathea	1074	-0.2158	0.0071	-30.5241	0.3446
Galathea intermedia	875	0.007	0.0052	1.3503	0.0729
Gammaridae	158	-0.0242	0.0227	-1.0665	0.0272
Gammarus duebeni	21	<0.0001	0.0412	<0.0001	0.0007
Gari fervensis	28	<0.0001	0.0928	<0.0001	0.0076
Glycera	2607	0.066	0.0055	12.0008	NA
Glyptocephalus cynoglossus	180	-2.4751	0.1586	-15.6076	0.203
Gobiidae	538	-0.0542	0.005	-10.7716	0.1384
Golfingia vulgaris	382	-0.0029	0.0157	-0.1851	0.0922
Goneplax rhomboides	810	-0.0222	0.0154	-1.439	0.5363
Goniada maculata	36	-0.2971	0.0223	-13.3022	0.0068
Gymnammodytes semisquamatus	46	0.2717	0.3118	0.8712	0.0217
Harmothoe impar	26	-0.1224	0.0688	-1.7807	0.0015
Harpacticoida	71	-0.7457	0.0334	-22.3307	0.0029
Hediste diversicolor	137	<0.0001	0.0178	<0.0001	0.0075
Heleobia stagnorum	12	<0.0001	0.0774	<0.0001	NA
Hippoglossoides platessoides	79	0.1032	0.0351	2.9375	0.0836

Table S2.2 continued

Species	Df	slope	t-value	p-value	% biomass
Hyale nilssoni	24	<0.0001	0.0847	<0.0001	0.0023
Hydroida	204	-0.1477	0.0214	-6.9144	0.0308
Hyperiidae	290	-0.019	0.0049	-3.9091	NA
Hyperoplus lanceolatus	16	0.1773	0.0326	5.4418	0.0149
Idotea	68	0.0457	0.0197	2.326	0.0066
Idotea granulosa	54	<0.0001	0.056	<0.0001	0.001
Inachus leptochirus	39	0.0343	0.0214	1.6063	0.012
Iphimedia	27	-0.0767	0.0286	-2.6768	0.0012
Iphinoe trispinosa	52	-0.5941	0.0656	-9.0504	NA
Isopoda	74	0.0478	0.0469	1.02	0.0053
Lacuna pallidula	15	<0.0001	0.1296	<0.0001	0.0009
Limacina retroversa	15	0.0128	0.3244	0.0395	0.0002
Limanda limanda	371	-0.0599	0.0176	-3.4017	0.3989
Liocarcinus	1288	-0.0744	0.0044	-16.9114	0.5675
Liocarcinus depurator	68	0.1102	0.0206	5.3601	0.0355
Liocarcinus holsatus	47	-0.18	0.02	-9.0211	0.0157
Liocarcinus pusillus	38	-0.1509	0.0192	-7.8766	0.0051
Littorina littorea	21	<0.0001	0.097	<0.0001	0.005
Littorina obtusata	15	<0.0001	0.1296	<0.0001	0.0036
Littorina saxatilis	27	<0.0001	0.0778	<0.0001	0.0038
Loliginidae	378	-0.0683	0.006	-11.3469	0.2244
Lumbrineris	1024	-0.2165	0.0159	-13.5811	0.0877
Macropodia rostrata	256	-0.0836	0.0163	-5.133	0.0802
Mactridae	12	-0.1676	0.0666	-2.5157	0.0065
Majidae	77	-0.3538	0.089	-3.9748	0.0115
Maldanidae	48	1.202	1.9609	0.613	0.0024
Malmgreniella	28	0.3168	0.0779	4.0648	0.0008
Maxmuelleria lankesteri	2173	-0.6442	0.0672	-9.5823	0.9437
Meganyctiphanes norvegica	112	-0.0167	0.0247	-0.6781	0.016

Table S2.2 continued

Species	Df	slope	t-value	p-value	% biomass
Melanogrammus aeglefinus	348	-0.3033	0.0566	-5.3603	0.6768
Merlangius merlangus	2104	0.0122	0.0145	0.8433	3.195
Microchirus variegatus	176	0.193	0.2457	0.7856	0.2145
Micromesistius poutassou	1572	-0.0661	0.0177	-3.7266	2.5098
Microsetella norvegica	55	-1.2636	0.2866	-4.4095	0.0056
Mollusca	2234	-0.1204	0.0036	-33.8855	NA
Monodonta	12	0.2375	0.3211	0.7395	0.0015
Myctophidae	31	0.0096	0.042	0.2276	0.0091
Mysidae	1035	0.0419	0.004	10.4937	NA
Mysidopsis angusta	2	<0.0001	0.1096	<0.0001	0.0002
Mytilus edulis	5	0.3483	0.0625	5.5742	0.001
Nematoda	123	<0.0001	0.0185	<0.0001	0.0023
Nemertea	303	0.0172	0.0068	2.5441	NA
Nephrops norvegicus	18123	-0.0272	0.0046	-5.9465	14.6755
Nephtys caeca	6976	-0.1712	0.0085	-20.1258	1.8897
Nereis	65	-0.023	0.0119	-1.936	0.015
Nucula	103	-0.109	0.0121	-9.0246	NA
Nudibranchia	12	0.6145	0.9348	0.6573	0.0099
Nyctiphanes couchii	334	-0.0004	0.0187	-0.0194	0.0118
Octopodidae	44	1.0016	0.1365	7.3386	0.1206
Oithona	347	0.1179	0.0103	11.4432	0.018
Ophelina	34	18.3927	3.5009	5.2537	NA
Ophiothrix fragilis	55	0.2875	0.0731	3.9313	0.0225
Ophiura	44	0.0811	0.0199	4.0869	0.0067
Ophiura albida	189	<0.0001	0.0141	<0.0001	0.0401
Ophiura ophiura	90	0.4401	0.0219	20.0589	0.0197
Ophiurida	792	-0.0355	0.0081	-4.3894	0.1882
Paguridae	1294	-0.0509	0.0043	-11.9679	0.4933
Pagurus bernhardus	577	-0.0909	0.0178	-5.1076	0.3267

Table S2.2 continued

Species	Df	slope	t-value	p-value	% biomass
Palaemon serratus	1117	-0.1793	0.041	-4.3712	0.6051
Palaemonidae	749	-0.066	0.0442	-1.4938	0.4085
Pandalina brevirostris	4	<0.0001	0.1268	<0.0001	0.0006
Pandalus	1974	-0.0199	0.0133	-1.4977	0.6315
Pandalus montagui	1044	-0.0812	0.0104	-7.8233	0.392
Paracalanus	61	0.1308	0.0231	5.6624	0.0021
Parasagitta elegans	134	0.0029	0.0263	0.1115	0.0093
Pasiphaea sivado	1031	-0.005	0.0077	-0.6473	0.3753
Patella vulgata	15	<0.0001	0.1058	<0.0001	0.003
Pectinaria koreni	633	-0.0639	0.0059	-10.849	NA
Pectinidae	101	0.0843	0.0155	5.4325	0.0781
Penaeus	68	<0.0001	0.0616	<0.0001	0.0134
Philine aperta	99	<0.0001	0.0773	<0.0001	0.01
Phoronis muelleri	77	-0.0352	0.0176	-2.0002	NA
Phyllodoce maculata	14	0.0397	0.0961	0.4132	0.0004
Pilumnus hirtellus	87	-0.0249	0.0176	-1.4133	0.0144
Pisidia longicornis	1191	0.0039	0.0032	1.2148	0.0936
Platyhelminthes	16	<0.0001	0.0272	<0.0001	0.0009
Pleuronectes platessa	2934	0.0779	0.0146	5.3288	0.3731
Pleuronectiformes	913	0.0075	0.0133	0.567	0.699
Polinices	15	<0.0001	0.4048	<0.0001	0.001
Pomatoceros triqueter	28	-0.0174	0.0179	-0.969	0.0012
Pomatoschistus minutus	69	0.2127	0.0416	5.1115	0.0156
Porcellana	158	0.0595	0.0379	1.571	0.0273
Processa canaliculata	335	-0.0462	0.0113	-4.0862	0.0466
Psammechinus miliaris	26	-0.5115	0.024	-21.3343	0.0057
Pseudocalanus elongatus	21331	0.1634	0.0086	18.9201	NA
Sabellaria spinulosa	127	0.0123	0.0133	0.9227	0.0073
Sabellidae	35	-0.1701	0.0551	-3.0882	0.0015
Scalibregma inflatum	31	-0.0915	0.0264	-3.4634	0.0022

Table S2.2 continued

Species	Df	slope	t-value	p-value	% biomass
Scomber scombrus	8	-0.1267	0.0831	-1.5252	0.0058
Semibalanus	93	<0.0001	0.0476	<0.0001	0.0055
Sepiola atlantica	114	-0.0996	0.011	-9.0386	0.0897
Serpulidae	12	<0.0001	0.0916	<0.0001	0.0004
Solea solea	31	0.1283	0.0848	1.5123	0.0256
Soleidae	20	6.2718	0.4231	14.8224	0.0076
Spionidae	22	0.0851	0.0386	2.2046	0.0008
Spisula solida	60	-0.006	0.0257	-0.232	0.0254
Spisula subtruncata	22	<0.0001	0.3167	<0.0001	0.0035
Sprattus sprattus	2378	-0.0109	0.0055	-1.9862	1.5065
Syllidae	38	-0.0153	0.1009	-0.1513	0.0008
Syngnathidae	68	0.041	0.0186	2.204	0.0195
Tellimya ferruginosa	26	<0.0001	0.154	<0.0001	0.0039
Tellina	63	0.0095	0.0213	0.4466	0.012
Temora	14798	0.0967	0.0075	12.8215	NA
Terebellidae	51	-0.1106	0.0292	-3.7897	0.016
Themisto abyssorum	171	-0.0122	0.1341	-0.091	0.0068
Thia scutellata	4	<0.0001	0.2468	<0.0001	0.0015
Timoclea ovata	77	<0.0001	0.0216	<0.0001	0.0118
Trachurus trachurus	12	-0.4853	0.1882	-2.579	0.0068
Trigla	96	0.4594	0.0537	8.5576	0.045
Trisopterus	213	0.1237	0.0528	2.3425	0.09
Trisopterus esmarkii	1470	-0.0028	0.0375	-0.0759	1.5067
Trisopterus minutus	348	-0.0564	0.018	-3.1321	0.3589
Turritella communis	53	-0.0138	0.0752	-0.1838	0.0115
Upogebia deltaura	162	-0.0705	0.0095	-7.4328	0.0833
Varicorbula gibba	50	-0.2932	0.0244	-11.9987	0.005
Xantho pilipes	140	-0.0752	0.1161	-0.6483	0.0991

1271

Table S2.3: The AIC values of all linear and polynomial models tested within this study. The optimal model (AIC value > 2 units lower) is highlighted in bold in each case.

Model	Response variable	Linear	Polynomial
PPMR ~ temperature	PPMR	**254903.3**	255022.9
	Predator mass	**5301.242**	5308.293
	Prey mass	143835.6	**143831.4**
	Prey count	**114131.7**	468990.4
	Prey richness	-85829.94	**-86088.3**
PPMR ~ temperature × fishing effort	PPMR	**246904.1**	246939.1
	Predator mass	**10427.64**	29361.44
	Prey mass	**137925.1**	137996.6
	Prey count	**113464.7**	468703.9
	Prey richness	-80542.45	**-80906.26**

3 Marine benthopelagic food webs of the North Sea (1997-2015)

Accepted with revisions in Scientific Data

3.1 Abstract

A major barrier to assessing the effects of global change on complex ecosystems is the scarcity of food web observations spanning the spatial and temporal scales needed to reveal significant change. This study aims to rectify this by presenting 4728 empirical food webs constructed every 50 km across the North Sea annually from 1997-2015. We also present a dynamic, reproducible framework for devising food webs at different spatial or temporal scales by integrating nearly four decades of standardised groundfish survey data with one of the world's most comprehensive stomach content databases. This time series of spatially resolved food webs should help enrich analyses of environmental change on food web structure and aid reliable benchmarking of ecosystem-based management in one of the world's most commercially important and anthropogenically influenced continental shelves.

3.2 Background

Food webs are ecological networks of species interactions that can provide perspective on the structure and functioning of ecosystems (Kortsch et al., 2019; O'Gorman et al., 2019; Pimm, 1982; Scharler et al., 2018). Food webs contain nodes which are organisms and edges that represent the flow of energy between organisms due to feeding interactions. Food webs have been used for many decades as a means to understand how environmental stressors alter ecological communities, providing insight into ecosystem complexity and resilience in the face of global change (Elton, 1927; Lindeman, 1941; Link, 2002; Odum, 1980; Pimm, 1982). Food webs are also attractive to policy makers and ecosystem managers as they can be used to condense complex ecosystem dynamics into simple metrics, enabling clear advice and the establishment of management benchmarks (Korpinen et al., 2022). For example, OSPAR uses food webs as a means to asses environmental status and the effectiveness of policy interventions to determine whether environmental change from anthropogenic activities is unsustainable or not (Schückel et al., 2023).

Given the increase of multiple anthropogenic pressures on marine environments (Díaz et al., 2019; Jouffray et al., 2020), tools to analyse system-level characteristics such as resilience are paramount to avoid unsustainable impacts and ecosystem degradation. The northeast Atlantic is subject to widespread anthropogenic pressures and yet remains home to extremely productive fisheries (Halpern et al., 2015, 2008). As a result, the North Sea has seen a dramatic decrease and geographic shifts in biodiversity (Hahn et al., 2023), ultimately impacting trophic interactions (Duffy et al., 2007), making it a great case study for the impacts of global change on food webs. However, the extensive data needed to construct food webs, e.g. on interactions between different species across their various life stages and geographic ranges are often not available, which has historically been a major limiting factor in food web research. To empirically capture trophic interactions, especially in open marine ecosystems, is often unachievable due to the unfeasible level of sampling required. The data that are available are often fragmentary, producing localised and static representations of space and time that can obscure the variability of trophic interactions. Consequently, a common critique of food web research is its lack of robust baselines and thus comparability to novel environmental contexts (Le Guen et al., 2019; Niquil et al., 2014). Recent methodological advances however, in sampling trophic interactions as well as collaborative efforts to publish large scale data has provided an opportunity to address such challenges. In this study, we make use of such recent advances and further address challenges within food web research by (a) generating an unprecedented number of food webs over multiple decades across the North Sea, and (b) proposing a dynamic, reproducible methodology for food web construction that can be applied consistently across different spatial and temporal scales. We focused on the North Sea to capture a substantial time-series that is has not yet been possible at larger scales. Other datasets, such as FISHGLOB (Maureaud et al., 2024) and additional fish stomach-content compilations (Pinnegar et al., 2023) could support extending food-web construction beyond the spatial scale considered here.

This dataset includes 4728 well-sampled empirical food webs spanning every 50 km across the North Sea over 18 years (Figure 3.1). Unlike traditional grid-based approaches, these food webs capture overlapping taxa and interactions by sampling within spatial and temporal radii. Constructed using novel stomach contents and

monitoring data as well as a reproducible, flexible methodology, our approach resolves incomplete predator diets, integrates both directly observed and literature-inferred predator-prey interactions, and ensures that trophic structures reflect locally observed communities. The resulting dataset captures North Sea ecosystem variability at a resolution not previously available, offering robust baselines for benchmarking and facilitating cross-scale comparisons of trophic interactions. The hope is that this resource will support advances in food web research and ecosystem-based management in a region heavily impacted by human activity, while also offering a transferable methodology for application in other marine systems worldwide.

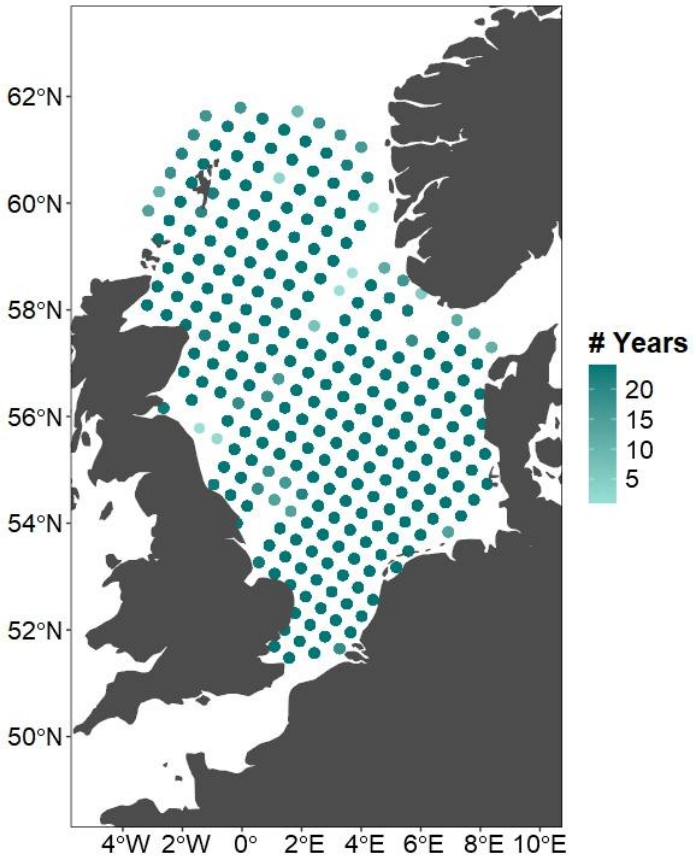

Figure 3.1: A map of the location of al 4728 food webs in the northeast Atlantic. Each point is the location of a food web, and replicates of each food web exist yearly (where possible) from 1997 to 2015. The colour of the point indicates the number of yearly replicates in each location.

3.3 Methods

3.3.1 Summary

This study draws on two primary empirical datasets to construct spatially and temporally explicit North Sea food webs: a standardised fish survey database, used to identify local fish taxa and estimate their abundance, biomass, and body size, and a stomach contents database, used to characterise consumer–resource interactions among fish predators and their prey. These datasets were combined with fish feeding-guild classifications and published functional-group diet information for non-fish prey taxa to infer trophic interactions across the wider food web. Together, these data were used to generate local food webs across the North Sea by combining information on species occurrence, predator diets, prey functional roles, and trophic interactions. The resulting dataset comprises 4728 empirical food webs spanning 1997–2015, with each web containing taxon identities, flux-weighted interactions, feeding groups, abundance, biomass, body-size information, spatial coordinates and sampling year. The different food web construction steps are detailed below and are summarised in a flow chart (Figure 3.2).

Figure 3.2: A flow chart summarising the data needed, steps and decisions taken as well as user-adjustable parameters used to construct the North Sea food webs.

3.3.2 Description of datasets used to construct the food webs

3.3.2.1 Fish survey

This dataset offers a standardised record of groundfish catches across the Northeast Atlantic spanning nearly four decades (Lynam and Riberio, 2022), drawing on extensive scientific trawl survey data from the ICES database of trawl surveys. A subset of -3.5 ° W to 8.5 ° E and 51.24 ° N to 61.75 ° N from 1997-2015 was used in this study due to the more limited availability of standardised data on commercial fishing as well as the extensive time-series available within this region. Here, the subsetted data are referred to as the fish survey database, which holds 3,334,387 abundance observations of 371 taxa sampled from 24,843 hauls from 1997-2015. The most common species in the fish survey are whiting (*Merlangius merlangus*), common dab (*Limanda limanda*), and haddock (*Melanogrammus aeglefinus*). The dataset reports taxa abundance at regular body size intervals and has been supplemented with information on biomass via routine sampling of length-mass relationships. This dataset was used to establish the fish predator taxa present in the environment for any given food web. Unfortunately, marine mammals and seabird data was not included due to limited availability at similar spatial and temporal scales.

3.3.2.2 Stomach contents

To establish the trophic interactions between consumers and resources, we used a data collation that includes DAPTSOM (Pinnegar et al., 2015) and ICES Year of the Stomach (ICES, 2010). This database is one of the most comprehensive archives of dietary data globally. Stomach samples were collected as early as 1837 and continued until 2016. The dataset used here brings together over 415,658 records of trophic interactions within 156,452 individual stomachs sampled from 6924 research hauls across the northeast Atlantic. The most common stomach samples are from Atlantic cod (*Gadus morhua*), whiting (*Merlangius merlangus*) and haddock (*Melanogrammus aeglefinus*). More information on this stomach contents data is detailed by Thompson et al., 2020. From here on, this dataset is referred to as the stomach contents database.

To clean and standardise the database, predator and prey taxa were checked for naming inconsistencies and unresolved taxonomic records were removed. Firstly, predator and prey taxa were renamed if there were obvious discrepancies, for

example “Octopus” was renamed to “Octopodidae” to match the Latin nomenclature used for the vast majority of observations. Unrefined data whereby the taxonomic resolution was not resolved to the family level or lower, including prey taxa labelled as “Decapoda”, “Chordata”, “Mollusca”, and “Arthropoda” were removed from the entire stomach contents database (13.37% of original dataset was deleted). To account for ontogenetic shifts in a species diet, feeding guilds were added to all fish predators in the stomach contents data (Thompson et al., 2025). Feeding guilds group predators based on similar feeding traits (size and abundance of prey in a diet) (Thompson et al., 2025). These feeding guilds consisted of planktivore (PL), benthivore (BE), bentho-piscivore (BP), and piscivore (PI). If the feeding guild could not be established directly, it was inferred by a predator of the same genus that was the most similar in size. However, predators that had no feeding guild information and less than ten observations across the entire stomach contents were removed from all datasets (0.05 % of original dataset was deleted), as there was not enough information to directly infer their diets.

3.3.3 The workflow used to construct the North Sea food webs

To construct spatially explicit food webs, the North Sea study area (−3.5° W to 8.5° E and 51.25° to 61.75° N) was divided into 50 × 50 km grid cells. The central longitude and latitude of each cell were used as focal points for constructing food webs. Fish species included in each food web were identified from all survey hauls conducted within a 100 km radius of the focal coordinate for a given year (1997–2015). This approach produced fuzzy boundaries between food webs, as overlapping 100 km radii introduced spatial continuity and dynamics absent in traditional hard-boundary delineations. To account for differences in sampling effort across the spatial region, a minimum of five and a maximum of ten hauls were taken per 100 km radius. If there were more than ten hauls present, the closest ten to the focal grid coordinate were selected. The fish species present were assigned a feeding guild following Thompson et al., 2025. The mean biomass (kg km^{-2}), abundance (individuals km^{-2}), and mean weight (g) within the 100 km radius were also recorded for each species. The next step involved subsetting the stomach contents database by year and the same 100 km radius around each focal grid coordinate to identify all possible prey taxa present in that particular space and time. This together with the subsetted fish

survey data determined the possible nodes within each food web and is referred to as the species master list.

To identify predator-prey interactions, local stomach contents records were subset according to each predator species identified in the fish survey. To ensure sufficient stomach content data were available to accurately characterize predator diets, when establishing trophic interactions, data from all years were combined for each local area. Consequentially when food webs are constructed, they rely on spatial variation of trophic interactions. However, the species composition represented spatial and temporal changes as only interactions between taxa known to be present according to the species masters list were included i.e. any diets are only inclusive of taxa observed within the local area within a given year. This approach was necessary because the temporal coverage of stomach content observations was too patchy to reliably assess changes in trophic interactions over time. This approach could be easily modified in our code if a different temporal resolution of trophic interactions is desired. Most predators in the stomach contents database are resolved to species level, making it straightforward to connect species in the food web based on this information. However, taxa resolved to genus level were renamed to taxa resolved to the species level from the same genus and within that grid coordinate in order to consolidate the nodes and trophic links within the food web. If no other taxa of the same species were present, then the taxa remained resolved to the genus level.

To evaluate whether sufficient data were available to represent each predator's diet, species accumulation (yield–effort) curves were constructed using the 'specaccum' function from the *vegan* R package (R Core Team, 2024). The expected total prey diversity for each predator was then estimated by fitting six model distributions ('lomolino', 'arrhenius', 'gleason', 'gitay', 'asymp', and 'logis') using the 'fitspecaccum' function, with the best-fitting model selected based on the lowest Akaike Information Criterion (AIC) value (Figure 3.3). A predator's diet was considered to be at a satisfactory level of completion when the observed number of prey taxa represented at least 75% of the total prey richness predicted by the selected model. If the predator species was not represented in the local stomach contents or its diet completion was below 75%, then local interactions from the predator species within the same genus that were most similar in size were included in the diet of that predator. This process was repeated iteratively until all predator diets were

sufficiently complete: 1. first by adding local data from all species of the same genus that were not more than double in size; 2. then from local data from species in the same feeding guild and most similar in size; 3. then from local data and all species within the same feeding guild that were not more than double the size; 4. finally from across the global stomach contents database by adding interactions observed for that predator species from the entire range of space and time. Statistics on how many diets were completed at each step are include in Table 3.1. On average across all food webs, 89% of fish predator species had a diet completion over 75%.

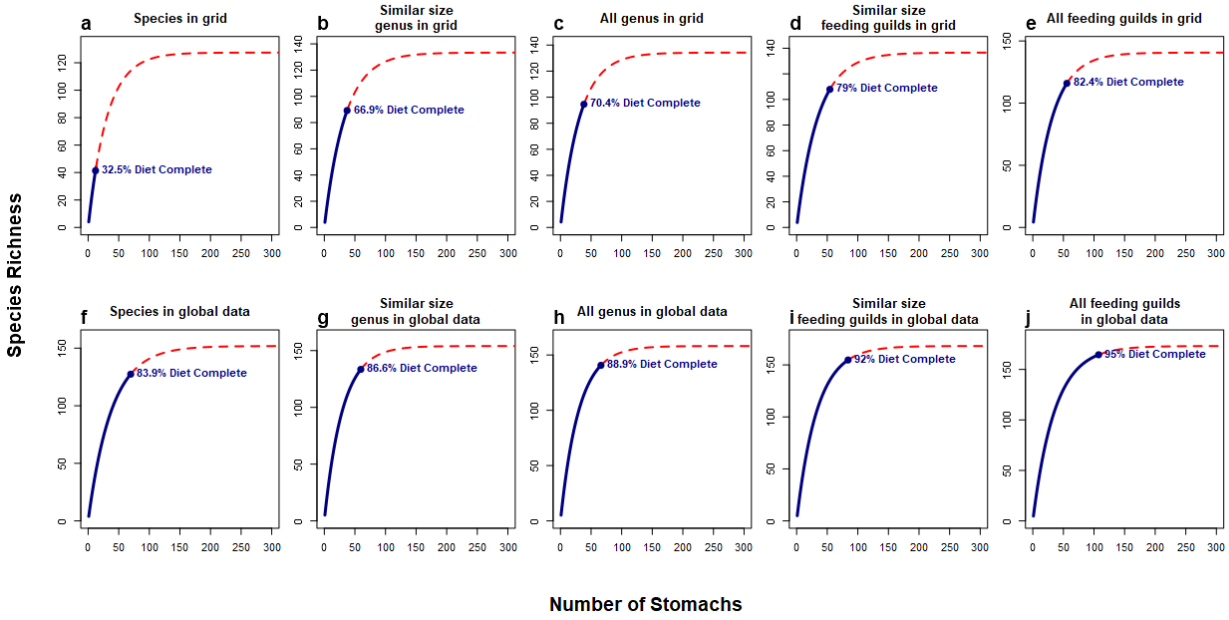

Figure 3.3: An example of species accumulation curves at each stage of food web construction for *Sprattus sprattus* at longitude -1.1 and latitude 59.3. The blue solid line indicates the observed prey species richness in the stomach contents and the dashed red line is the predicted prey species richness. A satisfactory level of diet completion was achieved when the empirical richness was 75% or more of the predicted prey species richness, i.e. in panel (d), thereby negating the need to add any further links to the diet from panels (e-j).

Table 3.1: The mean percentage of predators that reached a diet completion of above 75% across all 4865 food webs within the study, as determined by the species accumulation curve models.

Level of dietary resolution	**Percentage complete**	**Cumulative percentage complete**
Species within 100 km radius	0	0
Genus most similar in size within 100 km radius	16.6	16.6
Genus not more than double in size within 100 km radius	1.8	18.4
Feeding guild most similar in size within 100 km radius	12.2	30.6
Feeding guild not more than double in size within 100 km radius	4.6	35.2
Species within global stomach contents database	32.1	67.4
Genus most similar in size within global stomach contents database	5.9	73.2
Genus not more than double in size within global stomach contents database	0.4	73.6
Feeding guild most similar in size within global stomach contents database	5.5	79.1
Feeding guild not more than double in size within global stomach contents database	9.8	89.0

The body mass and abundance of the fish predators were taken directly from the local fish survey. The abundance of the non-fish prey was taken from the prey count indicated by the trophic interactions, and the biomass of the prey was calculated using this abundance multiplied by the individual weight recorded from the stomach contents. These measurements have some limitations such as the impact of digestion on estimates of prey weight; however, they are the best estimate in the

absence of biological survey data for prey taxa at the same spatiotemporal scale as the fish.

After establishing trophic interactions of the fish predator species, we attempted to determine trophic interactions between their prey. First, if the prey taxa were themselves fish, the previous steps of identifying interactions from the stomach contents database at the species, genus, and feeding guild level were completed for these taxa and their trophic adjacency matrices were constructed. Prey taxa that were not fish were assigned to one of the following feeding groups: herbivorous zooplankton, omnivorous zooplankton, decapods, hydrozoans, tunicates, barnacles, bivalves, bryozoans, omnivorous echinoderms, herbivorous echinoderms, herbivorous gastropods, omnivorous gastropods, cephalopods, omnivorous cnidarians, herbivorous cnidarians, and sponges and their diets were inferred based on a published North Sea food web model by Daskalov and Mackinson (2007). The inferred diet of each grouping is summarised in Table 3.2. For example, if a prey taxon was classified as omnivorous zooplankton taxon, it was assumed to feed on herbivorous zooplankton taxa based on the North Sea model (Daskalov and Mackinson, 2007; Mackinson and Daskalov, 2007). Accordingly, a feeding interaction was established between the omnivorous zooplankton taxa and all herbivorous zooplankton known to occur within the spatial scale of the food web. If the prey taxon was known to consume small teleost's (Daskalov and Mackinson, 2007; Mackinson and Daskalov, 2007), feeding interactions were created to all fish species that were under 10 cm in length at maturity. Some prey taxa consumed basal resources including phytoplankton, CPOM, FPOM, microalgae, macroalgae fungi, and bacteria (Daskalov and Mackinson, 2007; Mackinson and Daskalov, 2007), which are ubiquitous throughout the North Sea and thus were added to every food web.

Table 3.2: The different prey taxa groupings and their inferred diet from the North Sea Model by (Daskalov and Mackinson, 2007; Mackinson and Daskalov, 2007).

Prey Group	Diet
Herbivorous zooplankton	FPOM, Bacteria, Fungi, Phytoplankton
Omnivorous zooplankton	Herbivorous zooplankton, Omnivorous zooplankton, FPOM, Bacteria, Fungi, Phytoplankton
Decapods	Herbivorous zooplankton, Omnivorous zooplankton, CPOM, Decapoda, Bivalves, Herbivorous echinoderms, Omnivorous echinoderms, Hydrozoa, Herbivorous gastropoda, Omnivorous gastropoda
Hydrozoans	Herbivorous zooplankton, Omnivorous zooplankton
Tunicates	FPOM, Bacteria, Fungi, Phytoplankton
Barnacles	FPOM, Bacteria, Fungi, Phytoplankton
Bivalves	FPOM, Bacteria, Fungi, Phytoplankton
Bryozoans	FPOM, Bacteria, Fungi, Phytoplankton
Omnivorous echinoderms	Herbivorous zooplankton, Omnivorous zooplankton, Barnacles, Fungi, Macroalgae, CPOM, Bivalves
Herbivorous echinoderms	FPOM, Bacteria, Fungi, Phytoplankton
Herbivorous gastropods	FPOM, Bacteria, Fungi, Phytoplankton
Omnivorous gastropods	Herbivorous gastropoda, Omnivorous gastropoda, Bivalves, Bryozoa, Hydrozoa, Tunicate, Fungi, Macroalgae, CPOM
Cephalopods	Small teleosts, Herbivorous echinoderms, Omnivorous echinoderms, ivalves, Decapoda, Herbivorous gastropoda and Omnivorous gastropoda
Omnivorous cnidarians	Herbivorous zooplankton, Omnivorous zooplankton, Small teleosts
Herbivorous cnidarians	FPOM, Bacteria, Fungi, Phytoplankton
Sponges	FPOM, Bacteria, Fungi, Phytoplankton

To complete the food webs, all trophic interactions of the fish predators, fish prey and non-fish prey taxa were combined. Additional final checks included the removal of any isolated nodes and cannibalistic trophic links. A final rule whereby no consumer could be smaller than their prey was implemented. This was due to the highly size-structured nature of aquatic ecosystems (Petchey et al., 2008; Woodward et al., 2005), supported by a minimum predator-prey body mass ratio of 1.002 across the entire stomach contents database. A final attribute table was developed including taxon names (nodes), feeding group, abundance (N), and biomass (M) as well as the latitude, longitude, and year of the food web in question. The final feeding groups included fish, basal, and all the prey groups listed in Table 3.2. This created a total of 4865 well-sampled empirical food webs across the North Sea from 1997 – 2015 (see Figure 3.4 for an example). The largest food web included 320 nodes and 20,724 trophic links, and the smallest food web included 50 nodes and 543 trophic links.

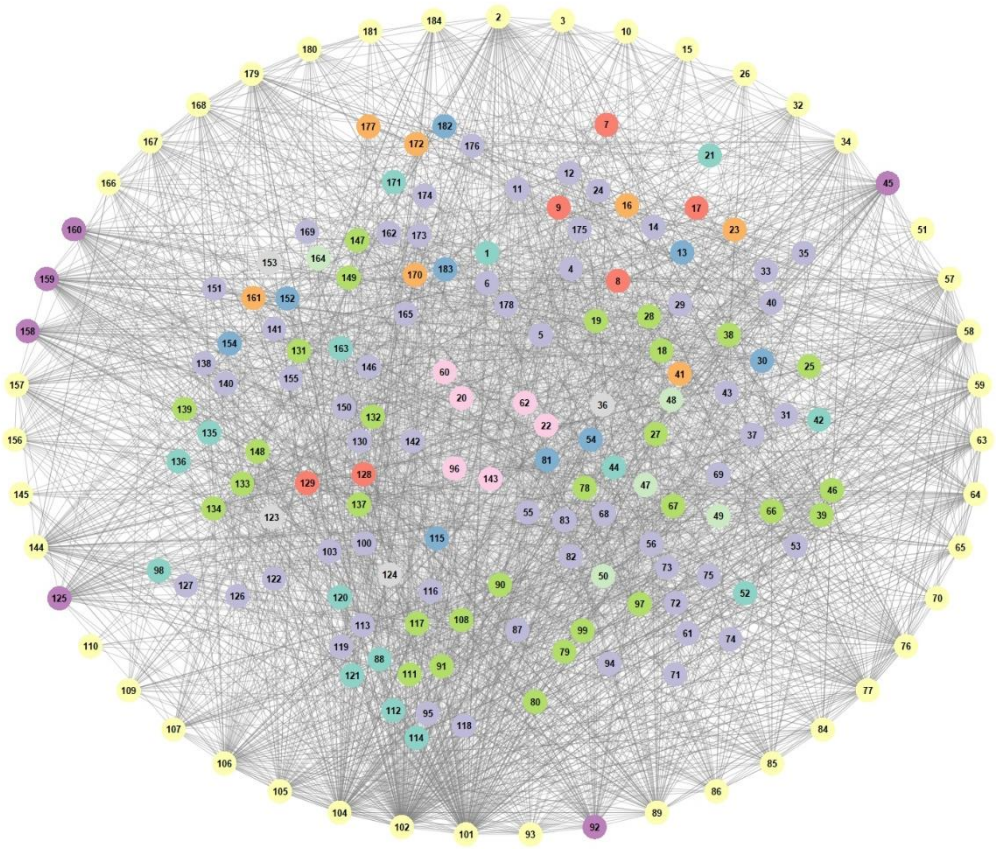

1 Abra
2 Amblyraja radiata_BP
3 Ammodytes_PL
4 Ampelisca aequicornis
5 Ampeliscidae
6 Amphipoda
7 Amphiura carchara
8 Amphiura chiajei
9 Amphiuridae
10 Anarhichas lupus_BE
11 Annelida
12 Aphrodita aculeata
13 Archaeogastropoda
14 Arcturidae
15 Argentina sphyraena_BP
16 Astacilla
17 Astropecten duplicatus
18 Atelecyclus rotundatus
19 Atlantopandalus propinqvus
20 Bacteria
21 Buccinum undatum
22 CPOM
23 Calanus tonsus
24 Caligus
25 Callianassa
26 Callionymus maculatus
27 Calocaris macandreae
28 Cancridae
29 Candacia armata
30 Cephalaspidea
31 Chaetognatha
32 Chelidonichthys cuculus_BE
33 Cirolana parva
34 Clupea harengus_PL
35 Cnidaria
36 Copelata
37 Corophiidae
38 Corystes cassivelaunus
39 Crangon allmanni
40 Cumacea
41 Cyclopoida
42 Cylichna cylindracea
43 Diastylis
44 Dinocardium
45 Doryteuthis
46 Dromiidae
47 Echinidae
48 Echinocardium cordatum
49 Echinocyamus pusillus
50 Echinodermata
51 Engraulis encrasicolus_PL
52 Ensis
53 Eudorellopsis deformis
54 Eulima
55 Eunice
56 Euphausia
57 Eutrigla gurnardus_BE
58 Eutrigla gurnardus_BP
59 Eutrigla gurnardus_PI
60 FPOM
61 Flabelligeridae
62 Fungi
63 Gadus morhua_BE
64 Gadus morhua_BP
65 Gadus morhua_PI
66 Galathea
67 Galatheidae
68 Glycera
69 Glycinde
70 Glyptocephalus cynoglossus_BE
71 Goniada maculata
72 Goniadidae
73 Haploops tubicola
74 Harmothoe
75 Harpinia antennaria
76 Hippoglossoides platessoides_BE
77 Hippoglossoides platessoides_BP
78 Hippolyte
79 Hyas araneus
80 Hyas coarctatus
81 Hydrobia
82 Hyperia galba
83 Hyperiidae
84 Hyperoplus lanceolatus_PI
85 Leucoraja naevus_BE
86 Leucoraja naevus_BP
87 Leucothoe spinicarpa
88 Limacina retroversa
89 Limanda limanda_BE
90 Liocarcinus depurator
91 Liocarcinus pusillus
92 Loliginidae
93 Lophius piscatorius_PI
94 Lophogaster typicus
95 Lysianassidae
96 Macroalgae
97 Macropipus tuberculatus
98 Mactra stultorum
99 Majidae
100 Meganyctiphanes norvegica
101 Melanogrammus aeglefinus_BE
102 Melanogrammus aeglefinus_BP
103 Melitidae
104 Merlangius merlangus_BP
105 Merlangius merlangus_PI
106 Merlangius merlangus_PL
107 Merluccius merluccius_PI
108 Metoporhaphis calcarata
109 Microstomus kitt_BE
110 Mullus surmuletus_BE
111 Munida
112 Mysella
113 Mysidae
114 Mytilus edulis
115 Natica
116 Nematoda
117 Nephrops norvegicus
118 Nephtys
119 Nereididae
120 Nucula
121 Octopodidae
122 Oedicerotidae
123 Oikopleura
124 Oikopleuridae
125 Ommastrephidae
126 Ophelia limacina
127 Opheliidae
128 Ophiura albida
129 Ophiuridae
130 Owenia fusiformis
131 Pagurus bernhardus
132 Pandalidae
133 Pandalus borealis
134 Pandalus montagui
135 Papyridea semisulcata
136 Papyridea soleniformis
137 Parapontophilus
138 Pectinaria californiensis
139 Philocheras gorei
140 Photis lacia
141 Phyllodoce
142 Phyllodocidae
143 Phytoplankton
144 Pleuronectes platessa_BE
145 Pollachius virens_PI
146 Polynoidae
147 Pontophilus
148 Portunidae
149 Processa hemphilli
150 Pseudocuma
151 Pycnogonum litorale
152 Retusa truncatula
153 Salpidae
154 Scalaria tenera
155 Scoletoma
156 Scomber scombrus_PL
157 Scyliorhinus canicula_BP
158 Sepia
159 Sepiola atlantica
160 Sepiolidae
161 Serpulidae
162 Sigalionidae
163 Solenidae
164 Spatangidae
165 Sphaerodorum gracilis
166 Sprattus sprattus_PL
167 Squalus acanthias_BP
168 Squalus acanthias_PI
169 Stenothoidae
170 Tanaididae
171 Tellinidae
172 Temora
173 Terebellidae
174 Themisto compressa
175 Themisto libellula
176 Thysanoessa inermis
177 Thysanoessa raschii
178 Tomopteris
179 Trachurus trachurus_PL
180 Trisopterus esmarkii_PL
181 Trisopterus minutus_BE
182 Turritella communis
183 Turritella exoleta
184 Zeus faber_PI

Feeding Group
Bivalves
fish
Omnivorous Zooplankton
Omnivorous Echinoderms
Ominivorous Gastropoda
Herbivorous Zooplankton
Decapoda
Basal
Tunicate
Cephalopoda
Herbivorous Echinoderms

Figure 3.4: An example food web constructed within a 100 km radius of -1.37 degrees longitude and 59.84 degrees latitude in 2005. The food web was visualised using an adaptation of the 'PlotWagonWheel' function in the *cheddar* package (Hudson et al., 2013) that allowed all basal resources to be plotted at the centre of the network. Each node is a taxon and the links drawn between nodes are trophic interactions. This food web contains 222 nodes and 10,230 links. If the species belonged to a feeding guild, then it is denoted by an underscore followed by either PI (Piscivore), PL (Planktivore), BP (Bentho-piscivore) or BE (Benthivore). The nodes are labelled by numbers and coloured by feeding group, with definitions provided in the graphical legend. The links are weighted by the amount of energy flux (g year $^{-1}$) calculated using the 'fluxing' function in the *fluxweb* R package (Gauzens et al., 2019).

A final step was to calculate the weight of the trophic interactions (equation 3.1). This was done using the fluxing function in the *fluxweb* package in R (Gauzens et al., 2019). The predictions produced by *fluxweb* are based on body mass scaling of trophic interactions (Gauzens et al., 2019; Vucic-Pestic et al., 2010). The model assumes a steady state system where losses by predation or physiological processes equal gains from consumption. The *fluxwe*b calculation is as below:

$$\sum_{\mathrm{j}} \mathrm{W_{ji}F_{i}e_{ij}} = \mathrm{X_{i}} + \sum_{\mathrm{j}} \mathrm{W_{ij}F_{j}}.$$

(equation 3.1)

where F_i is the sum of all ingoing energy flux from species j, W_{ij} defines the proportion of F_i obtained from species j, e defines species feeding efficiency, and X_i represents the energetic loss from species i.

The weight of each trophic link was added to the list of trophic interactions. Note that energy flux could not be calculated for 137 food webs due to the model being unable to balance the energy flux with the given food web structure, thus the final number of food webs in our database is 4728. An example of a food web can be seen in Figure 3.4.

3.4 Data Record

The food webs are saved as two r.data files: one named FWTL.rdata, which contains a list of all 4728 trophic adjacency matrices; and the other named FWFin.rdata, which includes a list of all 4728 attribute tables. The attribute tables include columns called nodes (taxon names), M (body mass), N (abundance), feeding group, year, longitude, and latitude (the central coordinates of the focal grid). Both data files can be found on the University of Essex Data Repository (https://dx.doi.org/10.5526/ERDR-00000242).

3.5 Technical Validation

A major validation step of the food web construction was the yield-effort curves for fish diets. This ensured that the sampling completion of each fish predator's diet was at least 75% of what could be expected (Figure 3.1). At each step of the food web construction, we calculated the percentage completion of each predator in each food web, with the mean results presented in Table 3.1. In preliminary work using smaller than 100 km radii to sample a predator's diet, completion statistics were noticeably lower hence we chose 100 km as a balance between the data needed for diet completion and spatial resolution. We also attempted to minimise any differences due to sampling bias or changes in sampling effort across the region by taking a minimum of five and a maximum of ten hauls from the fish survey per food web. Furthermore, the food webs were not based on predetermined sampling location but were placed in a standardised way by gridding the study region and finding coordinate focal points. Food webs were also visually inspected using the *cheddar* package in R to observe any inconsistencies or outliers.

3.6 Usage notes

The code for reconstructing food webs across spatial and temporal scales is available on the authors' GitHub (https://github.com/amyshurety/Northeast_Atlantic_Food_Web_Construction), and the corresponding data required are found in the University of Essex Data Repository (https://dx.doi.org/10.5526/ERDR-00000242). Due to the dynamic nature of the 100 km radius used to collate surveys conducted near each focal grid coordinate, adjacent food webs share data so spatial and temporal autocorrelation should be expected. In this food web compilation, we constructed food webs that

were 50 km apart but were representations of a 100 km radius each year. However, care was taken to produce a methodological approach that could be readily applied to new data and/or spatial and temporal scales. The space between, size of the radius, spatial and temporal scale of the food webs can be altered by changing the variables indicated in Table 3.3. If monthly subsetting of the fish survey is required, here we only subset by year, then lines 122-145 of the R code should be included into the workflow.

We hope that this dynamic methodology and the database of North Sea food webs pioneers new research into how ecosystem structure and function vary across large spatio-temporal scales, and in response to different environmental drivers, thereby underpinning robust evidence for ecosystem-based management of heavily stressed ecosystems.

Table 3.3: Variables use to construct different spatial and temporal elements of each food web.

Variable name	Description
grid_m	Number of kilometres used to divide the North Sea into grid squares (here we used 50,000 m i.e. 50 km)
grid_radius	Number of kilometres used as a radius from the centre of the focal grid coordinate (here we used 100,000 m i.e.100 km)
year_min	Minimum year of required fish survey which ranges from 1997 to 2020 (here we used 1997)
year_max	Maximum year of required fish survey which ranges from 1997 to 2020 (here we used 2015)
lat_min	Minimum latitude of required fish survey which ranges from 36.0013 to 61.3535 degrees (here we used 51.25 degrees)
lat_max	Maximum latitude of required fish survey which ranges from 36.0013 to 61.3535 degrees (here we used 61.75 degrees)
long_min	Minimum longitude of required fish survey which ranges from -15.2333 to12.6190 degrees (here we used -3.5 degrees)
long_max	Maximum longitude of required fish survey which ranges from -15.2333 to12.6190 degrees (here we used 8.5 degrees)
year_min_stom	Minimum year of required stomach contents data which ranges from 1836 to 2016 (here we used -Inf to include all the data)
year_max_stom	Maximum year of required stomach contents data which ranges from 1836 to 2016 (here we used -Inf to include all the data)
lat_min_stom	Minimum latitude of required stomach contents data which ranges from 43.6405 to 80.0830 degrees (here we used -Inf to include all the data)
lat_max_stom	Maximum latitude of required stomach contents data which ranges from 43.6405 to 80.0830 degrees (here we used Inf to include all the data)
long_min_stom	Minimum longitude of required stomach contents data which ranges from -56.6000 to 49.9665 degrees (here we used -Inf to include all the data)
long_max_stom	Maximum longitude of required stomach contents data which ranges from -56.6000 to 49.9665 degrees (here we used Inf to include all the data)

3.7 Code availability

The code used to construct the food webs is available here (https://github.com/amyshurety/Northeast_Atlantic_Food_Web_Construction). Users have a series of parameters, such as the temporal and spatial resolution to generate food webs, that they can adjust, as described in Table 3.3.

4 Commercial fishing makes North Sea food webs more sensitive to increasing temperature

4.1 Abstract

Food webs provide a framework for understanding how environmental change and human pressures propagate through ecosystems via direct and indirect pathways. In marine systems, climate change and commercial fishing are prominent stressors, yet their combined effects on ecosystem structure and resilience remain poorly resolved. Here, we quantify how large gradients in temperature and commercial fishing relates to the structure and energy flux of 4,728 spatially resolved North Sea food webs sampled from 1997–2015 using ecological network analysis. At high temperatures, mean trophic level was reduced and food web robustness reconfigured, but other trophic responses depended on concurrent intensity of commercial fishing. Food webs remained broadly comparable across temperatures under low fishing pressure, whereas at high levels of commercial fishing, increasing temperatures were associated with declines in complexity and total energy flux, reducing trophic flexibility and energetic capacity. The cumulative effects of temperature and commercial fishing thus reconfigured key structural and energetic foundations of resilience, shifting food webs toward more constrained yet energy-poor configurations. These results illustrate that many properties of food-web structure and function exhibit heightened sensitivity to temperature under high levels of concurrent commercial fishing. The capacity of marine ecosystems to sustainably deliver resources such as food under warming may therefore need to be reconsidered in light of the broader food web effects on energy flow and ecosystem resilience reported here.

4.2 Introduction

Marine ecosystems provide essential goods and services, including food provision, climate regulation, and nutrient cycling, that underpin human well-being and global economies (Beaumont et al., 2008, 2007; Galparsoro et al., 2014). Environmental global change such as increasing sea surface temperatures (SST) and human exploitation are reshaping these ecosystems (Halpern et al., 2015, 2008; Shurety et al., 2026), altering the quality and sustainability of these services. However, the combined ecosystem effects of these stressors remain poorly resolved. Food webs provide a powerful framework for disentangling interacting drivers of global change

because they represent trophic interactions, that is who eats whom and quantify both the magnitude and organisation of energy flow among species (du Pontavice et al., 2020; Lynam et al., 2017; Thompson et al., 2020). By capturing both direct and indirect pathways (Bascompte et al., 2005; Lynam et al., 2017; Nordström et al., 2009), food webs describe ecosystem structure and energy flux in ways directly linked to ecosystem resilience.

Holling (1973) defined ecosystem resilience as the capacity of a system to absorb disturbance and reorganise while retaining its fundamental structure, functioning, and feedback. Ecosystem resilience emerges from how energy is distributed, constrained, and buffered across trophic interactions (Scharler et al., 2018). The structure and functioning of food webs therefore provide a basis for understanding how resilience varies across ecosystems and environmental conditions (Elton, 1927; Lindeman, 1942b; Link, 2002; Odum, 1980; Pimm, 1982), but empirical progress has been limited by the scarcity of large, multi-species datasets. Recent advances in coordinated monitoring and data collation (Pinnegar, 2014; Thompson et al., 2025) now enable the construction of spatially resolved food webs across broad environmental gradients.

Here, we analyse a novel suite of North Sea food webs spanning large spatial gradients in temperature and commercial fishing, enabling us to test how these two stressors interact to alter natural systems. The North Sea has experienced pronounced warming (Atkins et al., 2025; Mohamed et al., 2025) and remains among the most intensively exploited marine ecosystems globally (Halpern et al., 2015, 2008), providing an ideal system in which to examine how these drivers jointly structure trophic networks across space. We quantify variation in trophic structure and energy flow using widely applied network-level metrics (Fath et al., 2019; Kay et al., 1989).

Previous research indicates that warmer marine regions tend to support higher biodiversity (Hillebrand, 2004; Yvon-Durocher et al., 2015), and because metabolic rates increase exponentially with temperature (Brown et al., 2004), species interactions are likely to become more frequent and intense. As temperatures rise, we therefore expect food webs to become more complex and interconnected (connectance), with species feeding across multiple trophic levels and exhibiting

broader diets (omnivory). As generalist interactions (omnivory) become more common under warming (Martins et al., 2025; O'Gorman et al., 2012), functional overlap among species is also likely to increase (trophic redundancy), redistributing energy across multiple pathways and enhancing the system's capacity to absorb species loss (Biggs et al., 2020; Kharrazi et al., 2020; Ulanowicz, 2009, 2004; Ulanowicz et al., 2009). Increasing interaction density may reduce compartmentalisation within networks (modularity) and generate more integrated systems in which energy moves through longer pathways (average path length, APL). However, as energy is distributed across increasingly similar and extended pathways, the overall constraint and organisation of energy flow may decline (average mutual information, AMI) (Ulanowicz, 2009, 2004; Ulanowicz et al., 2009). Furthermore, because warming favours smaller-bodied taxa and species at lower trophic levels (Brown et al., 2004; Cheung et al., 2013; Coghlan et al., 2022), we expect a downward shift in overall trophic structure (mean trophic level). Higher temperatures are also expected to elevate overall ecosystem activity and energy availability (total system throughflow, TST), creating opportunities for greater internal recycling of energy as networks become more interconnected (Finn cycling index, FCI) (Habedank et al., 2024; Yvon-Durocher et al., 2015). Taken together, increasing temperatures alone is expected to generate food webs that are more connected, energetically rich, and pathway-diverse, yet less tightly organised in their trophic structure (Figure 4.1).

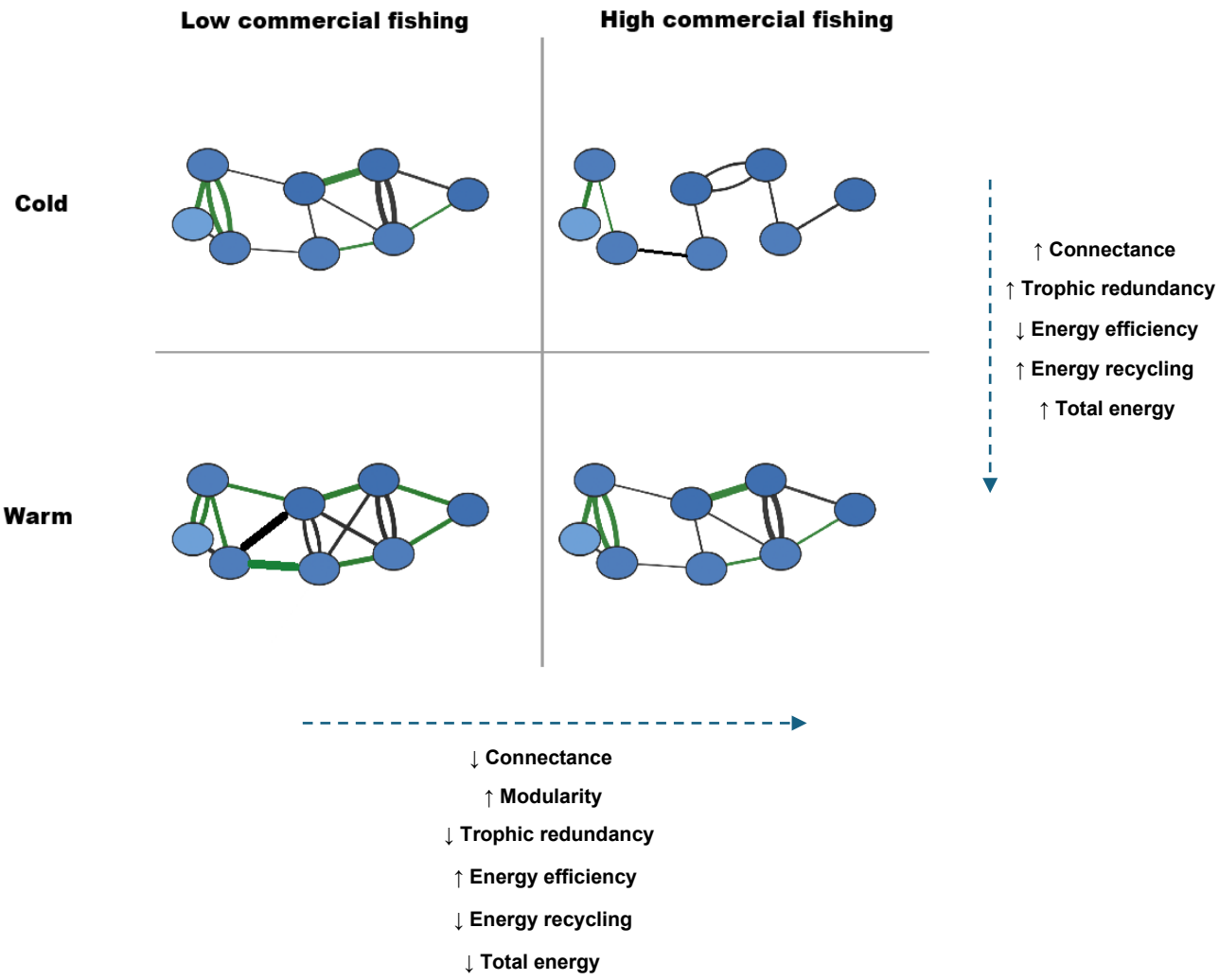

Figure 4.1: A conceptual diagram illustrating the expected changes in food web structure and function with increasing temperature and commercial fishing in the North Sea. The thickness of the links indicates the amount of energy within the trophic interaction; double links indicate redundancy and green links indicate those that hold recycled energy. The dashed arrows indicate an increase in either sea surface temperature or commercial fishing, and the smaller solid arrows indicate the expected direction of change in network-level metrics. We expect commercial fishing to dampen or offset temperature-induced increases in connectivity, redundancy, and energy flux, while amplifying temperature-driven declines in mean trophic level and modularity.

Commercial fishing, in contrast, imposes strong top-down pressure through the selective removal of large-bodied predators (Branch et al., 2010; Pauly et al., 1998),

truncating trophic structure and reducing mean trophic level. In doing so, commercial fishing may constrain the extent to which warming enhances trophic complexity. Although elevated temperatures are expected to promote greater interaction density (connectance), lengthen pathways (APL) due to broader feeding strategies (omnivory) (Martins et al., 2025; O'Gorman et al., 2012), the loss of higher trophic levels may limit such increases. Likewise, while increasing temperatures alone are expected to enhance trophic redundancy, biomass removal may reduce the pool of interacting species, thereby dampening temperature-driven gains in trophic redundancy and overall network connectivity. Furthermore, although increasing temperatures are expected to elevate system-wide activity and energy flux (TST) alongside greater internal recycling (FCI), sustained biomass extraction without compensatory production may reduce the energetic base required for these increases to occur, constraining temperature-related gains (Ito et al., 2023). Commercial fishing, by simplifying trophic pathways and limiting interaction diversity (Heymans et al., 2014a; Ito et al., 2023), may also moderate the expected temperature-driven decline in organisation (AMI), maintaining structurally constrained networks despite higher temperatures (Ulanowicz, 2009, 2004; Ulanowicz et al., 2009). We therefore expect commercial fishing to dampen or offset temperature-induced increases in connectivity, redundancy, and energy flux, while amplifying temperature-driven declines in trophic structure (mean trophic level) and compartmentalisation (modularity), such that under high fishing pressure, elevated temperature is unlikely to translate into greater trophic complexity or energetic expansion (Figure 4.1).

Ecosystem resilience is known to vary with the balance between organisation (structural constraint), redundancy (alternative pathways), and energy magnitude (functional capacity) (Gunderson et al., 2012; Holling, 1973), indicated by the robustness metric (Ulanowicz, 2009). Robustness is expected to decline where commercial fishing constrains energy throughput and redundancy, as diminished biomass and simplified trophic pathways reduce the capacity of the system to buffer perturbations (Figure 4.1). The combined impacts are therefore expected to shift structural properties in ways consistent with reduced resilience. Although food webs may become more flexible under increasing temperatures alone, commercial fishing reduces energy availability and pathway diversity (Heymans et al., 2014a; Ito et al.,

2023), increasing structural fragility and susceptibility to ecosystem-wide collapse under additional stress.

Here, we adopt a holistic food-web perspective to evaluate how increasing temperature and commercial fishing interact to jointly shape trophic organisation, energy flux, and ecosystem resilience within the North Sea. While the individual impacts of increasing temperatures and commercial fishing are relatively well understood, their cumulative effects on whole food webs remain comparatively unresolved. This research therefore advances our understanding of resilience dynamics in the region and strengthens the foundation for ecosystem-based management that accounts for impacts of climate change while maintaining sustainable levels of commercial fishing and long-term ecosystem resilience.

4.3 Methodology

4.3.1 Study Site

The North Sea study region spans from -3.5 ° W to 8.5 ° E and 51.25 to 61.75 ° N and experiences a temperate climate. It supports major ecosystem goods and services for many western European nations, including valuable commercial fisheries, mature oil and gas fields, rapidly expanding offshore wind infrastructure, and significant carbon sequestration. As a result, the North Sea is subject to some of the most intense anthropogenic pressures worldwide. At the same time, it has been the focus of extensive, often internationally coordinated research efforts, generating exceptionally rich datasets and long-term sampling records.

4.3.2 Data sources

4.3.2.1 fish survey data

For a more detailed explanation of the data sets and methodology used to construct the food webs please see chapter three, but we provide an overarching summary of the key steps here.

Fish community composition was obtained from the ICES DATRAS trawl survey database (Lynam and Riberio, 2022). To ensure consistency with available commercial fishing and environmental datasets, analyses were restricted to the period 1997–2015 and to hauls conducted within −3.5° W to 8.5° E and 51.24° to 61.75° N. The resulting dataset comprised 3,334,387 abundance observations of 371 taxa across 24,843 hauls. Abundances were recorded at regular body-size

intervals, and biomass estimates were derived from routine length–mass conversions. These data were used to identify locally occurring fish predators and to quantify their mean biomass, abundance, and body size within each food web.

4.3.2.2 Stomach contents data

Trophic interactions between predators and their prey were assembled from two major archives: DAPTSOM (Pinnegar et al., 2015) and ICES Year of the Stomach (ICES, 2010), collated following (Thompson et al., 2020). Although stomach samples span 1837–2016, only records from 1997–2015 were used to align with the fish survey data. The final dataset consisted of 415,658 trophic interaction records from 156,452 stomachs sampled across 6924 hauls. All taxonomic names were standardised, and entries unresolved above family level (e.g., “Decapoda”, “Chordata”, “Arthropoda”) were removed. Feeding guilds, such as planktivore, benthivore, bentho-piscivore, and piscivore, were assigned to all fish predators to account for ontogenetic dietary shifts (Thompson et al., 2025). Where direct corresponding feeding guild information was missing, feeding guilds were inferred from the most similar-sized congener. Predators lacking feeding-guild information and represented by fewer than ten observations were excluded.

4.3.3 Food-web construction

4.3.3.1 Spatial and temporal subsetting

The study region was divided into 50 × 50 km grid cells. Local food webs were generated for each grid-cell centroid and each year from 1997–2015 using all trawl survey hauls within a 100 km radius. To standardise sampling effort, a minimum of five and maximum of ten hauls were used, and when more than ten were available, the ten closest hauls were selected. All fish taxa detected within these hauls were included and assigned feeding guilds, whilst their mean biomass (kg km^{-2}), abundance (individuals km^{-2}), and body mass (g) were recorded. In parallel, the stomach contents database was subsetted by year and the same 100 km radius to identify all prey taxa present. Together, these two subsets defined the local species master list for each food web.

4.3.3.2 Assigning predator–prey interactions

To determine trophic interactions, all stomach contents observations from all years within the local 100 km radius were pooled for each predator species, ensuring

adequate coverage despite the patchy temporal distribution of stomach sampling. However, only interactions involving taxa present in the local species master list were retained (accounting for space and time). Genus-level observations were replaced by species-level names when a species from the same genus occurred locally; otherwise, genus-level nodes were retained.

Diet completeness for each predator was evaluated using species accumulation curves generated with the '*specaccum*' function (*vegan* package; Oksanen et al., 2007). Six accumulation models ("lomolino", "arrhenius", "gleason", "gitay", "asymp", "logis") were fitted using '*fitspecaccum*', and the best-fitting model was selected using the Akaike information criterion (AIC; Akaike, 1974). A diet was deemed satisfactorily represented when observed prey richness reached at least 75% of predicted richness.

Diets of predators failing this threshold were supplemented following an iterative hierarchy: 1. local data from congeneric species of similar size; 2. local congeneric species no more than twice the body size; 3. local species from the same feeding guild and of similar size; 4. local feeding-guild members no more than twice the size. If predator diet was still not satisfactorily complete, equivalent steps using the global stomach-content database were done. This procedure continued until diets reached the 75% completeness threshold. Across all food webs, the vast majority of predator diets (89%) met the sampling criterion, demonstrating strong coverage of dietary information. Nevertheless, all predators were included in the analysis, even those that were under sampled.

4.3.3.3 Prey–prey interactions

Prey taxa that were themselves fish underwent the same stomach-content procedure described above. Non-fish prey were assigned to one of sixteen feeding groups (Table 3.1) and their diets were inferred from the North Sea food-web model of (Daskalov and Mackinson, 2007; Mackinson and Daskalov, 2007). Interactions were established with all local taxa that fell within the inferred diet group. Basal resources, including phytoplankton, CPOM, FPOM, microalgae, macroalgae, fungi, and bacteria, were assumed ubiquitous and added to all food webs.

4.3.3.4 Biomass and abundance of prey

For non-fish prey, abundance was estimated directly from the number of occurrences in stomach contents, and biomass was calculated as abundance multiplied by recorded individual prey mass. Although digestion may affect prey mass estimates, these represented the best available estimates at the required spatiotemporal resolution.

4.3.3.5 Final assembly rules

All trophic interactions for fish predators, fish prey, and non-fish prey were combined to form each food web. Isolated nodes and cannibalistic links were removed. A final size-structuring constraint was imposed whereby no consumer could be smaller than its prey, justified by a minimum predator–prey mass ratio of 1.002 observed across the entire stomach-contents database. For each food web, a final attribute table was compiled including taxon names, feeding group, abundance, biomass, latitude, longitude, and year. Across 1997–2015, this procedure yielded 4865 food webs.

4.3.3.6 Weighting trophic interactions

Estimates of energy-flux (i.e. strengths of trophic interactions) were calculated using the '*fluxing*' function in the *fluxweb* package described by equation 4.1 (Gauzens et al., 2019), which estimates steady-state energy flows based on allometric scaling relationships (Petchey et al., 2008; Vucic-Pestic et al., 2010). The model assumes that energetic gains from consumption equal the sum of losses due to predation and physiological costs:

$$\sum_j W_{ji} F_i e_{ij} = X_i + \sum_j W_{ij} F_j.$$

(equation 4.1)

where W_{ij} is the proportion of consumer j's flux derived from prey i, F_i is total incoming flux to species i, e_{ij} is feeding efficiency, and X_i is metabolic loss. Flux calculations failed for 137 food webs due to being unable to balance (i.e. input equals output) energy flux with the given food web structure, resulting in a final dataset of 4728 flux-weighted food webs (Figure 4.2). The largest food web contained 320 nodes and 20,724 links, and the smallest contained 50 nodes and 543 links (Figure 4.2).

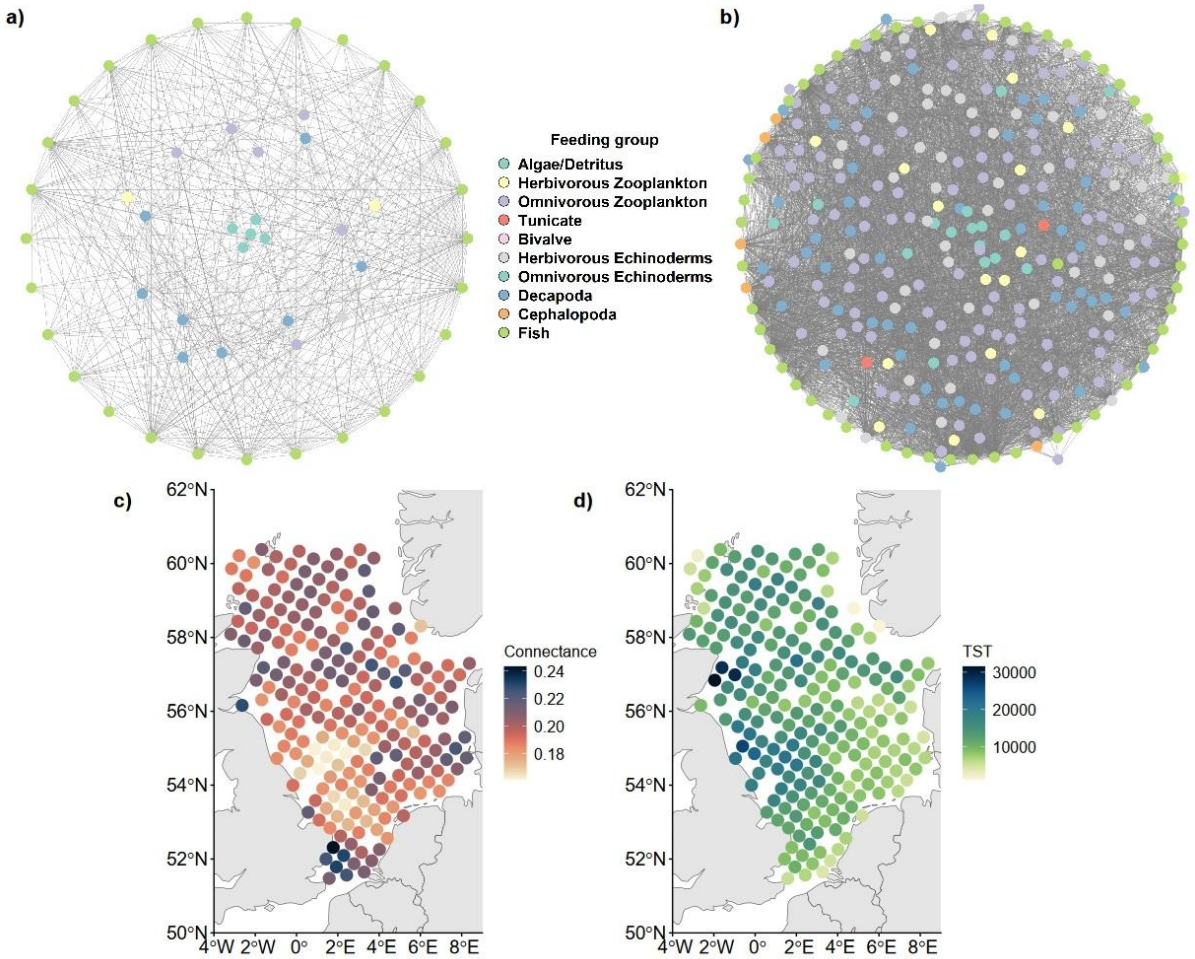

Figure 4.2: **a)** The smallest food web (50 nodes and 543 trophic interactions) used within this study illustrating the network within 50 km of the central coordinate of 4.78 ° E and 58.79 ° N 1859 in 2003. **b)** The largest food web (320 nodes and 20,724 trophic interactions) used within this study illustrating the network within 50 km of the central coordinate of -1.96 ° W and 56.84 ° N 1861 in 2003. The bottom panel contains maps illustrating the location of all 4728 food 1862 webs with their corresponding **c)** connectance and **d)** total system throughflow (TST) 1863 ($mgCm^{-2}year^{-1}$) values.

4.3.4 Environmental gradients

Daily sea surface temperature data (°C) from both satellite and in situ observations were extracted from the Copernicus open access data repository (Donlon et al., 2012; Good et al., 2020; Stark et al., 2007b). The mean sea surface temperature (henceforth 'temperature') for each food web was calculated by taking the mean temperature of all records from the given year and within a 100 km radius of the grid-cell centroid. Commercial fishing (hours per year) was taken from reconstructed

North Sea trawling effort from 1985 – 2015 (Couce et al., 2020) and a yearly mean was calculated for each food web from a 100 km radius around each grid-cell centroid. For visualisation purposes, the commercial fishing data was divided into three bins each containing an equal number of observations, and the median of each bin was calculated to and used to predict three bin-specific predictions of each metric. Furthermore, the proportion of commercial fishing that came from beam trawling was calculated. Other explanatory variables were linked to each food web including depth (m), salinity (ug/l), and chlorophyl, which were taken from the ICES open-source data portal (ICES Data Portal, Dataset on Ocean HydroChemistry, ICES, Copenhagen). A mean per year for each 100 km radius around each grid-cell centroid was calculated.

4.3.5 Network-level metrics

Food-web metrics provide quantitative measures of ecosystem structure and functioning. ENA offers a suite of metrics to characterise trophic interactions and energy flow within environmental networks (Baird and Ulanowicz, 1989; de la Vega et al., 2018; Mukherjee et al., 2015; Schückel et al., 2022). We calculated ENA metrics for all 4,728 food webs, many of which are recognised indicators under OSPAR (OSPAR, 2023).

Connectance represents the proportion of realised trophic interactions relative to all possible links in the network (Albert and Barabási, 2002), providing a measure of interaction density and overall system complexity. Mean trophic level describes the biomass-weighted position of species within the food web (Pauly et al., 1998) and is widely used to assess top-down impacts such as commercial fishing. Modularity quantifies the degree to which nodes form semi-independent clusters (Newman, 2006), with higher modularity potentially limiting the spread of perturbations across compartments (Krause et al., 2003; Stouffer and Bascompte, 2011). APL represents the mean number of trophic steps through which energy flows from basal resources to higher consumers (Hirata and Ulanowicz, 1986), reflecting the indirectness and potential dissipation of energy transfer within the system.

TST measures the total quantity of energy passing through all nodes in the network ($mgCm^{-1}year^{-1}$; Finn, 1976) and provides an index of ecosystem size and activity (Chen et al., 2011; Patrício and Marques, 2006). FCI quantifies the proportion of TST

that is recycled through feedback trophic loops (%; Finn, 1980, 1976), indicating the degree of internal energy retention within the food web. Omnivory describes the extent to which consumers feed across multiple trophic levels (Pimm and Lawton, 1978), capturing the prevalence of generalist interactions and cross-level energy flow. AMI measures the degree to which energy flows are organised and constrained within specific pathways (bits; Hirata and Ulanowicz, 1986; Rutledge et al., 1976), with higher values indicating more efficient and concentrated energy transfer (Fath et al., 2019). Redundancy reflects the extent to which energy is distributed across parallel, functionally similar pathways (bits; Ulanowicz, 1996), providing alternative routes for energy flow. Robustness, calculated as the ratio of AMI to redundancy (Ulanowicz, 2009), captures the balance between organisational efficiency and pathway diversity. Intermediate values are associated with systems operating within the “window of vitality,” where energy transfer is both efficient and sufficiently redundant to avoid structural fragility (Ulanowicz, 2009).

All food webs were mass balanced prior to analysis, ensuring that inputs equalled outputs at each node. Balancing was conducted using the balancing function in the *enaR* package (Borrett and Lau, 2014). Further details on metric calculation are provided in Table 1.1 and described in Kay et al., 1989 and Borrett and Lau, 2014. Example of metrics calculated for each food web across the North Sea can be found in Figure 4.2.

4.3.6 Statistical Analysis

All statistical analyses and visualisations were conducted using R v4.2.2 (R Core Team, 2024). A non-linear Generalized Additive Mixed Model (GAMM) was used to test the relationship between each metric and the main and interactive effects of temperature and commercial fishing. TST, FCI and commercial fishing were $\log_{10}$-transformed to meet the assumptions of normality and homogeneity. The model included additional continuous smoothers of salinity, depth (m), number of nodes and year, as well as random effect of the proportion of commercial fishing that was beam trawling. Spatial autocorrelation was adequately accounted for using an AR1 correlation structure (see Table S4.1). Model selection of the fixed and random effects for each metric was conducted using Akaike information criterion (AIC; Akaike, 1974). See all model formulas and diagnostics (Figure S4.1-4.11 and Table S4.2) in the supplementary material. To note the main effects of commercial fishing

was included in the model but are not discussed within this study (Table S4.3 and Figure S4.12).

The percentage change values represented in the results are the total deviation from the mean across the temperature gradient as a percentage of the metric mean from the original sample. This was the most intuitive way to understand a change in the metric due to temperature and commercial fishing as well as the most consistent with the figures presented. In the results section these values are represented as the percentage change for easier reading.

4.4 Results

The direction and magnitude of change in network-level metrics depended on temperature as well as the degree of commercial fishing, with largely non-linear relationships (Table 4.1, Figure 4.3). There were significant interactive effects of temperature and commercial fishing on several metrics, indicating that the responses to increasing temperature were contingent on the level of commercial fishing.

Table 4.1: The main effect of temperature and interactive effects of temperature and commercial fishing from GAMM models performed on each network metric. The main effects of commercial fishing can be found in the supplementary material (Table S4.3, Figure S4.12).

Metric	**Main effect of temperature**			**Interaction between temperature and commercial fishing**		
	edf	**F Value**	**P Value**	**edf**	**F Value**	**P Value**
Connectance	4.174	12.333	**< 0.005**	14.29	2.618	**< 0.005**
Mean trophic level	3.929	9.096	**< 0.005**	10.510	1.744	0.062
Modularity	1	0.247	0.619	8.041	2.937	**0.002**
Average path length	3.5	18.27	**< 0.005**	9.138	5.921	**< 0.005**
Total system throughflow	3.984	9.614	**< 0.005**	3.98	9.61	**< 0.005**
Finn cycling index	1	0.001	0.9735	1.914	1.95	0.0987
Omnivory	2.962	1.37	0.218	17.9	2.237	**0.002**
Redundancy	4.247	12.673	**< 0.005**	14.49	2.17	**0.006**
Average mutual Information	3.47	5.496	**< 0.005**	9.436	1.339	**< 0.005**
Robustness	3.665	6.624	**< 0.005**	10.505	1.446	0.146

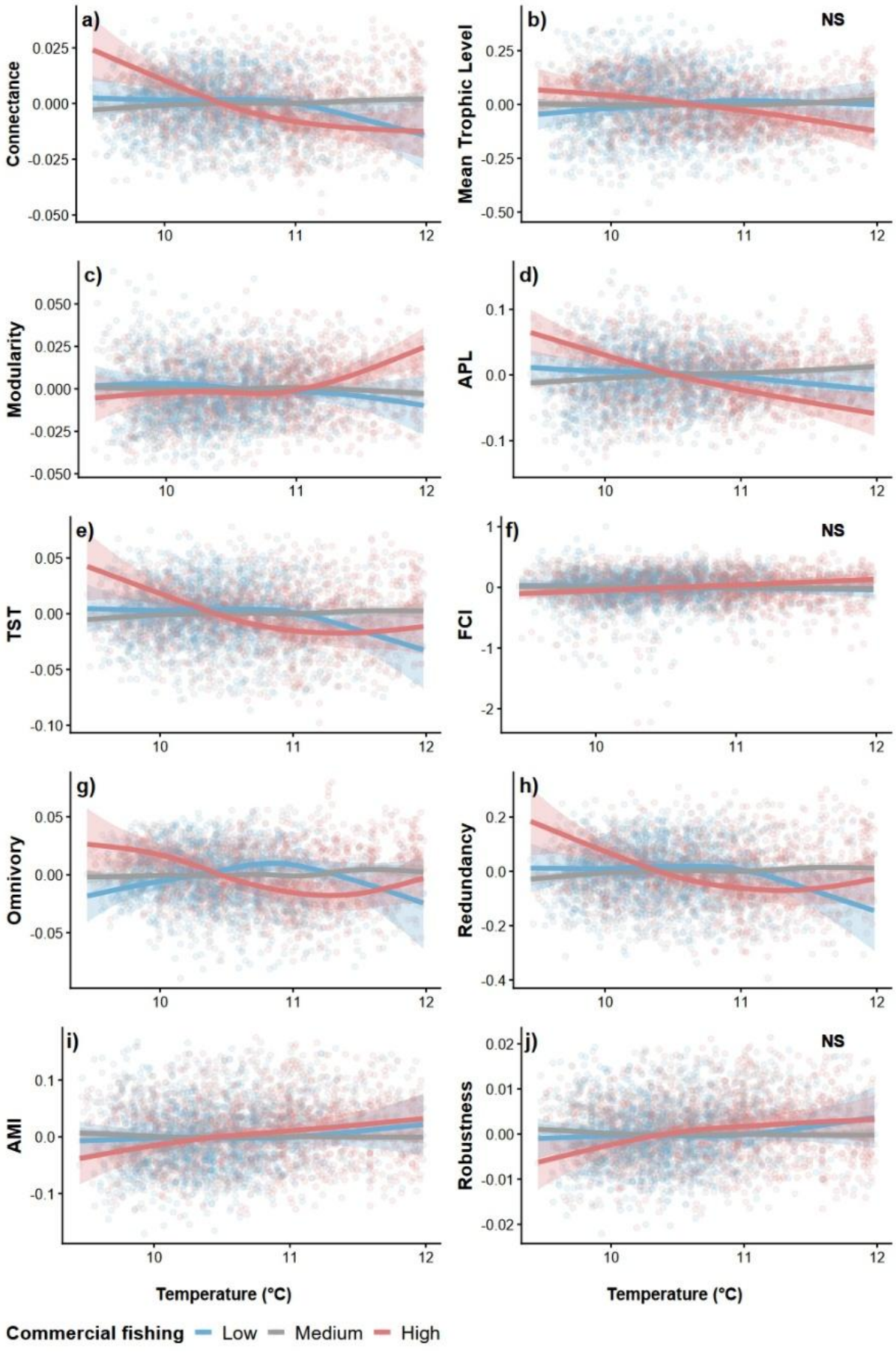
a)
Connectance
0.025
0.000
-0.025
-0.050
b)
NS
Mean Trophic Level
0.25
0.00
-0.25
-0.50
c)
Modularity
0.050
0.025
0.000
-0.025
-0.050
d)
APL
0.1
0.0
-0.1
e)
TST
0.05
0.00
-0.05
-0.10
f)
NS
FCI
1
0
-1
-2
g)
Omnivory
0.05
0.00
-0.05
h)
Redundancy
0.2
0.0
-0.2
-0.4
i)
AMI
0.1
0.0
-0.1
j)
NS
Robustness
0.02
0.01
0.00
-0.01
-0.02
10
11
12
Temperature (°C)
Commercial fishing
Low
Medium
High

1990

Figure 4.3: Partial effects of temperature (°C) and commercial fishing (hours yr^{-1}) on food-web metrics, estimated using generalized additive mixed models. Panels show: **a**) connectance (R^2 = 0.29); **b**) mean trophic level (R^2 = 0.33); **c**) modularity (R^2 = 0.15); **d**) average path length (APL; R^2 = 0.72); **e**) total system throughflow (TST, $mgCm^{-2}year^{-1}$; $\log_{10}$ transformed; R^2 = 0.975); **f**) FCI (%, $\log_{10}$ transformed, R^2 = 0.289); **g**), omnivory (R^2 = 0.403); **h**), redundancy (bits, R^2 = 0.975); **i**)**,** average mutual information (bits, AMI; R^2= 0.236) and **j**) robustness (R^2 = 0.669). To visualise interactions between commercial fishing ($\log_{10}$ transformed) and temperature, we show the temperature effect at low (100–1,720 hours $year^{-1}$), medium (1,720–4,620 hours $year^{-1}$), and high (4,620–27,800 hours $year^{-1}$) commercial fishing categories. Non-significant relationships are indicated by NS in the top-right corner of the panel.

Connectance exhibited significant interactive effects (Table 4.1 and Figure 4.3a). Contrary to expectations of temperature-driven increases, connectance declined consistently across the temperature gradient under both low (by −9%) and high commercial fishing (by −15.42%; Table 4.2), with the strongest declines observed under high commercial fishing (Figure 4.4). Mean trophic level significantly declined with increasing temperature (Table 4.1 and Figure S4.13), supporting expectations of trophic truncation, however, this response was not modified by commercial fishing (Table 4.1 and Figure 4.b). Modularity also showed significant interaction effects (Table 4.1 and Figure 4.3c), declining with temperature under low and moderate commercial fishing but increasing markedly under high commercial fishing (by 25.76%; Table 4.2 and Figure 4.4). Variation in APL was similarly significantly moderated by commercial fishing (Table 4.1 and Figure 4.3d), with temperature-associated increases only under intermediate and declines under high commercial fishing (by −4.54%; Table 4.2 and Figure 4.4).

Patterns in energy flux were likewise contingent on temperature and commercial fishing intensity. TST did not increase with rising temperature as predicted. Instead, a significant temperature and commercial fishing interaction (Table 4.1 and Figure 4.3e) revealed that TST declined across the temperature gradient under both low (by −0.91%) and high fishing (by −1.33%), while remaining relatively stable under moderate commercial fishing (increasing by 0.19%) (Table 4.2 and Figure 4.4). FCI showed no significant response to either temperature or commercial fishing (Table 4.1 and Table S4.4). Metrics associated with interaction breadth and pathway

diversity were similarly constrained. Omnivory did not increase with temperature alone but showed exacerbated declines across the temperature gradient in areas under high commercial fishing (by −3.65%; Table 4.1, 4.2; Figure 4.3g and Figure 4.4). Redundancy did significantly decline with increasing temperatures alone which was significantly moderated by commercial fishing (Table 4.1 and Figure 4.3h). A high level of commercial fishing further reduced redundancy (by −1.69%; Table 4.2 and Figure 4.4) compared to low levels of commercial fishing (by −1.24%; Table 4.2 and Figure 4.4). This indicated a reduction rather than the expected expansion of alternative trophic pathways with increased temperatures. Similarly in contrary to predictions AMI increased with temperature under both low (by 2.39%) and high commercial fishing (by 5.77%; Table 4.1, 4.2; Figure 4.3i and Figure 4.4). Robustness increased significantly across the temperature gradient and was not significantly altered by fishing intensity (Table 4.1 and Figure 4.3j).

In summary, rather than promoting widespread increases in complexity and energy flux, increasing temperature was associated with reduced connectivity, constrained throughput, and declining redundancy, with high commercial fishing amplifying this structural simplification, reduced energy flux and increased network organisation.

Table 4.2: Percentage change in food web metrics across the temperature gradient within each commercial fishing category. The commercial fishing categories were low (100–1,720 hours year^{-1}), medium (1,720–4,620 hours year^{-1}), and high (4,620–27,800 hours year^{-1}). The relationships were largely non-linear (see Figure 4.3). Positive and negative values denote the direction of deviation from the predicted mean. Metrics with an asterix denote statistically significant interactive relationships with temperature and commercial fishing.

Metric	**Low commercial fishing**	**Medium commercial fishing**	**High commercial fishing**
Connectance *	-9.32	2.44	-15.42
Mean Trophic Level	1.11	0.47	-4.73
Modularity *	-9.9	-3.11	25.76
APL *	-1.24	0.92	-4.54
TST *	-0.91	0.19	-1.33
FCI	-1.719	-0.777	5.629
Omnivory *	-0.76	0.525	-3.65
Redundancy *	-1.239	0.316	-1.686
AMI *	2.393	-0.638	5.777
Robustness	2.067	-0.557	4.187

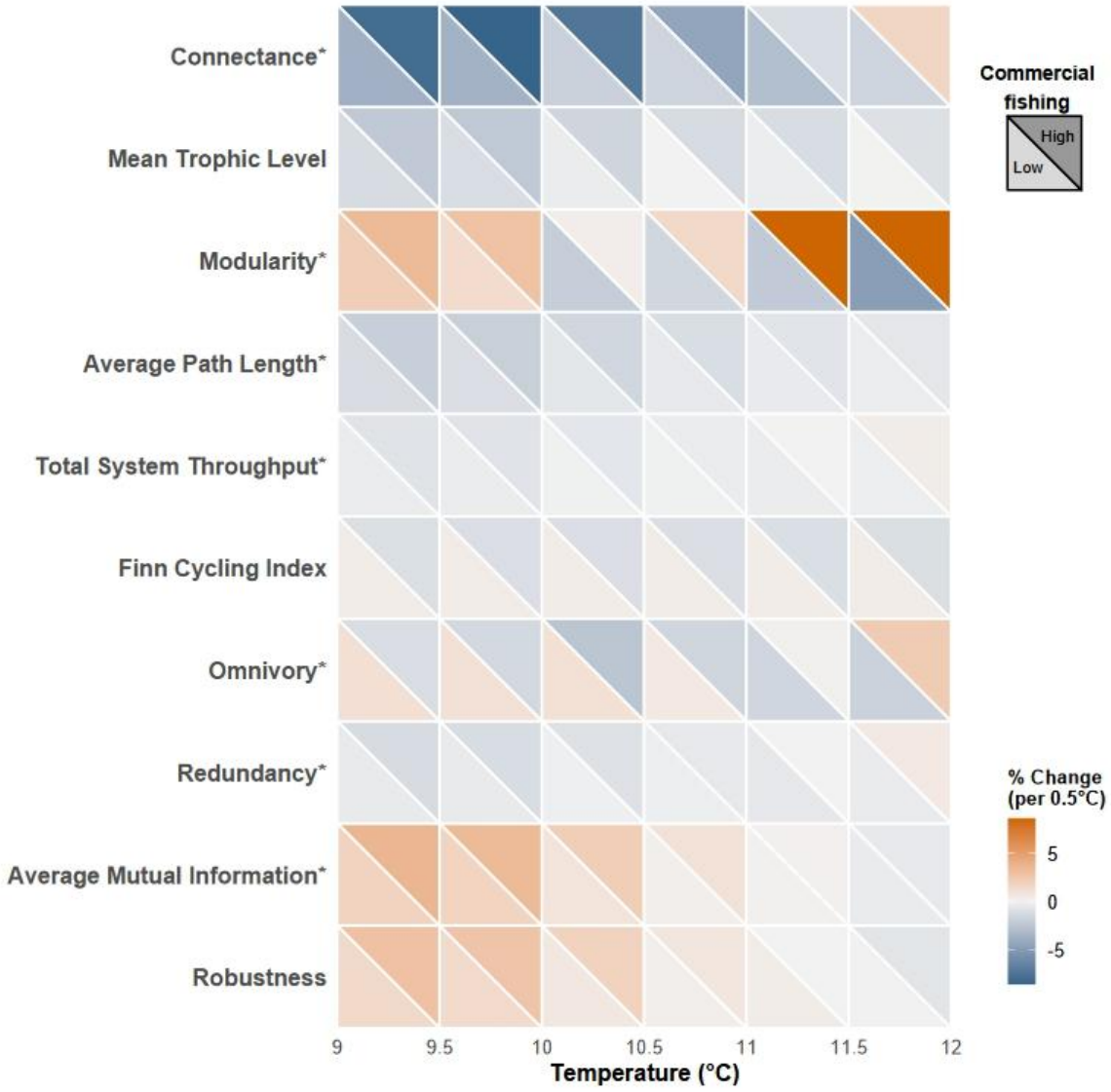

Figure 4.4: Percentage change (per 0.5 °C) in network-level metrics across the North Sea temperature gradient. Within each cell, the lower-left triangle represents low commercial fishing, and the upper-right triangle represents high commercial fishing. Positive values (orange) indicate increases with temperature, whereas negative values (blue) indicate declines. Metrics marked with an asterisk exhibited statistically significant temperature and commercial fishing interactions (see Table 4.1).

4.5 Discussion

Food webs of the North Sea exhibit substantial reorganisation in response to large spatial and temporal gradients in temperature and commercial fishing. The magnitude and direction of changes within the food webs depend on the interaction between these stressors, with commercial fishing markedly amplifying thermal

sensitivity. Commercial fishing therefore plays a pivotal role in determining whether the degree to which rising temperatures reinforce or erode particular components of ecosystem resilience in the North Sea. Commercial fishing, by truncating age structure, weakening predator control, and reducing interaction diversity, can erode stabilising dynamics and increase population variability and sensitivity to environmental conditions (Hsieh et al., 2006). Climate–fishing interactions have likewise been shown to amplify ecosystem responses to environmental conditions, accelerating regime shifts in the North Atlantic (Kirby and Beaugrand, 2009), further supporting the role of commercial fishing as a key moderator of thermal sensitivity of marine food webs. Moreover, unlike localised food-web studies, our analysis reveals that these responses emerge across broad spatiotemporal gradients and thousands of food webs, reinforcing evidence that temperature effects are conditional on concurrent anthropogenic pressures.

As expected, increasing temperature reduced mean trophic level, truncating energy pathways, consistent with patterns observed in other marine regions such as the Baltic Sea and San Jorge Gulf (Funes et al., 2022; Tomczak et al., 2013). However, several predicted temperature-driven increases in trophic complexity and energy flow were not consistently supported and were contingent on the degree of commercial fishing. Despite evidence of trophic truncation, overall food-web properties remain broadly comparable between colder and warmer regions of the North Sea under moderate levels of commercial fishing, with some metrics including modularity, and robustness showing limited divergence. In contrast, intense commercial fishing amplifies the thermal sensitivity of multiple food web properties in the North Sea. Contrary to expectations, connectance, APL, TST, redundancy, and omnivory only increased with temperature at moderate but declined under high commercial fishing. This demonstrated that biomass removal under high commercial fishing amplifies unexpected temperature-associated reductions in trophic complexity and energy flow. Increased temperatures have been shown to reduce predator persistence (Binzer et al., 2016) which together with the targeted removal of predators by commercial fishing (Pauly and Palomares, 2005) could result in the exacerbated simplification of food web structure. Furthermore, temperature-dependent changes in attack rates and handling times can alter the potential and strength of trophic interactions, potentially reducing connectance and energy flux as temperature

increases (Coll et al., 2008; Pauly et al., 1998). Energy flux in the English Channel and Eastern Mediterranean was also found to be particularly sensitive to fishing pressure, with energy flow declining with increasing commercial fishing (Corrales et al., 2018; Ito et al., 2023). These results also suggest that loss of omnivorous interactions is associated with simultaneous declines in energy availability and trophic flexibility, highlighting the disproportionate importance of generalist consumers for maintaining functional redundancy that supports ecosystem resilience (Kharrazi et al., 2016; Mukherjee et al., 2015; Schückel et al., 2015). Previous studies have shown that omnivory can stabilise food webs by dampening population oscillations and distributing energy across multiple pathways (Gellner and McCann, 2016; McCann and Hastings, 1997).

We further expected that increasing temperature in the North Sea would increase redundancy but reduce organisation (AMI), generating food webs that are more flexible yet less constrained. Instead, trophic redundancy declined while organisation increased with temperature, a pattern further exacerbated by high commercial fishing. The rise in AMI is consistent with the concurrent increase in modularity under high exploitation (Wechsler and Bascompte, 2024), suggesting the concurrent greater compartmentalisation may promote increasingly efficient energy flow. Empirical analyses suggest that modular organisation can buffer secondary extinction cascades while maintaining local efficiency of energy transfer (Rezende et al., 2009; Stouffer and Bascompte, 2011). Although modularity can buffer disturbances (Grilli et al., 2016; Stouffer and Bascompte, 2011), here greater compartmentalisation coincided with reduced total energy flow and less diverse trophic pathways, also critical when buffering disturbances (Fath et al., 2019).

Therefore we need to consider the balance between flexibility (redundancy) and efficiency (AMI) in energy pathways (Ulanowicz, 2009), i.e. robustness, which varied primarily with temperature and was not significantly moderated by commercial fishing, contrary to expectations that exploitation would further reduce it. As robustness reflects the trade-off between these properties, the opposing effects of temperature and commercial fishing on AMI and redundancy likely offset one another, resulting in little net change in robustness. Instead, robustness was lowest at thermal extremes, indicating a more balanced trade-off between trophic

redundancy and efficiency at intermediate temperatures in the North Sea. These characteristics are critical for ecosystem resilience, as redundancy supports adaptive capacity while organisation maintains efficient energy flow following disturbance (Scharler et al., 2018; Tomczak et al., 2013). However, as increasing temperature and high commercial fishing reduced pathway redundancy, concurrent increases in trophic organisation may mask underlying declines in resilience, creating systems that appear structurally robust yet possess diminished adaptive capacity. A similar disproportionate reduction in redundancy, associated with lowered resilience, has been observed in the Baltic Sea under both warming and fishing pressure (Tomczak et al., 2013). Such patterns are consistent with resilience theory whereby ecosystems can prioritise apparent structural organisation while losing adaptive capacity and approaching potential thresholds of regime shifts (Allen et al., 2014; Dakos et al., 2019; Scheffer and Carpenter, 2003).

The results demonstrate network-level responses to combined stressors using a novel set of food webs across a large spatiotemporal scale. Establishing empirical patterns in network-level metrics provides a benchmark against which change can be detected, interpreted, and managed (Fath et al., 2019; Heymans et al., 2014b). Here, concurrent increases in temperatures and high commercial fishing have shifted North Sea food webs from relatively complex, energy-rich, and redundant configurations in colder regions toward simpler and more specialised structures that hold less energy in warmer regions (Figure 4.5). As ecosystem resilience is structured by the balance between energy magnitude, pathway redundancy, and organisational constraint (Folke et al., 2016; Holling, 1973; Scharler et al., 2018; Walker et al., 2004), these combined pressures have altered this balance toward systems that are more tightly organised for efficient energy transfer but less flexible, thereby restructuring resilience across the region.

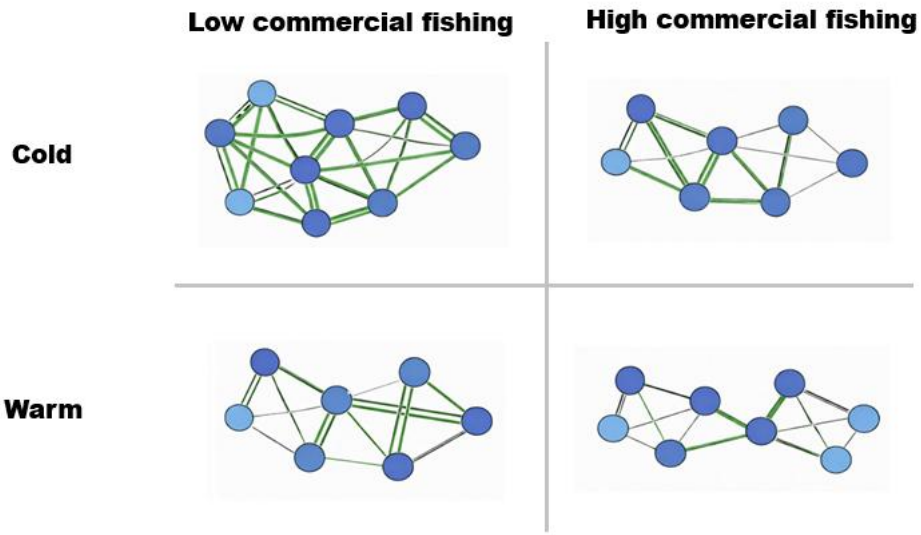

Figure 4.5: A conceptual diagram illustrating the observed changes in food web structure and function with increasing temperature and commercial fishing in the North Sea. The thickness of the links indicates the amount of energy within the trophic pathway; double links indicate redundancy and green links indicate those that hold recycled energy. The cumulative impacts of increasing temperatures and commercial fishing have resulted in ecosystems that are more tightly organised for efficient energy transfer but less flexible, thereby restructuring resilience across the North Sea.

Several network-level metrics that respond most strongly to combined increases in temperature and commercial fishing (e.g. TST, connectance, omnivory, redundancy) closely correspond to structural and functional properties targeted by international marine protection agreements such as OSPAR (Schückel et al., 2022). Our findings therefore complement and extend existing regional policy frameworks by clarifying empirically how food-web structure and energy flux shifts across large spatiotemporal gradients in environmental drivers such as temperature and commercial fishing. Furthermore, despite the relatively small thermal gradient, food webs at both the cold and warm extremes of the North Sea appear most sensitive to commercial fishing. Effective management should therefore prioritise sustainable fishing practices in areas approaching thermal extremes, a vulnerability likely to intensify under continued climate change (IPCC, 2023). Fixed management thresholds may consequently underestimate risk in northern temperate seascapes.

For example, omnivorous and generalist species in thermally stressed areas within key fishery grounds should be identified and protected as they are shown to disproportionally support energy flow and ecosystem resilience. Incorporating food-web responses to changes in temperature and commercial fishing into policy assessment and management frameworks could improve early detection of structural reorganisation, shifts in energy flow, and emerging changes in ecosystem resilience. Embedding network-level indicators within ecosystem-based management would support more spatially adaptive, climate-informed fisheries strategies, strengthening the capacity to sustain ecosystem resilience while maintaining the long-term delivery of marine ecosystem goods and services under continued warming.

4.6 Supplementary Material

Connectance GAMM Formula:

$$g(\mathbb{E}[Connectance_i]) = \beta_0 + s(Temperature_i) + s(\log_{10}\mathrm{FE}_i) + ti(Temperature_i, \log_{10}\mathrm{FE}_i) + s(n_i) + +s(\mathrm{Depth}_i) + s(\mathrm{Sal}_i) + b_{\mathrm{BeamClass}(i)} + s(\mathrm{Year}_i)$$

where $s(\cdot)$are penalized spline smooths, $ti(\cdot,\cdot)$is a tensor-product interaction smooth, $b_{\mathrm{BeamClass}} \sim \mathcal{N}(0, \sigma_b^2)$is a random effect, and residuals follow an exponential spatial correlation structure within years. *FE* is Fishing effort (hours per year), *n* is the number of nodes within the food web, *Sal* is salinity and *BeamClass* is the proportion of beam trawling within the fishing effort.

Mean Trophic Level GAMM Formula:

$$g(\mathbb{E}[MTL]) = \beta_0 + s(Temperature_i) + s(\log_{10}\mathrm{FE}_i) + ti(Temperature_i, \log_{10}\mathrm{FE}_i) + s(n_i) + s(\mathrm{Depth}_i) + s(\mathrm{Sal}_i) + b_{\mathrm{BeamClass}(i)} + s(\mathrm{Year}_i)$$

where $s(\cdot)$are penalized spline smooths, $ti(\cdot,\cdot)$is a tensor-product interaction smooth, $b_{\mathrm{BeamClass}} \sim \mathcal{N}(0, \sigma_b^2)$is a random effect, and residuals follow an exponential spatial correlation structure within years.

Modularity GAMM Formula:

$$g(\mathbb{E}[Modularity_i]) = \beta_0 + s(Temperature_i) + s(\log_{10}\mathrm{FE}_i) + ti(Temperature_i, \log_{10}\mathrm{FE}_i) + s(n_i) + s(\mathrm{Depth}_i) + s(\mathrm{Sal}_i) + b_{\mathrm{BeamClass}(i)} + s(\mathrm{Year}_i)$$

where $s(\cdot)$are penalized spline smooths, $ti(\cdot,\cdot)$is a tensor-product interaction smooth, $b_{\mathrm{BeamClass}} \sim \mathcal{N}(0, \sigma_b^2)$is a random effect, and residuals follow an exponential spatial correlation structure within years.

Average Path Length (APL) GAMM Formula:

$$g(\mathbb{E}[APL_i]) = \beta_0 + s(Temperature_i) + s(\log_{10}\mathrm{FE}_i) + ti(Temperature_i, \log_{10}\mathrm{FE}_i) + s(n_i) + s(\mathrm{Depth}_i) + s(\mathrm{Sal}_i) + b_{\mathrm{BeamClass}(i)} + s(\mathrm{Year}_i)$$

where $s(\cdot)$are penalized spline smooths, $ti(\cdot,\cdot)$is a tensor-product interaction smooth, $b_{\mathrm{BeamClass}} \sim \mathcal{N}(0, \sigma_b^2)$is a random effect, and residuals follow an exponential spatial correlation structure within years.

Total System Throughput (TST) GAMM Formula:

Let $Y_i = log_{10}(TST_i)$.

Then

$$g(\mathbb{E}[Y_i]) = \beta_0 + s(Temperature_i) + s(\log_{10}\mathrm{FE}_i) + ti(Temperature_i, \log_{10}\mathrm{FE}_i) + s(n_i) + b_{\mathrm{BeamClass}(i)} + s(\mathrm{Year}_i)$$

where $s(\cdot)$are penalized spline smooths, $ti(\cdot,\cdot)$is a tensor-product interaction smooth, $b_{\mathrm{BeamClass}} \sim \mathcal{N}(0, \sigma_b^2)$is a random effect, and residuals follow an exponential spatial correlation structure within years.

Finn Cycling Index (FCI) GAMM Formula:

Let $X_i = log_{10}(FCI_i)$.

Then

$$g(\mathbb{E}[X_i]) = \beta_0 + s(Temperature_i) + s(\log_{10}\mathrm{FE}_i) + ti(Temperature_i, \log_{10}\mathrm{FE}_i) + s(n_i) + s(\mathrm{Depth}_i) + s(\mathrm{Sal}_i) + b_{\mathrm{BeamClass}(i)} + s(\mathrm{Year}_i)$$

where $s(\cdot)$are penalized spline smooths, $ti(\cdot,\cdot)$is a tensor-product interaction smooth, $b_{\mathrm{BeamClass}} \sim \mathcal{N}(0, \sigma_b^2)$is a random effect, and residuals follow an exponential spatial correlation structure within years.

Omnivory GAMM Formula:

$$g(\mathbb{E}[Omnivory_i]) = \beta_0 + s(Temperature_i) + s(\log_{10}\mathrm{FE}_i) + ti(Temperature_i, \log_{10}\mathrm{FE}_i) + s(n_i) + s(\mathrm{Depth}_i) + s(\mathrm{Sal}_i) + b_{\mathrm{BeamClass}(i)} + s(\mathrm{Year}_i)$$

where $s(\cdot)$are penalized spline smooths, $ti(\cdot,\cdot)$is a tensor-product interaction smooth, $b_{\mathrm{BeamClass}} \sim \mathcal{N}(0, \sigma_b^2)$is a random effect, and residuals follow an exponential spatial correlation structure within years.

Redundancy GAMM Formula:

$$g(\mathbb{E}[Redundancy_i]) = \beta_0 + s(Temperature_i) + s(\log_{10}\mathrm{FE}_i) + ti(Temperature_i, \log_{10}\mathrm{FE}_i) + s(n_i) + s(\mathrm{Depth}_i) + s(\mathrm{Sal}_i) + b_{\mathrm{BeamClass}(i)} + s(\mathrm{Year}_i)$$

where $s(\cdot)$are penalized spline smooths, $ti(\cdot,\cdot)$is a tensor-product interaction smooth, $b_{\mathrm{BeamClass}} \sim \mathcal{N}(0, \sigma_b^2)$is a random effect, and residuals follow an exponential spatial correlation structure within years.

Average Mutual Information (AMI) GAMM Formula:

$$g(\mathbb{E}[AMI_i]) = \beta_0 + s(Temperature_i) + s(\log_{10}\mathrm{FE}_i) + ti(Temperature_i, \log_{10}\mathrm{FE}_i) + s(n_i) + b_{\mathrm{BeamClass}(i)} + s(\mathrm{Year}_i)$$

where $s(\cdot)$are penalized spline smooths, $ti(\cdot,\cdot)$is a tensor-product interaction smooth, $b_{\mathrm{BeamClass}} \sim \mathcal{N}(0, \sigma_b^2)$is a random effect, and residuals follow an exponential spatial correlation structure within years.

Robustness GAMM Formula:

$$g(\mathbb{E}[Robustness_i]) = \beta_0 + s(Temperature_i) + s(\log_{10}\mathrm{FE}_i) + ti(Temperature_i, \log_{10}\mathrm{FE}_i) + s(n_i) + b_{\mathrm{BeamClass}(i)} + s(\mathrm{Year}_i)$$

where $s(\cdot)$are penalized spline smooths, $ti(\cdot,\cdot)$is a tensor-product interaction smooth, $b_{\mathrm{BeamClass}} \sim \mathcal{N}(0, \sigma_b^2)$is a random effect, and residuals follow an exponential spatial correlation structure within years.

4.6.1 GAMM Diagnostics

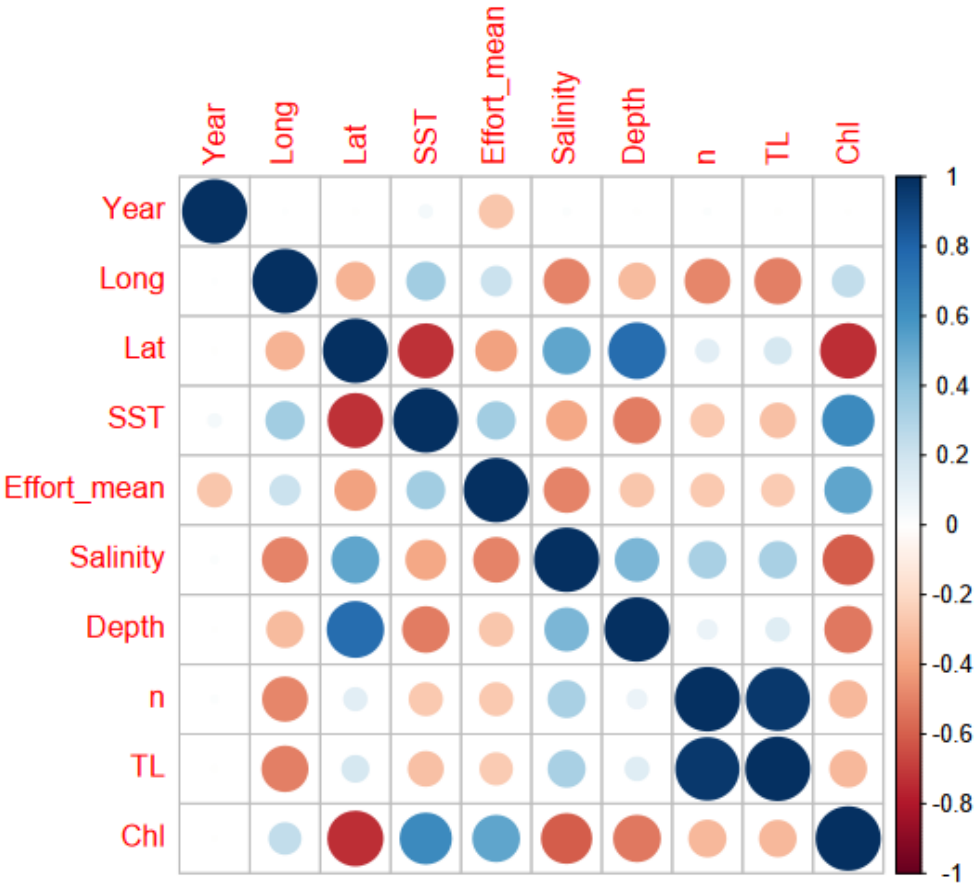

Figure S4.1: A correlation plot of all variables that could possibly be included in the GAMM metric models. Long is longitude, Lat is latitude, SST is mean sea surface temperature (°C), Effort_mean is the mean commercial fishing (hours year^{-1}), n is the number of nodes within a food web, TL is the number of trophic levels within a food web and Chl is chlorophyll. From these results TL and Chl were not included in any GAMM models due to high correlation with other variables.

Table S4.1: The results of the Moran's I test for each metric GAMM model. Moran's I is used to test the level of spatial autocorrelation within the mode. A close to zero Moran's I statistic and non-significant p value indicates little spatial autocorrelation.

Metric	**Moran I statistic**	**P Value**
Connectance	-2.772e-04	0.5
Mean trophic level	-2.772e-04	0.5
Modularity	-2.772e-04	0.5
APL	-2.772e-04	0.5
TST	-2.772e-04	0.5
FCI	-2.782e-04	0.5
Omnivory	-2.772e-04	0.5
Redundancy	-2.7724-04	0.5
AMI	-2.772e-04	0.5
Robustness	-2.772e-04	0.5

Table S4.2: The estimated results of the concurvity test of each GAMM model. Concurvity tests the degree of co-linearity between the model smoother predictors.

Metric	s(Temperature)	s(Commercial Fishing)	s(Temperature, Commercial Fishing)	s(number of nodes)	s(Depth)	s(Salinity)	s(Year)
Connectance	0.552	0.675	0.233	0.354	0.413	0.621	0.243
Mean trophic level	0.479	0.305	0.187	NA	0.436	0.709	0.226
Modularity	0.713	0.508	0.498	NA	0.607	0.424	0.506
APL	0.623	0.695	0.338	0.365	0.471	0.766	0.261
TST	0.512	0.671	0.287	0.176	NA	NA	0.239
FCI	0.751	0.53	0.453	0.326	0.562	0.682	0.27
Omnivory	0.638	0.61	0.207	0.393	0.79	0.763	0.261
Redundancy	0.576	0.695	0.255	0.359	0.287	0.728	0.261
AMI	0.562	0.54	0.292	0.181	NA	NA	0.249
Robustness	0.527	0.671	0.283	0.316	NA	NA	0.239

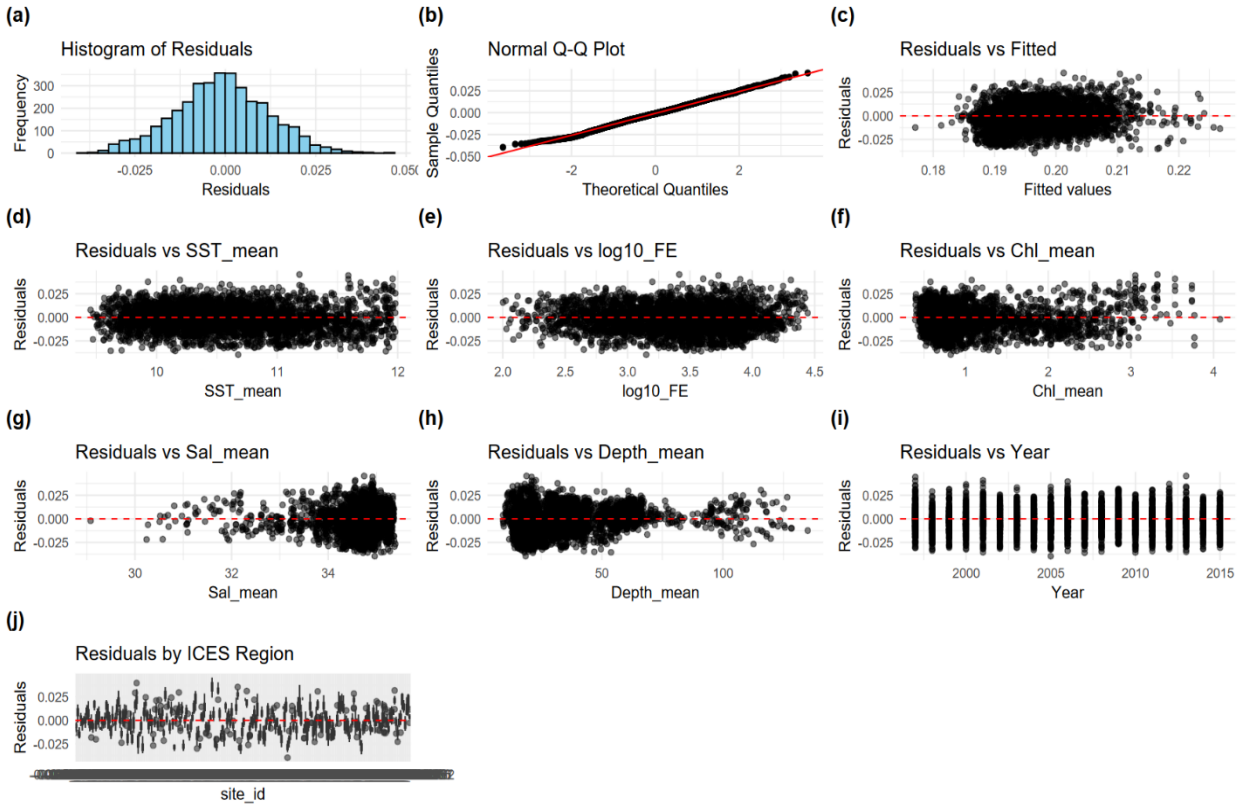

Figure S4.2: Diagnostic plots of the connectance GAMM including **a**) histogram of residuals, **b**) Q–Q plot of residuals, **c–j**) residuals patterns across fitted values, environmental predictors and year and regions.

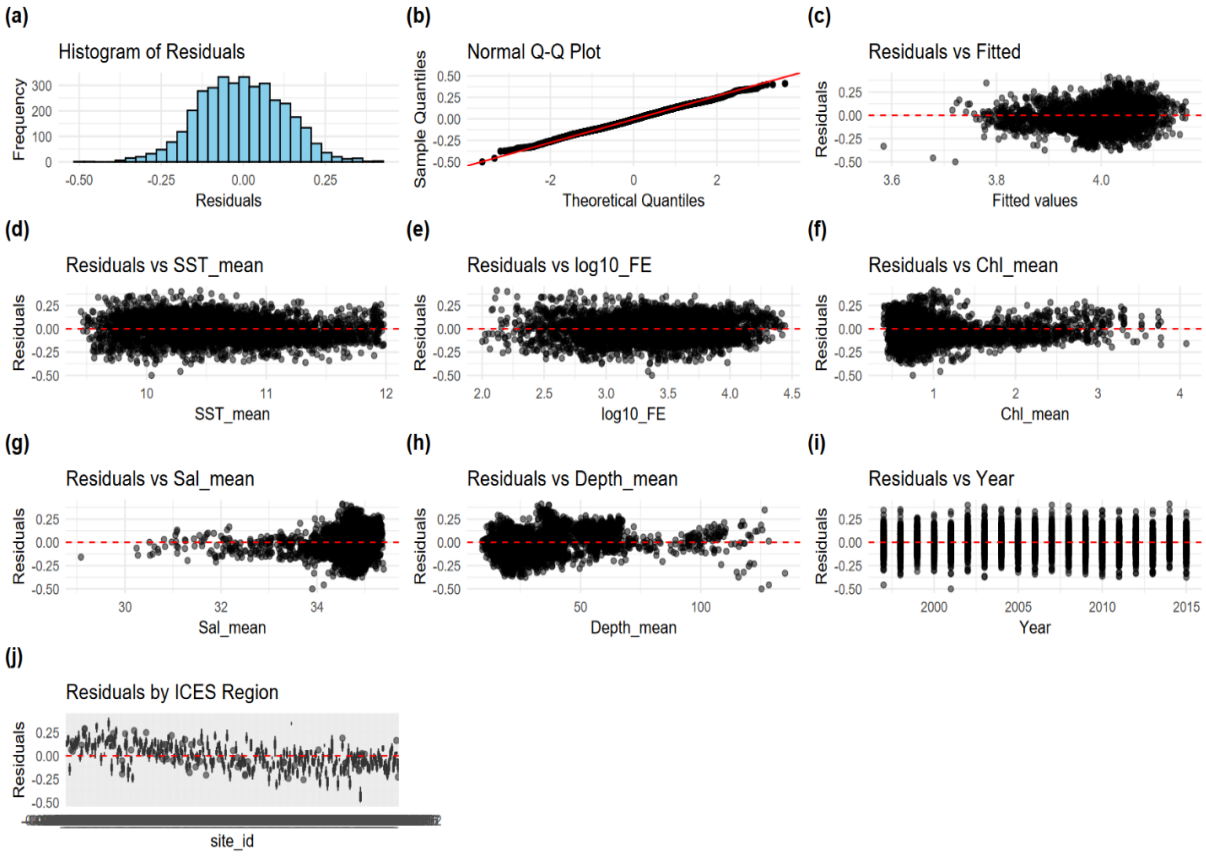

Figure S4.3: Diagnostic plots of the mean trophic level GAMM including **a**) histogram of residuals, **b**) Q–Q plot of residuals, **c–j**) residuals patterns across fitted values, environmental predictors and year and regions.

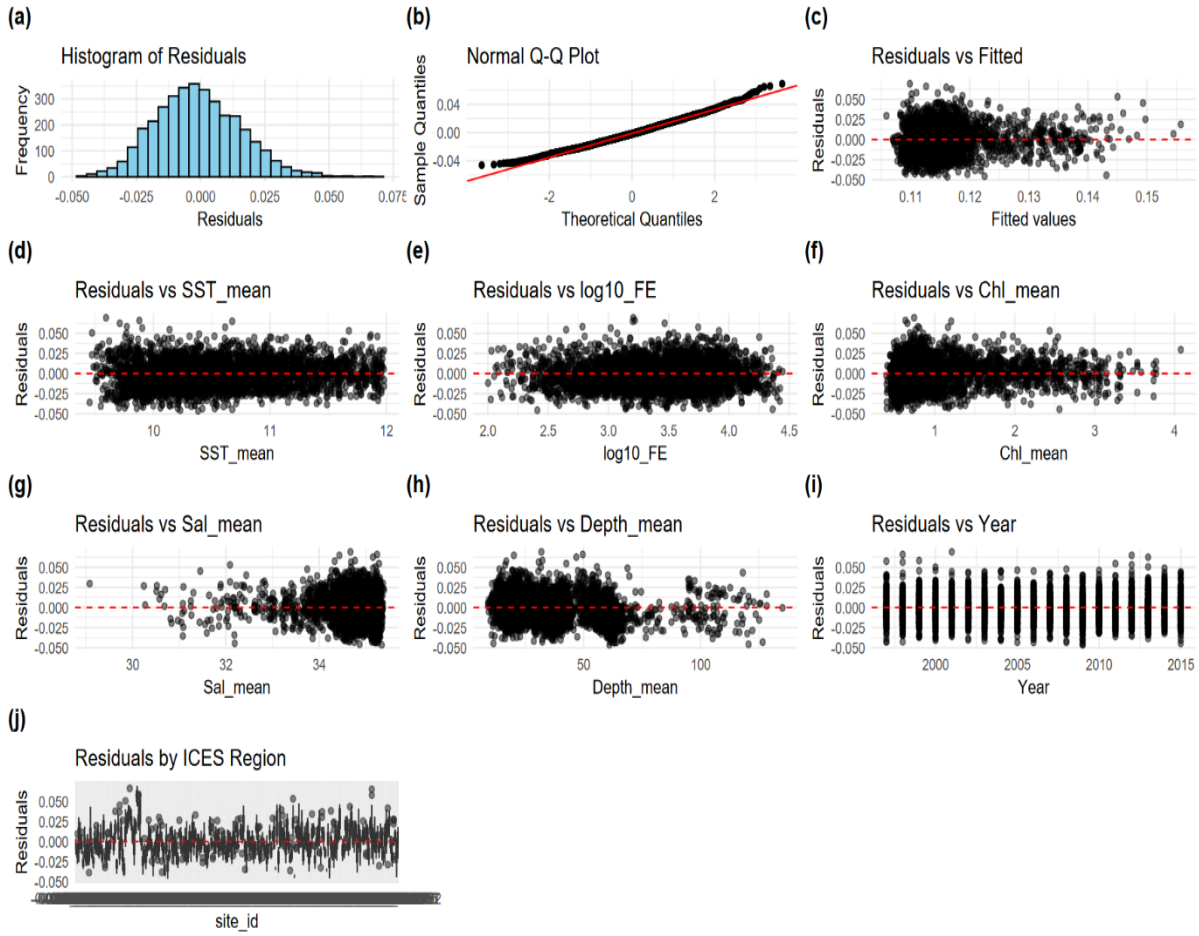

Figure S4.4: Diagnostic plots of the modularity GAMM including **a**) histogram of residuals, **b**) Q–Q plot of residuals, **c–j**) residuals patterns across fitted values, environmental predictors and year and regions.

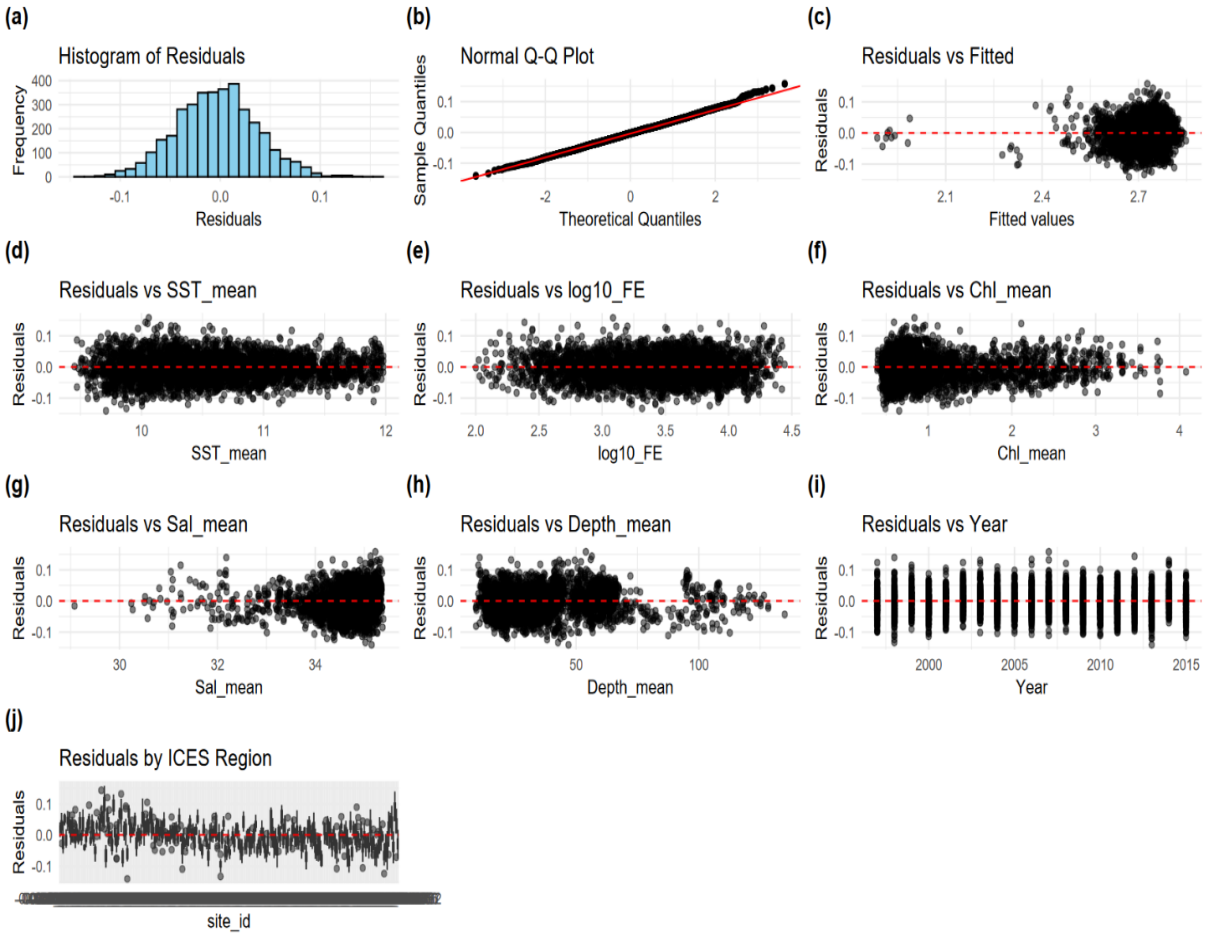

Figure S4.5: Diagnostic plots of the average path length (APL) GAMM including **a**) histogram of residuals, **b**) Q–Q plot of residuals, **c–j**) residuals patterns across fitted values, environmental predictors and year and regions.

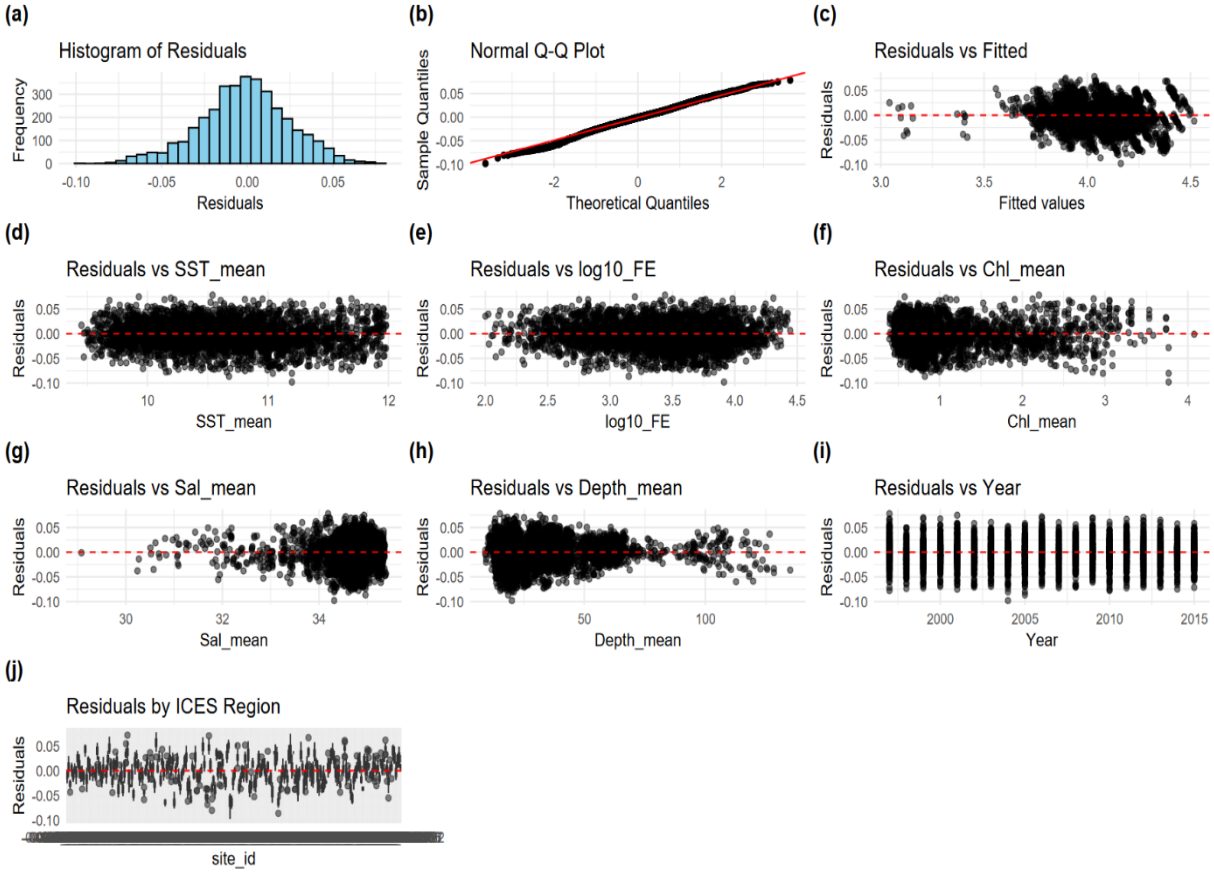

Figure S4.6: Diagnostic plots of the total system throughflow (TST) GAMM including **a**) histogram of residuals, **b**) Q–Q plot of residuals, **c–j**) residuals patterns across fitted values, environmental predictors and year and regions.

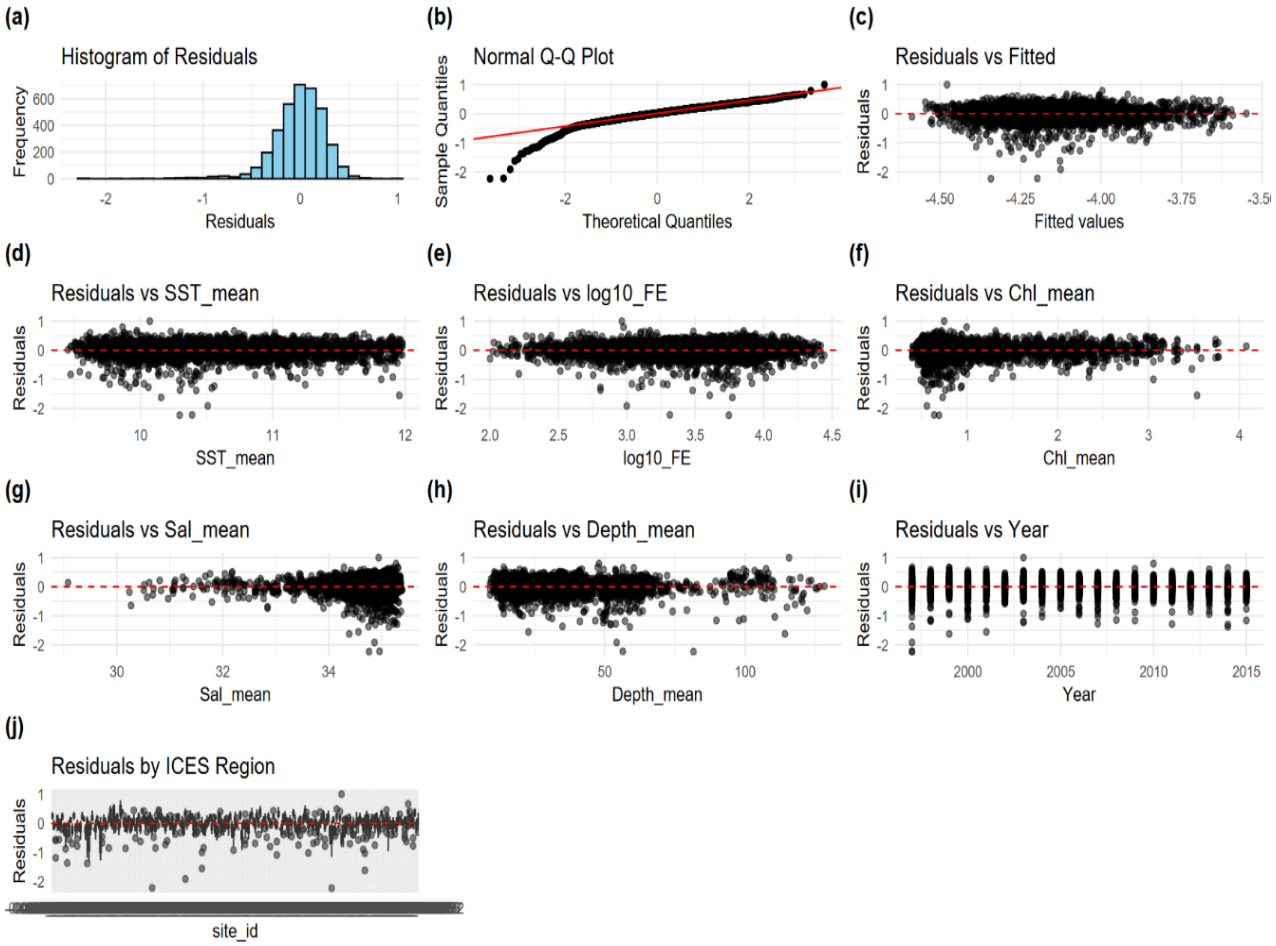

Figure S4.7: Diagnostic plots of the Finn cycling index (FCI) GAMM including **a**) histogram of residuals, **b**) Q–Q plot of residuals, **c–j**) residuals patterns across fitted values, environmental predictors and year and regions.

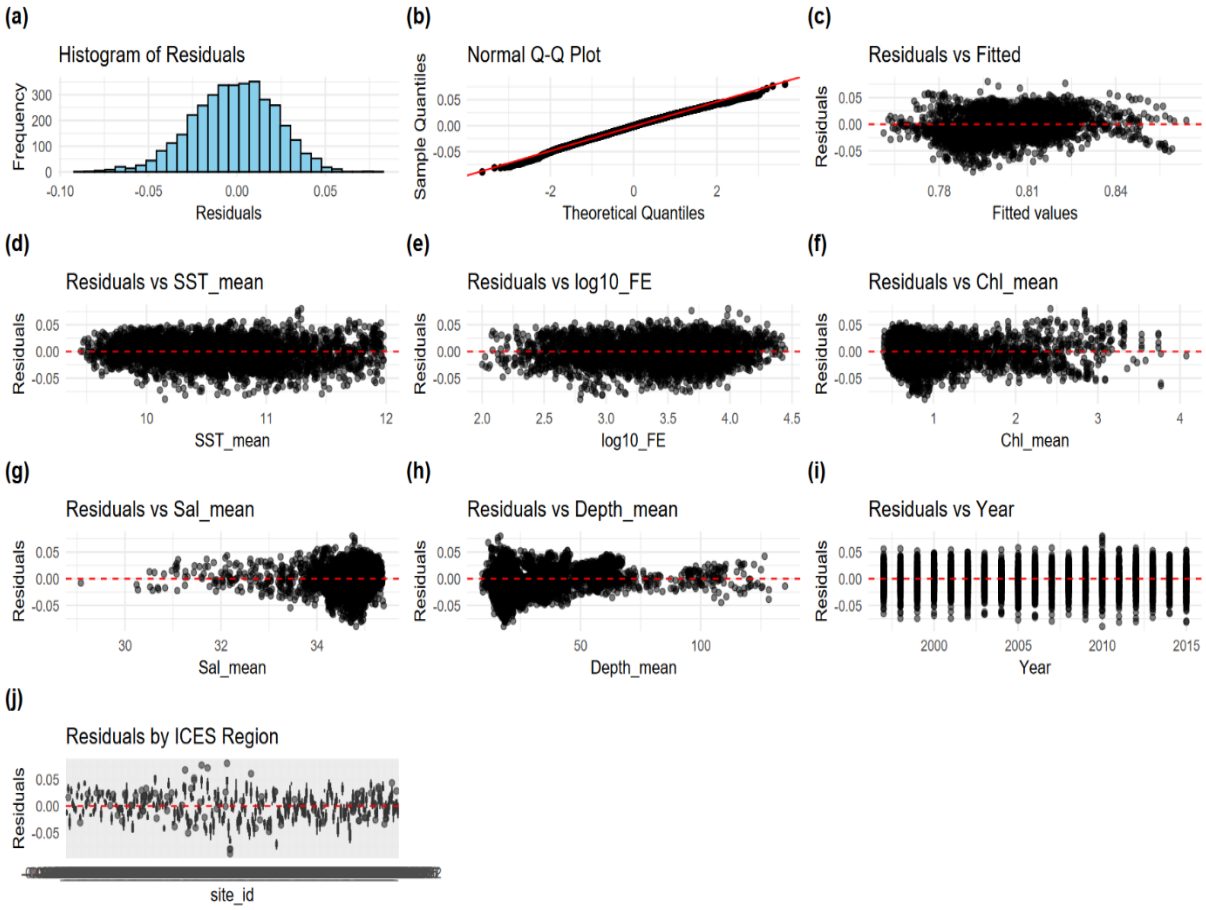

Figure S4.8: Diagnostic plots of the omnivory GAMM including **a**) histogram of residuals, **b**) Q–Q plot of residuals, **c–j**) residuals patterns across fitted values, environmental predictors and year and regions.

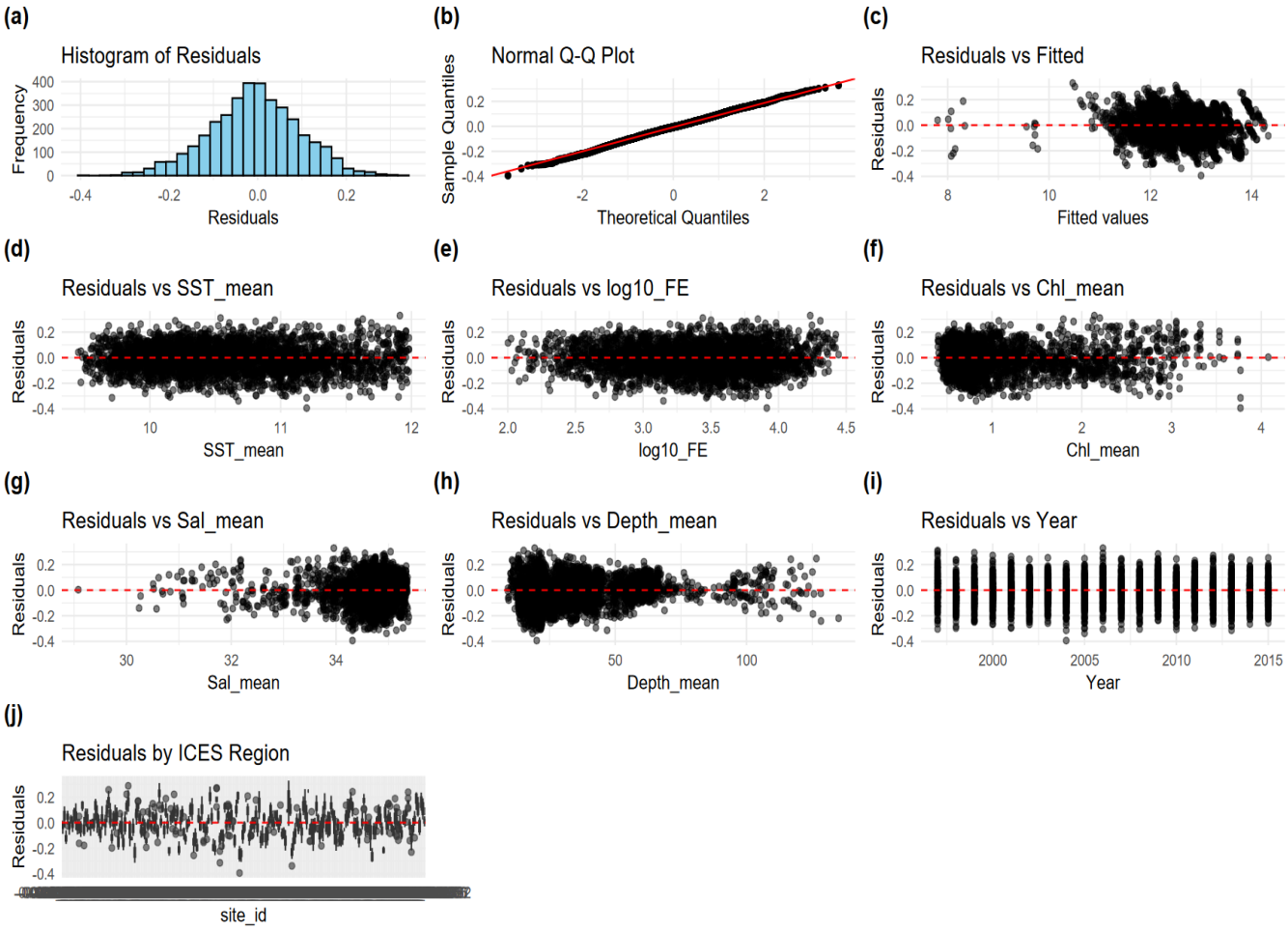

Figure S4.9: Diagnostic plots of the redundancy GAMM including **a**) histogram of residuals, **b**) Q–Q plot of residuals, **c–j**) residuals patterns across fitted values, environmental predictors and year and regions.

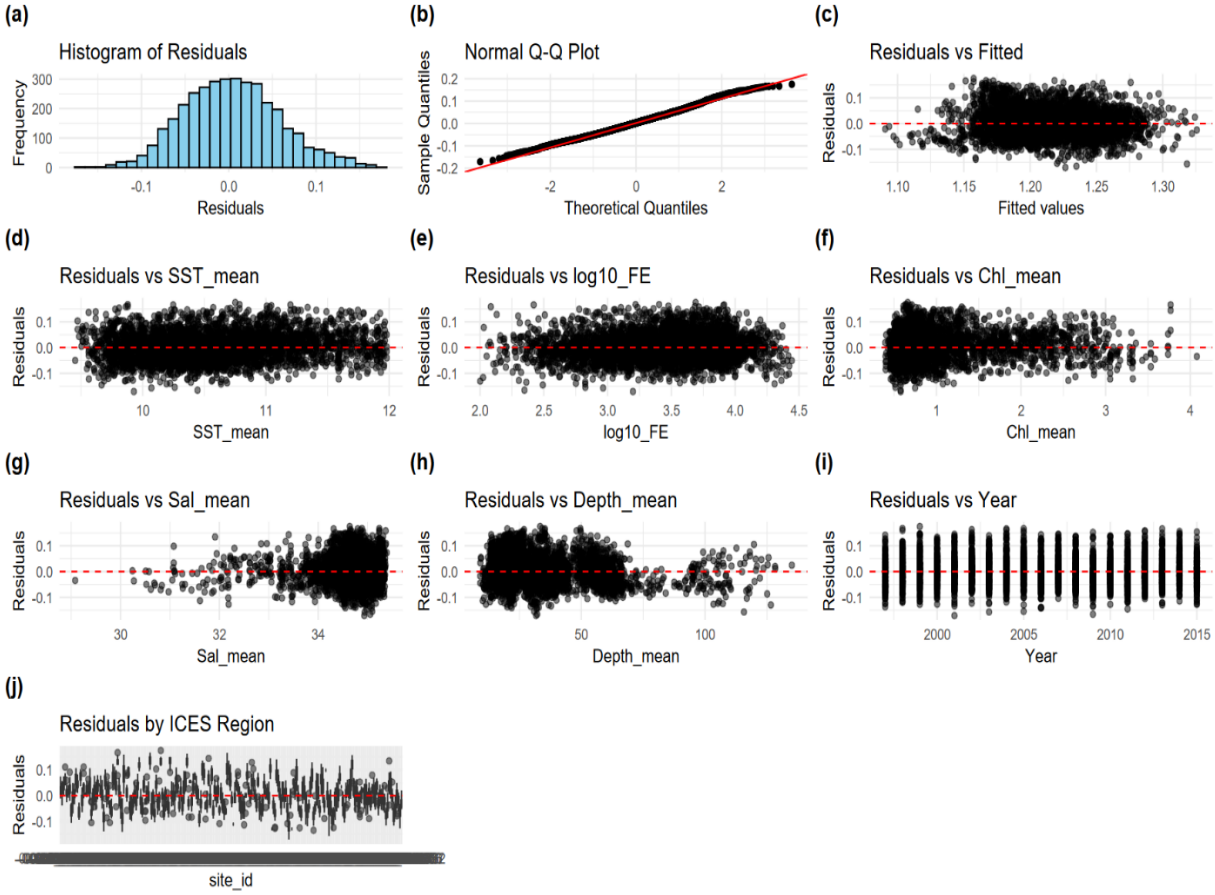

Figure S4.10: Diagnostic plots of the average mutual information (AMI) GAMM including **a**) histogram of residuals, **b**) Q–Q plot of residuals, **c–j**) residuals patterns across fitted values, environmental predictors and year and regions.

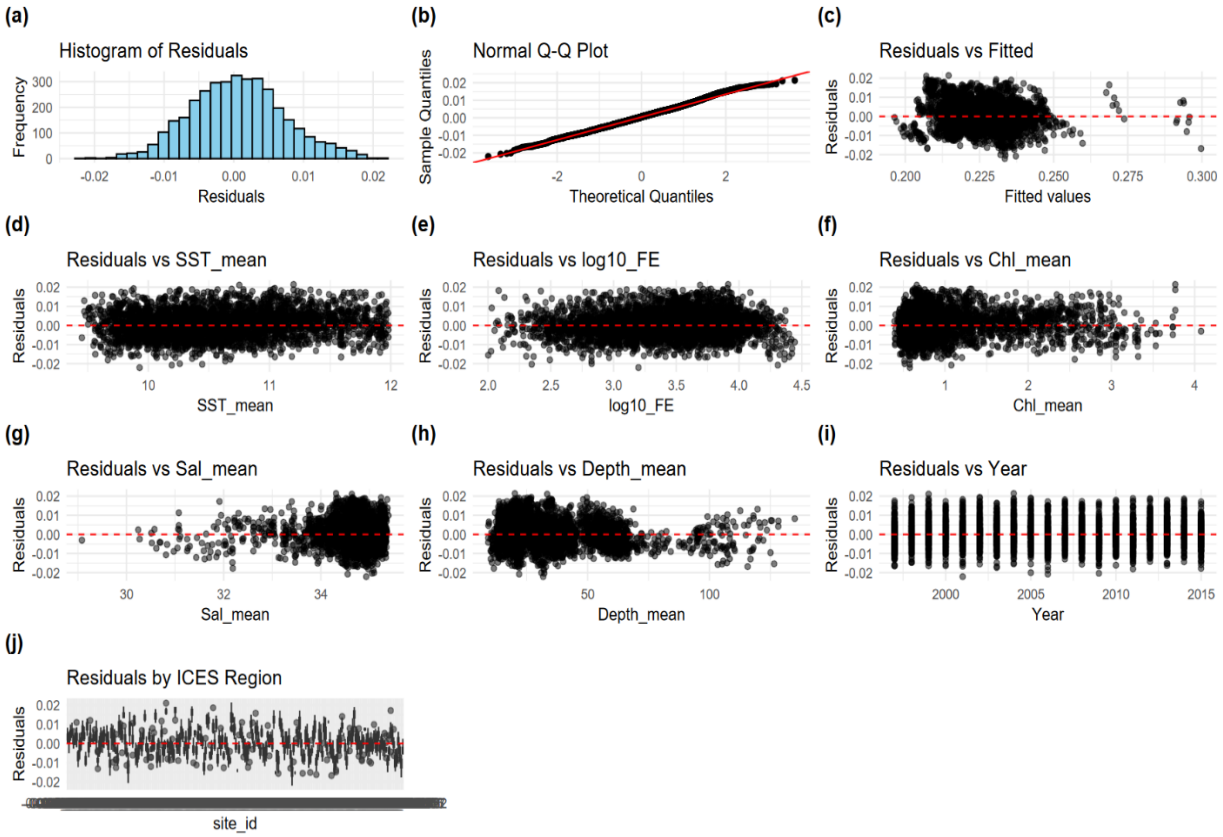

Figure S4.11: Diagnostic plots of the robustness GAMM including **a**) histogram of residuals, **b**) Q–Q plot of residuals, **c–j**) residuals patterns across fitted values, environmental predictors and year and regions.

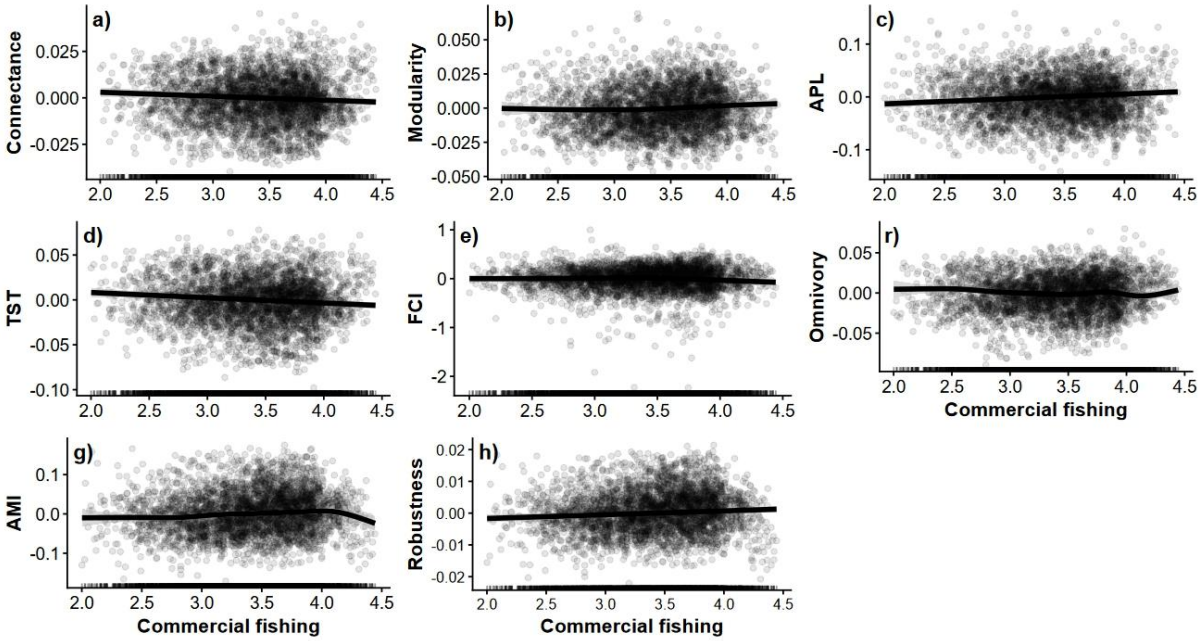

2329

2330 Figure S4.12: The significant main effects of commercial fishing (hours year^{-1}; $\log_{10}$
2331 transformed) on the partial residuals of **a)** connectance, **b)** modularity, **c)** average
2332 path length (APL), **d)** total system throughflow (TST, $\log_{10}$) transformed, **e)** Finn
2333 cycling index (FCI), **f)** omnivory, **g)** average mutual information (AM) and **h)**
2334 robustness.

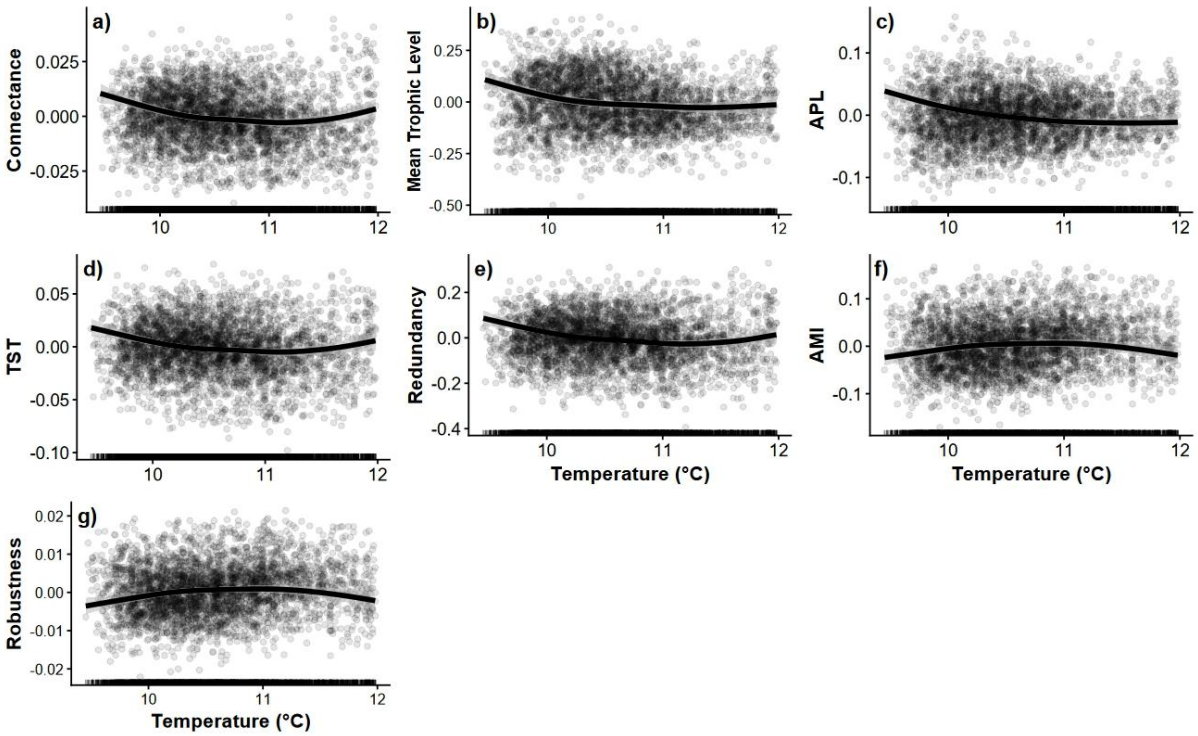

Figure S4.13: The significant main effects of temperature (°C) on the partial residuals of **a)** connectance, **b)** modularity, **c)** average path length (APL), **d)** total system throughflow (TST, $\log_{10}$) transformed, **e)** Finn cycling index (FCI), **f)** omnivory, **g)** average mutual information (AM) and **h)** robustness.

Table S3: The main effect of commercial fishing GAMM results for each metric.

Metric	**edf**	**F Value**	**P Value**
Connectance	1	8.525	**< 0.005***
Mean trophic level	5.197	1.829	0.102
Modularity	2.324	2.888	**0.033***
APL	1	13.33	**< 0.005***
TST	1	13.204	**< 0.005***
FCI	2.876	3.745	**0.023***
Omnivory	7.534	2.341	**0.01***
Redundancy	1	3.173	0.075
AMI	6.453	3.457	**0.002***
Robustness	1	9.108	**0.003***

5 Spatial scale determines temporal reconfiguration of North Sea ecosystem resilience

5.1 Abstract

Marine ecosystem resilience emerges from the organisation of trophic interactions that regulate energy transfer, biomass distribution, and other functional processes. The North Sea has experienced decades of commercial fishing and climate variability, yet the response of trophic structure, energy flux and associated variation in ecosystem resilience remain insufficiently resolved at ecologically relevant spatial scales. Here, we apply ecological network analysis to empirically derived food webs at a 50 km resolution across the North Sea from 1997 to 2015, assessing temporal and spatial variability in ecosystem structure, functioning, and resilience. Network metrics were used to characterise trophic complexity, energy throughput, recycling, pathway diversity, trophic organisation, and robustness and revealed that North Sea food webs underwent substantial reorganisation through time. Across the study period structural organisation and compartmentalisation of trophic interactions increased, together with the degree of energy recycling that they facilitated. Conversely, trophic connectivity, energetic capacity, and pathway diversity declined. These contrasting trends indicate that ecosystem resilience has been reconfigured rather than uniformly enhanced or eroded, with ecosystem functioning increasingly supported by more structured and efficiently routed energy flows but reduced functional redundancy to accommodate future disturbance. Spatial analyses revealed pronounced heterogeneity, with localised restructuring of food-web properties frequently coinciding with areas of changing fishing pressure. Regional trends often masked finer-scale variation in trophic structure and energy flux. Together, these findings demonstrate that ecosystem resilience is dynamic and scale dependent, underscoring the necessity of spatially explicit, ecosystem level indicators to inform ecosystem-based management under continued global change.

5.2 Introduction

Marine ecosystems provide essential services, including fisheries production and carbon cycling (Barbier, 2017). The continued provision of these services depends on ecosystem resilience, defined as the capacity of a system to absorb disturbance and reorganise while maintaining its essential structure and functioning (Fath and Scharler, 2018; Holling, 1973; Walker et al., 2004). Ecosystem resilience emerges from the organisation of ecological interactions that regulate energy transfer,

biomass distribution, and functional processes across trophic levels. When ecosystem resilience is high, ecosystems can buffer perturbations without undergoing fundamental shifts in structure or functioning, whereas erosion of resilience increases the likelihood of regime shifts and loss of ecosystem services (Folke, 2006; Holling, 2001).

Trophic interactions underpin ecosystem resilience by governing the transfer of energy from primary producers to higher trophic levels and maintaining the balance between organisation, redundancy, and energy recycling that stabilises ecological systems (Duffy et al., 2015; Ulanowicz, 2004). These interactions create pathways through which energy and matter flow, underpinning ecosystem functioning such as productivity and nutrient cycling, while also providing alternative routes that allow ecosystems to compensate for species loss or environmental change (Folke et al., 2016; Scharler et al., 2018). Anthropogenic impacts including ocean warming and commercial fishing can disrupt trophic structure e.g. through the loss of higher predators or reductions in primary production), thereby constraining these pathways and ultimately weakening resilience by limiting the system's capacity to redistribute energy and reorganise following disturbance (Frank et al., 2005; Tomczak et al., 2013, Scharler et al., 2018).

Food webs provide a valuable framework for quantifying trophic interactions and the organisation of energy flow (such as carbon or other nutrients) within ecosystems (Baird and Ulanowicz, 1989; Mukherjee et al., 2015). Because food webs explicitly represent trophic interactions among species and functional groups, they capture both the structure and functioning of ecological systems across multiple trophic levels. As such, their structure reflects emergent ecosystem properties, including complexity, redundancy, and ultimately ecosystem resilience, providing a means to assess how ecosystems vary through time (Kortsch et al., 2019; O'Gorman et al., 2019).

Global change drivers, including increasing sea surface temperatures (SST) and commercial fishing affect ecosystems through multiple pathways simultaneously by altering species composition, modifying interaction strengths, and reshaping energy flow through food webs (Clark et al., 2003; Kortsch et al., 2015; Shurety et al., 2026; Wood et al., 2024). Commercial fishing reduces the abundance of higher trophic

level predators, truncating trophic structure and constraining energy transfer through trophic levels (Frank et al., 2005; Pauly et al., 1998), while warming alters metabolic demand and ecosystem respiration, influencing the balance between production and dissipation (Brown et al., 2004; Coghlan et al., 2024; Yvon-Durocher et al., 2015). These cumulative pressures may therefore progressively alter ecosystem resilience. In this study we focus on the North Sea, decades of commercial fishing and climate variability have altered trophic relationships and assemblages (Frelat et al., 2022; Sguotti et al., 2022), raising fundamental questions about how food-web structure, functioning, and ecosystem resilience have shifted through time within the region.

Recent food-web assessments conducted by OSPAR within the Quality Status Report (Schückel et al., 2022) highlighted the need for integrated, ecosystem-scale indicators capable of capturing such system-wide changes in trophic structure and functioning across the North-East Atlantic. In particular, the pilot application of Ecological Network Analysis (ENA; Schückel et al., 2022) demonstrated that whole-food-web models can reveal cumulative and emergent changes that are not detectable using single-component indicators. However, this pilot assessment was spatially restricted to represent broad marine regions with single modelled food webs, limiting its ability to resolve regional-scale dynamics. Here, we apply ENA to empirically derived 50 x 50 km food webs spanning the North Sea (approximately 808,659 km²) over two decades (1997–2015), providing comprehensive spatial and temporal resolution of trophic organisation and energy transfer. By using empirically derived food webs rather than modelled representations, this study provides a direct assessment of long-term changes in ecosystem structure and functioning.

ENA provides a quantitative framework for assessing these emergent ecosystem properties by characterising patterns of energy transfer, organisation, and recycling within trophic networks, which together regulate ecosystem functioning including carbon transfer and biological productivity (Finn, 1976; Ulanowicz, 2004). To quantify these properties, we apply a suite of network-based metrics describing structural and functional aspects of food webs and their capacity to support and sustain ecosystem processes. Connectance captures overall trophic complexity (Newman and Girvan, 2004; Pimm, 1982), modularity reflects compartmentalisation within the network and the extent to which energy flows are distributed among semi-independent subsystems (Newman and Girvan, 2004), and total system throughflow (TST)

represents the overall magnitude of trophic flux, reflecting the total volume of energy transferred through the ecosystem (Finn, 1976). The Finn cycling index (FCI) measures the extent of energy recycling, which contributes to the retention and reuse of energy within the system (Finn, 1976), redundancy describes the availability of alternative pathways performing similar functional roles potentially supporting continuity of ecosystem processes under disturbance (Ulanowicz, 2004), and average mutual information (AMI) quantifies the organisation and efficiency of energy transfer, influencing how effectively energy and biomass are channelled through trophic levels (Ulanowicz, 2004). Robustness integrates these characteristics, reflecting the balance between organisation and redundancy and providing a system-level measure of resilience and the capacity of the ecosystem to sustain functioning under environmental change (Ulanowicz, 2009).

We treat ecosystem resilience as an emergent property of food webs that integrates the cumulative effects of multiple stressors rather than attributing observed changes to individual pressures. Given observed wide-scale reductions in commercial fishing pressure across much of the North Sea over recent decades (Figure 5.1), which could result in the partial recovery of biomass and rebuilding of trophic complexity (McClanahan, 2014; Rojo et al., 2021), ecosystem resilience may be expected to increase over the study period (1997–2015) (Figure 5.2). Such increases in resilience would be reflected in measurable changes to food-web structure and energy flux, including increases in system activity (TST) and recycling (FCI), strengthening of trophic complexity (increases in connectance, modularity, omnivory, and redundancy), and enhanced robustness arising from a more balanced trade-off between organisation (AMI) and redundancy. Increasing resilience may also manifest as recovery of trophic structure, reflected in increases in mean trophic level and associated increases in average path length, indicating expansion and strengthening of the trophic hierarchy. However, these potential gains in resilience must be considered alongside concurrent changes in SST (Figure 5.1), which can alter species distributions, modify interaction strengths, and reorganise energy pathways (Coghlan et al., 2024; Kortsch et al., 2019, 2015). As a result, ecosystem responses may not be uniform, and the combined influence of reduced fishing pressure and climate-driven environmental change are expected to produce spatially heterogeneous trends in food-web structure and resilience across the North Sea.

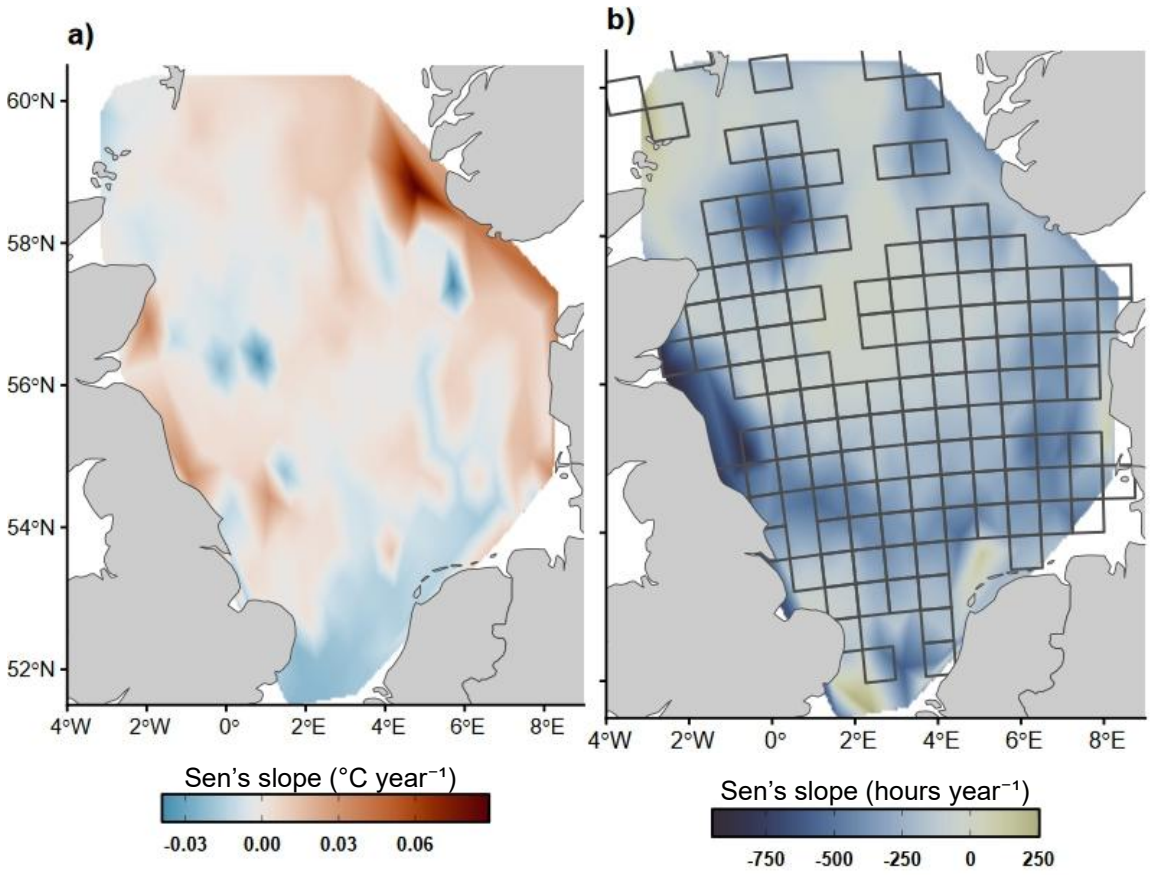

Figure 5.1: Temporal trends at 50 × 50 km grid scale in a) sea surface temperature (Sen's slope, °C year^{-1}), and b) commercial fishing effort (Sen's slope, hours year^{-1}). Temporal trends were calculated using Sen's slope, a non-parametric measure of trend magnitude calculated as the median of all pairwise slopes between observations over time. Site-level Sen's slope estimates were interpolated across the study region using bilinear interpolation (Akima interpolation), generating continuous raster surfaces of spatial trend patterns. Outlined grid cells represent areas where significant temporal trends were significant temporal trends were observed ($p \leq 0.05$).

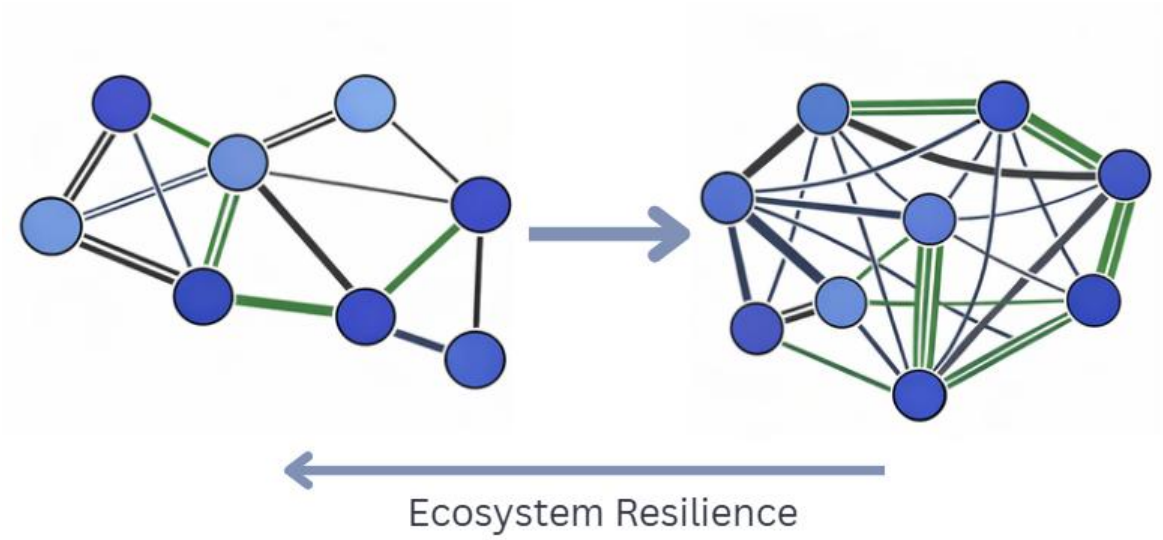

Figure 5.2: A conceptual diagram illustrating the expected changes in North Sea food webs leading to decreased ecosystem resilience. The thickness of the links indicates the amount of energy within the trophic interaction; double links indicate redundancy and green links indicate those that hold recycled energy. Increasing ecosystem resilience is expected to manifest from increases in system activity (TST) and recycling (FCI), strengthening of trophic complexity (increases in connectance, modularity, omnivory, and redundancy), re-establishment of trophic structure (increases in mean trophic level and APL), and enhanced robustness arising from a more balanced trade-off between organisation (AMI) and redundancy.

Previous studies have demonstrated the value of ENA and food-web approaches to detect system-wide changes that emerge from complex trophic interactions, enabling the assessment of ecosystem resilience across marine systems (Frelat et al., 2022; Mukherjee et al., 2015; Schückel et al., 2022). Building on this foundation, we make use of a novel empirical food-web database spanning two decades (1997–2015), enabling a comprehensive assessment of temporal and spatial variability in ecosystem resilience derived from North Sea food webs. This broader perspective compared to previous studies supports the development of quantitative empirical baselines for network-level metrics, allowing changes in organisation and energy flow to be interpreted relative to a reference state and improving our ability to detect shifts in ecosystem resilience. By advancing the operational application of ENA metrics at regional scales, this study contributes new evidence to support

ecosystem-based management and improve understanding of how marine ecosystems respond to global environmental change through time.

5.3 Methods

5.3.1 Environmental gradients

Daily sea surface temperature data (°C) from both satellite and in situ observations were extracted from the Copernicus open access data repository (Donlon et al., 2012; Good et al., 2020; Stark et al., 2007a). The mean sea surface temperature was calculated for each year. Commercial fishing (hours $year^{-1}$) was taken from reconstructed North Sea trawling effort from 1985 – 2015 (Couce et al., 2020) and a yearly mean was calculated for each year. The proportion of commercial fishing that came from beam trawling was calculated using the same reconstructed trawling effort data (Couce et al., 2020). Depth (m), salinity (ugl^{-1}), and chlorophyll were taken from the ICES open-source data portal (ICES Data Portal, Dataset on Ocean HydroChemistry, ICES, Copenhagen) and a yearly mean was calculated.

5.3.2 Food Webs

We made use of a novel database of food webs from across the North Sea from 1997 to 2015. Here we summarise how the food webs were constructed (see chapter three for full methodological details). Fish community composition (1997–2015) was derived from ICES DATRAS trawl surveys (Lynam and Riberio, 2022) within the defined study region, and trophic interactions were assembled from DAPTSOM (Pinnegar, 2014) and ICES Year of the Stomach databases (ICES, 2010) for the same period. The region was divided into 50 × 50 km grid cells, and annual local food webs were generated by spatially matching trawl and stomach-content data within a 100 km radius, producing a local species list and associated predator–prey links. Diet completeness was evaluated and supplemented using hierarchical size- and guild-based rules where necessary, and non-fish prey and basal resources were incorporated using established North Sea food webs models (Daskalov and Mackinson, 2007; Mackinson and Daskalov, 2007). Final food webs were assembled with size-structuring constraints and removal of isolated nodes, and interaction strengths were quantified using allometric steady-state, energy-flux modelling (Gauzens et al., 2019). After excluding unbalanced networks, this food web construction methodology resulted in 4,728 weighted food webs.

5.3.3 Network-level metrics

Food-web metrics provide a quantitative framework for describing structural and functional properties of ecosystems. ENA applies network theory to trophic systems and offers a suite of metrics that characterise how energy and interactions are organised within food webs (Baird and Ulanowicz, 1989; de la Vega et al., 2018; Scharler, 2012). We calculated a suite of ENA metrics including connectance, mean trophic level, modularity, APL, TST, FCI, Omnivory, redundancy, AMI and robustness, for all 4,728 food webs, many of which are recognised indicators of GES under the OSPAR Convention (Schückel et al., 2022).

Calculation of ENA metrics requires mass balance, whereby inputs equal outputs for each node. All food webs were balanced using the '*balancing*' function in the '*enaR*' package (Borrett and Lau, 2014), with further methodological details provided in Table 1.1 and described in Kay et al., 1989 and Borrett and Lau, 2014.

5.3.4 Statistical Analysis

All statistical analyses and visualisations were conducted using R v4.2.2 (R Core Team, 2024). Community composition was analysed using site-level presence–absence matrices constructed from the taxa recorded at each site. Species richness was calculated as the number of unique taxa recorded per site. Community dissimilarity among sites was quantified using Bray–Curtis dissimilarity. Non-metric multidimensional scaling (nMDS) was then used to visualise differences in community structure among sites. Environmental and spatial gradients were fitted onto the ordination using vector fitting, with sea surface temperature, commercial fishing effort, longitude and latitude included as continuous predictors. All analyses were conducted in R Software using the vegan package (Oksanen et al., 2007).

Non-linear Generalized Additive Mixed Models (GAMMs) were used to test the relationships between each network metric and year. FCI, TST, and commercial fishing were $\log_{10}$-transformed to meet the assumptions of normality and homogeneity. The models included additional continuous smoothers of chlorophyll (ug/l), salinity, depth (m), number of nodes, and year, as well as the random effect of the proportion of commercial fishing that was beam trawling. Spatial autocorrelation was adequately accounted for using an AR1 correlation structure. Model selection of the fixed and random effects for each metric was conducted using Akaike information criterion (AIC; Akaike, 1974). These models where the same ones developed in

Chapter 4, therefore all equations and diagnostics can be within the supplementary material of Chapter 4 (Table S4.1 and S4.2; Figure S4.1: S4.11). The percentage change of each metric and environmental gradient across year was calculated using the predicted metric value from the linear and GAMM models.

To quantify temporal trends at the 50 × 50 km grid scale, we calculated Sen's slope (Sen, 1968) from model-predicted annual values derived from the fitted GAMMs for each food-web metric in each grid cell across the North Sea over the study period (1997–2015). Sen's slope is a non-parametric estimate of trend magnitude, defined as the median of all pairwise slopes between observations over time, and provides a robust measure of temporal change that does not assume linearity. This yielded an estimate of the rate of change for each metric in each grid cell over the study period. Statistical significance of trends was assessed using associated p-values, with changes considered significant at $p \leq 0.05$. When analysing the results, it should be noted that site-level trends were estimated using Sen's slope for each site individually, whereas regional trends were calculated from the spatially averaged annual predictions.

Spatial patterns in ecosystem metrics were visualised using continuous raster surfaces derived from site-level trend estimates. The site-specific Sen's slopes were interpolated across the study region using bilinear interpolation on a regular latitude–longitude grid (akima interpolation, Akima, 1978), producing a continuous surface representing spatial variation in the direction and magnitude of change.

5.4 Results

5.4.1 Variation in community composition

Community composition varied across sites along clear environmental and spatial gradients. The nMDS ordination showed separation in community composition primarily along NMDS1, with sea surface temperature aligned with this main axis of variation. This suggests that warmer sites supported distinct community assemblages relative to cooler sites. Latitude was oriented in the opposite direction to temperature, indicating that part of the temperature-associated community shift may also reflect a broader north–south spatial gradient. Fishing effort was also aligned with the positive NMDS1 axis and was associated with regions of the ordination containing lower to intermediate realised species richness. Together,

these patterns suggest that community structure is jointly organised by temperature, fishing pressure and spatial location, with higher fishing effort potentially associated with reduced species richness.

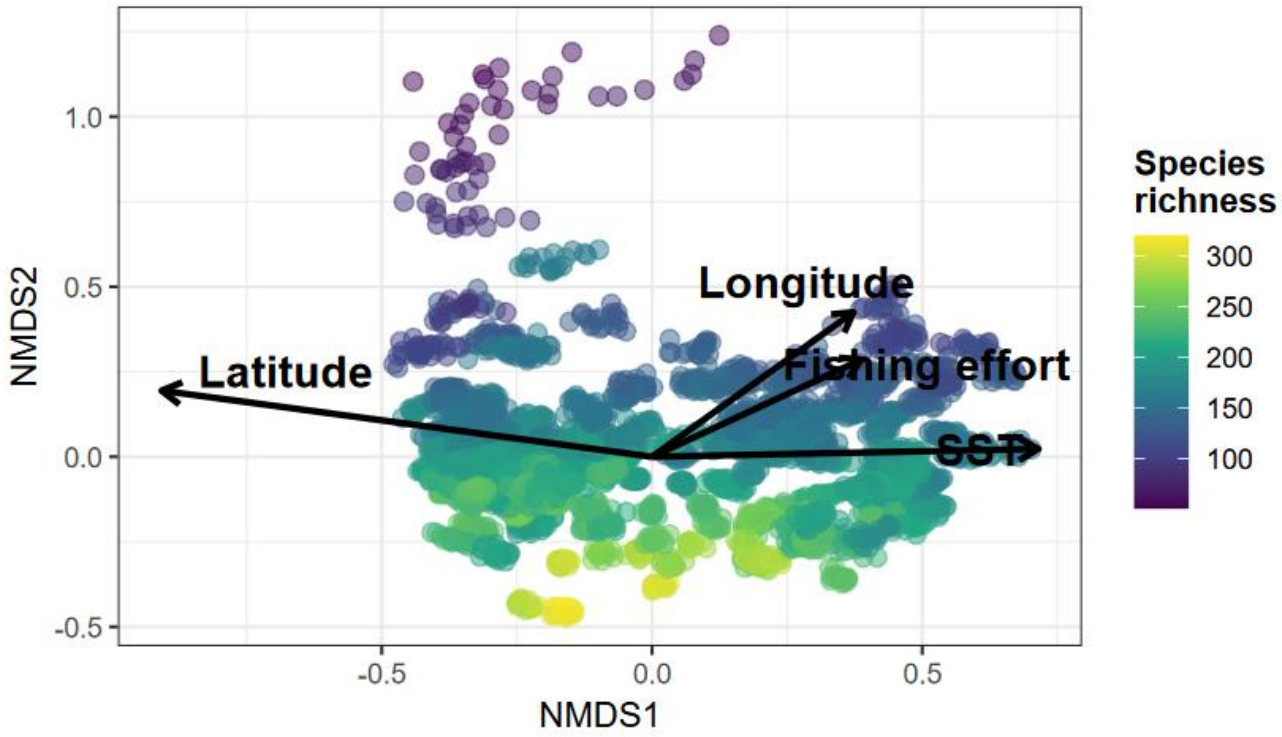

Figure 5.3: A nMDS illustrating variation in community composition across sites in relation to environmental and spatial gradients. The SST (sea surface temperature), fishing effort, longitude and latitude vectors indicate the direction of increasing values for each variable. Point colour represents the species richness (number of species) per site.

5.4.2 Temporal trends in food web structure and function at the North Sea scale

Connectance declined significantly over time, decreasing by 2.37% from 1997 to 2015, indicating a progressive reduction in the density of realised trophic interactions in contrast to our expectations of increasing trophic complexity under recovering resilience (Figure 5.4a, Figure 5.5 and Table 5.1). Mean trophic level increased while APL decreased, although neither metric was significantly associated with year (Table 5.1). Modularity, however, significantly increased by 6.35% through time, reflecting enhanced compartmentalisation of North Sea food webs (Figure 5.3b, Figure 4 and Table 5.1).

TST significantly declined by 0.26% from 1997 to 2015, indicating a reduction in the overall magnitude of energy flux within more recent food webs and suggesting lower system activity than expected under increasing ecosystem resilience (Figure 5.4c, Figure 5.5 and Table 5.1). However, FCI significantly increased by 2.65% over time (Figure 5.4d, Figure 5.5 and Table 5.1), indicating enhanced recycling of energy within the system, consistent with improved internal retention of energy despite declining throughput. Omnivory also increased through time, although the trend was not significant (Table 5.1), suggesting a weak tendency towards greater diet breadth.

Unexpectedly, redundancy declined significantly by 0.27% from 1997 to 2015, indicating reduced availability of alternative trophic pathways and suggesting diminished functional buffering capacity (Figure 5.4h, Figure 5.5 and Table 5.1). In parallel, AMI, reflecting the organisation and efficiency of energy transfer, significantly increased by 2.43% across the study period (Figure 5.4i, Figure 5.5 and Table 5.1), indicating increasingly structured and channelled energy flow. Robustness, which reflects the balance between organisation and redundancy, also increased significantly by 1.6% through time, driven primarily by the strengthening of network organisation (Figure 5.4j, Figure 5.5 and Table 5.1). Taken together, these results indicate that, over time, food webs have developed a more organised yet less complex trophic structure, characterised by declining connectance and redundancy, while retaining a greater proportion of recycled energy despite lower overall energy availability.

Table 5.1: The GAMM results for the effect of year on each metric. An asterix signifies a statistically significant relationship.

Metric	R^2	edf	F	p	% change
Connectance	0.292	1	7.849	0.005*	-2.365
Mean trophic level	0.324	1	0.888	0.346	0.573
Modularity	0.148	1.707	6.071	0.019*	6.346
Average Path Length	0.783	1	3.012	0.083	0.337
Total System Throughput	0.975	1	10.264	0.001*	-0.261
Finn Cycling Index	0.289	2.317	9.891	<0.001*	2.65%
Omnivory	0.403	1	0.607	0.436	0.324
Average Mutual Information	0.236	1	10.776	0.001*	-0.265
Redundancy	0.975	1	7.206	0.007*	2.434
Robustness	0.669	1	11.384	0.001*	1.599

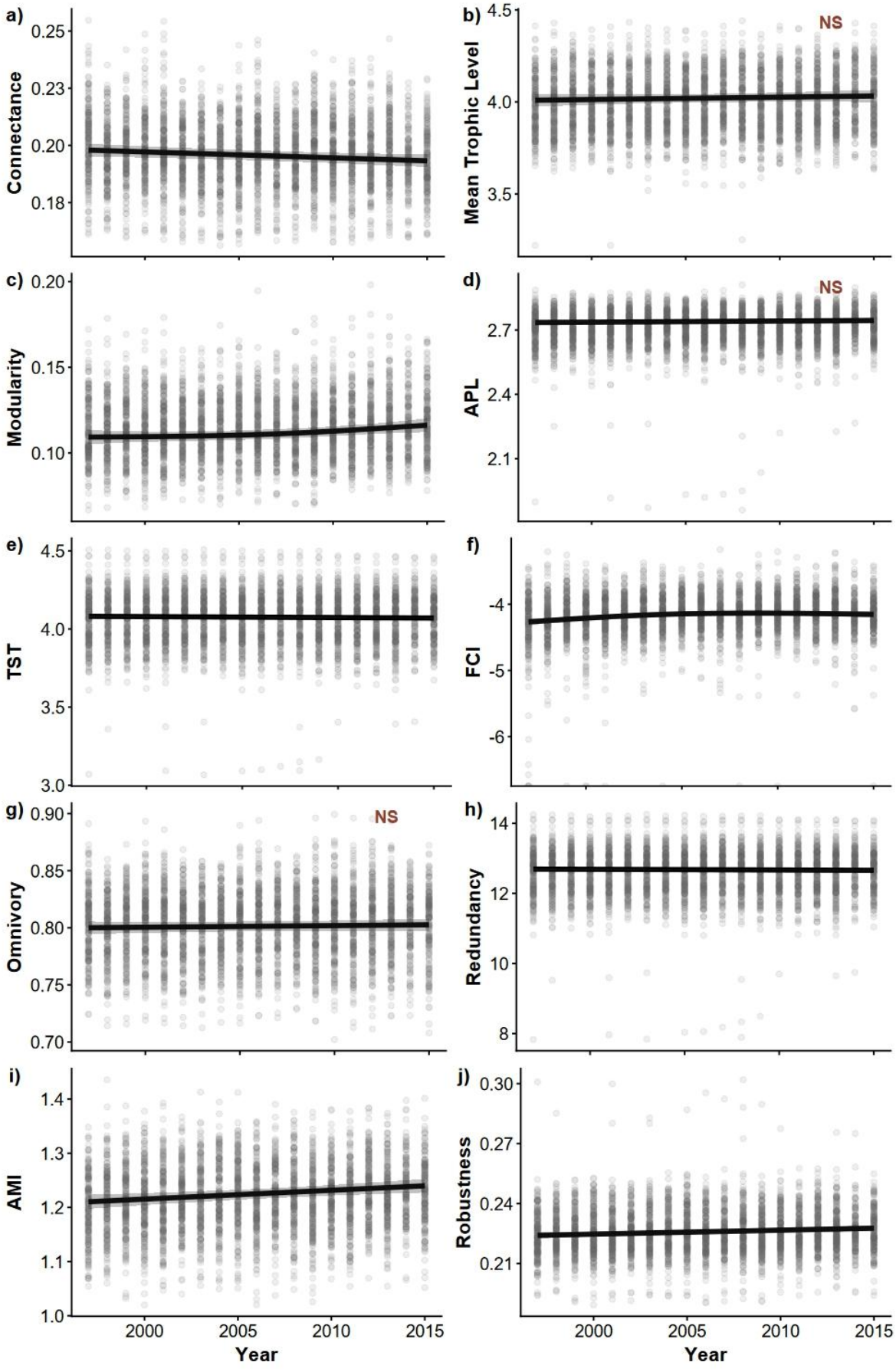
a)
Connectance
0.25
0.23
0.20
0.18
b)
Mean Trophic Level
4.5
4.0
3.5
NS
c)
Modularity
0.20
0.15
0.10
d)
APL
2.7
2.4
2.1
NS
e)
TST
4.5
4.0
3.5
3.0
f)
FCI
-4
-5
-6
g)
Omnivory
0.90
0.85
0.80
0.75
0.70
NS
h)
Redundancy
14
12
10
8
i)
AMI
1.4
1.3
1.2
1.1
1.0
j)
Robustness
0.30
0.27
0.24
0.21
2000
2005
2010
2015
Year
2000
2005
2010
2015
Year

2646

Figure 5.4: The predicted value of a) connectance, b) mean trophic level, c) modularity, d) average path length (APL), e) total system throughput ($mgCm^{-2}year^{-1}$; TST), f) Finn cycling index (%, FCI), g) omnivory, h) redundancy (bits), i) average mutual information (bits, AMI) and j) robustness across the study period (1997-2015). The predicted results and model fit are from GAMMs performed on each metric. All relationships with year were significant (Table 5.1).

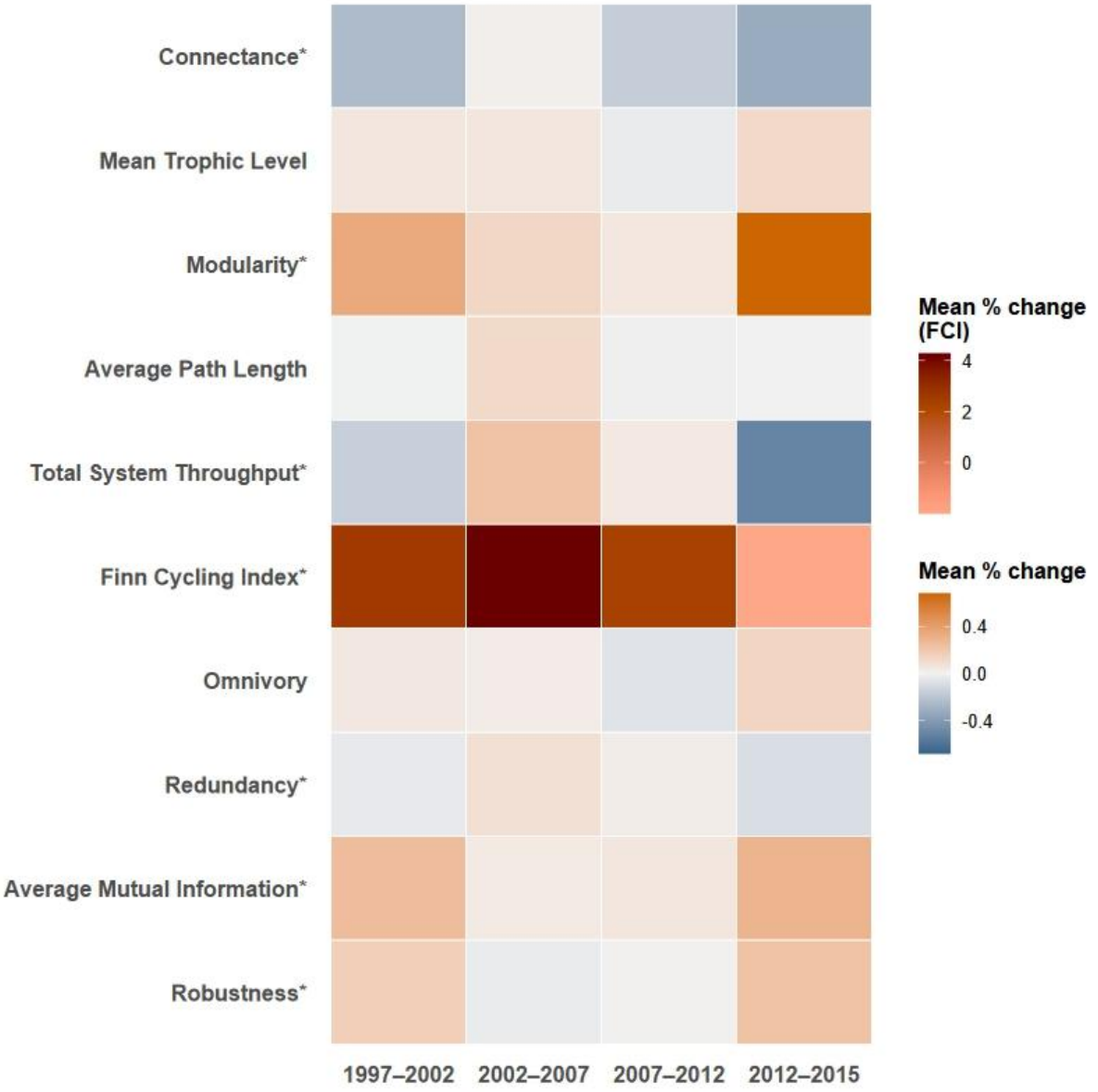

Figure 5.5: Temporal changes in network-level metrics across five-year time periods. Colour intensity indicates the direction and magnitude of mean percentage change within each bin. Finn Cycling Index (FCI) has a unique colour scale to accommodate the larger range of percentage change. Asterisks denote statistically significant trends between the metric and year (1997-2015) within the North Sea.

5.4.3 Temporal trends in food web structure and function at the local scale

Significant temporal changes in food-web structure at the 50 × 50 km grid scale were spatially heterogeneous across the North Sea. The density of trophic interactions declined broadly, with significant reductions in connectance widely dispersed across the region, reflecting a weakening of trophic connectivity (Figure 5.6a). At the same time, compartmentalisation increased throughout much of the North Sea, with widespread increases in modularity indicating greater subdivision of trophic interactions into more distinct sub-networks (Figure 5.6c). Trophic structure also showed evidence of regional strengthening, with trophic levels increasing across most areas, particularly in the southern North Sea, indicating a lengthening of trophic pathways (Figure 5.6b). This pattern was further supported by increases in average path length, especially in mid- and southern regions, reflecting expansion of energy transfer across a greater number of trophic steps (Figure 5.6d).

Changes in system functioning, reflected in the magnitude, organisation, and routing of energy flow, varied regionally. TST exhibited both increases and decreases across the North Sea, indicating spatial variability in overall energy transfer, with significant increases concentrated along the British coastline (Figure 5.6e). In parallel, redundancy also exhibited spatially heterogeneous trends, with significant increases primarily associated with coastal regions, indicating localised expansion in the availability of alternative trophic pathways supporting energy transfer (Figure 5.6i). More broadly, increases in the organisation and recycling of energy were observed throughout the North Sea, with widespread increases in AMI and FCI indicating progressively more structured energy flow and greater internal retention of energy within food webs (Figure 5.6f, h). Trophic flexibility also increased across much of the region, reflected in widespread increases in omnivory, particularly at mid-latitudes (Figure 5.6g). Together, these changes were accompanied by increases in robustness across multiple areas, indicating strengthening of the balance between organisation and pathway availability within regional food webs.

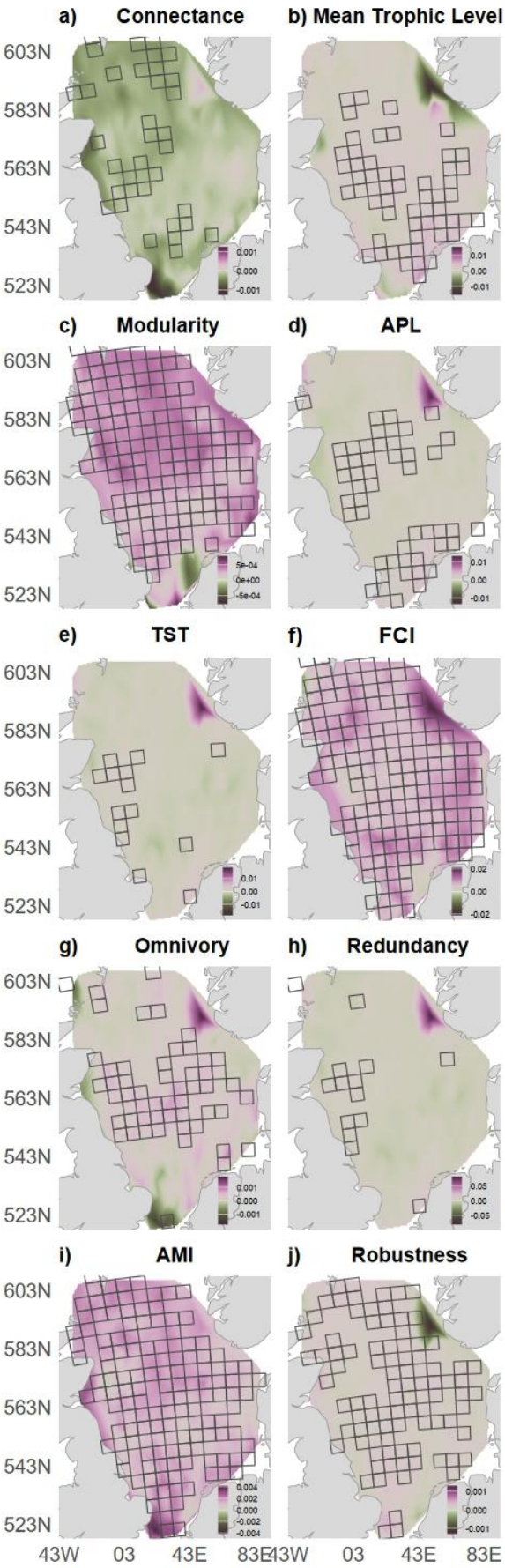
a) Connectance
b) Mean Trophic Level
c) Modularity
d) APL
e) TST
f) FCI
g) Omnivory
h) Redundancy
i) AMI
j) Robustness
603N
583N
563N
543N
523N
43W
03
43E
83E

2687

Figure 5.6: Temporal trends at the 50 x 50 km grid scale (Sen's slopes) in food web network metrics a) connectance, b) mean trophic level, c) modularity, d) average path length (APL), e) total system throughflow ($mgCm^{-2}year^{-1}$; TST), f) Finn cycling index (%, FCI), g) omnivory, h) average mutual information (bits, AMI), i) redundancy (bits) and j) robustness. If a 50 km grid cell was outlined, it indicates a significant temporal trend ($p \leq 0.05$) of that metric within that region. Temporal trends were calculated using Sen's slope, a non-parametric measure of trend magnitude calculated as the median of all pairwise slopes between observations over time. Site-level Sen's slope estimates were interpolated across the study region using bilinear interpolation (Akima interpolation), generating continuous raster surfaces of spatial trend patterns.

Grid cells exhibiting the highest density of significant temporal change in food web structure and function were clustered around the British coastline (Figure 5.6). This suggests locally concentrated restructuring of North Sea food web structure and function across time. Two grid cells showed significant temporal trends in eight metrics, indicating locally concentrated restructuring of food web structure and function (Figure 5.7). Overall, there was substantial spatial overlap between grid cells exhibiting multi-metric shifts and those experiencing significant changes in commercial fishing (Figure 5.1b and Figure 5.7). Specifically, 69.1% of grid cells showing significant temporal trends in two or more food-web metrics also exhibited concurrent significant temporal trends in commercial fishing.

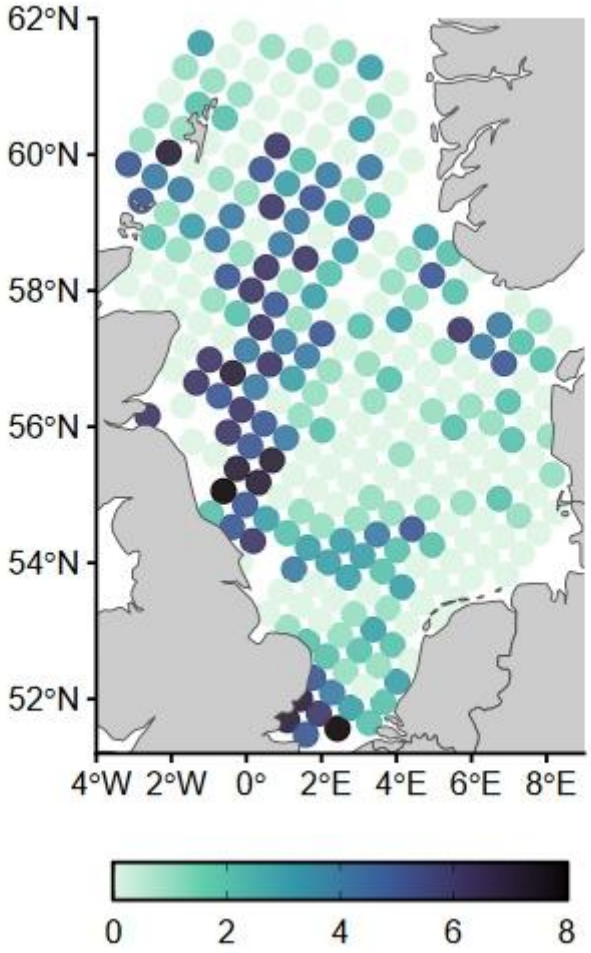

Figure 5.7: The number of metrics that showed a significant temporal trend within each North Sea grid cell.

5.5 Discussion

Within the North Sea, community structure is not fixed across space but varies with the environmental gradients and pressures experienced by local assemblages, including sea surface temperature and commercial fishing. These shifts in community composition can reshape food-web structure by altering the species interactions and energetic pathways that support ecosystem functioning. Here, we show that North Sea food webs underwent substantial reorganisation from 1997 to 2015, shifting towards more structured and compartmentalised configurations despite reductions in trophic connectivity and energetic capacity. Rather than exhibiting a uniform decline, ecosystem resilience was reconfigured through contrasting changes in structural and functional components, with declines in pathway diversity and energy throughput occurring alongside increased organisation,

recycling, and robustness. Therefore, there is overall less energy within North Sea food webs supporting biological activity, but what energy remains is being used more efficiently. This indicates that persistence of energy flow has become increasingly supported by the organisation and retention of energy within the system, rather than by extensive connectivity and energetic redundancy. As food webs consolidate into more organised configurations, energy flow becomes more efficiently routed through fewer pathways, allowing continued functioning under constrained energetic conditions while increasing reliance on the stability of remaining trophic interactions. Together, these changes indicate that resilience in North Sea food webs has shifted from being supported more by pathway diversity and energetic surplus to being increasingly maintained through increased organisation, compartmentalisation, and efficient retention of energy.

The structural and functional changes observed here reflect a shift in how resilience is maintained within the ecosystem. Increased organisation, compartmentalisation, and recycling improve the efficiency and persistence of energy transfer (Ulanowicz 2003, 2009), limiting the propagation of perturbations and enabling continued energy flow despite reduced overall availability (Krause et al., 2003; Stouffer and Bascompte, 2011). At the same time, reduced pathway diversity and energetic reserves indicate diminished buffering capacity, increasing reliance on fewer trophic pathways to maintain ecosystem processes (de Jonge and Schückel, 2021; Fulton et al., 2003; Heymans and Baird, 2000). Increased recycling suggests that energy is retained and reused more efficiently within the system, potentially compensating for reduced flux. For example, in the Gulf of Naples plankton food web, enhanced re-routing of energy through detrital and microbial pathways helped sustain trophic functioning during periods of reduced primary production (D'Alelio et al., 2016). Overall, rather than accumulating trophic links and energetic surplus, North Sea food webs appear to have consolidated into simpler but more organised networks that prioritise efficient routing and retention of energy.

This restructuring is consistent with ecological reorganisation following disturbance, as described by the Panarchy framework, in which ecosystems undergo cycles of growth, conservation, release, and reorganisation (Allen et al., 2014; Gunderson and Holling, 2006; Kharrazi et al., 2016). Declines in energetic throughput and pathway diversity indicate loss of energetic surplus and trophic pathways, while increases in

organisation and recycling reflect consolidation and optimisation of remaining energy flows. In this context, ecosystem resilience emerges through structural organisation and efficiency rather than through accumulation of complexity and redundancy. This suggests that North Sea food webs have stabilised into more organised but energetically constrained configurations, reflecting adaptation to continued or recent pressures rather than full recovery of trophic complexity found in the past, offering potential reduced capacity to adapt to future pressures (Folke et al., 2016; Scharler et al., 2018).

However, this restructuring was spatially heterogeneous, highlighting the scale dependence of ecosystem resilience and environmental pressure dynamics. While regional averages indicated reductions in energetic reserves and pathway diversity, spatially explicit analyses revealed widespread increases in compartmentalisation, recycling, and organisation, alongside localised strengthening of trophic structure and energy transfer in some areas. Differences between grid-level and regional trends demonstrate that spatial aggregation can potentially obscure localised restructuring processes.

Increases in mean trophic level in parts of the southern North Sea are consistent with rebuilding of trophic structure under reduced fishing pressure (McClanahan, 2014; Rojo et al., 2021), whereas weaker responses elsewhere indicate incomplete or uneven recovery. The observed pronounced restructuring along the British coastline, including increased trophic organisation, recycling, and energy transfer, indicates focal regions of trophic rebuilding and functional reorganisation. These findings demonstrate that ecosystem resilience pathways vary geographically, and that regional-scale indicators alone may underestimate localised recovery. Other studies have also found such spatial mismatches in ecosystem resilience. In the Tagus Estuary, Bay of Seine and Bay of Biscay, food-web network properties differed markedly when constructed at broader versus more restricted spatial extents, with key structural metrics changing depending on system boundaries (Nogues et al., 2022; Schückel et al., 2022; Vinagre et al., 2017).

The observed divergence between regional and local patterns reflects the spatially explicit nature of commercial fisheries as a pressure. Fishing effort and reductions in fishing mortality occur unevenly across the seascape due to management measures,

fleet behaviour, and species distributions (Holland, 2003; Truesdell et al., 2016), allowing potential recovery of trophic structure and functional pathways to emerge locally rather than uniformly across the ecosystem. Studies have found that the spatial distribution of fishing effort can be as important as total fishing mortality when determining environmental impacts (Truesdell et al., 2016). In contrast, climate-driven warming operates across broad spatial and temporal scales, influencing metabolic demand, species distributions, and energy flux (O'Gorman et al., 2019; Ullah et al., 2018). However, the absence of widespread local sea surface temperature trends alongside spatially explicit changes in food-web structure suggests that historical and contemporary fishing pressure remains a key driver of trophic restructuring within the region. Together, these findings further emphasise the importance of assessing ecosystem resilience at spatial scales aligned with the distribution of anthropogenic pressures. Future research would do well in explicitly understanding the link between food web dynamics and commercial fishing at spatially relevant scales.

Overall, resilience across the North Sea has undergone reorganisation rather than uniform decline or recovery from 1997 to 2015. Structural organisation, compartmentalisation, and persistence have strengthened, while energetic reserves and pathway diversity have declined or remained constrained. This indicates that resilience is increasingly supported by efficient routing and retention of energy rather than by high redundancy and energetic surplus. Such restructuring allows continued ecosystem functioning under sustained pressure but may increase vulnerability to future disturbance if remaining pathways are disrupted (Scharler et al., 2018; Ulanowicz et al., 2009). These findings highlight the importance of protecting energetic reserves, trophic pathway diversity, and biomass, particularly at spatial scales relevant to fisheries impacts. By applying empirical food webs and ENA across spatial and temporal scales, this study provides an integrated assessment of ecosystem resilience properties and supports the development of spatially explicit ecosystem-based management to maintain ecosystem resilience allowing the continued provision of ecosystem services under ongoing environmental change.

5.6 Supplementary material

All supplementary material needed for chapter 5 is included in the supplementary material of chapter 4 (Table S4.1 and S4.2; Figure S4.1: S4.11).

6 General Discussion

6.1 Summary

The transfer of energy within ecosystems underpins not only the survival of individual species but the functioning and persistence of entire ecological systems, characterised by ecosystem resilience. Energy moves among species and between their environment through a complex web of direct and indirect trophic interactions, collectively represented as food webs. These networks capture the pathways through which biomass and energy are redistributed, regulated, and maintained within ecosystems.

Food webs have become increasingly central in environmental research as recognition grows that anthropogenic pressures disrupt ecosystems through both direct and indirect pathways. Climate change and commercial fishing do not simply affect individual species, their impacts propagate through trophic interactions, altering energy flow and restructuring ecological communities. Understanding food webs is therefore fundamental to assessing multispecies persistence and ecosystem resilience under global change.

Although there is strong evidence demonstrating the value of food web approaches in environmental research, most historical case studies have been limited by data availability. As a result, food web research often relies on empirical food webs that are static representations constructed at relatively small spatial and temporal scales, limiting their ability to capture the dynamic and interconnected nature of marine ecosystems, or on modelled representations, which hold inherent uncertainty.

This thesis addresses these limitations through three primary objectives: (1) to construct robust, empirical, multi-species food webs capable of advancing research within the Northeast Atlantic; (2) to extend understanding of food web structure and function across unprecedented spatial and temporal scales; and (3) to examine how cumulative environmental gradients, specifically sea surface temperature (SST) and commercial fishing, jointly shape trophic dynamics. Together, these objectives provide a more realistic and integrative portrait of energy flow and ultimately ecosystem resilience within northern temperate marine ecosystems that are experiencing environmental global change.

Our initial findings demonstrate the sensitivity of even single pairwise trophic interactions to environmental gradients across the Northeast Atlantic, highlighting the relevance of examining food webs across spatial and temporal scales. Fundamental principles governing trophic structure, such as predator–prey body mass scaling, were shown to vary with SST and commercial fishing pressure. The body mass of prey species was found to be increasingly divergent from body size of predators within warmer regions of the Northeast Atlantic due to changing physiology. These results provide clear empirical evidence that the foundational rules structuring trophic interactions are dynamic across environmental gradients and establish a robust basis for scaling analyses from individual interactions to whole food webs across broader spatial and temporal gradients.

Analysis of multi-species food webs allows understanding of both direct and indirect effects on food web structure and function. To address this, in chapter three, we constructed 4,728 spatially resolved, weighted multi-species food webs across the North Sea at 50 km resolution, from 1997 to 2015. This unprecedented dataset provides a novel basis to examine ecosystem-wide variation across broad spatial, temporal and environmental gradients.

Analyses reveal that food web structure and function are jointly shaped by SST and the degree of commercial fishing. Warmer, lightly exploited systems tend to retain more complex and energetically diverse network configurations of trophic interactions, whereas warmer regions with a high degree of commercial fishing shift toward simplified but more efficient and tightly organised structures. This trade-off between complexity and efficiency underpins ecosystem resilience, reflecting the balance between adaptive capacity and functional persistence. While highly organised networks may conserve energy flow and maintain short-term functioning, they exhibit reduced flexibility to reorganise under additional or increased perturbation.

Together, these chapters demonstrate how environmental change is reshaping trophic interactions and food-web organisation across the Northeast Atlantic. Beginning with evidence that warming and commercial fishing alter predator–prey size relationships (chapter two), this thesis then scales these interaction-level changes to spatially explicit empirical food webs (chapter three) to examine how

ecosystem structure responds to environmental gradients (chapter four) and how these dynamics have unfolded through time (chapter five). Across these analyses, consistent patterns emerge in which interacting pressures of climate change and commercial fishing simplify food-web structure while increasing organisational constraint and reducing redundancy within energy pathways. These findings show that trophic interactions and energy transfer within Northeast Atlantic ecosystems are becoming more tightly structured but potentially less flexible, suggesting an increasing emphasis on conservation of existing function at the expense of adaptive potential, with implications for ecosystem resilience under continued environmental change. From a management perspective, the results suggest that climate adaptation and fisheries management cannot be addressed in isolation. Furthermore, spatial heterogeneity in food web responses highlights the necessity of geographically explicit management strategies.

The novelty of this thesis lies in scaling food web research across large spatial extents and multi-decadal timescales, providing a standardised baseline for detecting ecological change within inherently complex and variable marine systems. Such large-scale empirical benchmarking is rare but is essential for integrating food web science into policy and management frameworks. By contextualising and quantifying ecosystem complexity in a structured and interpretable way, food web approaches enable clearer detection of structural and functional shifts that would otherwise remain obscured within ecological variability. Collectively, the findings provide robust evidence of both regional and localised changes in food web structure and function across the Northeast Atlantic, identifying increasing SST and commercial fishing as dominant and interacting drivers of trophic reorganisation that ultimately reshape ecosystem resilience. Overall, this thesis provides an empirically grounded insight into the trophic dynamics of the Northeast Atlantic in the current context of environmental global change.

6.2 Chapter Contributions

6.2.1 Chapter two: Commercial fishing amplifies impacts of increasing temperatures on predator-prey interactions in marine ecosystems.

This chapter examines how SST and commercial fishing pressure interact to modify predator–prey mass ratios (PPMR) in Northeast Atlantic food webs. PPMR is a fundamental metric in food-web ecology, grounded in allometric theory, which explains that body mass strongly constrains trophic interactions through mechanisms such as gape limitation (predators struggle to handle or consume prey larger than themselves) and energetic requirements (predators avoid or do not perceive extremely small prey because they do not provide sufficient energetic return) (Reum et al., 2019a). PPMR therefore underpins many size-based and ecosystem models because it governs interaction strengths, energy transfer efficiency, and trophic stability (Gauzens et al., 2019; Petchey et al., 2008). Despite its widespread use, however, PPMR is typically treated as a fixed parameter in predictive modelling (Hartvig et al., 2011; Klecka, 2014). Here, we explicitly test this assumption by linking long-term stomach-content data to environmental drivers of increasing SST and commercial fishing.

We combine a large historical stomach-content dataset (1981–2016; >300,000 prey observations from 88 predator species) with SST and commercial fishing data to quantify environmental impacts on PPMR across the North Sea over 35 years. This extensive and unprecedented database reveals substantial temporal and spatial variability in predator–prey size relationships. Our results show that PPMR increases significantly with SST, indicating a growing size disparity between predators and their prey in warmer waters. Importantly, this SST effect is strongly amplified by commercial fishing. Contrary to expectations, predator body mass remains largely stable across SST and fishing gradients. Instead, increases in PPMR are driven primarily by reductions in prey body mass, predominantly through intra-specific (physiological) declines rather than shifts in prey species composition.

As prey become smaller, predators respond by selectively targeting the largest individuals within an increasingly small-bodied prey community. These foraging adjustments are consistent with optimal foraging theory and reflect compensation for declining prey size and energetic value (Brown et al., 1999; Pyke, 1984). Such behavioural responses have the potential to alter energy pathways within

ecosystems by modifying interaction strengths and restructuring trophic dynamics, with possible consequences for ecological resilience (Emmerson and Raffaelli, 2004; Jonsson and Ebenman, 1998).

Overall, this chapter provides robust empirical evidence across multiple ecosystems and multi-decadal timescales that PPMR systematically increases with SST and that commercial fishing intensifies this relationship. This chapter establishes a critical mechanistic link between environmental change and food web structure by identifying cumulative effects of climate change and fishing on trophic size relationships. These findings directly challenge the assumption of fixed PPMR values in size-based and ecosystem models, demonstrating instead that predator–prey size structure is dynamic and environmentally contingent. Incorporating environmentally responsive PPMR into predictive models (e.g. ADBM (Petchey et al., 2010); Fluxweb (Gauzens et al., 2019); and EcoSim (Christensen and Walters, 2004) could therefore improve forecasts of trophic dynamics and food-web stability in increasingly warm and heavily exploited marine systems.

6.2.2 Chapter three: Marine benthopelagic food webs of the North Sea (1997-2015)

Building on the findings from pairwise predator–prey interactions, this chapter advances the thesis by scaling up to the construction of whole food webs, enabling assessment of how environmental drivers reshape trophic structure at the ecosystem level. As food webs are composed of many interacting predator–prey relationships, the variability in PPMR identified in chapter two implies that entire trophic networks are likely to reorganise under environmental change. This motivates the need to move beyond individual interactions and reconstruct empirical food webs that capture how such changes propagate across species and trophic pathways. While predator–prey body mass ratios provide critical insight into variation in individual trophic interactions, they cannot capture how these changes propagate indirectly across species and trophic pathways. By integrating trophic interactions within a multi-species food web framework, this chapter enables a more holistic assessment of how SST and commercial fishing alter energy flow, species connectivity, and ecosystem functioning across the North Sea.

A major contribution of this chapter is overcoming longstanding limitations in food web research, which has historically relied on a small number of static and spatially

constrained networks that fail to represent the dynamic and interconnected nature of marine ecosystems. Using an extensive stomach contents database integrated with large-scale fish survey data and supplementary trophic information, this study reconstructs 4,728 spatially explicit empirical food webs across the North Sea. By incorporating overlapping spatial boundaries, accounting for incomplete dietary sampling, and inferring missing interactions using ecological analogues, this framework provides a more realistic and continuous representation of trophic structure across open marine systems. The inclusion of basal resources and lower trophic levels through functional groupings ensures whole-system representation, while weighting trophic links using allometric energy flux estimates allows quantification of functional properties beyond simple presence or absence of trophic interactions.

This chapter delivers, to our knowledge, the most comprehensive spatially and temporally resolved empirical food web dataset to date. Critically, it also establishes a dynamic, reproducible, and scalable methodology that enables consistent food web construction across regions and time periods. By moving from isolated trophic interactions to fully integrated, energy-weighted food webs, this work provides a robust empirical foundation for quantifying ecosystem structure, energy pathways, and resilience under global change. The food web dataset created here provides the empirical platform necessary to quantify ecosystem responses to environmental change. This enables subsequent chapters to examine how food web organisation responds to environmental gradients across space (chapter four) and how these structural properties have changed through space and time (chapter five).

6.2.3 Chapter four: Commercial fishing makes North Sea food webs more sensitive to increasing temperature.

This chapter makes a significant contribution to food web research by providing one of the first spatially extensive, empirically grounded assessments of how SST and commercial fishing jointly restructure trophic networks across the North Sea. By analysing the novel suite of 4,728 weighted North Sea food webs produced in chapter three across environmental gradients of SST and fishing, this chapter moves beyond local or single-system studies to quantify how food web structure and energy flow respond to interacting stressors at ecosystem scales. We applied Ecological Network Analysis (ENA), a quantitative framework that applies network theory and

energy flow principles to food webs to quantify how energy is transferred, organised, and distributed among species within ecosystems. This approach enables assessment of how ecosystem resilience varies across spatial and temporal gradients of environmental change. The results demonstrate that SST and commercial fishing do not act independently, but instead interact to jointly determine trophic organisation, energy magnitude, and pathway redundancy. Increasing temperatures in areas that have a high degree of commercial fishing results in food webs that are relatively simplified, more tightly organised, with energetically limited configurations. This restructuring reflects a shift in ecosystem resilience, where increased structural organisation and energetic efficiency occur alongside reduced redundancy and adaptive flexibility.

A key contribution of this chapter is the empirical demonstration that commercial fishing amplifies ecosystem sensitivity to warming, fundamentally altering how marine food webs respond to climate-driven increases in SST. This work highlights the mechanisms through which human pressures reshape the structural foundations of ecosystem resilience by identifying consistent declines in energy availability, trophic flexibility, and redundancy under combined stressors. Furthermore, by establishing regional patterns across the North Sea, this chapter provides a robust empirical baseline for detecting future change and strengthens the integration of food web research into ecosystem-based management. These findings advance understanding of how cumulative anthropogenic pressures reorganise marine ecosystems and emphasise the importance of managing climate change and fisheries jointly to preserve ecosystem resilience.

This scaling from trophic interactions to ecosystem structure also provides a mechanistic link with the findings of chapter two. In chapter two, interactions in environmental change were shown to alter predator–prey mass ratios, demonstrating that SST and commercial fishing reshape the body-size structure of trophic interactions. Because food webs are composed of many such interactions, changes in predator–prey size relationships can propagate through trophic networks, influencing interaction strengths, energy transfer, and ultimately whole-food-web organisation (Brose et al., 2006; Petchey et al., 2008; Reum et al., 2019b). Body-size scaling is a central organising principle of ecological networks and strongly constrains how energy moves between trophic levels (Brown et al., 2004, 1999;

Yodzis and Innes, 1992). Importantly, both chapter two and chapter four identify significant interactive effects between SST and commercial fishing, indicating that these drivers do not operate independently but instead combine to restructure marine ecosystems. The consistency of these findings across analytical scales suggests that climate-driven changes are heavily dependent on the concurrent degree of commercial fishing, from the level of individual predator–prey interactions to the structure, energy pathways, and resilience of entire food webs.

6.2.4 Chapter five: Spatial scale determines temporal reconfiguration of North Sea ecosystem resilience

In this chapter, the focus shifts from spatial gradients to temporal dynamics in food web structure and function. While previous analyses examined how environmental drivers shape trophic networks across space, here we assess how long-term environmental change has reorganised North Sea food webs through time. Using ENA on the empirical database of 4,728 weighted multi-species food webs constructed in chapter three, we demonstrate that food webs in 2015 were structurally simpler than those in 1997, characterised by reduced connectance and lower overall energy magnitude, yet consisted of more tightly organised energy pathways.

This reorganisation indicates a temporal shift in ecosystem resilience, reflecting the balance between adaptive capacity, supported by redundancy and alternative energy pathways, and persistence, supported by efficient and constrained energy transfer (Ulanowicz, 2009, 2004). The observed simplification alongside increased organisation suggests that North Sea food webs have moved towards conserving existing structure and function, potentially at the expense of flexibility to respond to future perturbations.

A further contribution of this chapter lies in resolving temporal change at more localised spatial scales. By analysing local 50 km × 50 km trends in food web dynamics, we show that regional trends can mask substantial local heterogeneity. In several areas, local trajectories diverge from basin-scale patterns, demonstrating that ecosystem reorganisation is not spatially uniform. This spatially explicit temporal perspective provides a more realistic understanding of how ecosystem resilience

evolves across heterogeneous marine systems and strengthens the case for geographically targeted ecosystem-based management.

Chapter four shows that SST and commercial fishing jointly restructure food-web organisation and energy flow across spatial gradients, while chapter five extends this analysis by examining how these processes have unfolded through time while also resolving finer-scale spatial variation. Although regional trajectories can mask substantial local heterogeneity, both chapters reveal consistent reconfiguration of ecosystem resilience, with food webs becoming simpler and more tightly organised, characterised by reduced redundancy and fewer alternative energy pathways.

Together, chapters four and five provide an unprecedented benchmarking of food web structure and function across spatial and temporal scales within a northern temperate marine ecosystem. These results advance understanding of the dynamic nature of food webs and the mechanisms underpinning ecosystem resilience under environmental change. By establishing a robust empirical baseline, this work enables future comparisons and provides a foundation for anticipating and managing ongoing and future restructuring of the North Sea.

6.3 Future Work

6.3.1 Strengthening and expanding the food web database

Despite the unprecedented scope of data used in this thesis, several limitations remain that future research could address, such as the temporal patchiness of observed trophic interactions. Since constructing these food webs, additional stomach contents data have become available within the North Sea (Pinnegar et al., 2023) as well as across other regions of the Atlantic (NOAA, 2023) and incorporating these records would extend temporal coverage and improve representation of trophic dynamics. Increased temporal resolution captures greater dietary variability and strengthens inference of long-term structural and functional change.

Another limitation was the availability of dietary information for lower and higher trophic levels, such as zooplankton, decapods, marine birds and mammals. Currently, trophic interactions for many basal and intermediate taxa are inferred from existing ecosystem models, restricting the proportion of directly observed links. Expanding empirical sampling of lower trophic levels would significantly improve food

web realism. Continued collaboration and data sharing will further enhance the robustness of the empirical food web database. Furthermore, the methodology developed here could also be extended to other ecosystems and time periods using emerging global resources such as FishGlob (Maureaud et al., 2024) and other trophic interaction databases.

Fishing effort data also remain a major constraint throughout the thesis. Fishing data largely constrained the time-period in which we could construct empirical food webs, as we could not find reliable commercial fishing data before 1997 or at a wide spatial scale. Improving the spatial and temporal resolution of commercial fishing effort records, through enhanced reporting and/or reconstruction approaches should be prioritised (for example Couce et al., 2020). Consistent and transparent reporting by commercial fisheries and management agencies is essential for understanding how exploitation alters trophic structure and affects ecosystem resilience. Standardising commercial fisheries catch reporting across ocean management jurisdictions is therefore a critical priority for improving global ocean governance. Marine ecosystems are highly interconnected, meaning environmental pressures and commercial fishing impacts can propagate far beyond focal regions such as the North Sea, highlighting the need for coordinated and comparable reporting practices.

Artificial intelligence tools, including generative models and machine-learning approaches, will help address limitations in historical data such as bias in the digestibility of prey, as well as reduce the extensive sampling effort required to construct food webs. Machine-learning techniques can be used to extrapolate temporal patterns in biomass, trophic structure, and environmental conditions across locations, while also addressing missing data and estimating energy fluxes between species. For example, Barel et al., 2023 applied multiple machine-learning techniques to predict microbial feeding interactions from species traits and taxonomy, demonstrating that models such as boosted-regression trees can accurately infer trophic links and reconstruct microbial food webs from empirical datasets.

6.3.2 Using empirical food webs to support predictive modelling

The spatially and temporally resolved food webs developed in this thesis provide a strong empirical foundation for predictive ecosystem modelling. These food webs

can be used to calibrate and validate dynamical ecosystem models, machine learning frameworks, and trait-based predictive approaches to forecast how trophic structure, energy flow, and ecosystem resilience may respond to future scenarios of global change. Such models could simulate perturbations including species extinctions, poleward species redistribution, and climate-induced changes in primary productivity altering detrital inputs, as well as evaluate management interventions such as reduced fishing pressure or stock rebuilding. Here are some examples:

Dynamical extinction cascade models (Zhao et al., 2016) provide one key application. These models quantify robustness using the R_{50} metric which is the proportion of species removals required to cause 50% secondary extinctions, based either on complete loss of resource species or sufficient energy flux from key resources. R_{50} is calculated by explicitly simulating how perturbations propagate through trophic networks. Applying such approaches would advance our assessment of how warming and fishing alter ecosystem resilience and help identify key species whose loss disproportionately destabilises food webs.

The empirical food webs developed here also provide a valuable opportunity to improve trait-based predictive food web models, such as the Allometric Diet Breadth Model (ADBM; Petchey et al., 2010), which predicts trophic interactions based primarily on body size and energetic constraints. While these models provide a powerful theoretical framework, they rely heavily on a few assumptions and lack extensive empirical validation at ecosystem scales (Petchey et al., 2010). The empirically derived trophic interactions and energy flux estimates generated in this thesis provide a robust benchmark against which predictive performance can be directly evaluated, reducing uncertainty associated with purely theoretical predictions. The extensive stomach contents database (Pinnegar et al., 2023) and other associated trait information databases provide opportunities to incorporate additional predictive parameters, such as feeding strategies, physiological constraints such as gape size, and realised diet breadth, improving model realism and predictive accuracy while reducing reliance on extensive future sampling of empirical data.

More broadly, integrating empirical food web structure into predictive frameworks improves ecological forecasting by capturing the mechanistic pathways through

which environmental change propagates across ecosystems (Rubbens et al., 2023). The food webs developed here provide a robust basis for forecasting ecosystem trajectories under future environmental conditions, identifying resilience thresholds, and supporting climate-informed ecosystem-based management because they capture real-world spatial and temporal variability. Similar forecasting approaches have already been demonstrated, for example, Trifonova et al., (2017) applied a dynamic Bayesian network to the North Sea ecosystem to predict how changes in fisheries catch propagate through trophic interactions and influence species abundances across the food web. The food-web framework developed in this study could substantially improve the temporal and spatial resolution of such predictions by incorporating fine-scale variability in species biomass, trophic interactions, and environmental conditions, enabling more detailed forecasts of how fishing and other pressures may reshape ecosystem structure across regions and through time.

6.3.3 Integrating Cumulative Stressors with Food Web Structure

Future research should integrate empirical food web data with cumulative impact assessment frameworks. Cumulative impact assessment frameworks are tools used in marine ecosystem management to evaluate the combined effects of multiple human activities and environmental pressures on marine ecosystems (Halpern et al., 2008; Korpinen, 2015). Spatial mapping of overlapping anthropogenic stressors provides a powerful method for identifying ecosystem vulnerability (Halpern et al., 2015, 2008; Kappel and Halpern, 2012). Applying this approach to the North Sea, and more broadly to other marine ecosystems, alongside the food-web construction framework presented here would help identify regions where warming, fishing, and other pressures co-occur and where food-web resilience is most at risk. Identifying spatially correlated stressors simplifies interpretation of ecosystem change by highlighting dominant driver combinations, rather than disentangling each stressor independently, which is often impossible to do with environmental datasets. Integrating cumulative impact mapping with food web structure would provide a mechanistic and spatially explicit framework for understanding how multiple stressors jointly reshape marine ecosystems.

6.3.4 Further embedding food web change within resilience theory

Linking empirical food-web restructuring to resilience theory can strengthen existing frameworks for interpreting ecosystem change. The Panarchy framework (Allen et al., 2014; Gunderson and Holling, 2006; Holling, 2001) conceptualises ecosystems as adaptive cycles of growth, conservation, release, and reorganisation, within which shifts in food-web organisation, energy throughput, and redundancy may signal transitions between resilience states. These transitions may involve tipping points and regime shifts. Future research could therefore use food-web metrics, such as redundancy, energy throughput, and organisational constraint, to detect such thresholds (Folke, 2006; Scheffer and Carpenter, 2003). Analysing temporal and spatial trajectories of food-web structure may reveal early warning signals of critical transitions, while dynamical simulations could help quantify ecosystem proximity to these thresholds.

Integrating these perspectives would enable more consistent benchmarking of ecosystem change, facilitate wider adoption and synthesis of ecosystem indicators, and support the development of early warning signals for ecosystem collapse and regime shifts. Embedding food-web analysis within resilience theory would move the field beyond descriptive network analysis toward a more predictive and mechanistic understanding of ecosystem stability, improving our ability to anticipate and manage ecological change under interacting global stressors.

6.3.5 Advancing Ecosystem-Based Indicators and Management

Future research should continue to support the development of ecosystem-level indicators required by regulatory bodies such as ICES and international agreements aimed at protecting the marine environment, including OSPAR. Effective marine management increasingly requires approaches that move beyond traditional single-species quotas and maximum sustainable yield frameworks toward indicators that capture whole ecosystem structure and function. Large, empirically derived food-web datasets such as those developed here provide a valuable foundation for this transition. By capturing spatial and temporal variability in trophic interactions and energy flow, they can help establish historical baselines of ecosystem structure, identify regions where ecosystems may be most vulnerable to cumulative pressures, and support forecasting of future ecosystem change under interacting stressors.

Integrating such food-web information into ecosystem-based management frameworks could therefore improve the capacity of marine governance to anticipate and respond to ongoing environmental change– a research opportunity I hope to be a part of in the future!

7 References

Agnetta, D., Badalamenti, F., Sweeting, C.J., Libralato, S., Pipitone, C., 2024. Erosion of fish trophic position: an indirect effect of fishing on food webs elucidated by stable isotopes.

Akaike, H., 1974. A new look at the statistical model identification. IEEE Trans. Autom. Control 19, 716–723. https://doi.org/10.1109/TAC.1974.1100705

Akima, H., 1978. A Method of Bivariate Interpolation and Smooth Surface Fitting for Irregularly Distributed Data Points. ACM Trans Math Softw 4, 148–159. https://doi.org/10.1145/355780.355786

Albert, R., Barabási, A.-L., 2002. Statistical mechanics of complex networks. Rev. Mod. Phys. 74, 47–97. https://doi.org/10.1103/RevModPhys.74.47

Albouy, C., Velez, L., Coll, M., Colloca, F., Le Loc'h, F., Mouillot, D., Gravel, D., 2014. From projected species distribution to food-web structure under climate change. Glob. Change Biol. 20, 730–741. https://doi.org/10.1111/gcb.12467

Allen, C.R., Angeler, D.G., Garmestani, A.S., Gunderson, L.H., Holling, C.S., 2014. Panarchy: Theory and Application. Ecosystems 17, 578–589. https://doi.org/10.1007/s10021-013-9744-2

Allesina, S., Bodini, A., Bondavalli, C., 2006. Secondary extinctions in ecological networks: Bottlenecks unveiled. Ecol. Model., Special Issue on the Fourth European Conference on Ecological Modelling 194, 150–161. https://doi.org/10.1016/j.ecolmodel.2005.10.016

Andersen, K.H., Beyer, J.E., 2015. Size structure, not metabolic scaling rules, determines fisheries reference points. Fish Fish. 16, 1–22. https://doi.org/10.1111/faf.12042

Atkins, J.R.C., Scaife, A.A., Graham, J.A., Tinker, J., Halloran, P.R., 2025. Recent European marine heatwaves are unprecedented but not unexpected. Commun. Earth Environ. 6, 792. https://doi.org/10.1038/s43247-025-02802-3

Báez, J.C., Gimeno, L., Real, R., 2021. North Atlantic Oscillation and fisheries management during global climate change. Rev. Fish Biol. Fish. 31, 319–336. https://doi.org/10.1007/s11160-021-09645-z

Baird, D., Ulanowicz, R.E., 1989. The Seasonal Dynamics of The Chesapeake Bay Ecosystem. Ecol. Monogr. 59, 329–364. https://doi.org/10.2307/1943071

Barbier, E.B., 2017. Marine ecosystem services. Curr. Biol. 27, R507–R510. https://doi.org/10.1016/j.cub.2017.03.020

Barel, J.M., Petchey, O.L., Ghaffouli, A., Jassey, V.E.J., 2023. Uncovering microbial food webs using machine learning. Soil Biol. Biochem. 186, 109174. https://doi.org/10.1016/j.soilbio.2023.109174

Barnes, C., Maxwell, D., Reuman, D.C., Jennings, S., 2010. Global patterns in predator–prey size relationships reveal size dependency of trophic transfer efficiency. Ecology 91, 222–232. https://doi.org/10.1890/08-2061.1

Bartley, T.J., McCann, K.S., Bieg, C., Cazelles, K., Granados, M., Guzzo, M.M., MacDougall, A.S., Tunney, T.D., McMeans, B.C., 2019. Food web rewiring in a changing world. Nat. Ecol. Evol. 3, 345–354. https://doi.org/10.1038/s41559-018-0772-3

Bascompte, J., Melián, C.J., Sala, E., 2005. Interaction strength combinations and the overfishing of a marine food web. Proc. Natl. Acad. Sci. 102, 5443–5447. https://doi.org/10.1073/pnas.0501562102

Baudron, A.R., Needle, C.L., Rijnsdorp, A.D., Tara Marshall, C., 2014. Warming temperatures and smaller body sizes: synchronous changes in growth of North Sea fishes. Glob. Change Biol. 20, 1023–1031. https://doi.org/10.1111/gcb.12514

Baum, J.K., Worm, B., 2009. Cascading top-down effects of changing oceanic predator abundances. J. Anim. Ecol. 78, 699–714. https://doi.org/10.1111/j.1365-2656.2009.01531.x

Bazin, S., Domaizon, I., Barouillet, C., Frossard, V., Sentis, A., 2025. Seasonal variations in planktonic food web structure affect stability by shifting the distribution of energy fluxes. Oikos n/a, e11528. https://doi.org/10.1002/oik.11528

Beaumont, N.J., Austen, M.C., Atkins, J.P., Burdon, D., Degraer, S., Dentinho, T.P., Derous, S., Holm, P., Horton, T., van Ierland, E., Marboe, A.H., Starkey, D.J., Townsend, M., Zarzycki, T., 2007. Identification, definition and quantification of goods and services provided by marine biodiversity: Implications for the ecosystem approach. Mar. Pollut. Bull. 54, 253–265. https://doi.org/10.1016/j.marpolbul.2006.12.003

Beaumont, N.J., Austen, M.C., Mangi, S.C., Townsend, M., 2008. Economic valuation for the conservation of marine biodiversity. Mar. Pollut. Bull. 56, 386–396. https://doi.org/10.1016/j.marpolbul.2007.11.013

Becker, R.A., Wilks, A.R., Brownrigg, R., Minka, T.P., Deckmyn, A., 2023. Maps: Draw Geographical Maps. https://doi.org/https://doi.org/10.32614/CRAN.package.maps (2023).

Belgrano, A. (Ed.), 2004. Aquatic food webs: an ecosystem approach. Oxford University Press, Oxford.

Berkeley, S.A., Hixon, M.A., Larson, R.J., Love, M.S., 2004. Fisheries Sustainability via Protection of Age Structure and Spatial Distribution of Fish Populations. Fisheries 29, 23–32. https://doi.org/10.1577/1548-8446(2004)29%5B23:FSVPOA%5D2.0.CO;2

Biggs, C.R., Yeager, L.A., Bolser, D.G., Bonsell, C., Dichiera, A.M., Hou, Z., Keyser, S.R., Khursigara, A.J., Lu, K., Muth, A.F., Negrete Jr., B., Erisman, B.E., 2020.

Does functional redundancy affect ecological stability and resilience? A review and meta-analysis. Ecosphere 11, e03184. https://doi.org/10.1002/ecs2.3184

Binzer, A., Guill, C., Rall, B.C., Brose, U., 2016. Interactive effects of warming, eutrophication and size structure: impacts on biodiversity and food-web structure. Glob. Change Biol. 22, 220–227. https://doi.org/10.1111/gcb.13086

Blackman, R.C., Ho, H.-C., Walser, J.-C., Altermatt, F., 2022. Spatio-temporal patterns of multi-trophic biodiversity and food-web characteristics uncovered across a river catchment using environmental DNA. Commun. Biol. 5, 259. https://doi.org/10.1038/s42003-022-03216-z

Blanchard, J.L., Dulvy, N.K., Jennings, S., Ellis, J.R., Pinnegar, J.K., Tidd, A., Kell, L.T., 2005. Do climate and fishing influence size-based indicators of Celtic Sea fish community structure? ICES J. Mar. Sci. 62, 405–411. https://doi.org/10.1016/j.icesjms.2005.01.006

Blanchard, J.L., Heneghan, R.F., Everett, J.D., Trebilco, R., Richardson, A.J., 2017. From Bacteria to Whales: Using Functional Size Spectra to Model Marine Ecosystems. Trends Ecol. Evol. 32, 174–186. https://doi.org/10.1016/j.tree.2016.12.003

Bodin, Ö., Crona, B., Ernstson, H., 2006. Social Networks in Natural Resource Management: What Is There to Learn from a Structural Perspective? Ecol. Soc. 11.

Bondavalli, C., Bodini, A., 2014. How interaction strength affects the role of functional and redundant connections in food webs. Ecol. Complex. 20, 97–106. https://doi.org/10.1016/j.ecocom.2014.09.004

Borrett, S.R., Lau, M.K., 2014. enaR: An R package for Ecosystem Network Analysis. Methods Ecol. Evol. 5, 1206–1213. https://doi.org/10.1111/2041-210X.12282

Boyce, D., Tittensor, D., Worm, B., 2008. Effects of temperature on global patterns of tuna and billfish richness. Mar. Ecol. Prog. Ser. 355, 267–276. https://doi.org/10.3354/meps07237

Boyce, D.G., Frank, K.T., Worm, B., Leggett, W.C., 2015. Spatial patterns and predictors of trophic control in marine ecosystems. Ecol. Lett. 18, 1001–1011. https://doi.org/10.1111/ele.12481

Branch, T.A., Watson, R., Fulton, E.A., Jennings, S., McGilliard, C.R., Pablico, G.T., Ricard, D., Tracey, S.R., 2010. The trophic fingerprint of marine fisheries. Nature 468, 431–435. https://doi.org/10.1038/nature09528

Brierley, A.S., Kingsford, M.J., 2009. Impacts of Climate Change on Marine Organisms and Ecosystems. Curr. Biol. 19, R602–R614. https://doi.org/10.1016/j.cub.2009.05.046

Brose, U., Williams, R.J., Martinez, N.D., 2006. Allometric scaling enhances stability in complex food webs. Ecol. Lett. 9, 1228–1236. https://doi.org/10.1111/j.1461-0248.2006.00978.x

Brown, J.H., Gillooly, J.F., Allen, A.P., Savage, V.M., West, G.B., 2004. TOWARD A METABOLIC THEORY OF ECOLOGY. Ecology 85, 1771–1789. https://doi.org/10.1890/03-9000

Brown, J.S., Laundré, J.W., Gurung, M., 1999. The Ecology of Fear: Optimal Foraging, Game Theory, and Trophic Interactions. J. Mammal. 80, 385–399. https://doi.org/10.2307/1383287

Bryndum-Buchholz, A., Boyce, D., Tittensor, D., Christensen, V., Bianchi, D., Lotze, H., 2020. Climate-change impacts and fisheries management challenges in the North Atlantic Ocean. Mar. Ecol. Prog. Ser. 648, 1–17. https://doi.org/10.3354/meps13438

Capuzzo, E., Lynam, C.P., Barry, J., Stephens, D., Forster, R.M., Greenwood, N., McQuatters-Gollop, A., Silva, T., van Leeuwen, S.M., Engelhard, G.H., 2018. A decline in primary production in the North Sea over 25 years, associated with reductions in zooplankton abundance and fish stock recruitment. Glob. Change Biol. 24, e352–e364. https://doi.org/10.1111/gcb.13916

Casey, J.M., Meyer, C.P., Morat, F., Brandl, S.J., Planes, S., Parravicini, V., 2019. Reconstructing hyperdiverse food webs: Gut content metabarcoding as a tool to disentangle trophic interactions on coral reefs. Methods Ecol. Evol. 10, 1157–1170. https://doi.org/10.1111/2041-210X.13206

Chen, Z., Qiu, Y., Xu, S., 2011. Changes in trophic flows and ecosystem properties of the Beibu Gulf ecosystem before and after the collapse of fish stocks. Ocean Coast. Manag. 54, 601–611. https://doi.org/10.1016/j.ocecoaman.2011.06.003

Cheung, W.W.L., Sarmiento, J.L., Dunne, J., Frölicher, T.L., Lam, V.W.Y., Deng Palomares, M.L., Watson, R., Pauly, D., 2013. Shrinking of fishes exacerbates impacts of global ocean changes on marine ecosystems. Nat. Clim. Change 3, 254–258. https://doi.org/10.1038/nclimate1691

Christensen, V., Walters, C.J., 2004. Ecopath with Ecosim: methods, capabilities and limitations. Ecol. Model., Placing Fisheries in their Ecosystem Context 172, 109–139. https://doi.org/10.1016/j.ecolmodel.2003.09.003

Clark, R.A., Fox, C.J., Viner, D., Livermore, M., 2003. North Sea cod and climate change – modelling the effects of temperature on population dynamics. Glob. Change Biol. 9, 1669–1680. https://doi.org/10.1046/j.1365-2486.2003.00685.x

Coghlan, A.R., Blanchard, J.L., Heather, F.J., Stuart-Smith, R.D., Edgar, G.J., Audzijonyte, A., 2022. Community size structure varies with predator–prey size relationships and temperature across Australian reefs. Ecol. Evol. 12, e8789. https://doi.org/10.1002/ece3.8789

Coghlan, A.R., Blanchard, J.L., Wotherspoon, S., Stuart-Smith, R.D., Edgar, G.J., Barrett, N., Audzijonyte, A., 2024. Mean reef fish body size decreases towards warmer waters. Ecol. Lett. 27, e14375. https://doi.org/10.1111/ele.14375

Coll, M., Libralato, S., Tudela, S., Palomera, I., Pranovi, F., 2008. Ecosystem Overfishing in the Ocean. PLoS ONE 3, e3881. https://doi.org/10.1371/journal.pone.0003881

Corrales, X., Coll, M., Ofir, E., Heymans, J.J., Steenbeek, J., Goren, M., Edelist, D., Gal, G., 2018. Future scenarios of marine resources and ecosystem conditions in the Eastern Mediterranean under the impacts of fishing, alien species and sea warming. Sci. Rep. 8, 14284. https://doi.org/10.1038/s41598-018-32666-x

Couce, E., Schratzberger, M., Engelhard, G.H., 2020. Reconstructing three decades of total international trawling effort in the North Sea. Earth Syst. Sci. Data 12, 373–386. https://doi.org/10.5194/essd-12-373-2020

Creamer, R.E., Hannula, S.E., Leeuwen, J.P.V., Stone, D., Rutgers, M., Schmelz, R.M., Ruiter, P.C. de, Hendriksen, N.B., Bolger, T., Bouffaud, M.L., Buee, M., Carvalho, F., Costa, D., Dirilgen, T., Francisco, R., Griffiths, B.S., Griffiths, R., Martin, F., Silva, P.M. da, Mendes, S., Morais, P.V., Pereira, C., Philippot, L., Plassart, P., Redecker, D., Römbke, J., Sousa, J.P., Wouterse, M., Lemanceau, P., 2016. Ecological network analysis reveals the inter-connection between soil biodiversity and ecosystem function as affected by land use across Europe. Appl. Soil Ecol., Soil biodiversity and ecosystem functions across Europe: A transect covering variations in bio-geographical zones, land use and soil properties 97, 112–124. https://doi.org/10.1016/j.apsoil.2015.08.006

Cumming, G.S., 2016. Heterarchies: Reconciling Networks and Hierarchies. Trends Ecol. Evol. 31, 622–632. https://doi.org/10.1016/j.tree.2016.04.009

Cumming, G.S., Peterson, G.D., 2017. Unifying Research on Social–Ecological Resilience and Collapse. Trends Ecol. Evol. 32, 695–713. https://doi.org/10.1016/j.tree.2017.06.014

Dakos, V., Matthews, B., Hendry, A.P., Levine, J., Loeuille, N., Norberg, J., Nosil, P., Scheffer, M., De Meester, L., 2019. Ecosystem tipping points in an evolving world. Nat. Ecol. Evol. 3, 355–362. https://doi.org/10.1038/s41559-019-0797-2

D'Alelio, D., Libralato, S., Wyatt, T., Ribera d'Alcalà, M., 2016. Ecological-network models link diversity, structure and function in the plankton food-web. Sci. Rep. 6, 21806. https://doi.org/10.1038/srep21806

Daskalov, G., Mackinson, S., 2007. TROPHIC MODELLING OF THE NORTH SEA.

Daskalov, G.M., Grishin, A.N., Rodionov, S., Mihneva, V., 2007. Trophic cascades triggered by overfishing reveal possible mechanisms of ecosystem regime shifts. Proc. Natl. Acad. Sci. U. S. A. 104, 10518–10523. https://doi.org/10.1073/pnas.0701100104

Daufresne, M., Lengfellner, K., Sommer, U., 2009. Global warming benefits the small in aquatic ecosystems. Proc. Natl. Acad. Sci. 106, 12788–12793. https://doi.org/10.1073/pnas.0902080106

de Jonge, V.N., Schückel, U., 2021. A comprehensible short list of ecological network analysis indices to boost real ecosystem-based management and policy making. Ocean Coast. Manag. 208, 105582. https://doi.org/10.1016/j.ocecoaman.2021.105582

de la Vega, C., Schückel, U., Horn, S., Kröncke, I., Asmus, R., Asmus, H., 2018. How to include ecological network analysis results in management? A case study of three tidal basins of the Wadden Sea, south-eastern North Sea. Ocean Coast. Manag. 163, 401–416. https://doi.org/10.1016/j.ocecoaman.2018.07.019

DeAngelis, D.L., 1980. Energy Flow, Nutrient Cycling, and Ecosystem Resilience. Ecology 61, 764–771. https://doi.org/10.2307/1936746

Díaz, S.M., Settele, J., Brondízio, E., Ngo, H., Guèze, M., Agard, J., Arneth, A., Balvanera, P., Brauman, K., Butchart, S., Chan, K.M.A., Garibaldi, L.A., Ichii, K., Liu, J., Subramanian, S., Midgley, G., Miloslavich, P., Molnár, Z., Obura, D., Pfaff, A., Polasky, S., Purvis, A., Razzaque, J., Reyers, B., Roy Chowdhury, R., Shin, Y.-J., Visseren-Hamakers, I., Willis, K., Zayas, C., 2019. The global assessment report on biodiversity and ecosystem services: Summary for policy makers. Intergovernmental Science-Policy Platform on Biodiversity and Ecosystem Services.

Doney, S.C., Ruckelshaus, M., Emmett Duffy, J., Barry, J.P., Chan, F., English, C.A., Galindo, H.M., Grebmeier, J.M., Hollowed, A.B., Knowlton, N., Polovina, J., Rabalais, N.N., Sydeman, W.J., Talley, L.D., 2012. Climate Change Impacts on Marine Ecosystems. Annu. Rev. Mar. Sci. 4, 11–37. https://doi.org/10.1146/annurev-marine-041911-111611

Donlon, C.J., Martin, M., Stark, J., Roberts-Jones, J., Fiedler, E., Wimmer, W., 2012. The Operational Sea Surface Temperature and Sea Ice Analysis (OSTIA) system. Remote Sens. Environ., Advanced Along Track Scanning Radiometer(AATSR) Special Issue 116, 140–158. https://doi.org/10.1016/j.rse.2010.10.017

du Pontavice, H., Gascuel, D., Reygondeau, G., Maureaud, A., Cheung, W.W.L., 2020. Climate change undermines the global functioning of marine food webs. Glob. Change Biol. 26, 1306–1318. https://doi.org/10.1111/gcb.14944

Ducrotoy, J.-P., Elliott, M., de Jonge, V.N., 2000. The North Sea. Mar. Pollut. Bull., Seas at the Millennium: an Environmental Evaluation 41, 5–23. https://doi.org/10.1016/S0025-326X(00)00099-0

Duffy, J.E., Cardinale, B.J., France, K.E., McIntyre, P.B., Thébault, E., Loreau, M., 2007. The functional role of biodiversity in ecosystems: incorporating trophic complexity. Ecol. Lett. 10, 522–538. https://doi.org/10.1111/j.1461-0248.2007.01037.x

Duffy, J.E., Reynolds, P.L., Boström, C., Coyer, J.A., Cusson, M., Donadi, S., Douglass, J.G., Eklöf, J.S., Engelen, A.H., Eriksson, B.K., Fredriksen, S., Gamfeldt, L., Gustafsson, C., Hoarau, G., Hori, M., Hovel, K., Iken, K.,

Lefcheck, J.S., Moksnes, P.-O., Nakaoka, M., O'Connor, M.I., Olsen, J.L., Richardson, J.P., Ruesink, J.L., Sotka, E.E., Thormar, J., Whalen, M.A., Stachowicz, J.J., 2015. Biodiversity mediates top–down control in eelgrass ecosystems: a global comparative-experimental approach. Ecol. Lett. 18, 696–705. https://doi.org/10.1111/ele.12448

Dunne, J.A., Williams, R.J., Martinez, N.D., 2002. Network structure and biodiversity loss in food webs: robustness increases with connectance. Ecol. Lett. 5, 558–567. https://doi.org/10.1046/j.1461-0248.2002.00354.x

Dye, S.R., Holliday, N.P., Hughes, S.L., Inall, M., Kennington, K., Smyth, T., Tinker, J., Andres, O., Beszczynska-Möller, A., 2013. Climate change impacts on the waters around the UK and Ireland: Salinity. MCCIP Sci. Rev. 2013 7 pages. https://doi.org/10.14465/2013.ARC07.060-066

Elton, C.S., 1927. Animal ecology. Sidgwick and Jackson, London, UK.

Emmerson, M., Raffaelli, D., 2004. Predator-Prey Body Size, Interaction Strength and the Stability of a Real Food Web on JSTOR [WWW Document]. URL https://www.jstor.org/stable/3505650?seq=1 (accessed 3.5.26).

Engelhard, G.H., Lynam, C.P., García-Carreras, B., Dolder, P.J., Mackinson, S., 2015. Effort reduction and the large fish indicator: spatial trends reveal positive impacts of recent European fleet reduction schemes. Environ. Conserv. 42, 227–236. https://doi.org/10.1017/S0376892915000077

Engelhard, G.H., Peck, M.A., Rindorf, A., C. Smout, S., Van Deurs, M., Raab, K., Andersen, K.H., Garthe, S., Lauerburg, R.A.M., Scott, F., Brunel, T., Aarts, G., Van Kooten, T., Dickey-Collas, M., 2014. Forage fish, their fisheries, and their predators: who drives whom? ICES J. Mar. Sci. 71, 90–104. https://doi.org/10.1093/icesjms/fst087

FAO, 2016. The State of World Fisheries and Aquaculture - 2016 (SOFIA) - Latest publications [WWW Document]. URL https://www.fao.org/fishery/en/publication/67906 (accessed 3.4.26).

Fath, B., Scharler, U., 2018. Systems Ecology: Ecological Network Analysis ☆, in: Reference Module in Earth Systems and Environmental Sciences. Elsevier, pp. 1083–1088. https://doi.org/10.1016/B978-0-12-409548-9.11171-6

Fath, B.D., Asmus, H., Asmus, R., Baird, D., Borrett, S.R., de Jonge, V.N., Ludovisi, A., Niquil, N., Scharler, U.M., Schückel, U., Wolff, M., 2019. Ecological network analysis metrics: The need for an entire ecosystem approach in management and policy. Ocean Coast. Manag. 174, 1–14. https://doi.org/10.1016/j.ocecoaman.2019.03.007

Fath, B.D., Scharler, U.M., Ulanowicz, R.E., Hannon, B., 2007. Ecological network analysis: network construction. Ecol. Model., Special Issue on Ecological Network Theory 208, 49–55. https://doi.org/10.1016/j.ecolmodel.2007.04.029

Fauchald, P., Skov, H., Skern-Mauritzen, M., Johns, D., Tveraa, T., 2011. Wasp-Waist Interactions in the North Sea Ecosystem. PLOS ONE 6, e22729. https://doi.org/10.1371/journal.pone.0022729

Fernandes, J.A., Cheung, W.W.L., Jennings, S., Butenschön, M., de Mora, L., Frölicher, T.L., Barange, M., Grant, A., 2013. Modelling the effects of climate change on the distribution and production of marine fishes: accounting for trophic interactions in a dynamic bioclimate envelope model. Glob. Change Biol. 19, 2596–2607. https://doi.org/10.1111/gcb.12231

Finn, J.T., 1980. Flow Analysis of Models of the Hubbard Brook Ecosystem. Ecology 61, 562–571. https://doi.org/10.2307/1937422

Finn, J.T., 1976. Measures of ecosystem structure and function derived from analysis of flows. J. Theor. Biol. 56, 363–380. https://doi.org/10.1016/S0022-5193(76)80080-X

Flanagan, P.H., Jensen, O.P., Morley, J.W., Pinsky, M.L., 2019. Response of marine communities to local temperature changes. Ecography 42, 214–224. https://doi.org/10.1111/ecog.03961

Folke, C., 2006. Resilience: The emergence of a perspective for social–ecological systems analyses. Glob. Environ. Change, Resilience, Vulnerability, and Adaptation: A Cross-Cutting Theme of the International Human Dimensions Programme on Global Environmental Change 16, 253–267. https://doi.org/10.1016/j.gloenvcha.2006.04.002

Folke, C., Biggs, R., Norström, A.V., Reyers, B., Rockström, J., 2016. Social-ecological resilience and biosphere-based sustainability science. Ecol. Soc. 21.

Forster, J., Hirst, A.G., 2012. The temperature-size rule emerges from ontogenetic differences between growth and development rates. Funct. Ecol. 26, 483–492. https://doi.org/10.1111/j.1365-2435.2011.01958.x

Forsyth, P.J., Kay, J.A., 1980. The Economic Implications of North Sea Oil Revenues. Fisc. Stud. 1, 1–28.

Frank, K.T., Petrie, B., Choi, J.S., Leggett, W.C., 2005. Trophic Cascades in a Formerly Cod-Dominated Ecosystem. Science 308, 1621–1623. https://doi.org/10.1126/science.1113075

Frelat, R., Kortsch, S., Kröncke, I., Neumann, H., Nordström, M.C., Olivier, P.E.N., Sell, A.F., 2022. Food web structure and community composition: a comparison across space and time in the North Sea. Ecography 2022. https://doi.org/10.1111/ecog.05945

Fulton, E., Smith, A., Johnson, C., 2003. Effect of complexity on marine ecosystem models. Mar. Ecol. Prog. Ser. 253, 1–16. https://doi.org/10.3354/meps253001

Funes, M., Saravia, L.A., Cordone, G., Iribarne, O.O., Galván, D.E., 2022. Network analysis suggests changes in food web stability produced by bottom trawl

fishery in Patagonia. Sci. Rep. 12, 10876. https://doi.org/10.1038/s41598-022-14363-y

Galparsoro, I., Borja, A., Uyarra, M.C., 2014. Mapping ecosystem services provided by benthic habitats in the European North Atlantic Ocean. Front. Mar. Sci. 1. https://doi.org/10.3389/fmars.2014.00023

Gauzens, B., Barnes, A., Giling, D.P., Hines, J., Jochum, M., Lefcheck, J.S., Rosenbaum, B., Wang, S., Brose, U., 2019. fluxweb: An R package to easily estimate energy fluxes in food webs. Methods Ecol. Evol. 10, 270–279. https://doi.org/10.1111/2041-210X.13109

Gellner, G., McCann, K.S., 2016. Consistent role of weak and strong interactions in high- and low-diversity trophic food webs. Nat. Commun. 7, 11180. https://doi.org/10.1038/ncomms11180

Genner, M.J., Sims, D.W., Southward, A.J., Budd, G.C., Masterson, P., Mchugh, M., Rendle, P., Southall, E.J., Wearmouth, V.J., Hawkins, S.J., 2010. Body size-dependent responses of a marine fish assemblage to climate change and fishing over a century-long scale. Glob. Change Biol. 16, 517–527. https://doi.org/10.1111/j.1365-2486.2009.02027.x

Goldenberg, J., Bisschop, K., D'Alba, L., Shawkey, M.D., 2022. The link between body size, colouration and thermoregulation and their integration into ecogeographical rules: a critical appraisal in light of climate change. Oikos 2022, e09152. https://doi.org/10.1111/oik.09152

Good, S., et al, et al, 2020. Global Ocean OSTIA Sea Surface Temperature and Sea Ice Analysis [WWW Document]. URL https://data.marine.copernicus.eu/product/SST_GLO_SST_L4_NRT_OBSERVATIONS_010_001/description (accessed 2.9.26).

Grilli, J., Rogers, T., Allesina, S., 2016. Modularity and stability in ecological communities. Nat. Commun. 7, 12031. https://doi.org/10.1038/ncomms12031

Gulev, et al, et al, 2023. Climate Change 2021 – The Physical Science Basis: Working Group I Contribution to the Sixth Assessment Report of the Intergovernmental Panel on Climate Change, 1st ed. Cambridge University Press. https://doi.org/10.1017/9781009157896

Gunderson, L.H., 2000. Ecological Resilience--In Theory and Application. Annu. Rev. Ecol. Syst. 31, 425–439.

Gunderson, L.H., Allen, C.R., Holling, C.S., 2012. Foundations of Ecological Resilience. Island Press.

Gunderson, L.H., Holling, C.S., 2006. Panarchy: understanding transformations in human and natural systems. Island Press, Washington.

Habedank, J., Horn, S., Baird, D., Lemke, P., Renz, J., Sidorenko, V., Wiltshire, K.H., 2024. Flipbook-ENA: Towards a dynamic Ecological Network Analysis under

changing environmental conditions. Ecol. Model. 496, 110834. https://doi.org/10.1016/j.ecolmodel.2024.110834

Hahn, S.J., Brandt, A., Sonnewald, M., 2023. Climate change and fisheries affect benthic composition and diversity in the North Sea — investigations at the Dogger Bank during three decades (1991–2021) | Marine Biodiversity | Springer Nature Link [WWW Document]. URL https://link.springer.com/article/10.1007/s12526-025-01539-8 (accessed 3.2.26).

Hák, T., Janoušková, S., Moldan, B., 2016. Sustainable Development Goals: A need for relevant indicators. Ecol. Indic. 60, 565–573. https://doi.org/10.1016/j.ecolind.2015.08.003

Halpern, B.S., Frazier, M., Potapenko, J., Casey, K.S., Koenig, K., Longo, C., Lowndes, J.S., Rockwood, R.C., Selig, E.R., Selkoe, K.A., Walbridge, S., 2015. Spatial and temporal changes in cumulative human impacts on the world's ocean. Nat. Commun. 6, 7615. https://doi.org/10.1038/ncomms8615

Halpern, B.S., Walbridge, S., Selkoe, K.A., Kappel, C.V., Micheli, F., D'Agrosa, C., Bruno, J.F., Casey, K.S., Ebert, C., Fox, H.E., Fujita, R., Heinemann, D., Lenihan, H.S., Madin, E.M.P., Perry, M.T., Selig, E.R., Spalding, M., Steneck, R., Watson, R., 2008. A Global Map of Human Impact on Marine Ecosystems. Science 319, 948–952. https://doi.org/10.1126/science.1149345

Harley, C.D.G., Randall Hughes, A., Hultgren, K.M., Miner, B.G., Sorte, C.J.B., Thornber, C.S., Rodriguez, L.F., Tomanek, L., Williams, S.L., 2006. The impacts of climate change in coastal marine systems. Ecol. Lett. 9, 228–241. https://doi.org/10.1111/j.1461-0248.2005.00871.x

Hartvig, M., Andersen, K.H., Beyer, J.E., 2011. Food web framework for size-structured populations. J. Theor. Biol. 272, 113–122. https://doi.org/10.1016/j.jtbi.2010.12.006

Hastings, A., 1988. Food Web Theory and Stability. Ecology 69, 1665–1668. https://doi.org/10.2307/1941143

Heath, M.R., 2005. Changes in the structure and function of the North Sea fish foodweb, 1973–2000, and the impacts of fishing and climate. ICES J. Mar. Sci. 62, 847–868. https://doi.org/10.1016/j.icesjms.2005.01.023

Heino, M., Pauli, B.D., Dieckmann, U., 2015. Fisheries-Induced Evolution. Annu. Rev. Ecol. Evol. Syst. 46, 461–480. https://doi.org/10.1146/annurev-ecolsys-112414-054339

Heneghan, R.F., Hatton, I.A., Galbraith, E.D., 2019. Climate change impacts on marine ecosystems through the lens of the size spectrum. Emerg. Top. Life Sci. 3, 233–243. https://doi.org/10.1042/ETLS20190042

Heymans, J.J., Baird, D., 2000. A carbon flow model and network analysis of the northern Benguela upwelling system, Namibia. Ecol. Model. 126, 9–32. https://doi.org/10.1016/S0304-3800(99)00192-1

Heymans, J.J., Coll, M., Libralato, S., Morissette, L., Christensen, V., 2014a. Global Patterns in Ecological Indicators of Marine Food Webs: A Modelling Approach. PLoS ONE 9, e95845. https://doi.org/10.1371/journal.pone.0095845

Heymans, J.J., Coll, M., Libralato, S., Morissette, L., Christensen, V., 2014b. Global Patterns in Ecological Indicators of Marine Food Webs: A Modelling Approach. PLOS ONE 9, e95845. https://doi.org/10.1371/journal.pone.0095845

Hillebrand, H., 2004. On the Generality of the Latitudinal Diversity Gradient. Am. Nat. 163, 192–211. https://doi.org/10.1086/381004

Hirata, H., Ulanowicz, R.E., 1986. Large-scale systems perspective on ecological modelling and analysis. Ecol. Model., Scope and Limit in the Application of Ecological Models to Environmental Management\3-I\2-IV 31, 79–104. https://doi.org/10.1016/0304-3800(86)90057-8

Hoegh-Guldberg, O., Bruno, J.F., 2010. The Impact of Climate Change on the World's Marine Ecosystems. Science 328, 1523–1528. https://doi.org/10.1126/science.1189930

Holland, D.S., 2003. Integrating spatial management measures into traditional fishery management systems: the case of the Georges Bank multispecies groundfish fishery. ICES J. Mar. Sci. 60, 915–929. https://doi.org/10.1016/S1054-3139(03)00097-3

Holling, C.S., 2001. Understanding the Complexity of Economic, Ecological, and Social Systems. Ecosystems 4, 390–405. https://doi.org/10.1007/s10021-001-0101-5

Holling, C.S., 1973. RESILIENCE AND STABILITY OF ECOLOGICAL SYSTEMS.

Howarth, L., Waggitt, J., Bolam, S., Eggleton, J., Somerfield, P., Hiddink, J., 2018. Effects of bottom trawling and primary production on the composition of biological traits in benthic assemblages. Mar. Ecol. Prog. Ser. 602, 31–48. https://doi.org/10.3354/meps12690

Hsieh, C., Reiss, C.S., Hunter, J.R., Beddington, J.R., May, R.M., Sugihara, G., 2006. Fishing elevates variability in the abundance of exploited species. Nature 443, 859–862. https://doi.org/10.1038/nature05232

Hsieh, C., Yamauchi, A., Nakazawa, T., Wang, W.-F., 2010. Fishing effects on age and spatial structures undermine population stability of fishes. Aquat. Sci. 72, 165–178. https://doi.org/10.1007/s00027-009-0122-2

Hudson, L.N., Emerson, R., Jenkins, G.B., Layer, K., Ledger, M.E., Pichler, D.E., Thompson, M.S., O'Gorman, E.J., Woodward, G., Reuman, D.C., 2013. Cheddar: analysis and visualisation of ecological communities in R 4, 99–104.

Hunsicker, M.E., Ciannelli, L., Bailey, K.M., Buckel, J.A., Wilson White, J., Link, J.S., Essington, T.E., Gaichas, S., Anderson, T.W., Brodeur, R.D., Chan, K.-S., Chen, K., Englund, G., Frank, K.T., Freitas, V., Hixon, M.A., Hurst, T., Johnson, D.W., Kitchell, J.F., Reese, D., Rose, G.A., Sjodin, H., Sydeman,

W.J., van der Veer, H.W., Vollset, K., Zador, S., 2011. Functional responses and scaling in predator–prey interactions of marine fishes: contemporary issues and emerging concepts. Ecol. Lett. 14, 1288–1299. https://doi.org/10.1111/j.1461-0248.2011.01696.x

Hurrell, J.W., 1995. Decadal Trends in the North Atlantic Oscillation: Regional Temperatures and Precipitation. Science 269, 676–679. https://doi.org/10.1126/science.269.5224.676

ICES, 2026. ICES DataPortal [WWW Document]. URL https://data.ices.dk/view-map?theme=201809 (accessed 2.9.26).

ICES, 2010. ICES Stomach Content.

Intergovernmental Panel On Climate Change (Ipcc), 2023. Climate Change 2021 – The Physical Science Basis: Working Group I Contribution to the Sixth Assessment Report of the Intergovernmental Panel on Climate Change, 1st ed. Cambridge University Press. https://doi.org/10.1017/9781009157896

Ito, M., Halouani, G., Cresson, P., Giraldo, C., Girardin, R., 2023. Detection of fishing pressure using ecological network indicators derived from ecosystem models. Ecol. Indic. 147, 110011. https://doi.org/10.1016/j.ecolind.2023.110011

Jennings, S., Pinnegar, J.K., Polunin, N.V.C., Warr, K.J., 2002. Linking size-based and trophic analyses of benthic community structure. Mar. Ecol. Prog. Ser. 226, 77–85. https://doi.org/10.3354/meps226077

Jennings, S., Warr, K.J., 2003. Smaller predator-prey body size ratios in longer food chains. Proc. R. Soc. B Biol. Sci. 270, 1413–1417. https://doi.org/10.1098/rspb.2003.2392

Jonsson, T., Ebenman, B., 1998. Effects of Predator–prey Body Size Ratios on the Stability of Food Chains. J. Theor. Biol. 193, 407–417. https://doi.org/10.1006/jtbi.1998.0708

Jouffray, J.-B., Blasiak, R., Norström, A.V., Österblom, H., Nyström, M., 2020. The Blue Acceleration: The Trajectory of Human Expansion into the Ocean. One Earth 2, 43–54. https://doi.org/10.1016/j.oneear.2019.12.016

Kappel, C.V., Halpern, B.S., 2012. Mapping Cumulative Impacts of Human Activities on Marine Ecosystems [WWW Document]. ResearchGate. https://doi.org/10.31230/osf.io/6exng

Kay, J.J., Graham, L.A., Ulanowicz, R.E., 1989. A Detailed Guide to Network Analysis, in: Wulff, F., Field, J.G., Mann, K.H. (Eds.), Network Analysis in Marine Ecology: Methods and Applications. Springer, Berlin, Heidelberg, pp. 15–61. https://doi.org/10.1007/978-3-642-75017-5_2

Kharrazi, A., Fath, B.D., Katzmair, H., 2016. Advancing Empirical Approaches to the Concept of Resilience: A Critical Examination of Panarchy, Ecological Information, and Statistical Evidence. Sustainability 8, 935. https://doi.org/10.3390/su8090935

Kharrazi, A., Yu, Y., Jacob, A., Vora, N., Fath, B.D., 2020. Redundancy, Diversity, and Modularity in Network Resilience: Applications for International Trade and Implications for Public Policy. Curr. Res. Environ. Sustain. 2, 100006. https://doi.org/10.1016/j.crsust.2020.06.001

Kirby, R.R., Beaugrand, G., 2009. Trophic amplification of climate warming. Proc. R. Soc. B Biol. Sci. 276, 4095–4103. https://doi.org/10.1098/rspb.2009.1320

Kirby, R.R., Beaugrand, G., Lindley, J.A., 2009. Synergistic Effects of Climate and Fishing in a Marine Ecosystem. Ecosystems 12, 548–561. https://doi.org/10.1007/s10021-009-9241-9

Klecka, J., 2014. Modelling Size Structured Food Webs Using a Modified Niche Model with Two Predator Traits. PLOS ONE 9, e99355. https://doi.org/10.1371/journal.pone.0099355

Korpinen, 2015, 2015. OSPAR Case Study on Cumulative Effects: Evaluation of the methods and analysis of their outcomes. CEFAS.

Korpinen, S., Andersen, J.H., 2016. A Global Review of Cumulative Pressure and Impact Assessments in Marine Environments. Front. Mar. Sci. 3. https://doi.org/10.3389/fmars.2016.00153

Korpinen, S., Uusitalo, L., Nordström, M.C., Dierking, J., Tomczak, M.T., Haldin, J., Opitz, S., Bonsdorff, E., Neuenfeldt, S., 2022. Food web assessments in the Baltic Sea: Models bridging the gap between indicators and policy needs. Ambio 51, 1687–1697. https://doi.org/10.1007/s13280-021-01692-x

Kortsch, S., Frelat, R., Pecuchet, L., Olivier, P., Putnis, I., Bonsdorff, E., Ojaveer, H., Jurgensone, I., Strāķe, S., Rubene, G., Krūze, Ē., Nordström, M.C., 2021. Disentangling temporal food web dynamics facilitates understanding of ecosystem functioning. J. Anim. Ecol. 90, 1205–1216. https://doi.org/10.1111/1365-2656.13447

Kortsch, S., Primicerio, R., Aschan, M., Lind, S., Dolgov, A.V., Planque, B., 2019. Food-web structure varies along environmental gradients in a high-latitude marine ecosystem. Ecography 42, 295–308. https://doi.org/10.1111/ecog.03443

Kortsch, S., Primicerio, R., Fossheim, M., Dolgov, A.V., Aschan, M., 2015. Climate change alters the structure of arctic marine food webs due to poleward shifts of boreal generalists. Proc. R. Soc. B Biol. Sci. 282, 20151546. https://doi.org/10.1098/rspb.2015.1546

Krause, A.E., Frank, K.A., Mason, D.M., Ulanowicz, R.E., Taylor, W.W., 2003. Compartments revealed in food-web structure. Nature 426, 282–285. https://doi.org/10.1038/nature02115

Kuparinen, A., Cano, J.M., Loehr, J., Herczeg, G., Gonda, A., Merilä, J., 2011. Fish age at maturation is influenced by temperature independently of growth. Oecologia 167, 435–443. https://doi.org/10.1007/s00442-011-1989-x

Le Guen, C., Tecchio, S., Dauvin, J.-C., De Roton, G., Lobry, J., Lepage, M., Morin, J., Lassalle, G., Raoux, A., Niquil, N., 2019. Assessing the ecological status of an estuarine ecosystem: linking biodiversity and food-web indicators. Estuar. Coast. Shelf Sci. 228, 106339. https://doi.org/10.1016/j.ecss.2019.106339

Levett, R., 1998. Sustainability Indicators—Integrating Quality of Life and Environmental Protection. J. R. Stat. Soc. Ser. A Stat. Soc. 161, 291–302. https://doi.org/10.1111/1467-985X.00109

Levin, S.A., 1998. Ecosystems and the Biosphere as Complex Adaptive Systems. Ecosystems 1, 431–436. https://doi.org/10.1007/s100219900037

Levine, S., 1980. Several measures of trophic structure applicable to complex food webs. J. Theor. Biol. 83, 195–207. https://doi.org/10.1016/0022-5193(80)90288-X

Li, Y., Chen, B., Yang, Z.F., 2009. Ecological network analysis for water use systems—A case study of the Yellow River Basin. Ecol. Model., Special Issue on Cross-Disciplinary Informed Ecological Network Theory 220, 3163–3173. https://doi.org/10.1016/j.ecolmodel.2009.08.007

Liang, C., Pauly, D., 2017a. Fisheries impacts on China's coastal ecosystems: Unmasking a pervasive 'fishing down' effect. PLOS ONE 12, e0173296. https://doi.org/10.1371/journal.pone.0173296

Liang, C., Pauly, D., 2017b. Fisheries impacts on China's coastal ecosystems: Unmasking a pervasive 'fishing down' effect. PLOS ONE 12, e0173296. https://doi.org/10.1371/journal.pone.0173296

Lindeman, R.L., 1942a. The Trophic-Dynamic Aspect of Ecology. Ecology 23, 399–417. https://doi.org/10.2307/1930126

Lindeman, R.L., 1942b. The Trophic-Dynamic Aspect of Ecology. Ecology 23, 399–417. https://doi.org/10.2307/1930126

Lindeman, R.L., 1941. Ecological Dynamics in a Senescent Lake.

Link, J., 2002. Does food web theory work for marine ecosystems? Mar. Ecol. Prog. Ser. 230, 1–9. https://doi.org/10.3354/meps230001

Link, J.S., Watson, R.A., 2019. Global ecosystem overfishing: Clear delineation within real limits to production. Sci. Adv. 5, eaav0474. https://doi.org/10.1126/sciadv.aav0474

Lynam, C., Riberio, J., 2022. A data product derived from Northeast Atlantic groundfish data from scientific trawl surveys 1983-2020. https://doi.org/https://doi.org/10.14466/CefasDataHub.126

Lynam, C.P., Llope, M., Möllmann, C., Helaouët, P., Bayliss-Brown, G.A., Stenseth, N.C., 2017. Interaction between top-down and bottom-up control in marine food webs. Proc. Natl. Acad. Sci. 114, 1952–1957. https://doi.org/10.1073/pnas.1621037114

Lynam, C.P., Piet, G., Volwater, J., 2022. Size Composition in Fish Communities [WWW Document]. URL https://oap.ospar.org/en/versions/2365-en-1-0-0-size-composition-fish-communities/ (accessed 3.2.26).

Mackinson, S., Daskalov, G., 2007. An ecosystem model of the North Sea to support an ecosystem approach to fisheries management: description and parameterisation 142.

Martins, G.M., Harley, C.D.G., Neto, A., Arenas, F., 2025. Temperature-mediated shifts in feeding behaviour and metabolism in an omnivorous rock pool prawn. PLOS One 20, e0335899. https://doi.org/10.1371/journal.pone.0335899

Maureaud, A.A., Palacios-Abrantes, J., Kitchel, Z., Mannocci, L., Pinsky, M.L., Fredston, A., Beukhof, E., Forrest, D.L., Frelat, R., Palomares, M.L.D., Pecuchet, L., Thorson, J.T., van Denderen, P.D., Mérigot, B., 2024. FISHGLOB_data: an integrated dataset of fish biodiversity sampled with scientific bottom-trawl surveys. Sci. Data 11, 24. https://doi.org/10.1038/s41597-023-02866-w

May, R., 1973. Qualitative Stability in Model Ecosystems - May - 1973 - Ecology - Wiley Online Library [WWW Document]. URL https://esajournals.onlinelibrary.wiley.com/doi/abs/10.2307/1935352 (accessed 3.4.26).

McCann, K., Hastings, A., 1997. Re–evaluating the omnivory–stability relationship in food webs. Proc. R. Soc. B Biol. Sci. 264, 1249–1254. https://doi.org/10.1098/rspb.1997.0172

McCann, K., Hastings, A., Huxel, G.R., 1998. Weak trophic interactions and the balance of nature. Nature 395, 794–798. https://doi.org/10.1038/27427

McClanahan, T., 2014. Recovery of functional groups and trophic relationships in tropical fisheries closures. Mar. Ecol. Prog. Ser. 497, 13–23. https://doi.org/10.3354/meps10605

McCormack, S.A., Melbourne-Thomas, J., Trebilco, R., Blanchard, J.L., Raymond, B., Constable, A., 2021. Decades of dietary data demonstrate regional food web structures in the Southern Ocean. Ecol. Evol. 11, 227–241. https://doi.org/10.1002/ece3.7017

Mohamed, B., Barth, A., Van der Zande, D., Alvera-Azcárate, A., 2025. Amplified warming and marine heatwaves in the North Sea under a warming climate and their impacts. Ocean Sci. 21, 2505–2525. https://doi.org/10.5194/os-21-2505-2025

Molinos, J.G., Donohue, I., 2010. Interactions among temporal patterns determine the effects of multiple stressors. Ecol. Appl. 20, 1794–1800. https://doi.org/10.1890/10-0018.1

Mollet, F.M., Poos, J.J., Dieckmann, U., Rijnsdorp, A.D., 2016. Evolutionary impact assessment of the North Sea plaice fishery. Can. J. Fish. Aquat. Sci. 73, 1126–1137. https://doi.org/10.1139/cjfas-2014-0568

Morris, Z.B., Weissburg, M., Bras, B., 2021. Ecological network analysis of urban–industrial ecosystems. J. Ind. Ecol. 25, 193–204. https://doi.org/10.1111/jiec.13043

Mukherjee, J., Scharler, U.M., Fath, B.D., Ray, S., 2015. Measuring sensitivity of robustness and network indices for an estuarine food web model under perturbations. Ecol. Model., Special Issue: Ecological Modelling for Ecosystem Sustainability: Selected papers presented at the 19th ISEM Conference, 28-31 October 2013, Toulouse, France 306, 160–173. https://doi.org/10.1016/j.ecolmodel.2014.10.027

Naeem, S., 2009. Biodiversity, Ecosystem Functioning, and Human Wellbeing: An Ecological and Economic Perspective. Oxford University Press.

Nakazawa, T., Ushio, M., Kondoh, M., 2011. Scale Dependence of Predator–Prey Mass Ratio: Determinants and Applications, in: Advances in Ecological Research. Academic Press, pp. 269–302. https://doi.org/10.1016/B978-0-12-386475-8.00007-1

Neuheimer, A.B., Grønkjær, P., 2012. Climate effects on size-at-age: growth in warming waters compensates for earlier maturity in an exploited marine fish. Glob. Change Biol. 18, 1812–1822. https://doi.org/10.1111/j.1365-2486.2012.02673.x

Newman, M.E.J., 2006. Modularity and community structure in networks. Proc. Natl. Acad. Sci. 103, 8577–8582. https://doi.org/10.1073/pnas.0601602103

Newman, M.E.J., Girvan, M., 2004. Finding and evaluating community structure in networks. Phys. Rev. E 69, 026113. https://doi.org/10.1103/PhysRevE.69.026113

Niquil, N., Baeta, A., Marques, J., Chaalali, A., Lobry, J., Patrício, J., 2014. Reaction of an estuarine food web to disturbance: Lindeman's perspective. Mar. Ecol. Prog. Ser. 512, 141–154. https://doi.org/10.3354/meps10885

NOAA, 2023. North Pacific Groundfish Diet Data Map | NOAA Fisheries [WWW Document]. NOAA. URL https://www.fisheries.noaa.gov/resource/map/north-pacific-groundfish-diet-data-map (accessed 3.4.26).

Nogues, Q., Araignous, E., Bourdaud, P., Halouani, G., Raoux, A., Foucher, É., Loc'h, F.L., Loew-Turbout, F., Ben Rais Lasram, F., Dauvin, J.-C., Niquil, N., 2022. Spatialized ecological network analysis for ecosystem-based management: effects of climate change, marine renewable energy, and fishing on ecosystem functioning in the Bay of Seine. ICES J. Mar. Sci. 79, 1098–1112. https://doi.org/10.1093/icesjms/fsac026

Nordström, M., Aarnio, K., Bonsdorff, E., 2009. Temporal variability of a benthic food web: patterns and processes in a low-diversity system. Mar. Ecol. Prog. Ser. 378, 13–26. https://doi.org/10.3354/meps07872

Nordström, M.C., Aarnio, K., Törnroos, A., Bonsdorff, E., 2015. Nestedness of trophic links and biological traits in a marine food web. Ecosphere 6, art161. https://doi.org/10.1890/ES14-00515.1

Odum, W.E., 1980. THE STATUS OF THREE ECOSYSTEM-LEVEL HYPOTHESES REGARDING SALT MARSH ESTUARIES: TIDAL SUBSIDY, OUTWELLING, AND DETRITUS-BASED FOOD CHAINS, in: Estuarine Perspectives. Academic Press, pp. 485–495. https://doi.org/10.1016/B978-0-12-404060-1.50045-9

O'Gorman, E.J., Fitch, J.E., Crowe, T.P., 2012. Multiple anthropogenic stressors and the structural properties of food webs. Ecology 93, 441–448. https://doi.org/10.1890/11-0982.1

O'Gorman, E.J., Petchey, O.L., Faulkner, K.J., Gallo, B., Gordon, T.A.C., Neto-Cerejeira, J., Ólafsson, J.S., Pichler, D.E., Thompson, M.S.A., Woodward, G., 2019. A simple model predicts how warming simplifies wild food webs. Nat. Clim. Change 9, 611–616. https://doi.org/10.1038/s41558-019-0513-x

Oksanen, J., Kindt, R., Legendre, P., O'Hara, B., Stevens, M.H.H., Oksanen, M.J., Suggests, M.A.S.S., 2007. The vegan package. Community ecology package.

Olafsdottir, A.H., Slotte, A., Jacobsen, J.A., Oskarsson, G.J., Utne, K.R., Nøttestad, L., 2016. Changes in weight-at-length and size-at-age of mature Northeast Atlantic mackerel (Scomber scombrus) from 1984 to 2013: effects of mackerel stock size and herring (Clupea harengus) stock size. ICES J. Mar. Sci. 73, 1255–1265. https://doi.org/10.1093/icesjms/fsv142

O'Leary, J.K., Micheli, F., Airoldi, L., Boch, C., De Leo, G., Elahi, R., Ferretti, F., Graham, N.A.J., Litvin, S.Y., Low, N.H., Lummis, S., Nickols, K.J., Wong, J., 2017. The Resilience of Marine Ecosystems to Climatic Disturbances. BioScience 67, 208–220. https://doi.org/10.1093/biosci/biw161

OpenAI, 2025. ChatGPT (GPT-5).

Ortiz, E., Ramos-Jiliberto, R., Arim, M., 2023. Prey selection along a predators' body size gradient evidences the role of different trait-based mechanisms in food web organization. PLOS ONE 18, e0292374. https://doi.org/10.1371/journal.pone.0292374

OSPAR, 2023, 2023. Food webs Thematic Assessment. In: OSPAR, 2023: Quality Status Report. London, UK.

Otto, S.B., Rall, B.C., Brose, U., 2007. Allometric degree distributions facilitate food-web stability | Nature [WWW Document]. URL https://www.nature.com/articles/nature06359 (accessed 3.1.26).

Pace, M.L., Cole, J.J., Carpenter, S.R., Kitchell, J.F., Pace, M.L., Cole, J.J., Carpenter, S.R., Kitchell, J.F., 1999. Trophic cascades revealed in diverse ecosystems. Trends Ecol. Evol. 14, 483–488. https://doi.org/10.1016/S0169-5347(99)01723-1

Patrício, J., Marques, J.C., 2006. Mass balanced models of the food web in three areas along a gradient of eutrophication symptoms in the south arm of the Mondego estuary (Portugal). Ecol. Model. 197, 21–34. https://doi.org/10.1016/j.ecolmodel.2006.03.008

Pauly, D., 2019. (PDF) Gasping Fish and Panting Squids: Oxygen, Temperature and the Growth of Water-Breathing Animals. ResearchGate.

Pauly, D., Christensen, V., Dalsgaard, J., Froese, R., Torres, F., 1998. Fishing Down Marine Food Webs. Science 279, 860–863. https://doi.org/10.1126/science.279.5352.860

Pauly, D., Palomares, M.-L., 2005. FISHING DOWN MARINE FOOD WEB: IT IS FAR MORE PERVASIVE THAN WE THOUGHT. Bull. Mar. Sci. 76.

Pecuchet, L., Blanchet, M.-A., Frainer, A., Husson, B., Jørgensen, L.L., Kortsch, S., Primicerio, R., 2020. Novel feeding interactions amplify the impact of species redistribution on an Arctic food web. Glob. Change Biol. 26, 4894–4906. https://doi.org/10.1111/gcb.15196

Perkins, D.M., Hatton, I.A., Gauzens, B., Barnes, A.D., Ott, D., Rosenbaum, B., Vinagre, C., Brose, U., 2022. Consistent predator-prey biomass scaling in complex food webs. Nat. Commun. 13, 4990. https://doi.org/10.1038/s41467-022-32578-5

Perkins, D.M., Reiss, J., Yvon-Durocher, G., Woodward, G., 2010. Global change and food webs in running waters. Hydrobiologia 657, 181–198. https://doi.org/10.1007/s10750-009-0080-7

Perry, A.L., Low, P.J., Ellis, J.R., Reynolds, J.D., 2005. Climate Change and Distribution Shifts in Marine Fishes. Science 308, 1912–1915. https://doi.org/10.1126/science.1111322

Petchey, O.L., Beckerman, A.P., Riede, J.O., Warren, P.H., 2008. Size, foraging, and food web structure. Proc. Natl. Acad. Sci. 105, 4191–4196. https://doi.org/10.1073/pnas.0710672105

Petchey, O.L., Belgrano, A., 2010. Body-size distributions and size-spectra: universal indicators of ecological status? Biol. Lett. 6, 434–437. https://doi.org/10.1098/rsbl.2010.0240

Petchey, O.L., Brose, U., Rall, B.C., 2010. Predicting the effects of temperature on food web connectance. Philos. Trans. R. Soc. B Biol. Sci. 365, 2081–2091. https://doi.org/10.1098/rstb.2010.0011

Petchey, O.L., McPhearson, P.T., Casey, T.M., Morin, P.J., 1999. Environmental warming alters food-web structure and ecosystem function. Nature 402, 69–72. https://doi.org/10.1038/47023

Pimm, S.L., 1982. Food webs, in: Food Webs. Springer Netherlands, Dordrecht, pp. 1–11. https://doi.org/10.1007/978-94-009-5925-5_1

Pimm, S.L., 1980. Properties of Food Webs. Ecology 61, 219–225. https://doi.org/10.2307/1935177

Pimm, S.L., Lawton, J.H., 1978. On feeding on more than one trophic level. Nature 275, 542–544. https://doi.org/10.1038/275542a0

Pinnegar, J., 2014. DAPSTOM (integrated database and portal for fish stomach records). https://doi.org/10.14466/CEFASDATAHUB.144

Pinnegar, J., Cooper, K., Thompson, M.S.A., 2023. DAPSTOM (integrated database and portal for fish stomach records). https://doi.org/10.14466/CEFASDATAHUB.144

Pinnegar, J.K., Goñi, N., Trenkel, V.M., Arrizabalaga, H., Melle, W., Keating, J., Óskarsson, G., 2015. A new compilation of stomach content data for commercially important pelagic fish species in the northeast Atlantic. Earth Syst. Sci. Data 7, 19–28. https://doi.org/10.5194/essd-7-19-2015

Plank, M.J., Kolding, J., Law, R., Gerritsen, H.D., Reid, D., 2017. Balanced harvesting can emerge from fishing decisions by individual fishers in a small-scale fishery. Fish Fish. 18, 212–225. https://doi.org/10.1111/faf.12172

Plank, M.J., Law, R., 2012. Ecological drivers of stability and instability in marine ecosystems. Theor. Ecol. 5, 465–480. https://doi.org/10.1007/s12080-011-0137-x

Poloczanska, E.S., Burrows, M.T., Brown, C.J., García Molinos, J., Halpern, B.S., Hoegh-Guldberg, O., Kappel, C.V., Moore, P.J., Richardson, A.J., Schoeman, D.S., Sydeman, W.J., 2016. Responses of Marine Organisms to Climate Change across Oceans. Front. Mar. Sci. 3. https://doi.org/10.3389/fmars.2016.00062

Pörtner, H.-O., Roberts, D.C., Tignor, M.M.B., Poloczanska, E.S., Mintenbeck, K., Alegría, A., Craig, M., Langsdorf, S., Löschke, S., Möller, V., Okem, A., Rama, B. (Eds.), 2022. Climate Change 2022: Impacts, Adaptation and Vulnerability. Contribution of Working Group II to the Sixth Assessment Report of the Intergovernmental Panel on Climate Change.

Post, D.M., 2002. Using Stable Isotopes to Estimate Trophic Position: Models, Methods, and Assumptions. Ecology 83, 703–718. https://doi.org/10.1890/0012-9658(2002)083%5B0703:USITET%5D2.0.CO;2

Preciado, I., Arroyo, N.L., González-Irusta, J.M., López-López, L., Punzón, A., Muñoz, I., Serrano, A., 2019. Small-scale spatial variations of trawling impact on food web structure. Ecol. Indic. 98, 442–452. https://doi.org/10.1016/j.ecolind.2018.11.024

Prugh, L.R., Stoner, C.J., Epps, C.W., Bean, W.T., Ripple, W.J., Laliberte, A.S., Brashares, J.S., 2009. The Rise of the Mesopredator. BioScience 59, 779–791. https://doi.org/10.1525/bio.2009.59.9.9

Pyke, G.H., 1984. Optimal Foraging Theory: A Critical Review. Annu. Rev. Ecol. Syst. 15, 523–575.

R Core Team, 2024. R Software. A language and environment for statistical computing. R Foundation for Statistical Computing.

Reum, J.C.P., Blanchard, J.L., Holsman, K.K., Aydin, K., Punt, A.E., 2019a. Species-specific ontogenetic diet shifts attenuate trophic cascades and lengthen food chains in exploited ecosystems. Oikos 128, 1051–1064. https://doi.org/10.1111/oik.05630

Reum, J.C.P., Holsman, K.K., Aydin, K.Y., Blanchard, J.L., Jennings, S., 2019b. Energetically relevant predator–prey body mass ratios and their relationship with predator body size. Ecol. Evol. 9, 201–211. https://doi.org/10.1002/ece3.4715

Reum, J.C.P., Hunsicker, M.E., 2012. Season and prey type influence size dependency of predator−prey body mass ratios in a marine fish assemblage. Mar. Ecol. Prog. Ser. 466, 167–175. https://doi.org/10.3354/meps09913

Rezende, E.L., Albert, E.M., Fortuna, M.A., Bascompte, J., 2009. Compartments in a marine food web associated with phylogeny, body mass, and habitat structure. Ecol. Lett. 12, 779–788. https://doi.org/10.1111/j.1461-0248.2009.01327.x

Riede, J.O., Brose, U., Ebenman, B., Jacob, U., Thompson, R., Townsend, C.R., Jonsson, T., 2011. Stepping in Elton's footprints: a general scaling model for body masses and trophic levels across ecosystems. Ecol. Lett. 14, 169–178. https://doi.org/10.1111/j.1461-0248.2010.01568.x

Rojo, I., Anadón, J.D., García-Charton, J.A., 2021. Exceptionally high but still growing predatory reef fish biomass after 23 years of protection in a Marine Protected Area. PLoS ONE 16, e0246335. https://doi.org/10.1371/journal.pone.0246335

Rooney, N., McCann, K., Gellner, G., Moore, J., n.d. Structural asymmetry and the stability of diverse food webs | Nature [WWW Document]. URL https://www.nature.com/articles/nature04887 (accessed 3.4.26).

Rubbens, P., Brodie, S., Cordier, T., Destro Barcellos, D., Devos, P., Fernandes-Salvador, J.A., Fincham, J.I., Gomes, A., Handegard, N.O., Howell, K., Jamet, C., Kartveit, K.H., Moustahfid, H., Parcerisas, C., Politikos, D., Sauzède, R., Sokolova, M., Uusitalo, L., Van den Bulcke, L., van Helmond, A.T.M., Watson, J.T., Welch, H., Beltran-Perez, O., Chaffron, S., Greenberg, D.S., Kühn, B., Kiko, R., Lo, M., Lopes, R.M., Möller, K.O., Michaels, W., Pala, A., Romagnan, J.-B., Schuchert, P., Seydi, V., Villasante, S., Malde, K., Irisson, J.-O., 2023. Machine learning in marine ecology: an overview of techniques and applications. ICES J. Mar. Sci. 80, 1829–1853. https://doi.org/10.1093/icesjms/fsad100

Rutledge, R.W., Basore, B.L., Mulholland, R.J., 1976. Ecological stability: An information theory viewpoint. J. Theor. Biol. 57, 355–371. https://doi.org/10.1016/0022-5193(76)90007-2

Rutterford, L.A., Genner, M.J., Engelhard, G.H., Simpson, S.D., Hunter, E., 2023. Fishing impacts on age structure may conceal environmental drivers of body size in exploited fish populations. ICES J. Mar. Sci. 80, 848–860. https://doi.org/10.1093/icesjms/fsad014

Scharler, U.M., 2012. Ecosystem development during open and closed phases of temporarily open/closed estuaries on the subtropical east coast of South Africa. Estuar. Coast. Shelf Sci., ECSA 46 Conference Proceedings 108, 119–131. https://doi.org/10.1016/j.ecss.2011.08.003

Scharler, U.M., Fath, B.D., Banerjee, A., Fang, D., Feng, L., Mukherjee, J., Xia, L., 2018. Resilience Measures in Ecosystems and Socioeconomic Networks, in: Mensah, P., Katerere, D., Hachigonta, S., Roodt, A. (Eds.), Systems Analysis Approach for Complex Global Challenges. Springer International Publishing, Cham, pp. 183–208. https://doi.org/10.1007/978-3-319-71486-8_11

Scheffer, M., Carpenter, S.R., 2003. Catastrophic regime shifts in ecosystems: linking theory to observation. Trends Ecol. Evol. 18, 648–656. https://doi.org/10.1016/j.tree.2003.09.002

Schneider, F.D., Scheu, S., Brose, U., 2012. Body mass constraints on feeding rates determine the consequences of predator loss. Ecol. Lett. 15, 436–443. https://doi.org/10.1111/j.1461-0248.2012.01750.x

Schückel, U., Kröncke, I., Baird, D., 2015. Linking long-term changes in trophic structure and function of an intertidal macrobenthic system to eutrophication and climate change using ecological network analysis. Mar. Ecol. Prog. Ser. 536, 25–38. https://doi.org/10.3354/meps11391

Schückel, U., Nogues, Q., Brito, J., Niquil, N., Blomqvist, M., Sköld, M., Hansen, J., Jakobsen, H., Morato, T., 2022. Pilot Assessment of Ecological Network Analysis Indices, The 2023 Quality Status Report for the North-East Atlantic. OSPAR Commission. OSPAR, London.

Schwarz, B., Barnes, A.D., Thakur, M.P., Brose, U., Ciobanu, M., Reich, P.B., Rich, R.L., Rosenbaum, B., Stefanski, A., Eisenhauer, N., 2017. Warming alters energetic structure and function but not resilience of soil food webs. Nat. Clim. Change 7, 895–900. https://doi.org/10.1038/s41558-017-0002-z

Sen, P.K., 1968. Estimates of the Regression Coefficient Based on Kendall's Tau. J. Am. Stat. Assoc. 63, 1379–1389. https://doi.org/10.1080/01621459.1968.10480934

Sguotti, C., Bischoff, A., Conversi, A., Mazzoldi, C., Möllmann, C., Barausse, A., 2022. Stable landings mask irreversible community reorganizations in an overexploited Mediterranean ecosystem. J. Anim. Ecol. 91, 2465–2479. https://doi.org/10.1111/1365-2656.13831

Shackell, N.L., Frank, K.T., Fisher, J.A.D., Petrie, B., Leggett, W.C., 2010. Decline in top predator body size and changing climate alter trophic structure in an oceanic ecosystem. Proc. R. Soc. B Biol. Sci. 277, 1353–1360. https://doi.org/10.1098/rspb.2009.1020

Sheridan, J.A., Bickford, D., 2011. Shrinking body size as an ecological response to climate change. Nat. Clim. Change 1, 401–406. https://doi.org/10.1038/nclimate1259

Shurety, A.L., Thompson, M.S.A., Couce, E., Cameron, T., O'Gorman, E.J., 2026. Commercial fishing amplifies impacts of increasing temperature on predator-prey interactions in marine ecosystems | Nature Communications.

Silberberger, M.J., Renaud, P.E., Kröncke, I., Reiss, H., 2018. Food-Web Structure in Four Locations Along the European Shelf Indicates Spatial Differences in Ecosystem Functioning. Front. Mar. Sci. 5. https://doi.org/10.3389/fmars.2018.00119

Stäbler, M., Kempf, A., Temming, A., 2018. Assessing the structure and functioning of the southern North Sea ecosystem with a food-web model. Ocean Coast. Manag. 165, 280–297. https://doi.org/10.1016/j.ocecoaman.2018.08.017

Stark, J.D., Donlon, C.J., Martin, M.J., McCulloch, M.E., 2007a. OSTIA : An operational, high resolution, real time, global sea surface temperature analysis system, in: OCEANS 2007 - Europe. Presented at the OCEANS 2007 - Europe, IEEE, Aberdeen, UK, pp. 1–4. https://doi.org/10.1109/OCEANSE.2007.4302251

Stark, J.D., Donlon, C.J., Martin, M.J., McCulloch, M.E., 2007b. OSTIA : An operational, high resolution, real time, global sea surface temperature analysis system, in: OCEANS 2007 - Europe. Presented at the OCEANS 2007 - Europe, IEEE, Aberdeen, UK, pp. 1–4. https://doi.org/10.1109/OCEANSE.2007.4302251

Stouffer, D.B., Bascompte, J., 2011. Compartmentalization increases food-web persistence. Proc. Natl. Acad. Sci. 108, 3648–3652. https://doi.org/10.1073/pnas.1014353108

Sunday, J.M., Bates, A.E., Dulvy, N.K., 2010. Global analysis of thermal tolerance and latitude in ectotherms. Proc. R. Soc. B Biol. Sci. 278, 1823–1830. https://doi.org/10.1098/rspb.2010.1295

Thébault, E., Fontaine, C., 2010. Stability of Ecological Communities and the Architecture of Mutualistic and Trophic Networks. Science 329, 853–856. https://doi.org/10.1126/science.1188321

Thompson, M.S.A., Couce, E., Schratzberger, M., Lynam, C.P., 2023. Climate change affects the distribution of diversity across marine food webs. Glob. Change Biol. 29, 6606–6619. https://doi.org/10.1111/gcb.16881

Thompson, M.S.A., Pontalier, H., Spence, M.A., Pinnegar, J.K., Greenstreet, S.P.R., Moriarty, M., Hélaouët, P., Lynam, C.P., 2020. A feeding guild indicator to

assess environmental change impacts on marine ecosystem structure and functioning. J. Appl. Ecol. 57, 1769–1781. https://doi.org/10.1111/1365-2664.13662

Thompson, M.S.A., Preciado, I., Maioli, F., Bartolino, V., Belgrano, A., Casini, M., Cresson, P., Eriksen, E., Hernandez-Milian, G., Jónsdóttir, I.G., Neuenfeldt, S., Pinnegar, J.K., Ragnarsson, S., Schückel, S., Schückel, U., Smith, B.E., Torres, M.Á., Webb, T.J., Lynam, C.P., 2025. Fish functional groups of the North Atlantic and Arctic oceans. Earth Syst. Sci. Data 17, 2447–2462. https://doi.org/10.5194/essd-17-2447-2025

Tirsgaard, B., Behrens, J.W., Steffensen, J.F., 2015. The effect of temperature and body size on metabolic scope of activity in juvenile Atlantic cod *Gadus morhua* L. Comp. Biochem. Physiol. A. Mol. Integr. Physiol. 179, 89–94. https://doi.org/10.1016/j.cbpa.2014.09.033

Tomczak, M.T., Heymans, J.J., Yletyinen, J., Niiranen, S., Otto, S.A., Blenckner, T., 2013. Ecological Network Indicators of Ecosystem Status and Change in the Baltic Sea. PLoS ONE 8, e75439. https://doi.org/10.1371/journal.pone.0075439

Trifonova, N., Maxwell, D., Pinnegar, J., Kenny, A., Tucker, A., 2017. Predicting ecosystem responses to changes in fisheries catch, temperature, and primary productivity with a dynamic Bayesian network model. ICES J. Mar. Sci. 74, 1334–1343. https://doi.org/10.1093/icesjms/fsw231

Truesdell, S.B., Hart, D.R., Chen, Y., 2016. Effects of spatial heterogeneity in growth and fishing effort on yield-per-recruit models: an application to the US Atlantic sea scallop fishery. ICES J. Mar. Sci. 73, 1062–1073. https://doi.org/10.1093/icesjms/fsv238

Tucker, M.A., Rogers, T.L., 2014. Examining predator–prey body size, trophic level and body mass across marine and terrestrial mammals. Proc. R. Soc. B Biol. Sci. 281, 20142103. https://doi.org/10.1098/rspb.2014.2103

Tylianakis, J.M., Morris, R.J., 2017. Ecological Networks Across Environmental Gradients. Annu. Rev. Ecol. Evol. Syst. 48, 25–48. https://doi.org/10.1146/annurev-ecolsys-110316-022821

Ulanowicz, R.E., 2009. The dual nature of ecosystem dynamics. Ecol. Model. 220, 1886–1892.

Ulanowicz, R.E., 2004. Quantitative methods for ecological network analysis. Comput. Biol. Chem. 28, 321–339. https://doi.org/10.1016/j.compbiolchem.2004.09.001

Ulanowicz, R.E., 1996. Trophic Flow Networks as Indicators of Ecosystem Stress, in: Polis, G.A., Winemiller, K.O. (Eds.), Food Webs. Springer US, Boston, MA, pp. 358–368. https://doi.org/10.1007/978-1-4615-7007-3_35

Ulanowicz, R.E., Goerner, S.J., Lietaer, B., Gomez, R., 2009. Quantifying sustainability: Resilience, efficiency and the return of information theory. Ecol. Complex. 6, 27–36. https://doi.org/10.1016/j.ecocom.2008.10.005

Ullah, H., Nagelkerken, I., Goldenberg, S.U., Fordham, D.A., 2018. Climate change could drive marine food web collapse through altered trophic flows and cyanobacterial proliferation. PLOS Biol. 16, e2003446. https://doi.org/10.1371/journal.pbio.2003446

Van Baalen, M., Křivan, V., Van Rijn, P.C.J., Sabelis, M.W., 2001. Alternative Food, Switching Predators, and the Persistence of Predator-Prey Systems. Am. Nat. 157, 512–524. https://doi.org/10.1086/319933

Vinagre, C., Costa, M.J., Dunne, J.A., 2017. Effect of spatial scale on the network properties of estuarine food webs. Ecol. Complex. 29, 87–92. https://doi.org/10.1016/j.ecocom.2017.01.004

von Schuckmann, K., Moreira, L., Cancet, M., Gues, F., Autret, E., Aydogdu, A., Castrillo, L., Ciani, D., Cipollone, A., Clementi, E., Cossarini, G., de Pascual-Collar, A., De Toma, V., Gehlen, M., Giesen, R., Drevillon, M., Fanelli, C., Hodges, K., Jandt-Scheelke, S., Jansen, E., Juza, M., Karagali, I., Lagemaa, P., Lien, V., Lima, L., Lyubartsev, V., Maljutenko, I., Masina, S., McAdam, R., Miraglio, P., Morrison, H., Panteleit, T.R., Pisano, A., Pujol, M.-I., Raudsepp, U., Raj, R., Stoffelen, A., Van Gennip, S., Veillard, P., Yang, C., 2024. The state of the ocean in the northeastern Atlantic and adjacent seas. State Planet 4-osr8, 1–32. https://doi.org/10.5194/sp-4-osr8-2-2024

Vucic-Pestic, O., Rall, B.C., Kalinkat, G., Brose, U., 2010. Allometric functional response model: body masses constrain interaction strengths. J. Anim. Ecol. 79, 249–256. https://doi.org/10.1111/j.1365-2656.2009.01622.x

Walker, B., Holling, C.S., Carpenter, S.R., Kinzig, A., 2004. Resilience, Adaptability and Transformability in Social–ecological Systems. Ecol. Soc. 9.

Wang, S., Brose, U., 2018. Biodiversity and ecosystem functioning in food webs: the vertical diversity hypothesis. Ecol. Lett. 21, 9–20. https://doi.org/10.1111/ele.12865

Watts, D.J., Strogatz, S.H., 1998. Collective dynamics of ‘small-world’ networks. Nature 393, 440–442. https://doi.org/10.1038/30918

Wechsler, D., Bascompte, J., 2024. Mechanistic interactions as the origin of modularity in biological networks. Proc. R. Soc. B Biol. Sci. 291, 20240269. https://doi.org/10.1098/rspb.2024.0269

Williams, R.J., Martinez, N.D., 2004. Limits to Trophic Levels and Omnivory in Complex Food Webs: Theory and Data. Am. Nat. 163, 458–468. https://doi.org/10.1086/381964

Wilson, M.T., Kimmel, D.G., 2021. Predator–prey mass ratios of mid-trophic level fishes in a coastal marine ecosystem vary with taxonomy and body size. Mar. Biol. 169, 13. https://doi.org/10.1007/s00227-021-04000-z

Wood, M.V., Carvalho, F.M., Castello, L., 2024. Fishing shrinks the size structure of exploited coral reef fishes in Brazil. Fish. Res. 275, 107029. https://doi.org/10.1016/j.fishres.2024.107029

Woodson, C.B., Schramski, J.R., Joye, S.B., 2018. A unifying theory for top-heavy ecosystem structure in the ocean. Nat. Commun. 9, 23. https://doi.org/10.1038/s41467-017-02450-y

Woodward, G., Ebenman, B., Emmerson, M., Montoya, J.M., Olesen, J.M., Valido, A., Warren, P.H., 2005. Body size in ecological networks. Trends Ecol. Evol. 20, 402–409. https://doi.org/10.1016/j.tree.2005.04.005

Wootton, H.F., Morrongiello, J.R., Schmitt, T., Audzijonyte, A., 2022. Smaller adult fish size in warmer water is not explained by elevated metabolism. Ecol. Lett. 25, 1177–1188. https://doi.org/10.1111/ele.13989

Yodzis, P., Innes, S., 1992. Body Size and Consumer-Resource Dynamics. Am. Nat. 139, 1151–1175. https://doi.org/10.1086/285380

Yvon-Durocher, G., Allen, A.P., Cellamare, M., Dossena, M., Gaston, K.J., Leitao, M., Montoya, J.M., Reuman, D.C., Woodward, G., Trimmer, M., 2015. Five Years of Experimental Warming Increases the Biodiversity and Productivity of Phytoplankton. PLOS Biol. 13, e1002324. https://doi.org/10.1371/journal.pbio.1002324

Zanzi, A., Holmes, S., 2017. Fisheries data from DCF Fishing Effort Regimes data calls.

Zhao, L., Zhang, H., O'Gorman, E.J., Tian, W., Ma, A., Moore, J.C., Borrett, S.R., Woodward, G., 2016. Weighting and indirect effects identify keystone species in food webs. Ecol. Lett. 19, 1032–1040. https://doi.org/10.1111/ele.12638